



LUND UNIVERSITY

Peatland dynamics in response to past and potential future climate change

A regional modelling approach

Chaudhary, Nitin

2017

Document Version:

Publisher's PDF, also known as Version of record

[Link to publication](#)

Citation for published version (APA):

Chaudhary, N. (2017). *Peatland dynamics in response to past and potential future climate change: A regional modelling approach*. [Doctoral Thesis (compilation), Lund University]. Lund University, Faculty of Science, Department of Physical Geography and Ecosystem Science.

Total number of authors:

1

General rights

Unless other specific re-use rights are stated the following general rights apply:

Copyright and moral rights for the publications made accessible in the public portal are retained by the authors and/or other copyright owners and it is a condition of accessing publications that users recognise and abide by the legal requirements associated with these rights.

- Users may download and print one copy of any publication from the public portal for the purpose of private study or research.
- You may not further distribute the material or use it for any profit-making activity or commercial gain
- You may freely distribute the URL identifying the publication in the public portal

Read more about Creative commons licenses: <https://creativecommons.org/licenses/>

Take down policy

If you believe that this document breaches copyright please contact us providing details, and we will remove access to the work immediately and investigate your claim.

LUND UNIVERSITY

PO Box 117
221 00 Lund
+46 46-222 00 00

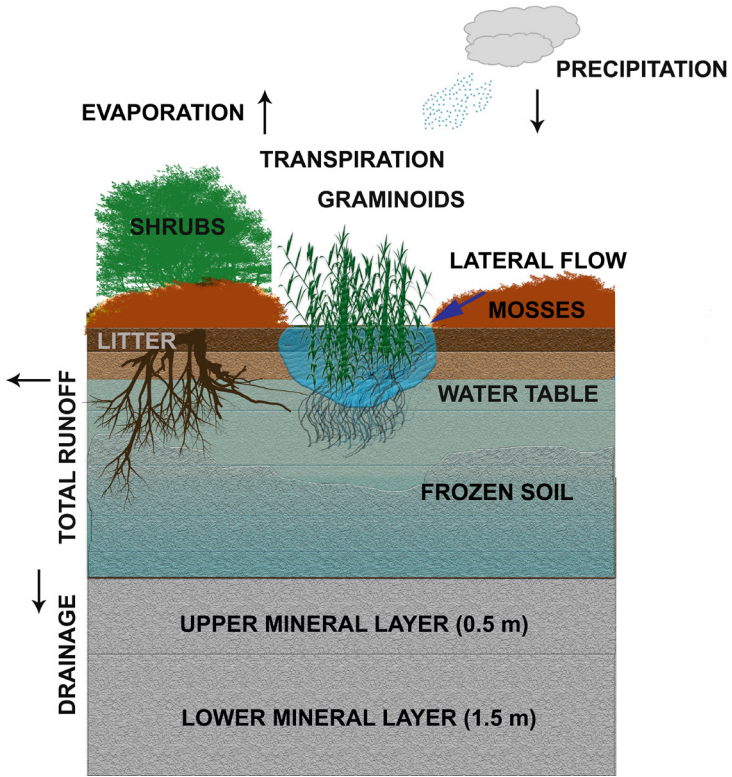
Peatland dynamics in response to past and potential future climate change

a regional modelling approach

NITIN CHAUDHARY

DEPARTMENT OF PHYSICAL GEOGRAPHY AND ECOSYSTEM SCIENCE | LUND UNIVERSITY





Peatland dynamics in response to past and potential future climate change

Peatland dynamics in response to past and potential future climate change

a regional modelling approach

Nitin Chaudhary



LUND
UNIVERSITY

DOCTORAL DISSERTATION

by due permission of the Faculty of Science, Lund University, Sweden

To be defended at Världen, Geocentrum I, Sölvegatan 12, Lund

Friday April 21st 2017, at 13.00

Faculty opponent

Dr. Mathew Williams

Global Change Research Institute

University of Edinburgh, UK

Organization LUND UNIVERSITY Department of Physical Geography and Ecosystem Science, Solvegatan 12, SE- 22362, Lund, Sweden Author: Nitin Chaudhary	Document name DOCTOROL DISSERTATION	
	Date of issue 20170325	
	Sponsoring organization DEFROST, a Nordic Centre of Excellence (NCoE) under the Nordic Top-level Research Initiative (TRI)	
Title: Peatland dynamics in response to past and potential future climate change Subtitle: A regional modelling approach		
<p>Abstract</p> <p>The majority of the northern peatlands developed during the Holocene as a result of a positive mass balance between net primary productivity (NPP) and heterotrophic decomposition rates. Over that time they have sequestered a huge amount of carbon in terrestrial ecosystems. A significant proportion of these areas also coincides with areas underlain by permafrost and shows a diverse range of peat accumulation patterns. Thus, for predicting and understanding the long-term evolution of peatland carbon stocks across the pan-Arctic, mechanistic representations of both peatland and permafrost dynamics are needed in the modelling framework. In this thesis, a novel implementation of dynamic multi-layer peatland and permafrost dynamics in the individual- and patch- based dynamic vegetation and ecosystem model (LPJ-GUESS) is described. The major emphasis of this work goes into enhancing the current understanding of the processes involved in the long-term peat accumulation and its internal dynamics, including how these systems are influenced by small-scale heterogeneity, vegetation dynamics and interactions with underlying permafrost. A simple two-dimensional microtopographical (2-DMT) model was also developed to address the established hypotheses concerning stability, behaviour and transformation of these microstructures and the effects of this small-scale heterogeneity on the coupled dynamics of vegetation, hydrology and peat accumulation. LPJ-GUESS was calibrated and validated using data from a mire in Stordalen, northern Sweden, and evaluated using data from multiple sites in Scandinavia and from Mer Bleue, Canada. It was subsequently applied across the pan-Arctic to advance the existing knowledge on carbon accumulation rates at different spatial and temporal scales, and also to demonstrate the potential implications of current warming on these climate sensitive ecosystems. Both of the models developed in this thesis performed satisfactorily when confronted with experimental data.</p> <p>LPJ-GUESS is quite robust in capturing peat accumulation and permafrost dynamics including reasonable vegetation and hydrological conditions at temporal and spatial scales across various climate gradients. The simulations improved our knowledge of peatland functioning in the past, present and future. It was found that Stordalen mire will continue to accumulate carbon in the coming decades but later will turn into a carbon source. It was also found that permafrost-free regions that are predicted to experience reduced rates of precipitation may lose significant amount of carbon in the future due to reductions in soil moisture. Conversely, peatlands currently underlain by permafrost could gain carbon due to an initial increase in soil moisture as a result of permafrost thawing. My modelling results also suggest that peatlands can show diverse range of behaviour with alternative compositional and structural dynamics depending on the initial topographical, climatic conditions, and plant characteristics, therefore, it will be challenging to represent such dynamics in current Earth System Models (ESMs). With the inclusion of aforementioned processes, LPJ-GUESS has now become quite robust. The resultant model can now be coupled with ESM where it can address issues related to peatland-mediated biogeochemical and biophysical feedbacks to climate change in the Arctic and globally.</p>		
Key words: Peatlands, permafrost, carbon accumulation, microtopography, LPJ-GUESS, Earth system models		
Classification system and/or index terms (if any)		
Supplementary bibliographical information		Language: English
ISSN and key title		ISBN (print): 978-91-85793-79-2 ISBN (PDF): 978-91-85793-80-8
Recipient's notes	Number of pages 227	Price
	Security classification	

I, the undersigned, being the copyright owner of the abstract of the above-mentioned dissertation, hereby grant to all reference sources permission to publish and disseminate the abstract of the above-mentioned dissertation.

Signature

Date: 25032017



Peatland dynamics in response to past and potential future climate change

a regional modelling approach

Nitin Chaudhary



LUND
UNIVERSITY

Department of Physical Geography and Ecosystem Science,
Faculty of Science, Lund University,
Sweden

A doctoral thesis at a university in Sweden is produced either as monograph or a collection of papers. In the latter case, the introductory part constitutes the formal thesis, which summarises the accompanying papers already published or manuscripts at various stages (in press, submitted or in preparation).

Coverphoto by: Nitin Chaudhary

Copyright: Nitin Chaudhary

Faculty of Science
Department of Physical Geography and Ecosystem Science

ISBN (print): 978-91-85793-79-2
ISSN (PDF): 978-91-85793-80-8

Printed in Sweden by Media-Tryck, Lund University
Lund 2017



This thesis is dedicated to the memory of my late father

One must have chaos in oneself to give birth to a dancing star

Contents

List of papers	1
List of Contribution	1
Abbreviations	2
Abstract	3
Sammanfattning	5
संसार	7
1. Introduction	9
1.1 Northern peatlands, their distribution and formation.....	13
1.2 Permafrost	15
1.3 Peatland vegetation and microtopography.....	17
1.4 Peatland modelling with a dynamic global vegetation model (DGVM)	19
2. Aim and Objectives	21
3. Description of LPJ-GUESS	23
3.1 LPJ-GUESS Peatland.....	24
3.2 Two-dimensional microtopographical model.....	27
4. Study area, data and experiments	29
5. Results and discussion	33
5.1 Implementing the current knowledge and progression in understanding of peatland development using LPJ-GUESS (Paper I).....	33
5.2 Predicting the past, present and future carbon accumulation rates across pan-Arctic (Paper II)	37
5.3 Modelling the coupled dynamics of vegetation-hydrology and peat accumulation (Paper III).....	39
5.4 Modelling soil thermal dynamics in high latitudes and high altitudes—a model intercomparison study (Paper IV).....	41
5.5 Future development and applications	43
6. Conclusions	47
Acknowledgements	49
Appendix	51
References	52

Papers I-IV

List of papers

- I. **Chaudhary, N.**, Miller, P. A., and Smith, B.: Modelling Holocene peatland dynamics with an individual-based dynamic vegetation model, *Biogeosciences Discussion*, doi:10.5194/bg-2016-319, in review, 2016.
- II. **Chaudhary, N.**, Miller, P. A., and Smith, B.: Modelling past, present and future carbon accumulation rates and permafrost distribution across the pan-Arctic, *Biogeosciences Discussion*, doi:10.5194/bg-2017-34, in review, 2017.
- III. **Chaudhary, N.**, Miller, P. A., and Smith, B.: Biotic and abiotic drivers of peatland growth and microtopography: a model demonstration. *Submitted to Ecosystems*
- IV. Ekici, A., Chadburn, S., **Chaudhary, N.**, Hajdu, L. H., Marmy, A., Peng, S., Boike, J., Burke, E., Friend, A. D., Hauck, C., Krinner, G., Langer, M., Miller, P. A., and Beer, C.: Site-level model intercomparison of high latitude and high altitude soil thermal dynamics in tundra and barren landscapes, *The Cryosphere*, 9, 1343-1361, doi:10.5194/tc-9-1343-2015, 2015.

List of Contribution

- I. NC implemented peatland dynamics in the customised Arctic version of LPJ-GUESS, designed the model study with guidance from the other authors, and performed the simulations. NC led the writing with all authors contributing.
- II. NC designed the model study and performed the model simulations and analysis. NC led the writing with all authors contributing.
- III. NC developed a two-dimensional microtopographical model based on a concept developed in discussion among the authors and performed the simulations. NC led the writing with all authors contributing.
- IV. The paper is a model intercomparison study carried out as a community effort with the aim of refining the representation of soil physical processes in cold region models. NC performed and contributed the LPJ-GUESS model simulations and provided input to the manuscript.

Abbreviations

ALD	Active layer depth
AR4	Fourth Assessment Report
AR5	Fifth Assessment Report
aWTP	Annual water table position
BP	Before present
CO ₂	Carbon dioxide
CH ₄	Methane
DGVM	Dynamic global vegetation model
DOC	Dissolved organic carbon
ESM	Earth System Model
GCM	Global Climate Model
GHGs	Greenhouse gases
Gr	Graminoids
HSS	High summergreen shrub
HTM	Holocene Thermal Maximum
IPCC	Intergovernmental Panel on Climate Change
K	Potassium
Kyr	Thousand years
LARCA	Long-term “apparent” rate of carbon accumulation
LPJ-GUESS	Lund-Potsdam-Jena General Ecosystem Simulator
LSE	Low evergreen shrub
LSS	Low summergreen shrub
M	Mosses
N	Nitrogen
NPP	Net primary productivity
NEE	Net ecosystem exchange
PFT	Plant functional type
PgC	Petagram Carbon
RCP	Representative concentration pathways
S	Shrubs
TgC	Teragram Carbon
TOPMODEL	TOPography based hydrological MODEL
WTP	Water table position
2-DMT	Two-dimensional microtopographical model
°C	Degree Celsius
°N	Degree North

Abstract

The majority of the northern peatlands developed during the Holocene as a result of a positive mass balance between net primary productivity (NPP) and heterotrophic decomposition rates. Over that time they have sequestered a huge amount of carbon in terrestrial ecosystems. A significant proportion of these areas also coincides with areas underlain with permafrost and shows a diverse range of peat accumulation patterns. Thus, for predicting and understanding the long-term evolution of peatland carbon stocks across the pan-Arctic, mechanistic representations of both peatland and permafrost dynamics are needed in the modelling framework. In this thesis, a novel implementation of dynamic multi-layer peatland and permafrost dynamics in the individual- and patch- based dynamic vegetation and ecosystem model (LPJ-GUESS) is described. The major emphasis of this work goes into enhancing the current understanding of the processes involved in the long-term peat accumulation and its internal dynamics, including how these systems are influenced by small-scale heterogeneity, vegetation dynamics and interactions with underlying permafrost. A simple two-dimensional microtopographical (2-DMT) model was also developed to address the established hypotheses concerning stability, behaviour and transformation of these microstructures and the effects of this small-scale heterogeneity on the coupled dynamics of vegetation, hydrology and peat accumulation. LPJ-GUESS was calibrated and validated using data from a mire in Stordalen, northern Sweden, and evaluated using data from multiple sites in Scandinavia and from Mer Bleue, Canada. It was subsequently applied across the pan-Arctic to advance the existing knowledge on carbon accumulation rates at different spatial and temporal scales, and also to demonstrate the potential implications of current warming on these climate sensitive ecosystems. Both of the models developed in this thesis performed satisfactorily when confronted with experimental data.

LPJ-GUESS is quite robust in capturing peat accumulation and permafrost dynamics including reasonable vegetation and hydrological conditions at temporal and spatial scales across various climate gradients. The simulations improved our knowledge of peatland functioning in the past, present and future. It was found that Stordalen mire will continue to accumulate carbon in the coming decades but later will turn into a carbon source. It was also found that permafrost-free regions that are predicted to experience reduced rates of precipitation may lose significant amount of carbon in the future due to reductions in soil moisture. Conversely, peatlands currently underlain with permafrost could gain carbon due to an initial increase in soil moisture as a result of permafrost thawing. My modelling results also suggest that peatlands can show diverse range of behaviour with alternative compositional and structural dynamics depending on the initial topographical and climatic conditions, and plant characteristics, therefore, it will be challenging to represent such dynamics in current Earth System Models (ESMs). With the inclusion of aforementioned processes, LPJ-GUESS has now become quite robust. The resultant model can now be coupled with

ESM where it can address issues related to peatland-mediated biogeochemical and biophysical feedbacks to climate change in the Arctic and globally.

Sammanfattning

En majoritet av de nordliga torvmarkerna utvecklades under holocen som ett resultat av en positiv massbalans mellan nettoprimärproduktion och heterotrofa nedbrytningshastigheter. Sedan dess har de lagrat stora mängder kol i terrestra ekosystem. En betydande del av dessa områden sammanfaller också med regioner med underliggande permafrost och uppvisar olika ackumulationsmönster av torv. Således, för att kunna förutse och förstå den långsiktiga utvecklingen av kollagret i torvmark i Arktiska områden, är det nödvändigt att använda mekanistiska framställningar av både torvmark och permafrost i modellering. I den här avhandlingen beskrivs en ny dynamisk flerskiktssimplemtering av torvmarker och permafrostodynamik i den individ- och patchbaserade dynamiska vegetations- och ekosystemmodellen LPJ-GUESS. Syftet med studierna i avhandlingen är att förbättra förståelsen av de processer som påverkar långsiktig torvackumulering och dess inre dynamik samt att inkludera hur dessa system påverkas av småskalig heterogenitet, vegetationsdynamik och interaktion med underliggande permafrost. En enkel tvådimensionell mikrotopografisk modell har också tagits fram för att undersöka etablerade hypoteser rörande stabilitet, beteende och transformation av dessa mikrostrukturer och effekter av denna småskaliga heterogenitet på kopplad dynamisk vegetation, hydrologi och torvackumulering. LPJ-GUESS kalibrerades och validerades med data från en myr i Stordalen i norra Sverige och utvärderades med data från flera platser i Skandinavien och Mer Bleue i Kanada. Modellen tillämpades sedan på regional nivå för att förbättra kunskapen om kolinlagringshastigheter för olika rums- och tidsupplösningar samt för att demonstrera potentiella följder av nuvarande uppvärmning på dessa klimat känsliga ekosystem. Båda modellerna som utvecklades i den här avhandlingen fungerade tillfredsställande vid jämförelser med experimentella data.

LPJ-GUESS är tämligen robust på att beskriva torvackumulering och permafrostodynamik med rimliga vegetations- och hydrologiska förhållanden för tids- och rumsupplösningar för olika klimatgradienter. Simuleringarna förbättrade vår kunskap om hur torvmarken utvecklades i det förflutna men också hur det utvecklas idag och kan komma att utvecklas i framtiden. Det visade sig att myren i Stordalen kommer att fortsätta att ackumulera kol de kommande årtiondena men senare kommer att övergå till en kolkälla. Det visade sig också att permafrostfria regioner som förutses erhålla reducerad mängd av nederbörd kan komma att förlora en signifikant mängd kol i framtiden till följd av minskad markfukt, medan torvmark med underliggande permafrost kan öka kolinlagringen på grund av en initial ökning i markfukt till följd av permafrostupptining, vilket undertrycker nedbrytning och förhöjer växtproduktion. Våra modelleringsresultat antyder även att torvmark kan uppvisa olika beteende med alternativ sammansättning och strukturell dynamik

beroende på initiala topografiska- och klimatologiska förhållanden, växtegenskaperna och det kommer i allmänhet att bli en utmaning att inkludera dem i nuvarande ESM:s. Dock så är LPJ-GUESS redo att användas i ESM:s i sin nuvarande form där den kan hantera problem relaterade till biogeokemiska och biofysikaliska återkopplingar till klimatförändringar i Arktis och globalt.

सार

जायदातर उत्तरी पीटलैंड का अधिकांश भाग होलोसीन के दौरान वकिसति होने का मुख्य कारण प्राथमिक उत्पादकता और अपघटन दर के बीच सकारात्मक द्रव्यमान संतुलन होना है। समय के साथ-साथ इन स्थलीय पारस्थितिकी तंत्र में बहुत अधिक कार्बन इकट्ठा हो गया। इन जगहों पर ठंडे बर्फ़ीली मैदान भी है और उसके परणामस्वरूप वभिन्न प्रकार के पीट पैटर्न दीखते हैं। पैन-आर्कटिक और क्पेत्रीय स्तर पर पीटलैंड कार्बन स्टॉक के व्यवहार की भवष्यवाणी के लिए मॉडलिंग ढांचे में इन दोनों वशिषताओं का प्रतनिधित्व करना आवश्यक है। इस थीसिस में, इंडविजुअल- और पैच-आधारित गतशील वनस्पतमॉडल (LPJ-GUESS) में गतशील बहु-पीट परत और परमफ्रॉस्ट का एक नया कार्यान्वयन वर्णित है। इस काम का मुख्य जोर दीर्घकालिक पीट संचय और इसकी आंतरिक गतशीलता में शामिल प्रक्रियाओं को समझने में और कैसे ये सिस्टम छोटे पैमाने पर वविधिता और वनस्पत की गतशीलता और अंतरनिहित परमफ्रॉस्ट के प्रभाव से बदलता है। स्थरिता, व्यवहार और इन माइक्रो स्ट्रक्चर के परिवर्तन और इस छोटे पैमाने पर वविधिता के प्रभाव और वनस्पत-जल वज्जान और पीट संचय के युग्मति गतशील के बारे में परकिल्पना को संबोधित करने के लिए एक सरल दो आयामी सूक्ष्म स्थलाकृतिक (2-डीएमटी/2-DMT) मॉडल भी वकिसति किया गया था। मॉडल को कैलब्रिरेटेड और मूल्यांकन स्टॉर्डेन में किया गया और स्कैंडिनेविया और मैर बलियू, कनाडा में कई साइटों पर परीक्षण किया गया। यह क्पेत्रीय पैमाने पर लागू किया गया था जो मौजूदा स्थानिक ज्ञान को वभिन्न स्थानिक और सैद्धांतिक स्तरों पर कार्बन संचय दर पर प्रक करने के लिए भी लागू किया गया था जो इन जलवायु संवेदनशील पारस्थितिकी तंत्रों पर वर्तमान गर्मी के संभावित प्रभावों का भी प्रदर्शन करता है। प्रायोगिक डेटा के सामने आने पर इस थीसिस में वकिसति किए गए दोनों मॉडल संतोषजनक तरीके से प्रदर्शन करते हैं।

लपज-गेस (LPJ-GUESS) वभिन्न जैव ग्रडियंट्स में लौकिक और स्थानिक स्तर पर उचित वनस्पत और जल वज्जान स्थितियों सहित पीट संचय और परमफ्रॉस्ट गतशीलता को कैप्चर करने में काफी मजबूत है। समिलेशन ने पछिले, वर्तमान और भवष्य में पीटलैंड के कामकाज के हमारे ज्ञान में सुधार किया है। यह पाया गया है की स्टोर्डलेन (Stordalen) आने वाले दशकों में

कार्बन जमा करना जारी रखेगा लेकिन बाद में कार्बन स्रोत बन जाएगा। यह भी पाया गया की मट्टी की नमी में कटौती के कारण परमाफ्रॉस्ट मुक्त क्षेत्रों को वर्षा की कम दरों के अनुभव होने से भवष्य में कार्बन की महत्वपूर्ण मात्रा में कमी आ सकती है। इसके विपरीत, वर्तमान में परमाफ्रॉस्ट पीटलैंड परमाफ्रॉस्ट थोवगि के परिणामस्वरूप मट्टी की नमी में प्रारंभिक वृद्धि के कारण कार्बन प्राप्त कर सकते हैं। नमी की स्थिति में यह प्रारंभिक वृद्धि अपघटन दर को दबा देती है और पौधों के उत्पादन को बढ़ाती है। मेरे मॉडलिंग परिणाम यह भी सुझाव देते हैं कि पीटलैंड प्रारंभिक स्थलाकृतिक, जलवायु परिस्थितियों और पौधे की विशेषताओं के आधार पर वैकल्पिक रचनात्मक और संरचनात्मक गतिशीलता के साथ विभिन्न प्रकार के व्यवहार को दिखा सकते हैं, इसलिए वर्तमान पृथ्वी सिस्टम मॉडल (ESM) में ऐसी गतिशीलता का प्रतिनिधित्व करना चुनौतीपूर्ण होगा। उपरोक्त प्रक्रियाओं को शामिल करने के साथ, एलपीजे-ग्यूस अब काफी मजबूत हो गया है। परिणामी मॉडल को अब ईएसएम (ESM) के साथ जोड़ा जा सकता है, जहां यह आर्कटिक और विश्व स्तर पर जलवायु परिवर्तन के लिए पीटलैंड-मध्यस्थता वाले बायोगाइकेमिकल और बायोफजिकल फीडबैक से संबंधित मुद्दों को हल कर सकता है।

1. Introduction

Northern peatlands share many features of upland and wetland ecosystems, in general, but exhibit some unique characteristics such as a shallow water table, anoxic biogeochemistry, carbon-rich soils and spatial heterogeneity influencing vegetation cover at micro (1–10 m) to macro ($> 10^4$ m) scales. It is a store house of recalcitrant dead organic mass mainly composed of *Sphagnum* species (Clymo, 1991). The dead organic matter is accumulated when the litter production is greater than the total peat decay. Because of this persistent sink, peatlands have stored large amounts of organic carbon, *i.e.*, approximately 30% of the present-day soil carbon pool (Fig. 1) and are considered one of the biggest carbon storage in the terrestrial ecosystem (ca. 350–500 PgC) (Gorham, 1991; Turunen et al., 2001; Yu et al., 2010), equivalent to earth's vegetation (ca. 550 PgC) and almost half of the atmospheric carbon dioxide (CO₂) (ca. 750 PgC) (IPCC, 2013).

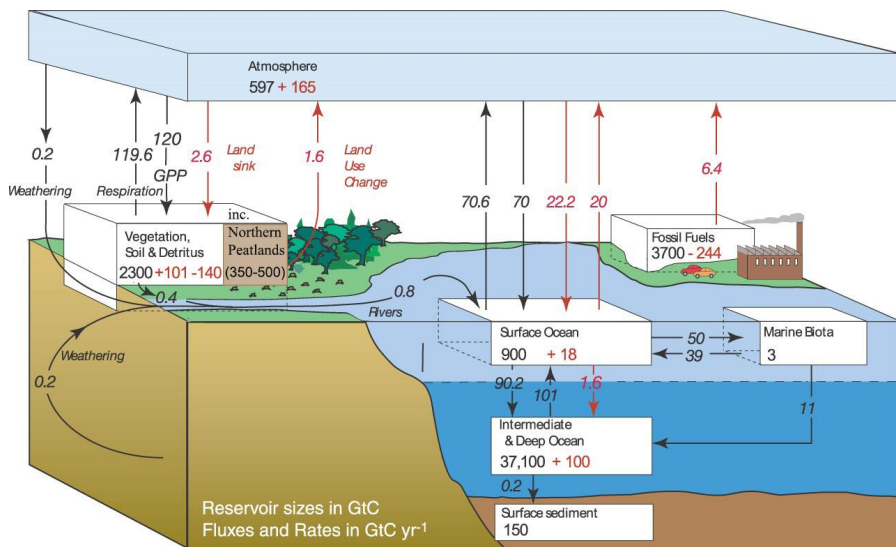


Figure 1 The global carbon cycle of the 1990s showing the carbon pools (PgC) and the annual carbon fluxes (PgC yr⁻¹). The red lines representing pre-industrial and black lines signify anthropogenic carbon fluxes and pools (Modified from IPCC, AR4, Chapter 7, Figure 3, page 515).

Peatlands are also a major source of methane (CH₄) contributing significantly to the greenhouse effect (IPCC 2013). The global peatland expansion and contraction are well correlated with past fluctuations in the atmospheric CH₄ concentration, hence facilitate in identifying the factors responsible for the peatland formation and

development (MacDonald et al., 2006). As per the proxy dataset, peatlands started forming since the last glacial maximum around 20 kyr BP (20 thousand years before present: 1950) but the majority of them were initiated during the mid-Holocene period around 8–12 kyr BP covering large areas from the north to south latitudes (Yu et al., 2010). More than 85% of these peat-rich complexes are present in northern latitude areas (between 45-75 °N) and a significant fraction of them are also underlain by frozen ground surface (continuous and discontinuous frozen ground), categorising peatlands into permafrost and non-permafrost peatlands (Tarnocai et al., 2009).

The current climate debate is mainly focused on the likely path the global average atmospheric CO₂ concentration might follow and its potential consequences on the global surface temperature (Le Quéré et al., 2016). The most optimistic future climate projections report at least 1.5–2 °C warming even if the CO₂ level stabilises (Fig. 2) (Peters et al., 2013; Friedlingstein et al., 2014). It is also predicted that the projected warming would be amplified in the northern high-latitude regions due to the associated biophysical and biogeochemical feedbacks and these regions may experience a warming of more than 5 °C (Arneth et al., 2010; Bathiany et al., 2010; Zhang et al., 2014). With this magnitude of warming, it is expected that the huge pristine peat-rich landscapes from Eurasia to North America would experience a dramatic upheaval sufficient to alter their existing carbon sink capacity (Christensen et al., 2004; Ise et al., 2008; Fan et al., 2013).

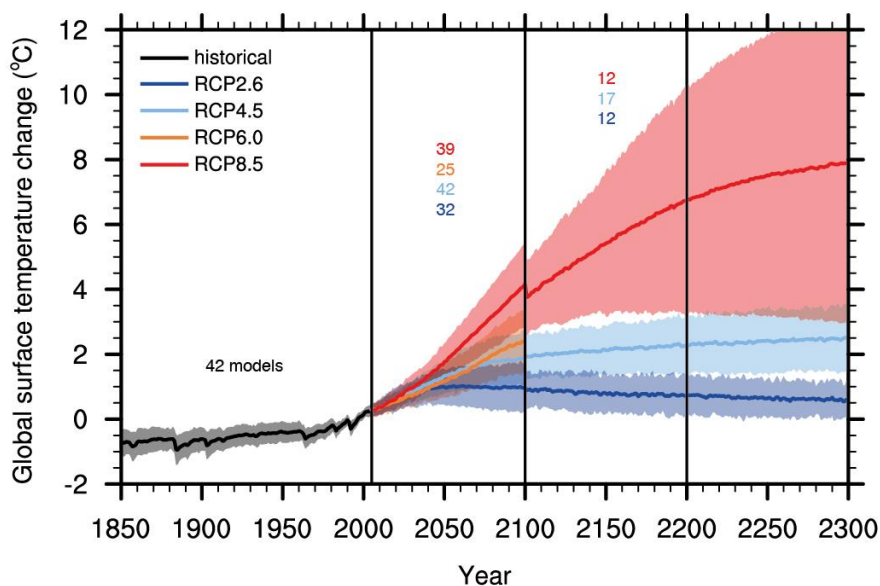


Figure 2 Warming projections (°C) under different emission scenarios. Zero is set at the average of 1986–2005 levels (IPCC AR5, Chapter 12, Figure 5, page 1054. The figure is reproduced with the kind permission of IPCC.

The first signs of these alterations have been noticed on the fringes and sensitive places across the modern peatland landscape (Yu et al., 2009; Loisel and Yu, 2013). In permafrost peatlands, recent evidences show an increase in the number of thermokarst lakes, peat subsidence, peat collapse and deeper active layer depth (ALD) due to higher atmospheric temperature leading to a complete shift from a recalcitrant moss-dominated vegetation community to dominance of non-peat-forming vegetation cover in many regions (Christensen et al., 2004; Johansson et al., 2006; Åkerman and Johansson, 2008; Swindles et al., 2015). On the other hand, the non-permafrost peatlands have been experiencing a drastic shift in their hydrological balance as a result of higher evapotranspiration (Lund et al., 2012). This accelerated rate of evapotranspiration under limited moisture conditions would potentially alter the internal biogeochemical processes of these ecosystems. Studies have also shown that higher temperature and limited moisture availability have deepened the water table, encouraging shrubs and trees to grow and modifying their present rate of carbon sequestration capacity (Sturm et al., 2005; Loranty and Goetz, 2012), a phenomenon widely reported across the pan-Arctic.

Conversely, large proportion of these peatland areas may also benefit from this accelerated rate of warming, higher precipitation rate, longer growing season and enhanced atmospheric CO₂ level (Lund et al., 2010; Charman et al., 2013). Warmer, longer growing seasons and elevated CO₂ promote plant productivity and high moisture level (driven by permafrost thaw or higher precipitation) compensates the temperature-driven decomposition rate (Yu, 2006). The combined effect of these factors would result in a substantive increase in peat accumulation rate. Currently, certain areas that were cold and perennially frozen with low carbon accumulation have been noticing a three- and four- fold increase in their productivity (Hinzman et al., 2005; Klein et al., 2013; Loisel and Yu, 2013). In future, their sink capacity may be further enhanced (Klein et al., 2013; Loisel and Yu, 2013) offsetting some negative effects of warming.

These findings and predictions highlight that peatland is a complex system that does not show a simple linear response to changing climate conditions and there is considerable uncertainty over the current and future state of peatland carbon balance. The main focus of this thesis is to determine whether these climate-sensitive ecosystems will remain a persistent carbon sink or their sequestration capacity will decline over the next 50-100 years making them a carbon source. To understand these convoluted issues, a predictive modelling approach is required that involves all the major key processes and mechanisms of the peatland carbon cycle. Though many peat growth models treat peatlands to varying degrees of complexity (see Table 1), the majority of them lack mechanistic representations of both multi-layer peatland and permafrost dynamics. Similarly, spatial heterogeneity may also be critically important in peatland development but this has unfortunately been ignored in many peatland modelling studies. The process-based dynamic multi-layer approach has been shown to capture reasonable peatland dynamics at the site scale (Bauer, 2004; Froliking et al.,

2010; Heinemeyer et al., 2010), but to my knowledge, such a scheme has not been adopted in the framework of dynamic global vegetation models (DGVMs) (see section 1.4) and also has not been applied in permafrost conditions. It is, therefore, essential to include these major detailed components in the present DGVMs to broaden the understanding of the internal processes and mechanisms of these complex systems. Once evaluated, these models can be used over large areas for assessing peat dynamics and regional carbon balance. The LPJ-GUESS DGVM provides a suitable platform to incorporate these important components in its framework and to study the long-term dynamics of peat formation and aggradation based on vegetation litter inputs and decomposition processes.

In this thesis, the implementation of new multi-layer peatland and permafrost dynamics in LPJ-GUESS, a dynamic global vegetation model (DGVM) is described. The vegetation and peatland carbon dynamics are simulated on multiple, connected patches to consider the functional and spatial heterogeneity in peatlands. The first paper (Paper I) focuses on the structure, processes understanding and performance of the model in permafrost and non-permafrost conditions and other independent sites spreading across the subarctic to temperate climate. In the next study (Paper II), the model was applied across the pan-Arctic to predict the past, present and future fate of long-term carbon pools in different climatic zones. The model predictions were evaluated against a number of reported long- and short-term carbon accumulation rates at regional and pan-Arctic scales. The third paper (Paper III) highlights the role of small-scale heterogeneity on the total peatland carbon balance and how closely microtopography is coupled with small-scale hydrology, peat accumulation and vegetation dynamics. The last study (Paper IV) focuses on model performance and evaluation with respect to other community models in predicting the soil physical processes in the cold climates.

1.1 Northern peatlands, their distribution and formation

Peatlands are transitional ecosystems mostly present in northern latitudes (Fig. 3) (Gorham, 1991) forming one of the biggest carbon reserves of all terrestrial ecosystems (Yu et al., 2010). Organic carbon stored in these ecosystems comprise one third of the global carbon deposits (Bridgham et al., 2006). Based on the present climate space, these ecosystems exist where the average annual temperature is between 2 and 10 °C and the annual precipitation ranges between 200 and 1000 mm (Yu et al., 2009). Moderate net primary productivity (NPP) coupled with depressed decomposition due to anoxic waterlogged conditions lead to sequestration of considerable amounts of carbon over the course of centuries (Clymo, 1991; Thormann and Bayley, 1997; Frohling et al., 2001). Peatlands have accumulated carbon at a rate of around 15–30 g C m⁻² y⁻¹ since the Holocene (Yu et al., 2009; Loisel et al., 2014). Overall, this imbalanced process has accumulated approximately 500±100 PgC across an area covering about 3.5 million km² (refer to Fig. 3) (Gorham, 1991; Turunen et al., 2002; Yu, 2012).

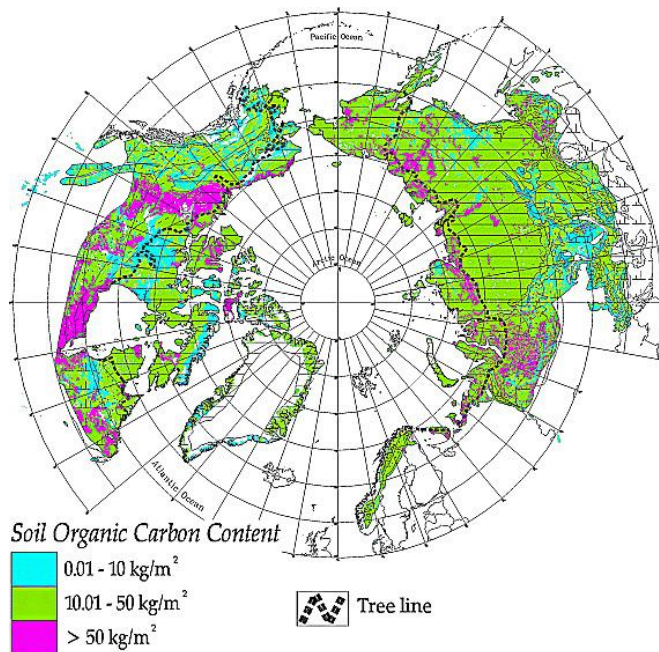


Figure 3 Soil organic carbon distribution in the northern latitude regions. Reproduced from Tarnocai et al. (2009) (Figure 3, page 6) with the kind permission of John Wiley and Sons under license no: 4073780673118

Peatland forms primarily either by paludification on a flat or depressed waterlogged mineral soil surface or on the moist surface that emerged from the ice or sea after deglaciation through isostatic rebound, or by filling up of shallow water bodies known as terristrialisation (Anderson and Foster, 2003; Kuhry and Turunen, 2006; MacDonald et al., 2006). The drainage of glacial lakes exposing the rich mineral soil also promoted these ecosystems (Vitt, 2006; Klein et al., 2013).

New land surface availability due to the retreat of massive ice caps (Dyke et al., 2004; Gorham et al., 2007), associated deglaciation warming (Kaufman et al., 2004), higher summer insolation (Berger and Loutr, 2003) marked by pronounced seasonality (Yu et al., 2009), emissions of greenhouse gases (GHGs) (MacDonald et al., 2006) together with elevated moisture conditions (Wolfe et al., 2000) are some other crucial factors that shaped and promoted the rapid expansion of peatlands in northern latitude regions.

Basal ages are commonly used as proxies to determine the approximate peatland inception period. Extensive basal databases indicate regional differences and a lag with respect to climate warming and ice retreat (MacDonald et al., 2006; Yu et al., 2010; Loisel et al., 2014). According to these datasets, the majority of the northern peatlands developed between ca. 8 and 12 kyr ago (see Fig. 4), after the deglaciation of the pan-Arctic region (MacDonald et al., 2006).

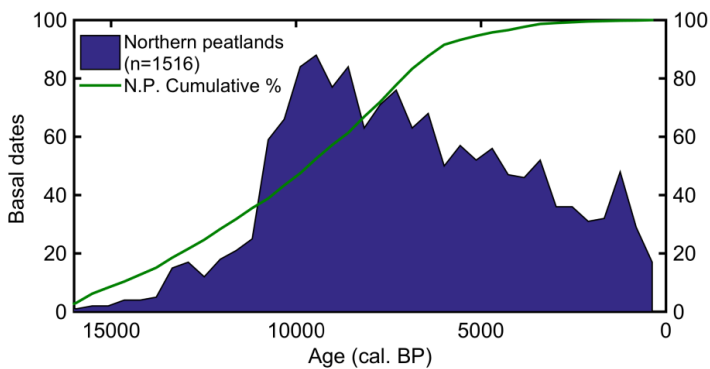


Figure 4 Observed peat basal ages and peat initiation histories plotted as a frequency curve and cumulative percentage (in green) for northern peatlands (used MacDonald et al. (2006) dataset to develop this plot)

1.2 Permafrost

Soils at or below 0 °C for at least two or more consecutive years are considered permafrost soils (Riseborough et al., 2008; Harris et al., 2009). The majority of northern peatlands overlap with low altitude permafrost areas (compare Fig. 3 and Fig. 5) (Tarnocai et al., 2009; Wania et al., 2009a, b; Kleinen et al., 2012). The peat deposits in combination with permafrost lead to assorted land structures such as palsa, peat plateaus and polygonal peat plateaus with shallow ALD (Vardy et al., 2000). The cold and frozen climate conditions prevalent in these regions create an inert environment suppressing the heterotrophic decomposition rate. The presence or absence of underlying permafrost also has diverse effects on peat accumulation and hydrology (Malmer et al., 2005). Having a strong coupling with all major biogeochemical components, any alterations in the present state of permafrost will have severe implications on the overall peatland carbon balance (Robinson and Moore, 2000).

Globally, permafrost peatlands store around 277 PgC which is equivalent to around 14% of the global soil carbon store (Tarnocai et al., 2009). In North America, permafrost peatlands store around 53.5 PgC, while non-permafrost peatlands store around 124.6 PgC with current sequestration rates of 6.6 and 22.6 TgC y⁻¹, respectively (Bridgman et al., 2006) equivalent to 12.9 g C m⁻² y⁻¹ for permafrost and 25.3 g C m⁻² y⁻¹ for non-permafrost peatlands (Wania et al., 2009a). This indicates how the frozen conditions in subarctic and arctic settings constrain peat accumulation by affecting aboveground vegetation and hydrology (Vardy et al., 2000). However, the presence of permafrost also promotes peat production by impeding drainage leading to moist and inundated conditions that lead to higher peat accumulation (Robinson and Moore, 2000). In turn, peat deposits and aboveground vegetation also affects permafrost by altering the soil physical properties and soil thermodynamics. Peat soils composed of organic recalcitrant carbon mass have, when dry, a low heat capacity and thermal conductivity which affects the presence and extent of permafrost underneath (Nicolson et al., 2007).

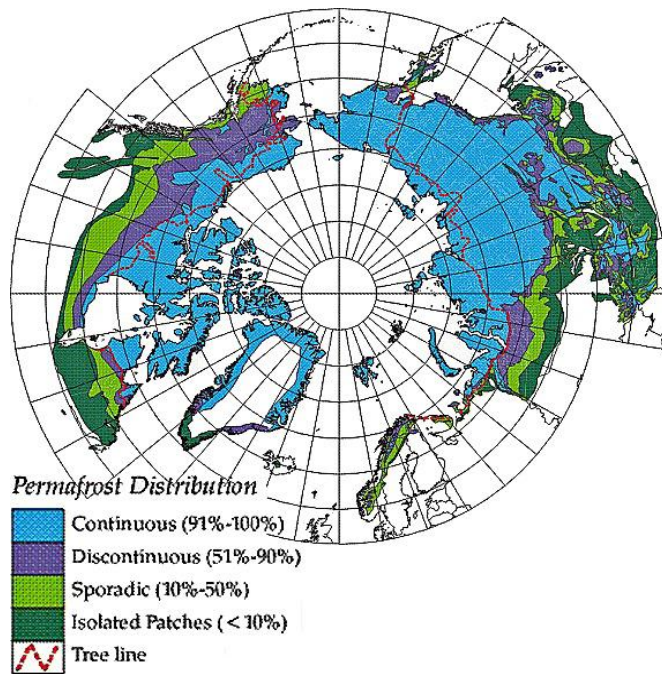


Figure 5 Permafrost distribution in the northern latitude regions. Reproduced from Tarnocai et al. (2009) (Figure 1) with the kind permission of John Wiley and Sons under license no: 4073780673118

1.3 Peatland vegetation and microtopography

The majority of peatlands are characterised by contrasting microstructures at different spatial scales (Weltzin et al., 2001; Belyea and Lancaster, 2002). At the micro scale (1–10 m), hummocks and hollows can be identified (Belyea and Clymo, 1998). Hummocks (see I in Fig. 6) are elevated features in the landscape where the water table is relatively lower than the surrounding sites leading to domination of shrubs and dry *Sphagnum* species (e.g. *S. fuscum* and *S. russowii*). Conversely, the deeper hollow areas (see III in Fig. 6) remain waterlogged and host tall productive and water-resistant species such as graminoids (e.g., *Carex rotundata*) and wet *Sphagnum* species (*S. balticum* and *S. riparium*). Mosses such as *S. lindbergi* grow in the intermediate areas known as lawns (see II in Fig. 6) and are found between the above two extremes. Open deep-water pools are also common in many peatlands and are often devoid of any vegetation (see IV in Fig. 6).

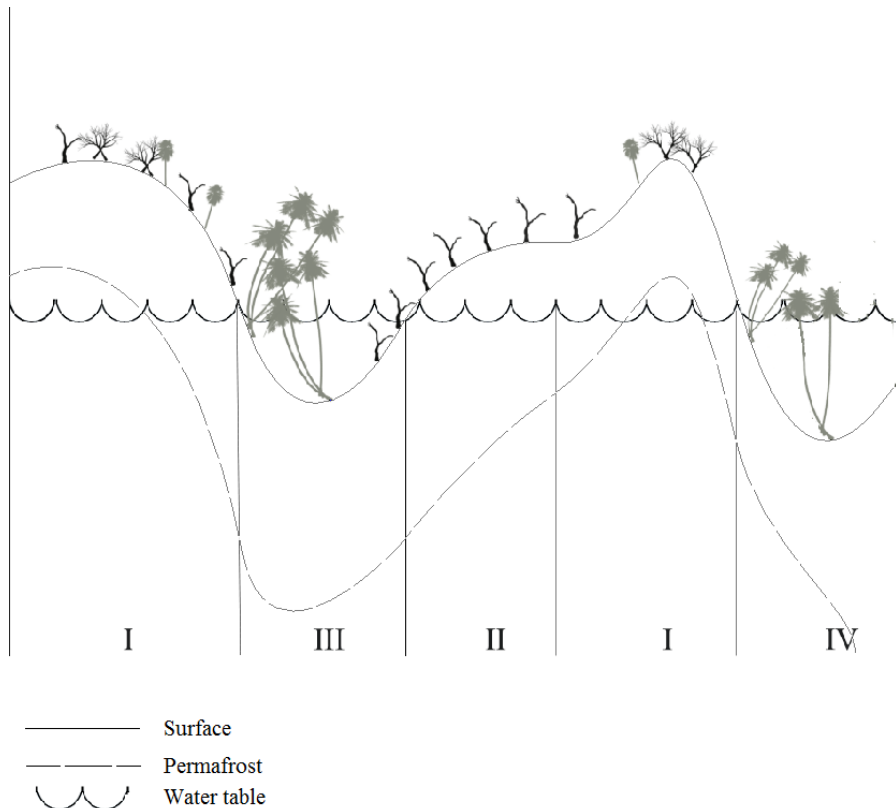


Figure 6 A schematic representation of different site classes found in the peatlands -hummocks (I), lawns (II), hollows (III) and pools (IV) and their permafrost and hydrology regimes. Modified from the source: Johansson et al. (2006).

These microstructures differ with regard to vegetation cover, hydrology, nutrient status, carbon accumulation and decomposition rates (Malmer et al., 2005). The proportion of these small-scale microstructures plays an important role in determining the long-term carbon fluxes in many peatlands (Malmer et al., 2005; Johansson et al., 2006). Changes in regional climatic conditions could have a profound impact on these micro-formations, modifying the peatland carbon balance from micro to macro scales (Johansson et al., 2006; Swindles et al., 2015).

1.4 Peatland modelling with a dynamic global vegetation model (DGVM)

Peatlands are transitional zones between upland mineral soils and wetland ecosystems (Clymo, 1991). Lately, effort have been made to incorporate peatland accumulation processes in different models (see Table 1) to understand their role in sequestering carbon and lowering the radiative forcing in the past (Frolking and Roulet, 2007; Wania et al., 2009a; Frolking et al., 2010; Kleinen et al., 2012; Tang et al., 2015b) and to know how these adaptive systems might behave in the present and potential future climatic conditions.

DGVMs are designed to study past, present and future vegetation patterns together with associated biogeochemical cycles and climate feedbacks at regional and global scales (Smith et al., 2001; Friedlingstein et al., 2006; Sitch et al., 2008; Strandberg et al., 2014; Zhang et al., 2014). They provide a suitable framework for the integration of both peatland and permafrost processes and to study their interactive response on high latitude climate. At present, most DGVMs lack both peatland and permafrost functionality (see Table 1) with a few exceptions (Wania et al., 2009a, b; Tang et al., 2015a). The two aforementioned models (Wania et al., 2009a, b; Tang et al., 2015a) however employed a relatively simple representation of peatland dynamics compared to a process-based dynamic multi-layer approach. Some other modelling groups (non-DGVMs) have also included peatland processes at varied degrees of complexity from simple two-layer to multiple-layer peat aggradation and decomposition schemes (Frolking et al., 2010; Morris et al., 2012; Alexandrov et al., 2016; Wu et al., 2016) but most of them lack permafrost. Nevertheless, they perform reasonably at single and multiple sites (Frolking et al., 2010; Wu et al., 2011; Morris et al., 2012) and also over large areas (see Table 1)(Kleinen et al., 2012; Schuldt et al., 2013; Stocker et al., 2014; Alexandrov et al., 2016).

Table 1. Comparison of functionality and scope of a representative set of current peatland models.

Schemes Models	Peatland	Permafrost	DGVM	Multiple annual peat layers	Spatial heterogeneity	Methane (Possible)	Coupled to ESM	Single site	Global/Regional application
This thesis	✓	✓	✓	✓	✓	✗ (Possible)	✗ (Possible)	✓	✓
Wu et al. (2016)	✓	✗	✗	✗	✗	✗	✓	✓	✓
Alexandrov et al. (2016)	✓	✗	✗	✗	✗	✗	✗	✗	✓
Tang et al. (2015b)	✓	✓	✓	✗	✗	✓	✗	✓	✓
Stocker et al. (2014)	✓	✗	✓	✗	✗	✗	✗	✗	✓
Morris et al. (2012)	✓	✗	✗	✗	✓	✗	✗	✓	✗
Schuldt et al. (2013)	✓	✗	✓	✗	✗	✓	✓	✓	✓
Kleinen et al. (2012)	✓	✗	✓	✗	✗	✗	✗	✓	✓
Heinemeyer et al. (2010)	✓	✗	✗	✓	✗	✗	✗	✓	✗
Frolking et al. (2010)	✓	✗	✗	✓	✗	✗	✗	✓	✗
Wania et al. (2009a)	✓	✓	✓	✗	✗	✓	✗	✗	✓
Ise et al. (2008)	✓	✗	✗	✗	✗	✗	✗	✓	✗
Bauer (2004)	✓	✗	✗	✓	✗	✗	✗	✓	✗
Hilbert et al. (2000)	✓	✗	✗	✗	✗	✗	✗	✓	✗
Clymo (1984)	✓	✗	✗	✗	✗	✗	✗	✓	✗
Ingram (1982)	✓	✗	✗	✗	✗	✗	✗	✓	✗

2. Aim and Objectives

The aim of this PhD project was to implement peatland and permafrost dynamics in a dynamic global vegetation model (LPJ-GUESS) and to evaluate it at different spatial and temporal scales.

The objectives were:

- I. To improve the current understanding of the processes and mechanisms involved in peatland development (Paper I)
- II. To assess the potential impact of climate change on the peatland carbon balance across the pan-Arctic and to understand its role in future (Paper II)
- III. To understand the role of small-scale heterogeneity on coupled vegetation-hydrology and peat accumulation (Paper III)
- IV. To evaluate LPJ-GUESS model performance in cold regions and to compare this performance to that of other land surface models (Paper IV)

3. Description of LPJ-GUESS

The Lund-Potsdam-Jena (LPJ) General Ecosystem Simulator (GUESS) is a generalised, process-based model of vegetation dynamics, plant physiology and the biogeochemistry of terrestrial ecosystems optimised for regional and global applications (Smith et al., 2001; Sitch et al., 2003; Miller and Smith, 2012). It simulates individual- and patch- based dynamics of vegetation structure and composition in changing climate and soil conditions. The model has been evaluated in numerous studies, e.g., Sitch et al. (2003), Gerten et al. (2004), Sitch et al. (2008), Piao et al. (2013) and Ekici et al. (2015) and is shown to simulate reasonable ecosystem dynamics, plant geography, and hydrological, biophysical and biogeochemical processes on regional and global scales. It gives a suitable framework for implementing peatland and permafrost dynamics and to study their long-term evolution and dynamics. Figure 7 outlines the steps involved in developing the two-dimensional microtopographical (2-DMT) and LPJ-GUESS Peatland models in this thesis.

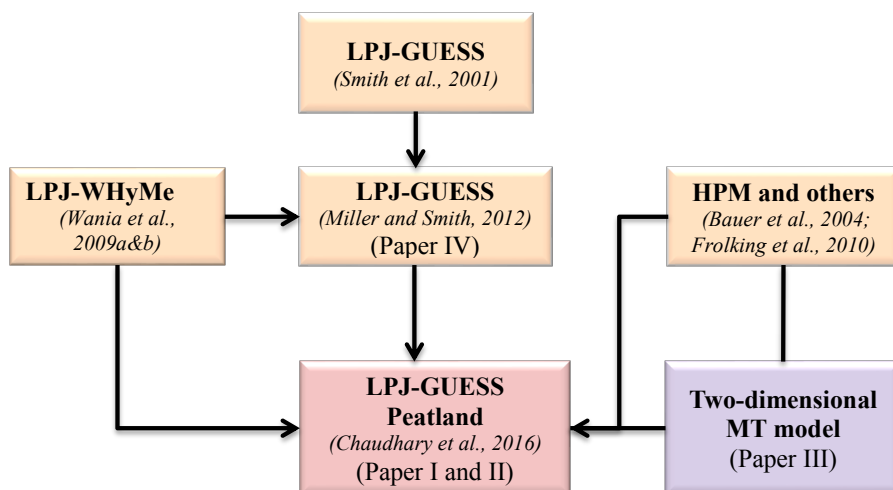


Figure 7 Flowchart depicting the steps involved in developing the two-dimensional microtopographical (2-DMT) and LPJ-GUESS Peatland models for this thesis. The model description can be found in each reference cited therein.

3.1 LPJ-GUESS Peatland

A customised Arctic version of LPJ-GUESS (Smith et al., 2001; Miller and Smith, 2012) is employed in three studies (Papers I-II and IV) in this thesis. It incorporates representations of hydrological, biophysical and biogeochemical processes characteristic of upland and peatland ecosystems of the tundra and taiga biomes (McGuire et al., 2012; Miller and Smith, 2012). I developed the model to include dynamic, multi-layer peat accumulation and permafrost dynamics (Miller and Smith, 2012; Chaudhary et al., 2016) (see Fig. 8). In the present approach, vegetation and peatland carbon dynamics are simulated on multiple, connected patches (approx. 10 ha) across the landscape to consider the functional and spatial heterogeneity of peatlands. The number of patches (total 10) is fixed at the outset of the simulation. In the first year, the model randomly distributes the carbon (after spinup) in each patch over the static mineral soil layers leading to an initially heterogeneous surface (different patch heights). These patches have their own soil column (composed of mineral and, eventually, peat layers) and dynamic vegetation properties. Vegetation in patches competes for water and sunlight and evolves as an outcome of this competition. However, there is no communication between patches except for the distribution of water. Each patch is separated vertically into four distinct layers. On the top is the dynamic single snow layer of variable thickness. Underneath it, litter/multiple peat layers of variable thickness exist. For Stordalen (see section 3), 4739 + 100 peat layers were simulated, i.e., one peat layer for each of the 4739 years after inception until the year 2000, followed by a 100-year projection from 2001 to 2100. Beneath these multiple peat layers there lies a mineral soil column composed of upper (0.5 m) and lower (1.5 m) mineral layers of fixed depth and finally a “padding” column of 48 m depth (with thicker sublayers).

To calculate the soil temperature, the peat column is subdivided into seven sublayers in the case of Stordalen, starting with the three sublayers and adding a new sublayer after every 0.5 m peat depth increment. The mineral soil layers (i.e., below the peat layers) are subdivided into 20 sublayers of 10 cm thickness. These sublayers play an important role in simulating the Arctic soil thermal dynamics at different depths. The soil temperature in the peat column and mineral soil is the result of presence/absence of insulating snow cover, phase change between water and ice, peat thickness, water input from precipitation and snowmelt and surface air temperature.

A traditional water bucket scheme was used to simulate the peatland hydrology where precipitation (rain or snowmelt) is considered the main source of water input. Water-balance processes such as evapotranspiration, drainage, surface, and base runoff determine the amount of water and ice in each layer and eventually determine the water table position (WTP). Peat layers above the WTP are assumed to remain

completely unsaturated. In the saturated layers, the amount of water and ice is limited to its water-holding capacity. The water and ice fractions in each peat layer of each individual patch are simulated daily, based on soil temperature in that layer on that particular day.

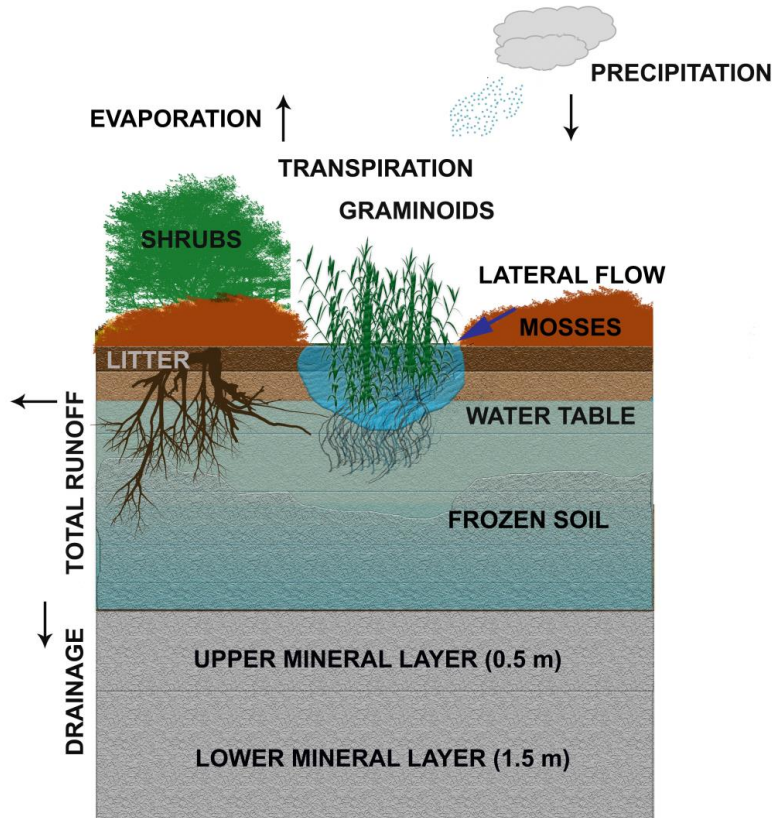


Figure 8 Schematic representation of peatland structure and function described in this thesis (Paper I). Dynamic peat layers accumulate above the static mineral soil layers (0.5+1.5 m). In the shallow peat, plant roots are present in both mineral and peat layers. Once the peat becomes sufficiently thick (2 m), all roots are confined to the peat layers.

The model also includes lateral flow of water between patches that has been missing from many earlier peatland models. Water is redistributed from the higher elevated patches (hummocks) to low depressions (hollows) using a simple lateral flow scheme in which the WTP of individual patches is held at the mean WTP of the landscape. As

the peat accumulates, the individual patches develop their own hydrologies and water-holding capacities leading to different water heights in each patch. The mean landscape WTP is calculated by taking the mean of the WTP across all patches at the end of the simulation in daily time step. This in turn affects the plant productivity and decomposition rate in each patch, which further modifies the surface conditions.

Five plant functional types (PFTs)—mosses (M), graminoids (Gr), summergreen and evergreen low shrubs (LSS and LSE) and summergreen high shrubs (HSS)—are considered. Each PFT has its own parameterisation of physiological processes related to photosynthetic pathway, leaf thickness, carbon allocation, plant phenology, and rooting depth (Miller and Smith, 2012). The PFTs establish only within the prescribed bioclimatic conditions and are also constrained by an annual average WTP (aWTP) limit. Shrubs grow in relatively dry conditions when the aWTP is deeper than 25 cm while mosses and graminoids thrive in relatively wet conditions. Mosses establish when the aWTP is between +5 and -50 cm and graminoids grow when the aWTP is above +10 cm. The establishment function is implemented once per annual time step based on the mean WTP of the previous 12 months.

The annual addition of peat layers together with annual average decomposition rate controlled by hydrological and thermal properties in each layer governs peat accumulation. Every year fresh litter is deposited on top of the mineral soil and decomposes for the entire year based on the surface soil temperature and moisture conditions. However, litter formed of plant dead roots is added directly to the peat layers corresponding to the location of the roots. The litter pool is composed of 17 plant parts (roots, seeds, wood and leaves) deposited by different PFTs based on their plant productivity, mortality and leaf turnover properties. These individual components decompose at different rates and this difference in decomposability between litter types is represented by the initial decomposition rate (k_0) (Aerts et al., 1999; Froliking et al., 2001), which declines over time as the peat becomes older.

At the start of the simulation, plants access water from the static upper (0.5 m) and lower (1.5 m) mineral soil layers. However, annually changing peat height necessitated a modified root fraction scheme which determines the amount of daily plant water uptake. In the standard set-up, plant roots fractions are prescribed in upper and lower mineral soil layers. In the modified implementation, the root fractions in the mineral soil layers are reduced linearly as peat accumulates and the corresponding reduction of root fractions is added in the peat layers, enabling PFT individuals to access water from the peat layers. Mosses are assumed to have shallow rooting depth and access water only from the top 50 cm of the peat surface. Other PFTs have deeper rooting depths that decline linearly as peat grows and they continue to access water from both mineral and peat soils. Once the peat height reaches 2 m, they access water only from the peat soil. A detailed description of the model can be found in Paper I.

3.2 Two-dimensional microtopographical model

In Paper III, I developed a simple two-dimensional microtopographical (2-DMT) model to investigate and understand the intricate relation between small-scale heterogeneity and coupled vegetation-hydrological dynamics, and the implications of divergent microtopographical behaviour on peatland carbon balances. The model shares peat accumulation and hydrological characteristics with LPJ-GUESS. Five different plant types have been considered in this study—shrubs, graminoids and three mosses dominant in their respective niches (wet, dry and intermediate peatland areas). The soil temperature in this model is calculated in a much simpler manner by adopting the simple analytical approach used in the LPJ-GUESS (Smith et al., 2001; Sitch et al., 2003), which in turn determines the amount of ice and water in the peat soil. Net primary productivity (NPP) is not simulated in 2-DMT. Rather, NPP is taken as an input to the model (from a separate LPJ-GUESS simulation for the same area), representing landscape-level primary productivity, and the model distributes it among plant types according to their productivity and dominance. The vegetation dynamics is determined by the position of the annual average WTP. The model used a simple lateral flow scheme (see above) that distributes water on the daily time-step across the patches (total 50). Figure 9 shows the schematic representation of 2-DMT and the details on this model can be found in Paper III.

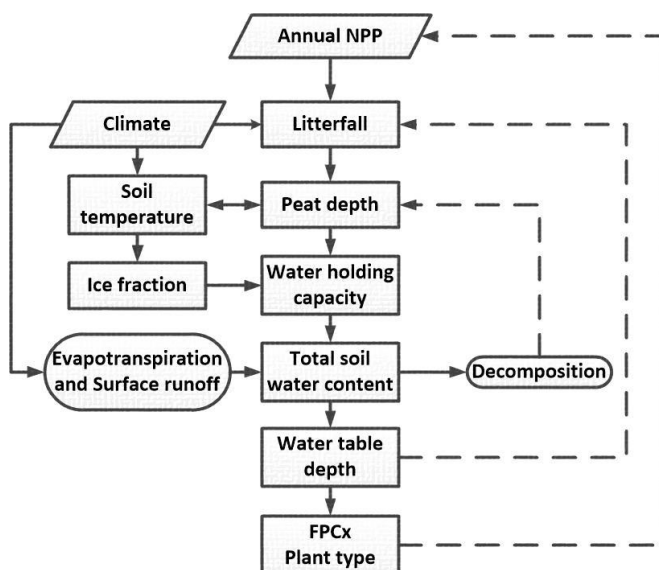


Figure 9 Schematic representation of the two-dimensional peat microtopographical model, 2-DMT. Model inputs are depicted by parallelograms, state variables are in rectangle boxes and processes are present in round boxes.

4. Study area, data and experiments

The LPJ-GUESS and 2-DMT models were tested and calibrated at Stordalen, a subarctic mire situated in the north of Sweden (68.36° N, 19.05° E, elevation 360 m a.s.l.). It is one of the most studied mixed mires in the world and was therefore considered appropriate for developing and evaluating the models (Papers I and III). Additionally, the performance of LPJ-GUESS was evaluated against the measurement and observations at Mer Bleue, a raised temperate peatland in Canada (45.40° N, 75.50° W, elevation 65 m a.s.l.). To further validate the performance of LPJ-GUESS across high-latitude climatic gradients, ten additional simulations were performed at different locations across Scandinavia (see Table 2 and Fig. 10) for which observations of peat depth were available; of these, three sites were evaluated against additional variables such as ecosystem carbon fluxes, WTP, long-term “apparent” rate of carbon accumulation (LARCA) and dominant plant type. These ten sites represent different types of peatlands with distinct initialisation periods from relatively new to old sites and diverse climatic zones from cold temperate to subarctic sites. In Paper II, the model was further applied at 180 randomly selected sites distributed among 10 zones across the pan-Arctic between 45 and 75° N to assess the effects of historical and projected climate on LARCA at regional scales. Each zone consists of 10–20 random points (see Paper II). The soil thermal dynamics and freezing-thawing properties of the model were tested and evaluated at four distinct cold sites ranging from high-latitude to high-altitude regions (see Paper IV). In Paper I, each simulation was run for 5 to 10 kyr based on the reported peat inception period, while in Paper II, all the points are run for 10 kyr. In Paper III, the model was run only for 1 kyr and in Paper IV, the simulations are done only for the recent climate (1901–2010). In the first two papers (Papers I and II), the simulations comprised three distinct climate forcing periods, the first, Holocene phase, lasted 5–10 kyr BP until 0 BP, assumed to be the year 1900. The second, historical phase ran from 1901 until the year 2000. Finally, the future scenario phase ran from the year 2001 until 2100. The detailed processing of Holocene climate forcing data was explained in Paper I. In Paper III, historical (last 1 kyr) and transient (1901–2000) runs were performed while only transient run (1901–2010) was carried out in Paper IV. Table 2 summarises the location and time periods for evaluating the model performance in this thesis, the validation datasets used and the model climate forcing data.

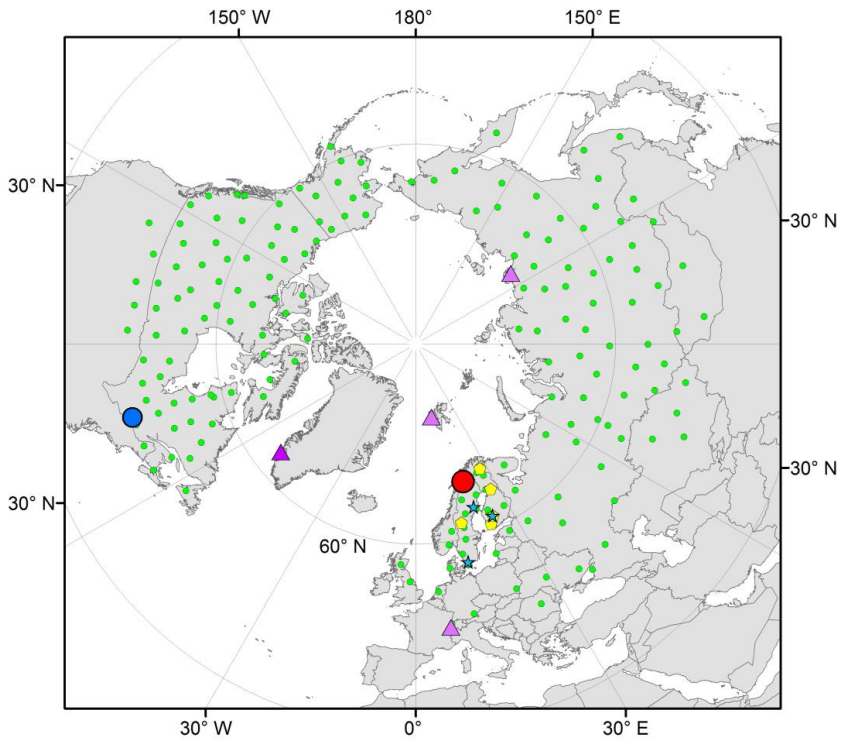







Figure 10 Map showing the selected study sites and randomly selected points used in this thesis (for symbols see Table 2).

Table 2. A summary of the simulations and model experiments described in this thesis: location, time periods for evaluating the model performance, validation datasets and climate forcing data used

Paper	Study site	Purpose of the simulation	Location(s)	Climate forcing data	Evaluation data	Period	Symbol in maps and Figure 10
I & III	Stordalen	Calibration & Evaluation	Scandinavia	Holocene climate anomalies ¹ + average observed climate (1913–1942) – Observed climate ² (1914–2000) – RCP8.5 and RCP2.6 ³ (2001–2100)	Peat depth ⁴ , LARCA ⁴ , NEE ⁵ , WTP ⁶ , ALD ⁶ , Vegetation dynamics ⁴ , Porosity ⁴ & Bulk density ⁴	4.7 (1.0) ⁷ kyr cal. BP-2100	
I	Mer Bleue	Evaluation	Canada	Holocene climate anomalies + average CRU climate (1901–1930) – CRU ⁸ climate (1901–2000) – RCP8.5 ³ (2001–2100)	Peat depth ⁹ & LARCA ⁹	8.4kyr cal. BP -2100	
I	3 sites	Evaluation	Scandinavia		Peat depth ¹⁰ , LARCA ¹⁰ , NEE ¹⁰ , WTP ¹⁰ & dominant PFT ¹⁰	5 to 10kyr cal. BP-2100	
I	5 sites	Evaluation	Scandinavia		Peat depth ¹¹	5 to 10kyr cal. BP-2100	
II	180 sites	Application & Evaluation	pan-Arctic		pan-Arctic ¹² & regional LARCA ¹³	10kyr cal. BP-2100	
IV	4 sites	Evaluation	Eurasia		WATCH ¹⁴ data (1901-2010)	Soil thermal properties & permafrost ¹⁵	1901-2010

¹ Miller and Smith, 2012

² Yang et al., 2012

³ Moss et al., 2010 and <http://tntcat.iiasa.ac.at/RcpDb/>; page visited 18th March 2017.

⁴ Kokfelt et al., 2010, Malmer et al., 2005 and Ryden et al., 1980

⁵ Deng et al., 2014 and Tang et al., 2015a

⁶ Tang et al., 2015a, b

⁷ Model was run for the last 1kyr in Paper III

⁸ Mitchell and Jones, 2005

⁹ Frolking et al., 2010 and Wang et al., 2014

¹⁰ Lund et al., 2007, Sagerfors et al., 2008 and Aurela et al., 2007

¹¹ Makila et al., 2001, Aurela et al., 2004, Tuittila et al., 2007, Valiranta et al., 2007 and Andersson and Schoning, 2010

¹² Yu et al., 2010 and Loisel et al., 2014

¹³ See Table 2 in Paper II

¹⁴ http://www.eu-watch.org/data_availability; page visited 18th March 2017

¹⁵ Ekici et al., 2015

5. Results and discussion

5.1 Implementing the current knowledge and progression in understanding of peatland development using LPJ-GUESS (Paper I)

Processes such as dynamic annual peat accumulation (Frolking et al., 2010), freezing-thawing (in subarctic and arctic conditions) (Wania et al., 2009a) and lateral flow (Belyea and Baird, 2006) are essential in the peatland modelling. Much of the understanding of these processes in peatland functioning is available in published literature (Yu et al., 2009; Frolking et al., 2010; Baird et al., 2013a; Baird et al., 2013b; Belyea, 2013; Frolking et al., 2013). My work builds upon the existing knowledge of these processes involved in long-term peat accumulation and its internal dynamics, including how these systems are influenced by small-scale heterogeneity, vegetation dynamics and underlying permafrost. My syntheses (see Table 1) showed that the current models (DGVMs and others) have not yet considered all aforementioned processes in their framework. Though many DGVMs (see Table 1) have simplified peat accumulation schemes, the majority of them lack permafrost as well as representations of small-scale heterogeneity questioning their applicability in areas where they occur. Hence, their inclusion in the modelling framework will be beneficial in predicting the past and future peatland dynamics not only at site scale but also in large areas (pan-Arctic). In this study, dynamic multi-layer peatland and permafrost dynamics are included in the Arctic version of LPJ-GUESS. Vegetation and peatland carbon dynamics are simulated on multiple, connected patches to account for the functional and spatial heterogeneity in peatlands (see Fig. 8). I used the resultant model representation to study the emergent patterns, variability and trends in the peatland ecosystems.

The model performed satisfactorily when confronted with experimental data, with modelled estimates such as long-term peat accumulation patterns, vegetation dynamics, carbon fluxes, permafrost, WTP, bulk density and porosity values (see Figs. 11 and 12). However, it was not able to reproduce the right peat accumulation pattern in some regions. This could be because of the unavailability of site-specific climate forcing data, peat inception period or dominant vegetation cover (presence of trees in some regions), an incorrect initial bulk density profile or the model's failure to capture the local hydrological conditions.

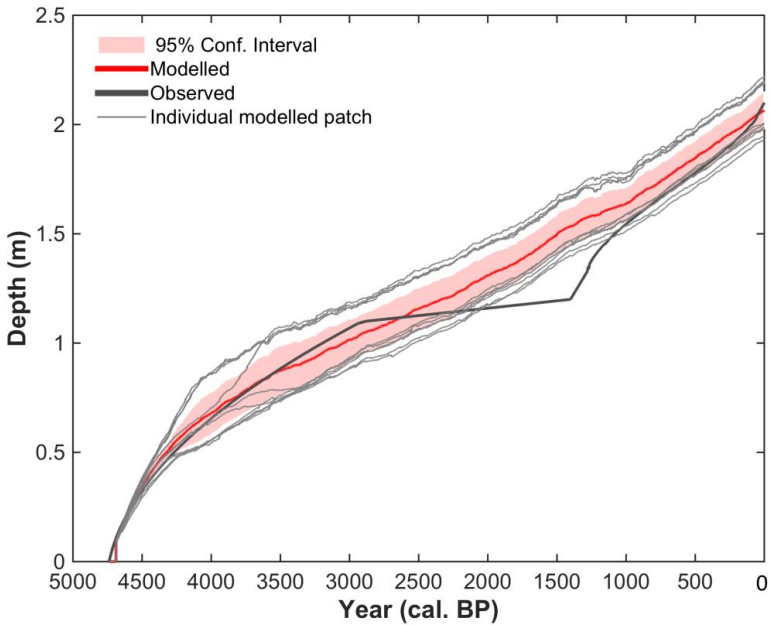


Figure 11 Comparison of mean landscape simulated peat depth (m) with inferred ages of peat layers of different depths in peat cores from the Stordalen mire. The light red shaded area shows the 95% confidence interval (CI) inferred from the variability among simulated patches at each site (shown in light grey lines).

The model simulated reasonable vegetation dynamics in the majority of the evaluation sites. However, in some instances, the dominant pattern was not captured well because plant dynamics is closely linked to the variability in local climate conditions. These biases and errors in climate data are likely to be higher in palaeoclimate simulations due to the absence of instrumental observations for validating the models. There could be additional bias also due to the interpolation procedure used during the conversion of global climate model (GCM) results into monthly anomalies. For instance, in Stordalen, between 700 and 1700 cal. BP graminoids were the dominant peat-forming vegetation but the model could not reproduce this phase due to the absence of decadal and centennial climate variability in the adopted climate-forcing data. This has resulted in an averaging out of high-moisture periods over time removing some wet episodes essential for graminoids to be sufficiently competitive (Fig. 12a).

The model has simulated reasonable ALD in hummocks and semi-wet patches (see Fig. 12b) with similar temporal pattern indicating that it is quite effective in capturing permafrost dynamics. The magnitude, variability and trend of the simulated annual ALD were close to the observed values. The simulated annual ALD was shallow in drier elevated areas while deeper in wet hollows, a phenomenon observed in many

permafrost peatlands (Johansson et al., 2013). Simulations also demonstrated that how the permafrost affects the productivity of vascular plants and the overall ecosystem. For instance, vascular plants have a deeper rooting depth and their access to water decreases significantly if the peat soil is frozen. This reduces their net productivity and in turn affects the total litter biomass. This condition marginally affects the mosses as they access water only from the top 50 cm of the soil. This is also a reason why mosses are the dominant PFT in majority of the subarctic settings.

Simulation results show that the bulk density does not increase with depth in the colder regions. Some studies also indicated the bulk density to be highly variable down the profile (Tomlinson, 2005; Baird et al., 2016). This is because the lower peat layers were frozen, didn't decompose significantly and their bulk densities remain lower relative to other partially frozen or unfrozen layers.

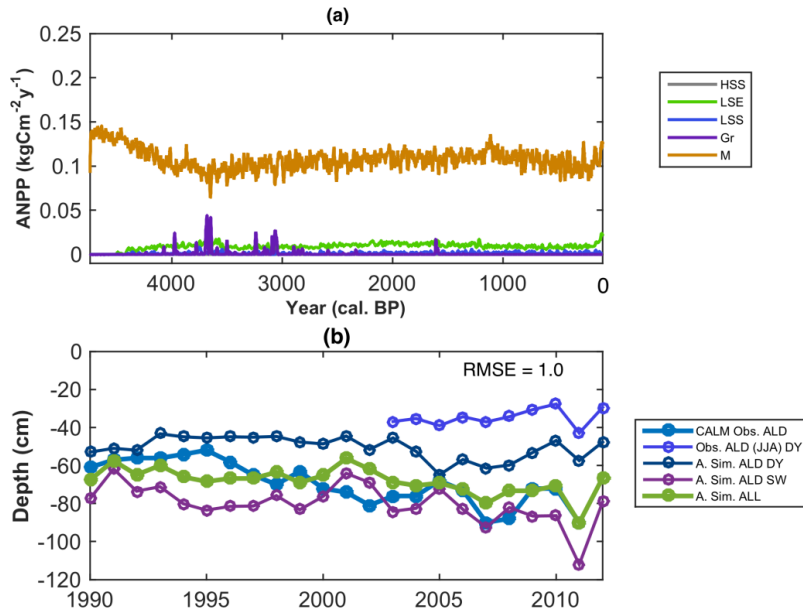


Figure 12 (a) Simulated annual net primary productivity (ANPP in $\text{kg C m}^{-2} \text{y}^{-1}$; 10-year moving average) of simulated PFTs. (b) Comparison between annual observed (CALM Obs.) and simulated (A. Sim. ALL) active layer depth (in cm) for 1990-2012 and annual average simulated ALD in semi-wet (A. Sim. SW) and dry patches (A. Sim. DY) at Stordalen mire. A separate short mean (June-August) ALD observation from the Stordalen in a dry elevated hummock site (Obs. ALD (JJA) DY) is also presented.

The above discussion shows that LPJ-GUESS is quite robust in capturing peat accumulation and permafrost dynamics including reasonable vegetation and hydrological conditions (see Fig. 8 in Paper I). The simulations also demonstrate that how these processes are intricately linked and help us in better understanding of the peatland functioning. The model also predicts the vulnerability of Stordalen mire to climate change and the results indicate that the mire may sequester more carbon until the middle of this century due to the prevailing mild climate conditions and then turn into a carbon source due to higher decomposition rate as a result of warming of soils and in more extreme case the permafrost might completely disappear.

These findings suggest that the model is capable of capturing the reasonable patterns, trends and variability associated with Stordalen mire and also reproduced satisfactory results at other sites (see Paper I); hence, it can be used to predict the past, present and future trends in carbon accumulation making a basis for my second study (Paper II). With incorporation of the aforementioned processes, LPJ-GUESS has now become quite robust and can be coupled with ESM to resolve the issues related to peatland-mediated biogeochemical and biophysical feedbacks to climate change in the Arctic as well as globally.

5.2 Predicting the past, present and future carbon accumulation rates across pan-Arctic (Paper II)

Many empirical studies have reported and compiled carbon accumulation rates across the pan-Arctic (Yu et al., 2009 and Table 3 in Paper II) and the recent syntheses by Loisel et al. (2014) highlighted certain gaps in some key regions such as eastern Siberia, Far East and European Russia due to the remoteness, inaccessibility and harsh climate conditions. My process-based peatland and permafrost modelling complements the empirical knowledge and fills the existing gaps related to carbon accumulation rates at different spatial and temporal scales and demonstrates the potential implications of current warming on these ecosystems. In this thesis (Paper II), LPJ-GUESS was employed at 180 randomly selected points distributed among 10 zones across the pan-Arctic (45–75 °N) to determine the carbon accumulation rates and to examine the implications of the projected climate change on peatland carbon dynamics.

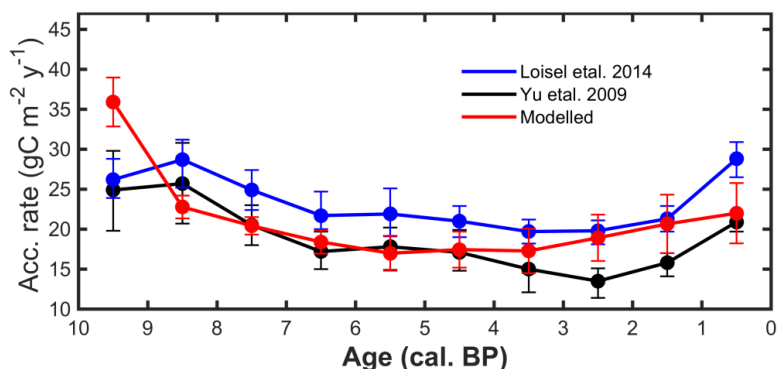


Figure 13 Simulated and observed mean carbon accumulation rate ($\text{g C m}^{-2} \text{y}^{-1}$) for each 1 kyr period for the last 10 kyr. Red: simulated mean (and standard error of the means) carbon accumulation rates based on 180 random sites. Blue and black points observed carbon accumulation rates ($\text{g C m}^{-2} \text{y}^{-1}$) based on 127 (Loisel et al., 2014) (blue points) and 33 sites (Yu et al., 2009) (black points) across northern peatlands with error bars showing standard errors of the means.

My result shows that the mean modelled LARCA ($20.8 \pm 12.3 \text{ g C m}^{-2} \text{y}^{-1}$) across the pan-Arctic falls within the reported range ($18.6\text{--}22.9 \text{ g C m}^{-2} \text{y}^{-1}$) for the northern peatlands (see Fig. 13) (Yu et al., 2009; Loisel et al., 2014). The reported value obtained from Loisel et al. (2014) is more comprehensive ($n = 127$) than that of Yu et al. (2009), which contains only 33 sites, and with limited or no sites from many important peat-rich regions such as the Hudson Bay Lowlands, the British Isles, western and eastern Siberia. However, the Loisel et al. (2014) dataset is not

completely representative of the pan-Arctic region either (see above). This dataset includes points mainly from peat rich complexes, whereas shallow peat basins are underrepresented (MacDonald et al., 2006; Gorham et al., 2007; Korhola et al., 2010). Furthermore, their dataset was limited to area north of 69 °N. Inclusion of shallow peatland complexes and more arctic sites in their syntheses might conceivably bring down the mean observed LARCA value closer to the modelled LARCA. However, the temporal pattern and overall trend of the modelled, regionally-averaged carbon accumulation rates ($n = 180$) for the last 10 kyr agrees reasonably closely with the published syntheses (Fig. 14a) and is also consistent with many reported regional estimates (see Paper II, Table 3).

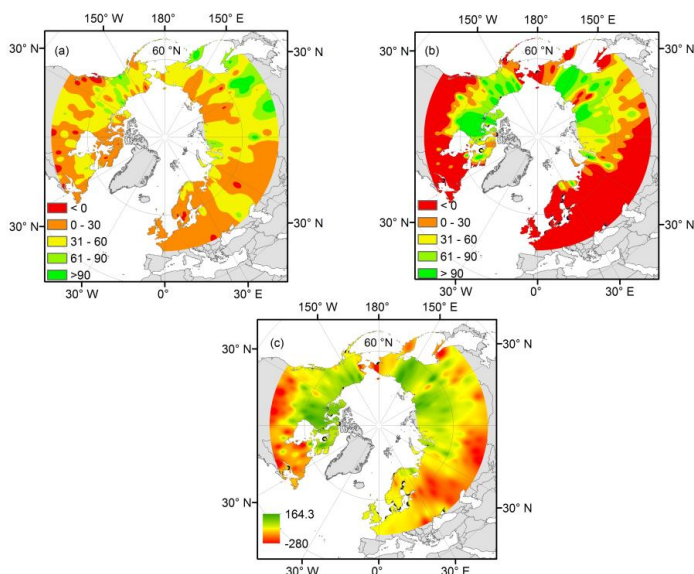


Figure 14 Modelled mean carbon accumulation rate ($\text{g C m}^{-2} \text{y}^{-1}$) interpolated among simulation points for (a) 1990-2000, (b) 2090-2100; (c) Net change in total accumulation rate (b-a).

The results show that the carbon sequestration capacity of major peat-rich regions such as Siberia, Far East Russia, Alaska and western and northern Canada would be enhanced by 2100. In contrast, regions such as Scandinavia, Europe, Russia and central and eastern Canada may turn into carbon sources (Fig. 14b,c). This indicates a shift in the carbon balance of major peat-rich regions. However, the projected readjustment affects the pan-Arctic carbon accumulation rate marginally and is predicted to decrease from $20.8 \text{ g C m}^{-2} \text{y}^{-1}$ to $20.78 \text{ g C m}^{-2} \text{y}^{-1}$ under extreme (RCP8.5) climatic conditions. Simulation results also highlighted that permafrost-free regions predicted to experience reduced rates of precipitation may lose significant amount of carbon in the future due to reduction in soil moisture; in contrast, peatlands currently underlain with permafrost could gain carbon in the coming decades due to an initial increase in soil moisture as a result of permafrost thawing (see Fig. 5 in Paper II).

5.3 Modelling the coupled dynamics of vegetation-hydrology and peat accumulation (Paper III)

Scaling is an important issue in peatland science because the majority of peatlands are marked with small-scale microstructures known as hummocks and hollows (see Fig. 6) (Weltzin et al., 2001; Belyea and Lancaster, 2002) and this small-scale heterogeneity has a strong influence on peatland carbon balance and regulates carbon fluxes at micro to macro scales (Malmer et al., 2005). The issues related to representation of such heterogeneity and their generalisation in GCMs are often discussed but not implemented due to sheer complexity and resource availability. In Paper III a simple 2-DMT model was developed to address the hypotheses concerning the stability, behaviour and transformation of these microstructures and the effects of the small-scale heterogeneity on coupled dynamic of vegetation-hydrology and peat accumulation. The main focus of this study is on understanding the processes operating at or near the peatland surface as well as across the peat column and how they are closely linked to and impact the overall peatland carbon balance.

I found a very interesting result which shows that peatlands can exhibit cyclical pattern in some patches (see Fig. 15). Shrubs and hummock mosses in some elevated areas (patches) replaced each other and the transition period lasted 50–150 years (Fig. 15a). During the transition, both the plant types coexisted. High rate of litter deposition by hummock mosses led to domination of shrubs as the WTP drew down from the surface. However, relatively high decomposition rate of shrub litter reduced the growth rate of peat column and soon the WTP approached the surface leading to favourable conditions for the hummock mosses to flourish. Similar cyclicality was also observed between lawn and hummock mosses but for a shorter duration (Fig. 15b). These dynamics may be crucial for the evolution of large-scale peatland carbon balance under changing climate conditions. However, it is likely challenging to emulate with accuracy due to the strong influence of internal feedbacks suggested by my simulation results (see Fig. 5 in Paper III).

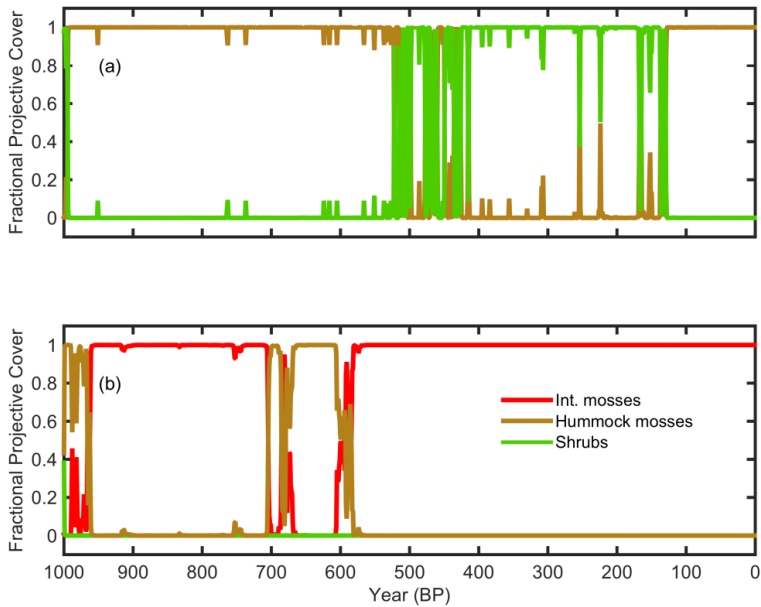


Figure. 15 (a) Cyclicity between shrubs and hummock mosses is apparent from ca. 600 cal. BP and (b) in intermediate and hummock mosses from ca. 950 cal. BP

Generally, the results indicate that peatland can show diverse ranges of behaviour with alternative compositional and structural dynamics depending on the initial topographical and climatic conditions, and plant characteristics. Some patches showed a cyclical behaviour while other remain stable over the course of the simulation but overall the peatland loses its initial surface roughness. Hence, this varied transformational behaviour of microstructures poses certain challenges to the representation of such dynamics in ESMs, allowing their potentially important implications for regional and global carbon balances and biogeochemical and biophysical feedbacks to the atmosphere to be explored and quantified.

5.4 Modelling soil thermal dynamics in high latitudes and high altitudes—a model intercomparison study (Paper IV)

Defining soil physical properties such as snow insulation, soil freezing and thawing and sub-surface conditions like water/ice content and soil texture are crucial for modelling the right soil thermal dynamics at high-latitudes and high-altitudes. Paper IV in this thesis presents a comparison of six different land surface models to identify the importance of physical processes in capturing observed temperature dynamics in soils. The model comparison is carried out at four different sites distributed from Alpine to high Arctic and wet polygonal tundra to non-permafrost Arctic. The study emphasised that the inclusion of detailed snow dynamics in the land surface models is important as the variation in the snow depth affects the topsoil temperature and its inclusion may further enhance the model predictive power. In the snow-free season, dynamic vegetation cover and organic/litter layer influence the topsoil temperature predictions and considering such dynamics is essential. On the other hand, dynamic heat-transfer parameters (volumetric heat capacity and heat conductivity) in snow representation appear less important because of the missing processes such as wind drift. We found some discrepancies in modelling subsoil temperature between the land surface models. These discrepancies in predicting the subsoil temperature stem from different hydrological and thermal dynamics in model formulations and the analysis indicates that the right subsoil temperature can be captured using a detailed soil-physics scheme. LPJ-GUESS modelled reasonable topsoil (see Fig. 16) and subsoil temperatures but its predictions can be improved further by including multi-snow layer scheme and detailed representation of dynamic organic surface layer and hydrology. In the subsequent study (Paper I), some of these issues were addressed and a dynamic multi-layer peatland and hydrology were incorporated in the model.

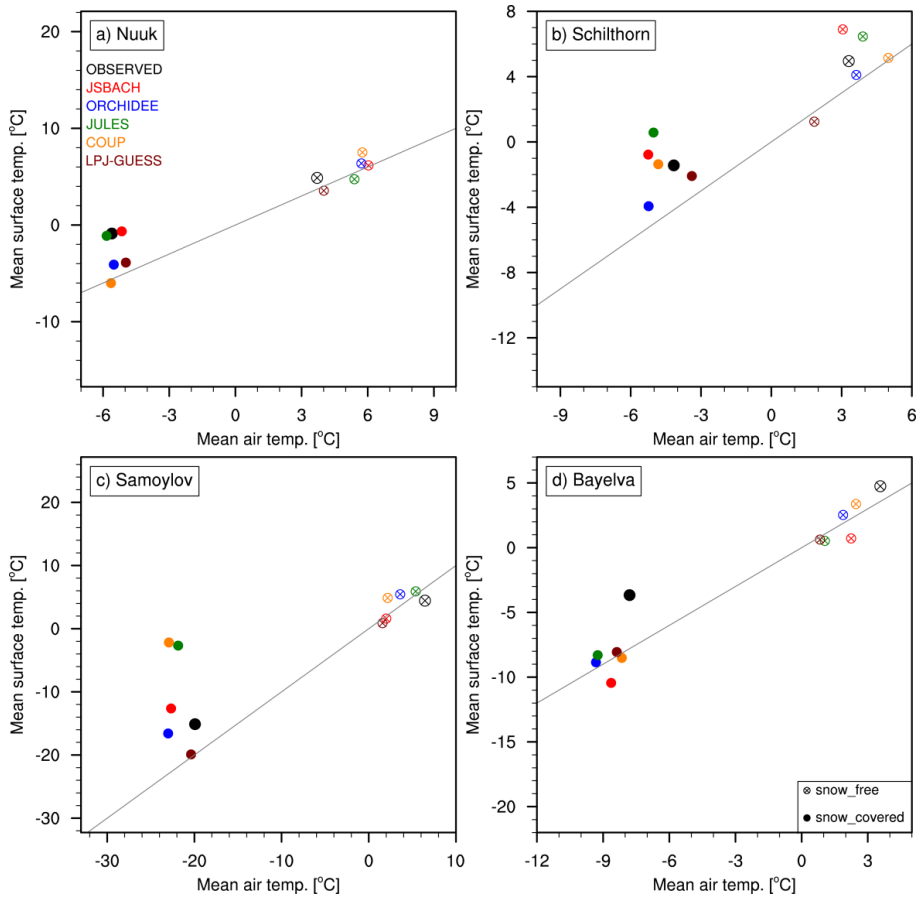


Figure 16 Scatter plots showing air/topsoil temperature relation from observations and models at each site for snow and snow-free seasons. Snow season is defined separately for observations and each model, by taking snow depth values over 5 cm to represent the snow-covered period. The average temperature of all snow covered (or snow free) days of the simulation period is used in the plots. Markers distinguish snow and snow free seasons and colors distinguish models. Gray lines represent the 1:1 line.

5.5 Future development and applications

In this thesis, the advantages of LPJ-GUESS peatland have been highlighted and the model has been shown to capture reasonable peat and permafrost dynamics. The model can further be improved or extended incorporating the following features:

- Peatland is a major source of methane, one of the potent GHG (Lai, 2009). Methane emissions are controlled by some crucial factors such as anaerobic biogeochemistry, soil moisture, plant types and quality of litter (Whiting and Chanton, 1993). Similarly, transport of dissolved organic carbon (DOC) in peatlands is also critical for their carbon balance. Multiyear observations show that export of DOC is between 10 and 20 g C m⁻² y⁻¹ and it has the same order of magnitude as LARCA in many peatlands (Roulet et al., 2007; Nilsson et al., 2008). In LPJ-GUESS, both these components exist in different versions that can be incorporated in the multi-layer peat scheme to simulate more realistic carbon budget and GHG flux estimations.
- Soil moisture above the WTP is essential for moss growth, CH₄ emissions, decomposition and plant productivity (Clymo, 1991). However, currently, the model (this version) uses a simple water bucket scheme and peat layers above the WTP are assumed to be completely unsaturated. The existing hydrology scheme can be further improved to strengthen the current predictive power of the model and associated mechanisms.
- Trees are one of the essential dominant PFTs in many peatlands and their inclusion can further benefit the model simulations in tree-dominated bogs (Lund et al., 2007). However, currently, there are issues in dealing with carbon produced by the trees. Dead litter components such as woody debris and trunks leave a huge mass of carbon affecting the peat layers, distorting the hydrology schemes. Further research is required to deal with this issue.
- Paper IV highlights the importance of including dynamic snow scheme in capturing the topsoil temperature. The model predictions can further be improved by including the multi-layer snow scheme in the cold regions (Ekici et al., 2015).
- Palsa formation and collapse are quite common in subarctic and arctic conditions (Swindles et al., 2015). They influence the peat formation rate and small-scale heterogeneity. The model can further be strengthened if the process related to palsa formation such as ice expansion and compression are added. This will help in capturing the events related to palsa development and collapse. The thawing of ground can lead to soil subsidence (Johansson et al., 2006), a phenomena which is

being noticed in many degraded palsa mires such as Stordalen. Inclusion of soil expansion and compression scheme can help in capturing these processes.

- Wind plays an important role in ecosystem functioning but surprisingly has not been considered in majority of the studies and its inclusion will strengthen the simulations (Malmer et al., 2005). For instance, exposure to wind may contribute to reduce plant productivity, abrasion of palsa site, snowdrift and degradation of hummocks sites. Therefore, considering wind and associated factors may certainly reduce some uncertainty.
- Natural disturbances such as fire play an important role in peatland functioning (van Bellen et al., 2012). Little is known about peatland recovery after fire and how they affect palsa formation as well as how they influence plant demography. Its inclusion (peat combustion) in LPJ-GUESS can help in understanding the role fire played in the past and its consequences on permafrost and vegetation dynamics. Many peatlands are currently under huge pressure due to anthropogenic influence and accounting for them in the modelling framework is challenging but a suitable strategy is needed for its representation.
- Many northern peatlands are currently lacking additional nutrients, especially nitrogen (N) and potassium (K). The role of nutrients in these peatlands need to be evaluated by incorporating them in model nutrient biogeochemistry (Smith et al., 2014). It is necessary to understand how these ecosystems may behave in the future due to nutrient loading. Recently, LPJ-GUESS included plant and soil N dynamics in its framework and the updated model can be synced in with the multi-layer peat scheme to simulate the effects of N on peatland functioning.
- My simple modelling approach showed that the inclusion of different mosses (dominant in their respective niches) can help to understand more detailed processes in peatland functioning such as eco-hydrological feedbacks but the question arises as to whether including additional plants in DGVMs will add any further predictive power to the model. This needs to be tested.
- Many tropical peatlands have different processes and are not known in detail. Their inclusion in LPJ-GUESS can make it more robust and can be used to carry out global simulations to simulate the global carbon accumulation rates and to quantify CH₄ budget (Yu et al., 2010; Kurnianto et al., 2015).
- Crout et al. (2009) showed that a well-established and popular wetland CH₄ model is over-complicated and can achieve the same predictive success in much simpler form. Models are often more complicated than they need to be. Based on this observation, the 2-DMT can further be improved by including dynamic vegetation cover constrained by climate conditions, soil expansion and compression schemes.

The improved model can be used to conduct a comparative study of the parsimonious approach and DGVM models.

- The extensive peat inception database (≈ 1500 basal age points; MacDonald et al., 2006) indicates regional differences in the timing of peat initiation. Other such datasets also exist (Gorham et al., 2007; Korhola et al., 2010) and can be combined. The collated dataset can then be interpolated and utilised for prescribing the model (see Fig. A1 in appendix). This interpolated dataset removes the uncertainty related to different timings of peat initiation as a result of the remnants of ice sheets or some other local factors.
- A knowledge of the underlying topography (below the peat deposit) is required for modelling the peat initiation periods but no such dataset exists. However, the current topography can be utilised for this purpose and can be combined with TOPMODEL approach to identify the timing of peat initiation. The simulated results can be compared with the observed datasets (see Fig. A1).
- Currently, static wetland maps are used to prescribe the model simulation in large areas (Wania et al., 2009a). Using the TOPMODEL approach (Kleinen et al., 2012; Stocker et al., 2014), the dynamic inundated area can be calculated which can further be utilised to delineate the past, present and future peatland distribution; it may also be used to predict the likely peat inception periods.
- In some peatlands, bulk density increases with depth due to compaction (Clymo, 1991) but other studies show no net increase (Tomlinson, 2005; Baird et al., 2016). My results indicate that the bulk density doesn't increase with depth in the subarctic conditions and is quite variable. It is an interesting finding and can be tested at other sites in different climate gradients to understand how it varies down the peat profile.
- The role of natural pipes is important in distributing water, solutes, dissolved gases and sediments (Smart et al., 2013). Very little is known about these natural pipes and its implications on peatland functioning. Further research is required how to include such processes in peatland models.
- The peatland stores huge amount of carbon and is not known how they influence the current rate of warming through biophysical and biogeochemical feedbacks (Frolking et al., 2013). LPJ-GUESS can be coupled with the recent ESMs to account for the potentially important (and hypothesised) role of peatlands in the climate system.

6. Conclusions

The main objectives of this thesis were to improve the current understanding of the peatland processes and mechanisms by implementing a detailed peatland and permafrost dynamics in LPJ-GUESS and to assess the implications of changing climate drivers on these sensitive carbon storehouses across the pan-Arctic. I demonstrated that a novel mechanistic multi-layer peat accumulation and decomposition scheme performed fairly well at site and regional scales and model findings are consistent with a broad range of observations.

The main findings of this thesis are:

- LPJ-GUESS is quite robust and can capture the vegetation, physical and hydrological dynamics essential for simulating peatland dynamics at local and regional scales.
- LPJ-GUESS can predict reasonable long-term carbon accumulation rates and the permafrost distribution across the pan-Arctic. My findings may reduce some of the uncertainties related to future peatland and permafrost distributions.
- The results show that climate change can cause many regions to become a carbon source while other regions may enhance their sink capacity across the pan-Arctic, but overall the pan-Arctic sink capacity will remain largely unchanged (similar to 2000) by the end of the century (2100), even under the high-end scenario (RCP8.5).
- The permafrost distribution will drastically reduce and will be limited to central and eastern parts of Siberia and the north Canadian region by the late 21st century, disappearing from large parts of western Siberia and southern parts of Canada, and with very little presence in Scandinavia.
- The small-scale spatial heterogeneity is an important component in many peatlands and to generalize them in large-scale land surface schemes is challenging.
- LPJ-GUESS has captured reasonably the soil thermal dynamics in distinct cold regions and could be further improved by adding a physical multi-layer snow scheme.

In future, I plan to incorporate CH₄ biogeochemistry and nutrient dynamics and the updated model will be used to assess the implications of projected climate change and atmospheric CO₂ on peatland vegetation and GHG exchange across the pan-Arctic. Another plan is to couple the LPJ-GUESS with the atmospheric component of a regional ESM to examine the role of peatland-mediated biogeochemical and biophysical feedbacks to climate change in the Arctic and globally.

Acknowledgements

I am thankful to Benjamin Smith for his guidance and support since I was a master's student. To have him as my main supervisor during my PhD studies and benefit from his excellent scientific guidance has been one of the best things for me being a PhD student. You always inspire me!

I want to thank Paul A. Miller, my PhD co-supervisor who has also been a great encouragement since my master's days. Thank you Paul for everything. You have been my big support!

I am thankful to DEFROST project for funding my PhD project. A major thanks goes to entire peatland community and modellers for sharing their vast knowledge.

I also want to thanks Joe Siltberg for always taking time to help with technical issues concerning model development.

My heart-felt thanks to all the PhD students. Tomas, Anders A., Bjarki and Fabien I really enjoyed your company. Also thankful to my colleagues at the Department of Physical Geography and Ecosystem Science, Lund University.

Special thanks to Rafael and Ricardo for helping me with technical aspects. I would also like to express my gratitude to Economics and Administration department for helping me out with day to day stuff.

Many thanks to my friends in Lund, Halmstad and other Swedish Cricket Clubs for making my journey enjoyable.

At last but most importantly, I am thankful to my late father for believing in me.

My deepest thanks to my biggest guru, my mother for her unconditional love. I am grateful to my lovely wife for her support and my darling daughter for her refreshing presence in my life. Also, big thanks to my other family members (Rahul, Tina, Sunny and others) and friends for their encouragement.

Some thoughts...

When I was a kid I always used to think what exists beyond my house, my locality...

Then I found there is a vast space outside my imagination...

A lot of people with so many different qualities....

Later, I found I am a part of a community, a state and a country...

Then, I realized I am a part of a global community...

After that, I realized that we are special living beings in a unique planet that only hosts life in this Solar system....

Stars bigger than our Sun also exist came to my knowledge later ...

After that, I realized there are multiple stars, galaxies in the universe...

Beyond that our knowledge is limited...

We don't know what exists beyond that....

What is the shape, size and extent of the universe

That always makes me crazy... because beyond that we don't know what exists ...

Then, one day I felt we may be a part of a simulation operating at different scales (dimensions)...

I find myself a random variable in my own space but may be I am a constant or a parameter depending upon which perspective you look in. ...

And, this randomness can be controlled or directed with right guidance of other stable variables (my supervisors) or random variables (my friends) which we often find in nature

Or all of us are random- helping or destroying each other in this evolution process...

Appendix

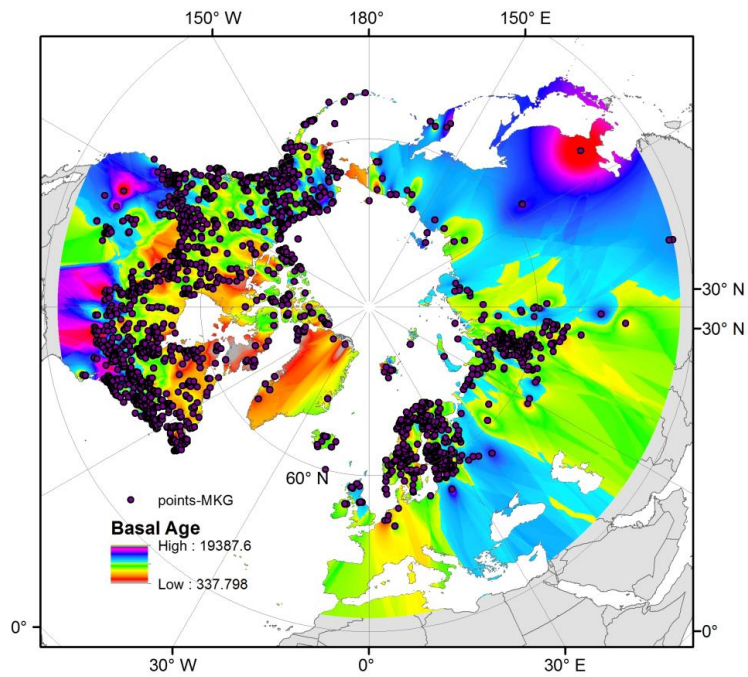


Figure A1 A map developed by interpolating > 2500 observed peat inception points. The dataset is prepared by combining peat inception points of MacDonald et al. (2006), Gorham et al. (2007), Korhola et al. (2010) and other published peat inception observations.

References

- Aerts, R., Verhoeven, J.T.A., Whigham, D.F. (1999) Plant-mediated controls on nutrient cycling in temperate fens and bogs. In *Ecology*: pp 2170-2181.
- Åkerman, H.J. and Johansson, M. (2008) Thawing permafrost and thicker active layers in sub-arctic Sweden. *Permafrost and Periglacial Processes*, **19**(3), 279-292.
- Alexandrov, G.A., Brovkin, V.A., Kleinen, T. (2016) The influence of climate on peatland extent in Western Siberia since the Last Glacial Maximum. *Scientific Reports*, **6**.
- Anderson, R. and Foster, D. (2003) Development and Expansion of Peatlands in Central New England from 14000 BP to Present. Harvard Forest Data Archive: HF074.
- Andersson, S. and Schoning, K. (2010) Surface wetness and mire development during the late Holocene in central Sweden. *Boreas*, **39**(4), 749-760.
- Arnth, A., Harrison, S.P., Zaehle, S., Tsigaridis, K., Menon, S., Bartlein, P.J., Feichter, J., Korhola, A., Kulmala, M., O'Donnell, D., Schurgers, G., Sorvari, S., Vesala, T. (2010) Terrestrial biogeochemical feedbacks in the climate system. *Nature Geoscience*, **3**(8), 525-532.
- Aurela, M., Laurila, T., Tuovinen, J.P. (2004) The timing of snow melt controls the annual CO₂ balance in a subarctic fen. *Geophysical Research Letters*, **31**(16), 4.
- Aurela, M., Riutta, T., Laurila, T., Tuovinen, J.P., Vesala, T., Tuittila, E.S., Rinne, J., Haapanala, S., Laine, J. (2007) CO₂ exchange of a sedge fen in southern Finland - The impact of a drought period. *Tellus Series B-Chemical and Physical Meteorology*, **59**(5), 826-837.
- Baird, A.J., Belyea, L.R., Morris, P.J. (2013a) Upscaling of Peatland-Atmosphere Fluxes of Methane: Small-Scale Heterogeneity in Process Rates and the Pitfalls of "Bucket-and-Slab" Models. In *Carbon Cycling in Northern Peatlands*, American Geophysical Union: pp 37-53.
- Baird, A.J., Comas, X., Slater, L.D., Belyea, L.R., Reeve, A.S. (2013b) Understanding Carbon Cycling in Northern Peatlands: Recent Developments and Future Prospects. In *Carbon Cycling in Northern Peatlands*, American Geophysical Union: pp 1-3.
- Baird, A.J., Milner, A.M., Blundell, A., Swindles, G.T., Morris, P.J. (2016) Microform-scale variations in peatland permeability and their ecohydrological implications. *Journal of Ecology*, **104**(2), 531-544.
- Bathiany, S., Claussen, M., Brovkin, V., Raddatz, T., Gayler, V. (2010) Combined biogeophysical and biogeochemical effects of large-scale forest cover changes in the MPI earth system model. *Biogeosciences*, **7**(5), 1383-1399.

- Bauer, I.E. (2004) Modelling effects of litter quality and environment on peat accumulation over different time-scales. *Journal of Ecology*, **92**(4), 661-674.
- Belyea, L.R. (2013) Nonlinear Dynamics of Peatlands and Potential Feedbacks on the Climate System. In *Carbon Cycling in Northern Peatlands*, American Geophysical Union: pp 5-18.
- Belyea, L.R. and Baird, A.J. (2006) Beyond "The limits to peat bog growth": Cross-scale feedback in peatland development. *Ecological Monographs*, **76**(3), 299-322.
- Belyea, L.R. and Clymo, R.S. (1998) Do hollows control the rate of peat bog growth? In: Standen V, Tallis JH, Meade R (eds) *Patterned mires and mire pools: origin and development; flora and fauna*. British Ecological Society, London, 55-65.
- Belyea, L.R. and Lancaster, J. (2002) Inferring landscape dynamics of bog pools from scaling relationships and spatial patterns. *Journal of Ecology*, **90**(2), 223-234.
- Berger, A. and Loutr, M.F. (2003) Insolation values for the climate of the last 10 million years. *Quaternary Science Reviews*, **10**(4), 297-317.
- Bridgman, S.D., Megonigal, J.P., Keller, J.K., Bliss, N.B., Trettin, C. (2006) The carbon balance of North American wetlands. *Wetlands*, **26**(4), 889-916.
- Charman, D.J., Beilman, D.W., Blaauw, M., Booth, R.K., Brewer, S., Chambers, F.M., Christen, J.A., Gallego-Sala, A., Harrison, S.P., Hughes, P.D.M., Jackson, S.T., Korhola, A., Mauquoy, D., Mitchell, F.J.G., Prentice, I.C., van der Linden, M., De Vleeschouwer, F., Yu, Z.C., Alm, J., Bauer, I.E., Corish, Y.M.C., Garneau, M., Hohl, V., Huang, Y., Karofeld, E., Le Roux, G., Loisel, J., Moschen, R., Nichols, J.E., Nieminen, T.M., MacDonald, G.M., Phadtare, N.R., Rausch, N., Sillasoo, U., Swindles, G.T., Tuittila, E.S., Ukonmaanaho, L., Valiranta, M., van Bellen, S., van Geel, B., Vitt, D.H., Zhao, Y. (2013) Climate-related changes in peatland carbon accumulation during the last millennium. *Biogeosciences*, **10**(2), 929-944.
- Chaudhary, N., Miller, P.A., Smith, B. (2016) Modelling Holocene peatland dynamics with an individual-based dynamic vegetation model. *Biogeosciences* (in review).
- Christensen, T.R., Johansson, T.R., Akerman, H.J., Mastepanov, M., Malmer, N., Friborg, T., Crill, P., Svensson, B.H. (2004) Thawing sub-arctic permafrost: Effects on vegetation and methane emissions. *Geophysical Research Letters*, **31**(4).
- Clymo, R.S. (1984) The limits to peat bog growth. *Philosophical Transactions of the Royal Society of London Series B-Biological Sciences*, **303**(1117), 605-654.
- Clymo, R.S. (1991) Peat growth. *Quaternary Landscapes*. Eds Shane LCK, Cushing EJ. Minneapolis, University of Minnesota Press., 76-112.
- Crout, N.M.J., Tarsitano, D., Wood, A.T. (2009) Is my model too complex? Evaluating model formulation using model reduction. *Environmental Modelling & Software*, **24**(1), 1-7.

- Deng, J., Li, C., Frolking, S., Zhang, Y., Bäckstrand, K., Crill, P. (2014) Assessing effects of permafrost thaw on C fluxes based on multiyear modeling across a permafrost thaw gradient at Stordalen, Sweden. *Biogeosciences*, **11**(17), 4753-4770.
- Dyke, A.S., Giroux, D., Robertson, L. (2004) Paleovegetation Maps, Northern North America, 18000 to 1000 BP. Geol. Surv. Can. Open File 4682, Ottawa, Canada.
- Ekici, A., Chadburn, S., Chaudhary, N., Hajdu, L.H., Marmy, A., Peng, S., Boike, J., Burke, E., Friend, A.D., Hauck, C., Krinner, G., Langer, M., Miller, P.A., Beer, C. (2015) Site-level model intercomparison of high latitude and high altitude soil thermal dynamics in tundra and barren landscapes. *The Cryosphere*, **9**(4), 1343-1361.
- Fan, Z.S., McGuire, A.D., Turetsky, M.R., Harden, J.W., Waddington, J.M., Kane, E.S. (2013) The response of soil organic carbon of a rich fen peatland in interior Alaska to projected climate change. *Global Change Biology*, **19**(2), 604-620.
- Friedlingstein, P., Andrew, R.M., Rogelj, J., Peters, G.P., Canadell, J.G., Knutti, R., Luderer, G., Raupach, M.R., Schaeffer, M., van Vuuren, D.P., Le Quere, C. (2014) Persistent growth of CO₂ emissions and implications for reaching climate targets. *Nature Geosci*, **7**(10), 709-715.
- Friedlingstein, P., Cox, P., Betts, R., Bopp, L., Von Bloh, W., Brovkin, V., Cadule, P., Doney, S., Eby, M., Fung, I., Bala, G., John, J., Jones, C., Joos, F., Kato, T., Kawamiya, M., Knorr, W., Lindsay, K., Matthews, H.D., Raddatz, T., Rayner, P., Reick, C., Roeckner, E., Schnitzler, K.G., Schnur, R., Strassmann, K., Weaver, A.J., Yoshikawa, C., Zeng, N. (2006) Climate-carbon cycle feedback analysis: Results from the (CMIP)-M-4 model intercomparison. *Journal of Climate*, **19**(14), 3337-3353.
- Frolking, S., Roulet, N., Lawrence, D. (2013) Issues Related to Incorporating Northern Peatlands into Global Climate Models. In *Carbon Cycling in Northern Peatlands*, American Geophysical Union: pp 19-35.
- Frolking, S. and Roulet, N.T. (2007) Holocene radiative forcing impact of northern peatland carbon accumulation and methane emissions. *Global Change Biology*, **13**(5), 1079-1088.
- Frolking, S., Roulet, N.T., Moore, T.R., Richard, P.J.H., Lavoie, M., Muller, S.D. (2001) Modeling northern peatland decomposition and peat accumulation. *Ecosystems*, **4**(5), 479-498.
- Frolking, S., Roulet, N.T., Tuittila, E., Bubier, J.L., Quillet, A., Talbot, J., Richard, P.J.H. (2010) A new model of Holocene peatland net primary production, decomposition, water balance, and peat accumulation. Article Thesis.
- Gerten, D., Schaphoff, S., Haberlandt, U., Lucht, W., Sitch, S. (2004) Terrestrial vegetation and water balance - hydrological evaluation of a dynamic global vegetation model. *Journal of Hydrology*, **286**(1-4), 249-270.

- Gorham, E. (1991) Northern peatlands - role in the carbon-cycle and probable responses to climatic warming. *Ecological Applications*, **1**(2), 182-195.
- Gorham, E., Lehman, C., Dyke, A., Janssens, J., Dyke, L. (2007) Temporal and spatial aspects of peatland initiation following deglaciation in North America. *Quaternary Science Reviews*, **26**(3-4), 300-311.
- Harris, C., Arenson, L.U., Christiansen, H.H., Etzemuller, B., Frauenfelder, R., Gruber, S., Haeberli, W., Hauck, C., Holzle, M., Humlum, O., Isaksen, K., Kaab, A., Kern-Lutschg, M.A., Lehning, M., Matsuoka, N., Murton, J.B., Nozli, J., Phillips, M., Ross, N., Seppala, M., Springman, S.M., Muhll, D.V. (2009) Permafrost and climate in Europe: Monitoring and modelling thermal, geomorphological and geotechnical responses. *Earth-Science Reviews*, **92**(3-4), 117-171.
- Heinemeyer, A., Croft, S., Garnett, M.H., Gloor, E., Holden, J., Lomas, M.R., Ineson, P. (2010) The MILLENNIA peat cohort model: predicting past, present and future soil carbon budgets and fluxes under changing climates in peatlands. *Climate Research*, **45**(1), 207-226.
- Hilbert, D.W., Roulet, N., Moore, T. (2000) Modelling and analysis of peatlands as dynamical systems. *Journal of Ecology*, **88**(2), 230-242.
- Hinzman, L.D., Bettez, N.D., Bolton, W.R., Chapin, F.S., Dyrugerov, M.B., Fastie, C.L., Griffith, B., Hollister, R.D., Hope, A., Huntington, H.P., Jensen, A.M., Jia, G.J., Jorgenson, T., Kane, D.L., Klein, D.R., Kofinas, G., Lynch, A.H., Lloyd, A.H., McGuire, A.D., Nelson, F.E., Oechel, W.C., Osterkamp, T.E., Racine, C.H., Romanovsky, V.E., Stone, R.S., Stow, D.A., Sturm, M., Tweedie, C.E., Vourlitis, G.L., Walker, M.D., Walker, D.A., Webber, P.J., Welker, J.M., Winker, K., Yoshikawa, K. (2005) Evidence and implications of recent climate change in northern Alaska and other arctic regions. *Climatic Change*, **72**(3), 251-298.
- Ingram, H.A.P. (1982) Size and shape in raised mire ecosystems - a geophysical model. *Nature*, **297**(5864), 300-303.
- IPCC. (2007): *Climate Change 2007: The Physical Science Basis*. Contribution of Working Group I to the Fourth Assessment Report of the Intergovernmental Panel on Climate Change [Solomon, S., D. Qin, M. Manning, Z. Chen, M. Marquis, K.B. Averyt, M. Tignor and H.L. Miller (eds.)]. Cambridge University Press, Cambridge, United Kingdom and New York, NY, USA.
- IPCC. (2013) *Climate Change 2013: The Physical Science Basis*. Contribution of Working Group I to the Fifth Assessment Report of the Intergovernmental Panel on Climate Change (eds Stocker TF, Qin D, Plattner G-K, Tignor M, Allen SK, Boschung J, Nauels A, Xia Y, Bex V, Midgley PM), NY, USA.
- Ise, T., Dunn, A.L., Wofsy, S.C., Moorcroft, P.R. (2008) High sensitivity of peat decomposition to climate change through water-table feedback. *Nature Geoscience*, **1**(11), 763-766.

- Johansson, M., Callaghan, T.V., Bosio, J., Akerman, H.J., Jackowicz-Korczynski, M., Christensen, T.R. (2013) Rapid responses of permafrost and vegetation to experimentally increased snow cover in sub-arctic Sweden. *Environmental Research Letters*, **8**(3).
- Johansson, T., Malmer, N., Crill, P.M., Friborg, T., Akerman, J.H., Mastepanov, M., Christensen, T.R. (2006) Decadal vegetation changes in a northern peatland, greenhouse gas fluxes and net radiative forcing. *Global Change Biology*, **12**(12), 2352-2369.
- Klein, E.S., Yu, Z., Booth, R.K. (2013) Recent increase in peatland carbon accumulation in a thermokarst lake basin in southwestern Alaska. In *Palaeogeography Palaeoclimatology Palaeoecology*: pp 186-195.
- Kleinen, T., Brovkin, V., Schuldt, R.J. (2012) A dynamic model of wetland extent and peat accumulation: results for the Holocene. *Biogeosciences*, **9**(1), 235-248.
- Kokfelt, U., Reuss, N., Struyf, E., Sonesson, M., Rundgren, M., Skog, G., Rosen, P., Hammarlund, D. (2010) Wetland development, permafrost history and nutrient cycling inferred from late Holocene peat and lake sediment records in subarctic Sweden. *Journal of Paleolimnology*, **44**(1), 327-342.
- Korhola, A., Ruppel, M., Seppa, H., Valiranta, M., Virtanen, T., Weckstrom, J. (2010) The importance of northern peatland expansion to the late-Holocene rise of atmospheric methane. *Quaternary Science Reviews*, **29**(5-6), 611-617.
- Kuhry, P. and Turunen, J. (2006) The Postglacial Development of Boreal and Subarctic Peatlands. In *Boreal Peatland Ecosystems* (R.K. Wieder & D.H. Vitt, eds), Springer Berlin Heidelberg, Berlin, Heidelberg: pp 25-46.
- Kurnianto, S., Warren, M., Talbot, J., Kauffman, B., Murdiyarto, D., Frohling, S. (2015) Carbon accumulation of tropical peatlands over millennia: a modeling approach. *Global Change Biology*, **21**(1), 431-444.
- Lai, D.Y.F. (2009) Methane Dynamics in Northern Peatlands: A Review. *Pedosphere*, **19**(4), 409-421.
- Le Quéré, C., Andrew, R.M., Canadell, J.G., Sitch, S., Korsbakken, J.I., Peters, G.P., Manning, A.C., Boden, T.A., Tans, P.P., Houghton, R.A., Keeling, R.F., Alin, S., Andrews, O.D., Anthoni, P., Barbero, L., Bopp, L., Chevallier, F., Chini, L.P., Ciais, P., Currie, K., Delire, C., Doney, S.C., Friedlingstein, P., Gkritzalis, T., Harris, I., Hauck, J., Haverd, V., Hoppema, M., Klein Goldewijk, K., Jain, A.K., Kato, E., Körtzinger, A., Landschützer, P., Lefèvre, N., Lenton, A., Lienert, S., Lombardozzi, D., Melton, J.R., Metzl, N., Millero, F., Monteiro, P.M.S., Munro, D.R., Nabel, J.E.M.S., Nakaoka, S.I., O'Brien, K., Olsen, A., Omar, A.M., Ono, T., Pierrot, D., Poulter, B., Rödenbeck, C., Salisbury, J., Schuster, U., Schwinger, J., Séférian, R., Skjelvan, I., Stocker, B.D., Sutton, A.J., Takahashi, T., Tian, H., Tilbrook, B., van der Laan-Luijkx, I.T., van der Werf, G.R., Viovy, N., Walker, A.P., Wiltshire, A.J., Zaehle, S. (2016) Global Carbon Budget 2016. *Earth Syst. Sci. Data*, **8**(2), 605-649.

- Loisel, J. and Yu, Z.C. (2013) Recent acceleration of carbon accumulation in a boreal peatland, south central Alaska. *Journal of Geophysical Research-Biogeosciences*, **118**(1), 41-53.
- Loisel, J., Yu, Z.C., Beilman, D.W., Camill, P., Alm, J., Amesbury, M.J., Anderson, D., Andersson, S., Bochicchio, C., Barber, K., Belyea, L.R., Bunbury, J., Chambers, F.M., Charman, D.J., De Vleeschouwer, F., Fialkiewicz-Koziel, B., Finkelstein, S.A., Galka, M., Garneau, M., Hammarlund, D., Hinchcliffe, W., Holmquist, J., Hughes, P., Jones, M.C., Klein, E.S., Kokfelt, U., Korhola, A., Kuhry, P., Lamarre, A., Lamentowicz, M., Large, D., Lavoie, M., MacDonald, G., Magnan, G., Makila, M., Mallon, G., Mathijssen, P., Mauquoy, D., McCarroll, J., Moore, T.R., Nichols, J., O'Reilly, B., Oksanen, P., Packalen, M., Peteet, D., Richard, P.J.H., Robinson, S., Ronkainen, T., Rundgren, M., Sannel, A.B.K., Tarnocai, C., Thom, T., Tuittila, E.S., Turetsky, M., Valiranta, M., van der Linden, M., van Geel, B., van Bellen, S., Vitt, D., Zhao, Y., Zhou, W.J. (2014) A database and synthesis of northern peatland soil properties and Holocene carbon and nitrogen accumulation. *Holocene*, **24**(9), 1028-1042.
- Loranty, M.M. and Goetz, S.J. (2012) Shrub expansion and climate feedbacks in Arctic tundra. *Environmental Research Letters*, **7**(1), 3.
- Lund, M., Christensen, T.R., Lindroth, A., Schubert, P. (2012) Effects of drought conditions on the carbon dioxide dynamics in a temperate peatland. *Environmental Research Letters*, **7**(4).
- Lund, M., Lafleur, P.M., Roulet, N.T., Lindroth, A., Christensen, T.R., Aurela, M., Chojnicki, B.H., Flanagan, L.B., Humphreys, E.R., Laurila, T., Oechel, W.C., Olejnik, J., Rinne, J., Schubert, P., Nilsson, M.B. (2010) Variability in exchange of CO₂ across 12 northern peatland and tundra sites. *Global Change Biology*, **16**(9), 2436-2448.
- Lund, M., Lindroth, A., Christensen, T.R., Strom, L. (2007) Annual CO₂ balance of a temperate bog. *Tellus Series B-Chemical and Physical Meteorology*, **59**(5), 804-811.
- MacDonald, G.M., Beilman, D.W., Kremenetski, K.V., Sheng, Y., Smith, L.C., Velichko, A.A. (2006) Rapid early development of circumarctic peatlands and atmospheric CH₄ and CO₂ variations. *Science*, **314**(5797), 285-288.
- Makila, M., Saarnisto, M., Kankainen, T. (2001) Aapa mires as a carbon sink and source during the Holocene. *Journal of Ecology*, **89**(4), 589-599.
- Malmer, N., Johansson, T., Olsrud, M., Christensen, T.R. (2005) Vegetation, climatic changes and net carbon sequestration in a North-Scandinavian subarctic mire over 30 years. *Global Change Biology*, **11**(11), 1895-1909.
- McGuire, A.D., Christensen, T.R., Hayes, D., Heroult, A., Euskirchen, E., Kimball, J.S., Koven, C., Lafleur, P., Miller, P.A., Oechel, W., Peylin, P., Williams, M., Yi, Y. (2012) An assessment of the carbon balance of Arctic tundra: comparisons among observations, process models, and atmospheric inversions. *Biogeosciences*, **9**(8), 3185-3204.

- Miller, P.A. and Smith, B. (2012) Modelling Tundra Vegetation Response to Recent Arctic Warming. *Ambio*, **41**, 281-291.
- Mitchell, T.D. and Jones, P.D. (2005) An improved method of constructing a database of monthly climate observations and associated high-resolution grids. *International Journal of Climatology*, **25**(6), 693-712.
- Morris, P.J., Baird, A.J., Belyea, L.R. (2012) The DigiBog peatland development model 2: ecohydrological simulations in 2D. *Ecohydrology*, **5**(3), 256-268.
- Moss, R.H., Edmonds, J.A., Hibbard, K.A., Manning, M.R., Rose, S.K., van Vuuren, D.P., Carter, T.R., Emori, S., Kainuma, M., Kram, T., Meehl, G.A., Mitchell, J.F.B., Nakicenovic, N., Riahi, K., Smith, S.J., Stouffer, R.J., Thomson, A.M., Weyant, J.P., Wilbanks, T.J. (2010) The next generation of scenarios for climate change research and assessment. *Nature*, **463**(7282), 747-756.
- Nicolson, D.J., Romanovsky, V.E., Alexeev, V.A., Lawrence, D.M. (2007) Improved modeling of permafrost dynamics in a GCM land-surface scheme. *Geophysical Research Letters*, **34**(8).
- Nilsson, M., Sagerfors, J., Buffam, I., Laudon, H., Eriksson, T., Grelle, A., Klemedtsson, L., Weslien, P., Lindroth, A. (2008) Contemporary carbon accumulation in a boreal oligotrophic minerogenic mire - a significant sink after accounting for all C-fluxes. *Global Change Biology*, **14**(10), 2317-2332.
- Peters, G.P., Andrew, R.M., Boden, T., Canadell, J.G., Ciais, P., Le Quere, C., Marland, G., Raupach, M.R., Wilson, C. (2013) COMMENTARY: The challenge to keep global warming below 2 degrees C. *Nature Climate Change*, **3**(1), 4-6.
- Piao, S., Sitch, S., Ciais, P., Friedlingstein, P., Peylin, P., Wang, X., Ahlstrom, A., Anav, A., Canadell, J.G., Cong, N., Huntingford, C., Jung, M., Levis, S., Levy, P.E., Li, J., Lin, X., Lomas, M.R., Lu, M., Luo, Y., Ma, Y., Myneni, R.B., Poulter, B., Sun, Z., Wang, T., Viivy, N., Zaehle, S., Zeng, N. (2013) Evaluation of terrestrial carbon cycle models for their response to climate variability and to CO₂ trends. *Global Change Biology*, **19**(7), 2117-2132.
- Riseborough, D., Shiklomanov, N., Etzelmuller, B., Gruber, S., Marchenko, S. (2008) Recent advances in permafrost modelling. *Permafrost and Periglacial Processes*, **19**(2), 137-156.
- Robinson, S.D. and Moore, T.R. (2000) The influence of permafrost and fire upon carbon accumulation in high boreal peatlands, Northwest Territories, Canada. *Arctic Antarctic and Alpine Research*, **32**(2), 155-166.
- Roulet, N.T., Lafleur, P.M., Richard, P.J.H., Moore, T.R., Humphreys, E.R., Bubier, J. (2007) Contemporary carbon balance and late Holocene carbon accumulation in a northern peatland. *Global Change Biology*, **13**(2), 397-411.
- Ryden, B.E., Fors, L., Kostov, L. (1980) Physical Properties of the Tundra Soil-Water System at Stordalen, Abisko. *Ecological Bulletins*(30), 27-54.

- Sagerfors, J., Lindroth, A., Grelle, A., Klemedtsson, L., Weslien, P., Nilsson, M. (2008) Annual CO₂ exchange between a nutrient-poor, minerotrophic, boreal mire and the atmosphere. *Journal of Geophysical Research-Biogeosciences*, **113**(G1), 15.
- Schuldt, R.J., Brovkin, V., Kleinen, T., Winderlich, J. (2013) Modelling Holocene carbon accumulation and methane emissions of boreal wetlands - an Earth system model approach. *Biogeosciences*, **10**(3), 1659-1674.
- Sitch, S., Huntingford, C., Gedney, N., Levy, P.E., Lomas, M., Piao, S.L., Betts, R., Ciais, P., Cox, P., Friedlingstein, P., Jones, C.D., Prentice, I.C., Woodward, F.I. (2008) Evaluation of the terrestrial carbon cycle, future plant geography and climate-carbon cycle feedbacks using five Dynamic Global Vegetation Models (DGVMs). *Global Change Biology*, **14**(9), 2015-2039.
- Sitch, S., Smith, B., Prentice, I.C., Arneth, A., Bondeau, A., Cramer, W., Kaplan, J.O., Levis, S., Lucht, W., Sykes, M.T., Thonicke, K., Venevsky, S. (2003) Evaluation of ecosystem dynamics, plant geography and terrestrial carbon cycling in the LPJ dynamic global vegetation model. *Global Change Biology*, **9**(2), 161-185.
- Smart, R.P., Holden, J., Dinsmore, K.J., Baird, A.J., Billett, M.F., Chapman, P.J., Grayson, R. (2013) The dynamics of natural pipe hydrological behaviour in blanket peat. *Hydrological Processes*, **27**(11), 1523-1534.
- Smith, B., Prentice, I.C., Sykes, M.T. (2001) Representation of vegetation dynamics in the modelling of terrestrial ecosystems: comparing two contrasting approaches within European climate space. *Global Ecology and Biogeography*, **10**(6), 621-637.
- Smith, B., Warlind, D., Arneth, A., Hickler, T., Leadley, P., Siltberg, J., Zaehle, S. (2014) Implications of incorporating N cycling and N limitations on primary production in an individual-based dynamic vegetation model. *Biogeosciences*, **11**(7), 2027-2054.
- Stocker, B.D., Spahni, R., Joos, F. (2014) DYPTOP: a cost-efficient TOPMODEL implementation to simulate sub-grid spatio-temporal dynamics of global wetlands and peatlands. *Geoscientific Model Development*, **7**(6), 3089-3110.
- Strandberg, G., Kjellstrom, E., Poska, A., Wagner, S., Gaillard, M.J., Trondman, A.K., Mauri, A., Davis, B.A.S., Kaplan, J.O., Birks, H.J.B., Bjune, A.E., Fyfe, R., Giesecke, T., Kalnina, L., Kangur, M., van der Knaap, W.O., Kokfelt, U., Kunes, P., Latalowa, M., Marquer, L., Mazier, F., Nielsen, A.B., Smith, B., Seppa, H., Sugita, S. (2014) Regional climate model simulations for Europe at 6 and 0.2 k BP: sensitivity to changes in anthropogenic deforestation. *Climate of the Past*, **10**(2), 661-680.
- Sturm, M., Schimel, J., Michaelson, G., Welker, J.M., Oberbauer, S.F., Liston, G.E., Fahnestock, J., Romanovsky, V.E. (2005) Winter biological processes could help convert arctic tundra to shrubland. *Bioscience*, **55**(1), 17-26.

- Swindles, G.T., Morris, P.J., Mullan, D., Watson, E.J., Turner, T.E., Roland, T.P., Amesbury, M.J., Kokfelt, U., Schoning, K., Pratte, S., Gallego-Sala, A., Charman, D.J., Sanderson, N., Garneau, M., Carrivick, J.L., Woulds, C., Holden, J., Parry, L., Galloway, J.M. (2015) The long-term fate of permafrost peatlands under rapid climate warming. *Scientific Reports*, **5**, 6.
- Tang, J., Miller, P.A., Crill, P.M., Olin, S., Pilesjo, P. (2015a) Investigating the influence of two different flow routing algorithms on soil-water-vegetation interactions using the dynamic ecosystem model LPJ-GUESS. *Ecohydrology*, **8**(4), 570-583.
- Tang, J., Miller, P.A., Persson, A., Olefeldt, D., Pilesjo, P., Heliasz, M., Jackowicz-Korczynski, M., Yang, Z., Smith, B., Callaghan, T.V., Christensen, T.R. (2015b) Carbon budget estimation of a subarctic catchment using a dynamic ecosystem model at high spatial resolution. *Biogeosciences*, **12**(9), 2791-2808.
- Tarnocai, C., Canadell, J.G., Schuur, E.A.G., Kuhry, P., Mazhitova, G., Zimov, S. (2009) Soil organic carbon pools in the northern circumpolar permafrost region. *GLOBAL BIOGEOCHEMICAL CYCLES*, **23**.
- Thormann, M.N. and Bayley, S.E. (1997) Decomposition along a moderate-rich fen-marsh peatland gradient in boreal Alberta, Canada. *Wetlands*, **17**(1), 123-137.
- Tomlinson, R.W. (2005) Soil carbon stocks and changes in the Republic of Ireland. *Journal of Environmental Management*, **76**(1), 77-93.
- Tuittila, E.S., Valiranta, M., Laine, J., Korhola, A. (2007) Quantifying patterns and controls of mire vegetation succession in a southern boreal bog in Finland using partial ordinations. *Journal of Vegetation Science*, **18**(6), 891-902.
- Turunen, J., Tahvanainen, T., Tolonen, K., Pitkanen, A. (2001) Carbon accumulation in West Siberian mires, Russia. *GLOBAL BIOGEOCHEMICAL CYCLES*, **15**(2), 285-296.
- Turunen, J., Tomppo, E., Tolonen, K., Reinikainen, A. (2002) Estimating carbon accumulation rates of undrained mires in Finland - application to boreal and subarctic regions. *Holocene*, **12**(1), 69-80.
- Valiranta, M., Korhola, A., Seppa, H., Tuittila, E.S., Sarmaja-Korjonen, K., Laine, J., Alm, J. (2007) High-resolution reconstruction of wetness dynamics in a southern boreal raised bog, Finland, during the late Holocene: a quantitative approach. *Holocene*, **17**(8), 1093-1107.
- van Bellen, S., Garneau, M., Ali, A.A., Bergeron, Y. (2012) Did fires drive Holocene carbon sequestration in boreal ombrotrophic peatlands of eastern Canada? *Quaternary Research*, **78**(1), 50-59.
- Vardy, S.R., Warner, B.G., Turunen, J., Aravena, R. (2000) Carbon accumulation in permafrost peatlands in the Northwest Territories and Nunavut, Canada. *Holocene*, **10**(2), 273-280.

- Wang, M., Moore, T.R., Talbot, J., Richard, P.J.H. (2014) The cascade of C:N:P stoichiometry in an ombrotrophic peatland: from plants to peat. *Environmental Research Letters*, **9**(2).
- Wania, R., Ross, I., Prentice, I.C. (2009a) Integrating peatlands and permafrost into a dynamic global vegetation model: 1. Evaluation and sensitivity of physical land surface processes. *GLOBAL BIOGEOCHEMICAL CYCLES*, **23**.
- Wania, R., Ross, I., Prentice, I.C. (2009b) Integrating peatlands and permafrost into a dynamic global vegetation model: 2. Evaluation and sensitivity of vegetation and carbon cycle processes. *GLOBAL BIOGEOCHEMICAL CYCLES*, **23**.
- Weltzin, J.F., Harth, C., Bridgham, S.D., Pastor, J., Vonderharr, M. (2001) Production and microtopography of bog bryophytes: response to warming and water-table manipulations. *Oecologia*, **128**(4), 557-565.
- Whiting, G.J. and Chanton, J.P. (1993) Primary production control of methane emission from wetlands. *Nature*, **364**(6440), 794-795.
- Wieder, R.K. (2001) Past, present, and future peatland carbon balance: An empirical model based on Pb-210-dated cores. *Ecological Applications*, **11**(2), 327-342.
- Wolfe, B.B., Edwards, T.W.D., Aravena, R., Forman, S.L., Warner, B.G., Velichko, A.A., MacDonald, G.M. (2000) Holocene paleohydrology and paleoclimate at treeline, north-central Russia, inferred from oxygen isotope records in lake sediment cellulose. *Quaternary Research*, **53**(3), 319-329.
- Wu, J.H., Roulet, N.T., Moore, T.R., Lafleur, P., Humphreys, E. (2011) Dealing with microtopography of an ombrotrophic bog for simulating ecosystem-level CO₂ exchanges. *Ecological Modelling*, **222**(4), 1038-1047.
- Wu, Y.Q., Verseghy, D.L., Melton, J.R. (2016) Integrating peatlands into the coupled Canadian Land Surface Scheme (CLASS) v3.6 and the Canadian Terrestrial Ecosystem Model (CTEM) v2.0. *Geoscientific Model Development*, **9**(8), 2639-2663.
- Yang, Z., Sykes, M.T., Hanna, E., Callaghan, T.V. (2012) Linking Fine-Scale Sub-Arctic Vegetation Distribution in Complex Topography with Surface-Air-Temperature Modelled at 50-m Resolution. *Ambio*, **41**, 292-302.
- Yu, Z.C. (2006) Holocene carbon accumulation of fen peatlands in boreal western Canada: A complex ecosystem response to climate variation and disturbance. *Ecosystems*, **9**(8), 1278-1288.
- Yu, Z.C. (2012) Northern peatland carbon stocks and dynamics: a review. *Biogeosciences*, **9**(10), 4071-4085.
- Yu, Z.C., Beilman, D.W., Jones, M.C. (2009) Sensitivity of Northern Peatland Carbon Dynamics to Holocene Climate Change. In *Carbon Cycling in Northern Peatlands* (A.J. Baird, L.R. Belyea, X. Comas, A.S. Reeve & L.D. Slater, eds): pp 55-69.

- Yu, Z.C., Loisel, J., Brosseau, D.P., Beilman, D.W., Hunt, S.J. (2010) Global peatland dynamics since the Last Glacial Maximum. *Geophysical Research Letters*, **37**, 5.
- Zhang, W., Jansson, C., Miller, P.A., Smith, B., Samuelsson, P. (2014) Biogeophysical feedbacks enhance the Arctic terrestrial carbon sink in regional Earth system dynamics. *Biogeosciences*, **11**(19), 5503-5519.

Paper I

Modelling Holocene peatland dynamics with an individual-based dynamic vegetation model

Nitin Chaudhary, Paul A. Miller and Benjamin Smith
5 Department of Physical Geography and Ecosystem Science, Lund University,
Sölvegatan 12, SE- 22362 Lund, Sweden

Correspondence to: N. Chaudhary (nitin.chj@gmail.com)

10 **Abstract.** Dynamic global vegetation models (DGVMs) are designed for the study of past, present and future vegetation patterns together with associated biogeochemical cycles and climate feedbacks. However, most DGVMs do not yet have detailed representations of permafrost and non-permafrost peatlands, which are an important store of carbon particularly at high latitudes. We demonstrate a new implementation of peatland dynamics in a customised “Arctic” version of the LPJ-GUESS DGVM, simulating the long-term evolution of selected northern peatland ecosystems and assessing the effect of
15 changing climate on peatland carbon balance. Our approach employs a dynamic multi-layer soil with representation of freeze-thaw processes and litter inputs from a dynamically-varying mixture of the main peatland plant functional types: mosses, shrubs and graminoids. The model was calibrated and tested for a sub-arctic mire in Stordalen, Sweden, and validated at a temperate bog site in Mer Bleue, Canada. A regional evaluation of simulated carbon fluxes, hydrology and vegetation dynamics encompassed additional locations spread across Scandinavia. Simulated peat accumulation was found
20 to be generally consistent with published data and the model was able to capture reported long-term vegetation dynamics, water table position and carbon fluxes. A series of sensitivity experiments were carried out to investigate the vulnerability of high latitude peatlands to climate change. We found that the Stordalen mire may be expected to sequester more carbon in the first half of the 21st century due to milder and wetter climate conditions, a longer growing season, and the CO₂ fertilization effect, turning into a carbon source after mid-century because of higher decomposition rates in response to warming soils.

25 1 Introduction

Peatlands are a conspicuous feature of northern latitude landscapes (Yu et al., 2010), of key importance for regional and global carbon balance and potential responses to global climate change. In the past 10,000 years (10 kyr) they have sequestered 550 ±100 PgC across an area of approximately 3.5 million km² (Gorham, 1991; Turunen et al., 2002; Yu, 2012). Peatlands are one of the major natural sources of methane, contributing significantly to the greenhouse effect (Whiting and
30 Chanton, 1993; Lai, 2009; IPCC, 2013). Around 19% (3556 × 103 km²) of the soil area of the northern peatlands coincides with low altitude permafrost (Tarnocai et al., 2009; Wania et al., 2009a). Permafrost changes the peat accumulation process by altering plant productivity and decomposition, affecting the carbon sequestration rate (Robinson and Moore, 2000). Thawing of permafrost exposes the organic carbon stored in the frozen soil which then becomes available for decomposition by soil microbes (Zimov et al., 2006).

35 Dynamic global vegetation models (DGVMs) are used to study past, present and future vegetation patterns from regional to
global scales, together with associated biogeochemical cycles and climate feedbacks, in particular through the carbon cycle
(Cramer et al., 2001; Friedlingstein et al., 2006; Sitch et al., 2008; Strandberg et al., 2014; Zhang et al., 2014). Only a few
DGVMs include representations of the unique vegetation, biophysical and biogeochemical characteristics of peatland
ecosystems (Wania et al., 2009a, b; Kleinen et al., 2012; Stocker et al., 2014; Tang et al., 2015a). Model formulations of
40 multiple peat layer accumulation and decay have been proposed and demonstrated at the site scale (Bauer et al., 2004;
Frolking et al., 2010; Heinemeyer et al., 2010) but have not yet, to our knowledge, been implemented within the framework
of a DGVM. However, peatland processes are included in some other types of model frameworks (Morris et al., 2012;
Alexandrov et al., 2016; Wu et al., 2016) and been shown to perform reasonably for peatland sites. Large area simulations of
regional peatland dynamics have been performed by (Kleinen et al., 2012; Schuldt et al., 2013; Stocker et al., 2014;
45 Alexandrov et al., 2016) (see Table S1).

Climate warming is amplified in northern latitudes, relative to the global mean trend, due to associated carbon-climate
feedbacks (IPCC, 2013). Current climate models predict that the northern high latitudes, where most of the peatlands and
permafrost areas are present, could experience warming of more than 5°C by 2100 (Hinzman et al., 2005; Christensen et al.,
2007; IPCC, 2013). A warming climate may alleviate the constraints on biological activity imposed by very low
50 temperatures, leading to higher productivity and decomposition rates. The resultant shift in the balance between plant
production and decomposition will alter the carbon balance, potentially leading to enhanced carbon sequestration in some
peatlands (Yu, 2012; Charman et al., 2013) while inducing a carbon (CO₂ and CH₄) source in others (Wieder, 2001; Ise et
al., 2008; Fan et al., 2013). Permafrost peatlands may respond quite differently to non-permafrost peatlands in changing
climate conditions. Increases in soil temperature may accelerate permafrost decay (Åkerman and Johansson, 2008) and
55 thereby modify the moisture balance of the peat soil, which could in turn alter the above ground vegetation composition and
carbon balance of the permafrost peatlands (Christensen et al., 2004; Johansson et al., 2006).

We demonstrate a new implementation of peatland dynamics in the LPJ-GUESS DGVM, aiming to emulate the long-term
dynamics of northern peatland ecosystems and to assess the effect of changing climate on peatland carbon balance at the
regional scale and across climatic gradients. To our knowledge, our new model implementation is unique in combining a
60 dynamic representation of vegetation composition and function, suitable for application at global to regional scale, with an
explicit representation of permafrost and peat accumulation dynamics. We build on previous work by implementing a
dynamic multi-layer approach (Bauer et al., 2004; Frolking et al., 2010; Heinemeyer et al., 2010) to peat formation and
composition with existing representations of soil freezing-thawing functionality, plant physiology and peatland vegetation
dynamics (Wania et al., 2009a) in a customised “Arctic” version of LPJ-GUESS (Miller and Smith, 2012). Uniquely among
65 existing large-scale (regional-global) models, we thus account for feedbacks associated with hydrology, peat properties and
vegetation dynamics, providing a basis for understanding how these feedbacks affect peat growth on the relevant centennial-

millennial time-scales and in different climatic situations. We evaluate the model at a range of observational study sites across the northern high latitudes, and perform a model sensitivity analysis to explore the potential fate of peatland carbon in response to variations in temperature, atmospheric CO₂ and precipitation change in line with 21st century projections from climate models.

2 Model Overview

2.1 Ecosystem modelling platform

We employed a customised Arctic version of the Lund-Potsdam-Jena General Ecosystem Simulator (LPJ-GUESS; Smith et al., 2001; Miller and Smith, 2012) as the ecosystem modelling platform for our study. LPJ-GUESS is a process-based model that couples an individual-based vegetation dynamics scheme to biogeochemistry of terrestrial vegetation and soils (Smith et al., 2001). Vegetation structure and dynamics follow an individual- and patch-based representation in which plant population demography and community structure evolve as an emergent outcome of competition for light, space and soil water among simulated plant individuals, each belonging to one of a defined set of plant functional types (PFTs) with different functional and morphological characteristics (see below).

In this paper, we employ a customised Arctic implementation of LPJ-GUESS that incorporates differentiated representations of hydrological, biophysical and biogeochemical processes characteristic of upland and peatland ecosystems of the tundra and taiga biomes, as well as plant functional types (PFTs) specific to Arctic ecosystems (Fig. 1) (McGuire et al., 2012; Miller and Smith, 2012). Five PFTs characteristic of peatlands – mosses (M), graminoids (Gr), low summergreen and evergreen shrubs (LSS and LSE) and high summergreen shrubs (HSS) – are included in the present study. These PFTs have different parameterizations of physiological processes, for instance relating to photosynthesis, leaf thickness, carbon allocation, phenology, and rooting depth. Full parameters sets for these PFTs are given in Miller and Smith (2012).

New functionality was incorporated in LPJ-GUESS in this study in order to represent the dynamics of peat formation and aggradation based on vegetation litter inputs and decomposition processes. To this end, we adapted the dynamic multi-layer approach used in Bauer et al., 2004, Heinemeyer et al., 2010 and Frolking et al., 2010 generalised for regional application.

The new implementation is detailed in sections 2.1.1-2.1.7 below.

A one-dimensional soil column is represented for each patch (defined below), divided vertically into four distinct layers: a snow layer of variable thickness, one dynamic litter/peat layer of variable thickness corresponding to each simulation year (e.g. 4739 + 100 layers by the end of the simulations, described in Section 2.4 below, for Stordalen), a mineral soil column with a fixed depth of 2 m consisting of two sublayers: an upper mineral soil sublayer (0.5 m) and a lower mineral soil sublayer (1.5 m), and finally a “padding” column of 48 m depth (with 10 sublayers) allowing the simulation of accurate soil thermal dynamics (Wania et al., 2009a). The insulation effects of snow, phase changes in soil water, precipitation and snowmelt input and air temperature forcing are important determinants of daily soil temperature dynamics at different

depths.

2.1.1 Litterfall

100 Peat accumulation is determined by the annual addition of new layers of litter at the top of the soil column. Litter is characterized as fresh, undecomposed plant material composed of dead plant debris such as wood, leaves and fine roots. PFTs accumulate carbon in the litter pool at different rates according to their productivity, mortality and leaf turnover properties. Litter is assumed to decompose at a rate dependent on the PFT and tissue type it originates from (Table 1). Graminoid litter is assumed to decompose faster than that of shrubs and mosses. Woody litter mass from shrubs decomposes
105 relatively slowly because it is made up of hard cellulose and lignin (Aerts et al., 1999; Moore et al., 2007). Moss litter decomposes slowest due to its recalcitrant properties (Clymo et al., 1991; Aerts et al., 1999; Moore et al., 2007). Fresh litter debris decomposes on the surface through exposure to surface temperature and moisture conditions until the last day of the year. The decomposed litter carbon is assumed to be released as respiration directly to the atmosphere while any remaining litter mass is treated as a new individual peat layer from the first day of the following year, which then underlies the newly
110 accumulating litter mass. This layer can be composed of up to 17 carbon components (g C m^{-2}), namely leaf, root, stem and seeds from shrubs, mosses and graminoids (see Table 1) and the model keeps a track of these layer components as they decompose through time.

2.1.2 Peat accumulation and decomposition

Peat consists of partially decomposed litter mass. Accumulation occurs when net primary productivity (NPP) is higher than
115 the decomposition rate, leading to carbon accumulation. Two functionally-distinct layers, the acrotelm and catotelm, are found in most peatland sites. The acrotelm is the top layer in which water table fluctuates leading to both aerated and anoxic conditions. Due to uneven wetness, litter decomposes aerobically as well as anaerobically in the acrotelm (Clymo, 1991; Frolking et al., 2002). This layer also plays the critical role in determining plant composition. The catotelm exists below the permanent annual water table position (WTP) and remains waterlogged throughout the year, creating anoxic conditions,
120 which in turn attenuate the decomposition rate and promote peat accumulation. The boundary between these two layers is marked by the transition from the living plant parts to the dead plant parts and annual WTP.

Our model implicitly divides the total peat column into two parts—acrotelm and catotelm—demarcated by annual WTP, as determined by the hydrology scheme described below. Every year, a new litter layer is deposited over previously accumulated peat layers. After several years due to high carbon mineralization rates in the acrotelm layer (or upper peat
125 layers above the annual WTP), the litter mass loses its structural integrity and transforms into peat, eventually becoming integrated into the saturated rising catotelm mass. The rate of change of total peat mass is the total peat production minus total peat loss due to decomposition (Clymo, 1984):

$$\frac{dM}{dt} = A - K M \quad (1)$$

where M (kg C m^{-2}) is the total peat mass, A is the annual peat input ($\text{kg C m}^{-2} \text{ yr}^{-1}$), and K is the decomposition rate (yr^{-1}).

- 130 Total peat depth is derived from the dynamic bulk density values calculated for individual peat layers. The decomposition process is simulated on annual time step based on the decomposability of the constituent litter types in each layer and the soil physical and hydraulic properties of that layer. This difference in decomposability between litter types is represented by the initial decomposition rate (k_0 – see Eq. 2 and Table 1) (Aerts et al., 1999; Frohling et al., 2001; Moore et al., 2007). The initial decomposition rates are assumed to decline over time using a simplified first order reduction equation (Clymo et al., 135 1998; Frohling et al., 2001):

$$k_i = k_0 \left(\frac{m_t}{m_0} \right) \quad (2)$$

- where i refers to a litter component in a certain peat layer, k_0 is the initial decomposition rate, m_0 is the initial mass and m_t is the mass remaining after some point in time (t). Peat water content and soil thermal dynamics are simulated at different depths (see below) and have a multiplicative effect on the daily decomposition rate (K) of each litter component in each 140 layer following Lloyd and Taylor (1994) and Ise et al. (2008):

$$K_i = k_i T_m W_m \quad (3)$$

- where k_i is the decomposition rate of the layer i component (see Eq. 2) and T_m and W_m are the temperature and moisture multipliers, respectively. Following Ise et al. (2008), we assume that peat decomposition is highest at field capacity and lowest during very wet conditions. However, we allowed the peat to decompose in very dry conditions when the annual WTP drops below -40 cm (WTP takes negative (positive) values when the water table is below (above) the peat surface) and the volumetric water content (θ) goes below 0.01 in the peat layers (Eq. 4 and Table 2). 145

$$W_m = \begin{cases} 1 - 0.975 \left(\frac{\theta - \theta_{opt}}{1.0 - \theta_{opt}} \right)^\alpha, & \theta > \theta_{opt} \\ 1 - \left(\frac{\theta_{opt} - \theta}{\theta_{opt}} \right)^\alpha, & \theta > 0.01 \text{ and } \theta \leq \theta_{opt} \\ \beta, & \theta \leq 0.01 \text{ and } WTP < -40 \end{cases} \quad (4)$$

- 150 where θ_{opt} is the field capacity (0.75) and optimum volumetric water content when W_m becomes 1 and α is a parameter that affects the shape of the dependency of decay on θ , set to 5 and β (0.064) is a minimum decomposition rate during very dry conditions when WTP goes below -40 cm (see Fig. A1). The temperature multiplier is exponentially related to the peat temperature (see Eq. 5 and Table 2) (Frohling et al., 2002). Peat is assumed not to decompose under frozen conditions when the fraction of ice content is greater than zero.

$$155 \quad T_m = \begin{cases} 0, & T_i < T_{\min} \text{ and } I > 0 \\ \left(\frac{T_i - T_{\min}}{|T_{\min}|}\right)^{0.5}, & T_{\min} < T_i < 0^\circ\text{C} \\ Q_{10}^{T_i/10}, & T_i > 0^\circ\text{C} \end{cases} \quad (5)$$

where T_i is the peat temperature in peat layer (i), T_{\min} is the lowest temperature (-4°C) below which heterotrophic decomposition ceases, I is the ice content in each peat layer (i) and Q_{10} is the proportional increase in decomposition rate for a 10°C increase in temperature; set to 2 (Fig. A1).

160 Compaction and the loss of peat mass due to decomposition modify the structural integrity of peat layers (Clymo, 1984) potentially inducing changes in bulk density with depth. Some previous studies have found that the lower bulk density of newly accumulated peat layers increases as peat decomposes and becomes compressed due to overlying peat mass (Clymo, 1991) although bulk density often shows no net increase with depth in the catotelm (Tomlinson, 2005; Baird et al., 2016). Following Frohking et al. (2010), we assume that bulk density is a non-linear function of total mass remaining ($\mu = M_i/M_o$) (see Eq. 6 and Table 2).

$$165 \quad \rho(\mu_i) = \rho_{\min} + \frac{\Delta\rho}{1 + \exp(-(40(1-\mu_i)-34))} \quad (6)$$

where ρ_{\min} is the minimum bulk density (40 kg m^{-3}), $\Delta\rho$ is the difference between this minimum (80 kg m^{-3}), and a maximum bulk density (120 kg m^{-3}), μ_i is the total mass remaining in peat layer i , M_o is the initial peat layer mass and M_i is the peat layer mass remaining after some point in time.

2.1.3 Permafrost/Freezing-thawing cycle

170 Freezing and thawing of peat and mineral soil layers is an important feature in permafrost peatlands, determining plant productivity, decomposition and hydrological dynamics (Christensen et al., 2004; Johansson et al., 2006; Wania et al., 2009b). To simulate permafrost, peat layer decomposition and cycles of freezing and thawing, the soil temperature at different depths must be calculated correctly. In the Arctic version of LPJ-GUESS as described by Miller and Smith (2012), mineral soil layers (i.e. below the peat layers added in this study) are subdivided into 20 sublayers of 10 cm thickness to
 175 calculate soil temperature at different depths. In our implementation, new peat layers are added on top of these mineral soil layers. To overcome computational constraints for millennial simulations we aggregate the properties of the individual annual peat layers into thicker sublayers for the peat temperature calculations, beginning with three sublayers of equal depth and adding a new sublayer to the top of previous sublayers after every 0.5 m of peat accumulation. This resulted, for example, in seven aggregate sublayers for the Stordalen simulations described in Section 2.4. The result is a soil column with
 180 a dynamic number of peat sublayers, 20 mineral soil layers and multiple ‘padding’ layers to a depth of 48 m. A single layer of snow is included, as in existing versions of the model. Following Wania et al. (2009a), the soil temperature profile in each layer is calculated daily by numerically solving the heat diffusion equation. Soil temperature is driven by surface air

temperature which acts as the upper boundary condition. Soil temperature in each annual peat layer is then updated daily and equal to the numerical sublayer to which it belongs. The amount of water and ice present in the sublayers together with their physical composition (mineral, organic or peat fractions) determine the thermal properties (soil thermal conductivities and heat capacities) of each sublayer. Freezing and thawing of soil water (see below) is modelled using the approach in following Wania et al. (2009a). The fraction of air and water is updated daily based on the soil temperature in each sublayer while the fraction of peat and organic matter is influenced by the degree of peat layer decomposability. In the sublayers, the fraction of mineral content is based on Hillel (1998). A full description of the soil temperature and permafrost scheme in the Arctic version of LPJ-GUESS is available in Miller and Smith (2012) and references therein.

2.1.4 Hydrology

Precipitation is the major source of water input in the majority of peatlands. In our model, precipitation is treated as rain or snow depending upon the daily surface air temperature. When temperature falls below the freezing point (0°C assumed), water is stored as a snow above the peat layers. Snow melts when the air temperature rises above the freezing point and is also influenced by the amount of precipitation on that day (Choudhury et al., 1998). We assume that the peatland can hold water up to +20 cm above the peat surface. Water is removed from the peat layers through evapotranspiration, drainage, surface and base runoff. A traditional water bucket scheme is adopted to simulate peatland hydrology (Gerten et al., 2004):

$$W = P - ET - R - DR \pm LF \quad (7)$$

where W is the total water input, P is the precipitation, ET is the evapotranspiration rate, R is the total runoff, DR for the vertical drainage and LF (see section 2.1.7 below) is the lateral flow within the landscape depending upon the relative position of the patch. We add water (rain or snowmelt) from the current WTP to the top of the peat column formed by individual peat layers giving a new WTP in each time step. In our model peat layers above the WTP are thus assumed to remain unsaturated. We simulate water and ice in each peat layer of each individual patch and convert them into water and ice content by dividing the amount of ice and water with total water holding capacity. If a layer is totally frozen (100% ice), then it cannot hold additional water. In partially frozen soil, the sum of the fractions of water and ice is limited to water holding capacity of the respective layer. WTP is updated daily based on existing WTP, W , the total drainage porosity and permeability of the peat layers. WTP is expressed in cm in this paper, with a value of 0 indicating a water table at the peat surface.

Evaporation can only occur when the snowpack is thinner than 1 cm and is calculated following the approach of Gerten et al. (2004), as in the standard version of LPJ-GUESS:

$$ET = 1.32 \cdot E \cdot W_c^2 \cdot F \quad (8)$$

215 where E is the climate-dependent equilibrium evapotranspiration (cm), W_c is the water content on the top 10 cm of the peat soil and F is the fraction of modelled area subject to evaporation, i.e. not covered by vegetation (Gerten et al., 2004).

Runoff is an exponential function of WTP (Wania et al., 2009a):

$$R = BR + \begin{cases} e^{0.01 \text{ WTP}}, & \text{WTP} > \text{TH} \\ 0, & \text{WTP} \leq \text{TH} \end{cases} \quad (9)$$

220 where TH is the WTP threshold, set to -30 cm (Table 2) and BR is the base runoff proportional to the total peat depth (D) is estimated as:

$$BR = u D \quad (10)$$

where u is a parameter (see Table 2) which determines rate of increase in the base runoff with increase in the peat depth (D), set to 0.45 (Frolking et al., 2010). Loss of the water through drainage/percolation depends on the permeability of peat layers and the saturation limit of the mineral soil underneath. Percolation ceases if the mineral layers are saturated with water, 225 incoming rainfall or snowmelt leading instead to an increase in WTP. Peat layer density is assumed to increase due to compression when highly decomposed by anoxic decomposition (Frolking et al., 2010). This results in declining permeability, affecting the flow of water from the peat layers to the mineral soil. The permeability of each peat layer (i) is calculated as a function of peat layer bulk density (Eq. 11) (Frolking et al., 2010). The amount of water draining from the peat column to the mineral soil is calculated by integrating permeability across all the peat layers (i).

$$230 \quad \kappa_i = 10 e^{-0.058\rho_i} \quad (11)$$

where κ_i is the permeability (0-1) and ρ_i is the bulk density of peat layer (i). Change of porosity (Φ) due to compaction is captured by a relationship to bulk density:

$$\Phi_i = 1 - \frac{\rho_i}{\rho_o} \quad (12)$$

235 where ρ_o is the particle bulk density of the organic matter (800 kg m⁻³; see Table 2). Finally, water infiltrating from the peat to the mineral soil layers is treated as the input to the standard LPJ-GUESS hydrology scheme described in Smith et al. (2001) and Gerten et al. (2004).

2.1.5 Root distribution and water uptake

240 In the customized Arctic version of LPJ-GUESS, the mineral soil column is 2 m deep and partitioned into two layers, an upper mineral soil layer of 0.5 m and lower mineral soil layer of 1.5 m. The fraction of roots in these two layers is prescribed for different PFTs (Table 1) and used to calculate daily water uptake. Dynamic peat layers on top of the mineral soil layers necessitated a modification to the way plants access water from both the peat layers and the underlying mineral soil. In the beginning of the peat accumulation process, plant roots are present both in peat and upper and lower mineral soil layers but

245 their mineral soil root distribution declines linearly as peat grows (see Fig. 2) and the corresponding mineral layer reduction
is used to access water from the peat layers. Mosses are assumed only to take up water from the top 50 cm of the mineral soil
in the beginning but once the peat depth exceeds 50 cm they only take water from the peat layers (top 50 cm of the peat
layer). Other PFTs can continue to take up water both from the mineral and peat soils until peat depth reaches 2 m, and from
only from the peat soil thereafter.

250

2.1.6 Establishment and mortality

PFTs are able to establish within prescribed bioclimatic limits reflective of their distributional range (Miller and Smith,
2012) but are also limited by the position of the annual-average WTP (Table 1). Shrubs are vulnerable to waterlogged and
255 anoxic conditions (Malmer et al., 2005) and establish only when annual WTP is deeper than 25 cm relative to the surface.
Mosses and graminoids, by contrast, thrive in wet conditions and establish under WTP +5 to -50 cm (mosses) and above -10
cm (graminoids). The establishment function is implemented once per annual time step, based on mean WTP for the
previous 12 months. LPJ-GUESS includes a prognostic wildfire module (Thonicke et al., 2001; Smith et al., 2014). In high-
latitude peatlands, the risk of natural fire events increases in prolonged dry and warm conditions and this is simulated by the
260 model. Fires lead to vegetation mortality but are assumed not to lead to combustion of peat carbon in our implementation.

2.1.7 Microtopographical structure

Many studies have highlighted the importance of surface micro-formations in peatland dynamics (Weltzin et al., 2001;
265 Nungesser, 2003; Belyea and Malmer, 2004; Belyea and Baird, 2006; Sullivan et al., 2008; Pouliot et al., 2011). The
patterned surface creates a distinctive environment with contrasting plant cover, nutrient status, productivity and
decomposition rates in adjacent microsites. Such spatial heterogeneity is typically ignored in peatland modelling studies, but
can be critically important for peatland development and carbon balance. In our approach, multiple vegetation patches are
simulated to account for such spatial heterogeneity. The model is initialised with a random surface represented by uneven
270 heights of individual patches (10 in the simulations performed here). Water is redistributed from the higher elevated sites to
low depressions through lateral flow (LF) (see Eq. 7). We equalize the WTP of individual patches to match the mean WTP
of the landscape on a daily time step. Patches lose water if their WTP is above the mean WTP of the landscape while the
lower patches receive water (see Eqs. 13-15). This in turn affects the PFT composition, productivity and decomposition rate
in each patch, and peat accumulation over time. We calculate the landscape WTP and add and remove the amount of water
275 from each patch required to match the landscape WTP.

$$\text{MWTP} = \sum \text{PWTP}_i / n \quad (13)$$

where MWTP is the mean WTP across all the patches, PWTP_i is the water table position in individual patches (i) and n is the
total number of patches. The water to be added to or removed from each patch with respect to mean WTP (MWTP) in each

280 patch, i.e. lateral flow (LF) is given by:

$$DWTP_i = PWT P_i - MWTP \quad (14)$$

$$LF_i = DWTP_i \cdot \Phi_a \quad (15)$$

285 where $DWTP_i$ is the difference in the patch (i) and $MWTP$ and LF_i is the total water to be added or removed with respect to $MWTP$ in each patch (i). If the WTP is below the surface then the total water is calculated by the difference in WTP (water heights) multiplied by average porosity (Φ_a). When the WTP is above the surface then Φ_a is not included in the calculation. This exchange of water between patches is implemented after the daily water balance calculation (Eq 7).

290 2.2 Study area

2.2.1 Stordalen

The model was developed based on observations and measurements at Stordalen, a subarctic mire situated 9.5 km east of the
295 Abisko Research Station in northern Sweden (68.36° N, 19.05° E, elevation 360 m a.s.l.) (Fig. 3). Stordalen is one of the most studied mixed mire sites in the world and it has been part of the International Biological Program since 1970 (Rosswall et al., 1975; Sonesson, 1980). It is characterized by four major habitat types: (1) elevated, nutrient poor areas with hummocks and shallow depressions (ombrotrophic), (2) relatively nutrient rich wet depressions (minerotrophic), (3) pools and (4) small streams exchanging water from the catchment (Rosswall et al., 1975). Our simulations represent a mixed
300 landscape of (1) and (2). The mire is mainly covered with mosses such as *Sphagnum fuscum* and *S. russowii*. Shrubs such as *Betula nana*, *Andromeda polifolia* and *Vaccinium uliginosum* are present in dry hummock areas where the WTP remains relatively low, while hollows are mainly dominated by tall productive graminoids, e.g. *Carex rotundata* and *Eriophorum vaginatum* (Malmer et al., 2005). The Stordalen catchment is in the discontinuous permafrost zone. The elevated areas are mainly underlain with permafrost and wet depressions are largely permafrost free and waterlogged. Permafrost underlying
305 elevated areas has been degraded as a result of climate warming in recent decades, with an increase in wet depressions modifying the overall carbon sink capacity of the mire (Christensen et al., 2004; Malmer et al., 2005; Johansson et al., 2006; Swindles et al., 2015). The annual average temperature of the Stordalen was -0.7°C for the period 1913-2003 (Christensen et al., 2004) and 0.49°C for the period 2002-2011 (Callaghan et al., 2013). The warmest month is July and coldest February. The mean annual average precipitation is low but increased from 30.4 cm (1961-1990) to 36.2 cm (1997-2007) (Johansson et al., 2013).
310 Overviews of the ecology and biogeochemistry of Stordalen are provided by Sonesson (1980), Malmer et al. (2005) and Johansson et al. (2006). Ecosystem respiration in Stordalen is lower than commonly observed in other northern peatlands due to low mean temperatures, a short frost-free season and the presence of discontinuous permafrost that keeps the thawed soil cooler and restricts the decomposition rate (Lindroth et al., 2007). Based on radioisotope dating of peatland and lake sequences supplemented with Bayesian modelling, Kokfelt et al. (2010) inferred that the peat initiation started ca.

315 4700 calendar years before present (cal. BP) in the northern part and ca. 6000 cal. BP in the southern part.

2.2.2 Mer Bleue

To evaluate the generality of the model for regional applications, we compared its predictions to observations and
320 measurements at Mer Bleue (45.40° N, 75.50° W, elevation 65 m a.s.l.), a raised temperate ombrotrophic bog located around
10 km east of Ottawa, Ontario (Fig. 3). The peat accumulation in this area initiated ca. 8400 cal. B.P and the mean depth is
around 4-5 m. The northwest arm of the bog is dome shaped with peat depths reaching 5-6 m near the central areas (Frolking
et al., 2010; Roulet et al., 2007). The bog surface is characterized by hummock and hollow topography. This bog is mostly
covered with Sphagnum mosses (*S. capillifolium*, *S. magellanicum*) and also dominated by a mixture of evergreen
325 (*Chamaedaphne calyculata*, *Rhododendron groenlandicum*, *Kalmia angustifolia*) and deciduous shrubs (*Vaccinium*
myrtilloides). A sparse cover of sedges (*Eriophorum vaginatum*) with some small trees (*Picea mariana*, *Larix laricina*,
Betula populifolia) is also present in the peatland (Bubier et al., 2006; Moore et al., 2002). The climate of the area is cool
continental with the annual average temperature being $6.0 \pm 0.8^\circ\text{C}$ for the period 1970 to 2000. The warmest month is July
($20.9 \pm 1.1^\circ\text{C}$) and coldest January ($-10.8 \pm 2.9^\circ\text{C}$). The average monthly temperature remains above 0°C from the April until
330 November and above 10°C between May and September. The mean annual average precipitation is 91 cm of which 23.5 cm
falls as a snow from December to March. The total precipitation is spread evenly across the year with a maximum of 9 cm in
July and a minimum of 5.8 cm in February.

2.2.3 Additional evaluation sites

To evaluate the performance of the model across high-latitude climatic gradients, simulations were performed at 8 locations
335 across Scandinavia for which observations of peat depth and/or other variables of relevance to our study (ecosystem C
fluxes, WTP, vegetation composition and cover) were available (Table 4). These sites represent different types of peatlands
with distinct initialization periods (from relatively new to old sites) and climate zones (from cold temperate to subarctic
sites) (Fig. 3).

2.3 Model forcing data

340 The model requires daily climate fields of temperature, cloudiness and precipitation as input. Holocene climate forcing series
for Stordalen and Mer Bleue were constructed by the delta-change method, i.e. applying relative anomalies derived from the
gridcell nearest to the location of the site from millennium time-slice experiments using the UK Hadley Centre's Unified
Model (UM) (Miller et al., 2008), to the average observed monthly climate of the sites. Daily values were obtained by
interpolating between monthly values for Stordalen from the year 5 kyr cal. BP and for Mer Bleue from the year 10 kyr cal.
345 BP until the year 2000. For Stordalen we used the dataset of Yang et al. (2012) from the period 1913-1942, and for Mer

350 Bleue we used average monthly data from the CRU TS 3.0 global gridded climate data set (Mitchell and Jones, 2005) from
the period 1901 to 1930. We then linearly interpolated the values between the millennium time slices. This method conserves
the interannual variability for temperature and precipitation throughout the simulation. The version of the UM used in this
study was HadSM3, an atmospheric general circulation model (AGCM) coupled to a simple mixed layer ocean and sea ice
355 model with $2.5 \times 3.75^\circ$ spatial resolution (Pope et al., 2000). The high spatial resolution (50 m), modern observed climate
dataset was developed by Yang et al. (2012) for the Stordalen site. In this dataset, the observations from the nearest weather
stations and local observations were included to take into account the effects of the Tornetråsk lake close to the Stordalen
catchment. The monthly precipitation data (1913-2000) for Stordalen at 50 m resolution were downscaled from 10 min
360 resolution using CRU TS 1.2 data (Mitchell and Jones, 2005), a technique quite common for cold regions (Hanna et al.,
2005). The precipitation data was also corrected by including the influences of topography and also by using historical
measurements of precipitation from the Abisko research station record. Finally, monthly values of Holocene temperature
were interpolated to daily values, monthly precipitation totals were distributed randomly among the number (minimum 10)
of rainy days per month from the climate dataset and the monthly CRU values of cloudiness for the first 30 years from the
year 1901-1930 were repeated for the entire simulation period. We added random variability to the daily climate values by
365 drawing random values from a normal distribution with monthly mean (μ) and standard deviation (σ) of the monthly
observed climate were used for Stordalen from the period of 1913-1942 and for Mer Bleue, 30 years of monthly CRU values
from the period of 1901-1930 were used. For the additional evaluation sites, we used the randomly generated daily climate
CRU values of temperature and precipitation from the period 1901-1930. Past, annual atmospheric CO₂ concentration values
from 5000 cal. BP for Stordalen and 10000 cal. BP for Mer Bleue to the year 2000 were obtained by linear interpolation
370 between the values used as a boundary conditions in the UM time-slice simulations (Miller et al., 2008). The CO₂
concentration values used to force the UM simulations were linearly interpolated to an annually varying value between
prescribed averages for each millennium. From 1901 to 2000 observed annual CO₂ from atmospheric or ice core
measurements were used (McGuire et al., 2012).

2.4 Simulation Protocol

370 2.4.1 Holocene hindcast experiments

The model was first initialised for 500 years from “bare ground” using the first 30 years of Holocene climate data to attain an
approximate equilibrium of vegetation and carbon pools with respect to mid-Holocene climate. The mineral and peat layers
were forced to remain saturated for the entire initialization period. The peat decomposition, soil temperature and water
balance calculations were not started until the peat column became sufficiently thick (0.5 m). This initialisation strategy was
375 essential in order to avoid sudden collapse of the peat in very dry conditions. After initialization, the model was forced with
continuous Holocene climate from the year 4700 cal. BP until the year 1912, after which the observed climate of the
Stordalen site was used for the transient run until the year 2000. This experiment is referred to as the standard model

experiment (STD). In the case of Mer Bleue, a similar procedure was adopted, but here the model was forced with continuous climate from the year 8400 cal. BP until the year 1900 and then the CRU climate was used for the transient run until the year 2000. Model parameters were identical in both cases, apart from those relating to local hydrology (u, TH – Eqs. 9 and 10) - see Table 2. This is to adjust the simulations with the local WTP. We refer to this experiment as the validation model experiment (VLD).

2.4.2 Hindcast experiment – regional climate gradient

The model was run at the eight additional evaluation sites spread across Scandinavia (Table 4; s2.2.3), comparing simulated peat accumulation to peat depth reported in the literature. Three sites were selected for additional evaluation of carbon fluxes, WTP and dominant vegetation cover (Fig. 3 and Table 4 and 5). These simulations used a similar set up as in STD experiment with respect to bulk density and local hydrology. Accurate prediction of total carbon accumulation across northern and high latitude peatlands is dependent on the right inception period, initial bulk density values and the local hydrology. The model was run within the most probable period of peat inception mentioned in the literature (Table 4).

2.4.3 Climate change experiment

To investigate the sensitivity of vegetation distribution, peat formation and peatland carbon balance to climate change, future experiments using RCP2.6 and RCP8.5 (Moss et al., 2010) 21st century climate change projections were performed, extending the STD experiment, which ends in 2000, until 2100. Climate output from the Coupled Model Intercomparison Project Phase 5 (CMIP5) runs with the MRI-CGCM3 general circulation model (GCM) was used to provide future climate forcing (Yukimoto et al., 2012). Climate sensitivity of MRI-CGCM3 is 2.60 K which is rather low compared to other models in CMIP5 (Andrews et al., 2012). Atmospheric CO₂ concentrations for the RCP2.6 and RCP8.5 emissions scenarios were obtained from the website of the International Institute for Applied Systems Analysis (IIASA)-<http://tntcat.iiasa.ac.at/RcpDb/>. Simulations were performed for the Stordalen site. Responses of the model to single factor and combined future changes in temperature, precipitation and atmospheric CO₂ were examined in separate simulations (Table 3). Model output variables examined include cumulative peat age profile, total peat accumulation, net ecosystem exchange (NEE), annual and monthly WTP, active layer depth (ALD) and measures of vegetation PFT composition and productivity.

3 Results

3.1 Hindcast experiment

3.1.1 Stordalen

In the standard (STD) experiment, a total of 94.6 kg C m⁻² (91.4-98.9 kg C m⁻²) of peat was accumulated over 4700 years, leading to a cumulative peat depth profile of 2.1 m (1.9-2.2 m) predicted for the present day (Fig. 4), comparable to the

observed peat depth of 2.06 m reported by Kokfelt et al. (2010). The trajectory of peat accumulation since the mid-Holocene inception is also similar to the reconstruction based on radioisotope dating of the peat core sequence in combination with Bayesian modelling (Kokfelt et al., 2010) (Fig 4). Total NPP ranged from 0.06-0.18 kg C m⁻² yr⁻¹ during the simulation while the soil decay losses were between 0.05 and 0.15 kg C m⁻² yr⁻¹. Hence, the carbon uptake by the Stordalen mire ranged between -0.03 and 0.10 kg C m⁻² yr⁻¹ (Figs. 5a, 5c and A2). The long-term mean accumulation rate of the mire was 0.04 cm yr⁻¹ or 20 g C m⁻² yr⁻¹. Mean annual WTP drew down to -10 cm in the beginning and fluctuated between -10 to -25 cm for the entire simulation period, but decreased to a value below -25 cm in the last 100 years due to comparatively higher temperatures during this period (Fig. 5e). The model initially had an uneven surface where the majority of the patches were suitable for moss growth because of the shallow peat depth and an annual WTP near the surface (Figs. 5e and 6a). Moss-dominated areas accumulated more carbon as they become highly recalcitrant due to saturated conditions and low initial decomposition rate (see Table 1). At around 4300 cal. BP, shrubs started to establish because of a lower annual WTP as peat depth increased (Figs. 5e, 6a and A3). When the peat was shallow, plant roots were present in both the mineral and peat layers. Since the majority of lower peat and mineral layers were frozen, the water required for the plant growth was limited, which then limited the productivity of shrubs and graminoids. However, since the upper peat layers were not completely frozen the moss productivity was not limited to the same extent as they could take up the water from upper 50 cm of the peat surface (Figs. 6a and 7a). The total ice fraction was between 40 and 60% for the majority of the simulation period indicating that the peat soil was partially frozen from the beginning (Fig. A4). The fraction of ice present in the peat soil is influenced by mean annual air temperature (MAAT) and peat thickness (section 2.1.3). Increasing MAAT can lead to a reduction in the fraction of ice present in the peatland if the peat is sufficiently shallow. However, in thicker peat profiles the influence of temperature was lower due to the thermal properties of the thicker peat layers. From Figure 7a, it is clear that at the end of the simulation period the lower layer (see X in Fig. 7a) was almost completely frozen but upper and middle layers were partially frozen (see Z in Fig. 7a) leading to a mean annual active layer depth (MAAD) of 0.64 m (Fig. 7c). When the peat layers had decomposed sufficiently and lost more than 70% of their original mass (M₀), their bulk density increased markedly. The observed monthly and annual WTP for the semi-wet patches and mean annual ALD were very near to the simulated values (see Figs. 8, 9 and A5). The simulated bulk density varies between 40-102 kg m⁻³ and the mean annual bulk density of the full peat profile was initially around 40 kg m⁻³, increasing to 50 kg m⁻³ as the peat layers grew older. Some studies (Clymo, 1991; Novak et al., 2008) noted a decline in bulk density with depth due to compaction. However, the simulated peat column does not exhibit such a decline with depth, instead being highly variable down the profile as found in other studies (Tomlinson, 2005; Baird et al., 2016). Freezing of the lower layers inhibited decomposition, with the result that bulk densities remained higher relative to other partially frozen or unfrozen layers. The pore space and permeability are linked to the compaction of peat layers. Therefore, when the peat bulk density increased, pore space declined from 0.95 to 0.93 reducing the total permeability of peat layers that in turn reduced the amount of percolated water from the peat layers to the mineral soil.

3.1.2 Mer Bleue

445 In the VLD experiment, a total of 227.9 kg C m⁻² (192.6-249.1 kg C m⁻²) peat was accumulated over the simulation period, resulting in a peat profile of around 4.2 m (3.6-4.6 m) (Fig. 4), which may be compared to the observed peat depth of 5 m reported by Frolking et al. (2010). The trajectory of peat accumulation is similar to the reconstruction based on radiocarbon dates for core MB930 by Frolking et al. (2010) for the first 6 kyr after which it diverges (Fig 4). The likely explanation for this late-Holocene divergence is discussed in section 4.1.1. Total NPP ranged from 0.1-0.5 kg C m⁻²yr⁻¹ in the course of the simulation while the soil carbon fluxes ranged between 0.12 and 0.25 kg C m⁻² yr⁻¹. Therefore, the simulated carbon sequestration rate was in the range -0.2 to 0.3 kg C m⁻² yr⁻¹ (Figs. 5b, 5d and A3). NPP increased during the simulation period reaching 0.5 kg C m⁻² by the end of the simulation. Though both shrubs and mosses were the dominant PFTs from the beginning of the simulation, mosses were replaced by graminoids during certain phases of peatland history and in the last 1000 years of the simulation (Fig. 6c). The mean accumulation rate was 0.05 cm yr⁻¹ or 27.1 g C m⁻² yr⁻¹. After the initialization period, annual WTP dropped to -50 cm and later stabilised between -30 to -60 cm (Fig. 5f). The initial average bulk density of the peat profile was around 40 kg C m⁻³, increasing to 93.4 kg C m⁻³ as peat grew older while the pore space declined from 0.95 to 0.89.

3.2 Hindcast experiment – regional climate gradient

The majority of modelled peat depth values were in good agreement with published data (see Fig. 10 a, b and Table 4). At certain locations, notably Kontolanrahka (60.78° N, 22.78° E), Fajemyr (56.27° N, 13.55° E) and Lilla Backsjömyren (62.41°N, 14.32°E) modelled peat depth was substantially different from observations reported in the literature (see Table 4 and Fig. 10). This could be because of the unavailability of site-specific climate forcing data (simulations were forced by interpolated station data from the CRU global gridded dataset), an incorrect initial bulk density profile or failure of the model to capture the local hydrological conditions. Fajemyr is a temperate tree bog and we have not considered litter coming from trees (T) and high evergreen shrubs (HSE) in this study, providing an additional potential reason for the underestimation of simulated peat depth at this site. However, the modelled dominant vegetation cover, WTP and long-term apparent rate of carbon accumulation (LARCA)¹ were within the published ranges for all three sites with some discrepancies in short-term carbon fluxes (Table 5). Modelled dominant vegetation cover is similar to the observed cover except in Fajemyr where tree was also one of the dominant PFTs. Modelled LARCA values were also similar to observed values for the two sites (Fajemyr and Siikaneva) while no observed LARCA value was reported for Degerö Stormyr. Slightly wetter conditions were

¹ LARCA is calculated by dividing total cumulative carbon (peat thickness) by the corresponding time interval (basal age)

simulated than observed at Degerö and Siikaneva. NEE outputs for the three sites are comparable to the range of observed NEE values although with some differences (Fig. 11 and Table 5).

3.3 Climate change experiments

In the future scenario experiments, the surface air temperature increased by approximately 4.8°C and 1.5°C in the T8.5 and T2.6 experiments by 2100, respectively, relative to the year 2000. The significantly higher temperature increase in the T8.5 experiment leads to complete disappearance of permafrost from the peat soil (Fig. 7c,d). Higher soil temperatures are associated with higher decomposition rates (Eq. 5) but since the MAAT is near to the freezing point (-0.7°C) at Stordalen a slight increase in temperature in the first 50 years leads only to a marginal increase in decomposition. However, melting of ice in the peat and mineral soils in combination with a milder climate and longer growing season lead to higher plant productivity (Fig. 6b and 7b). Therefore, the increase in decomposition is compensated by higher plant productivity leading to an initial increase in the peat depth in the both T8.5 and T2.6 experiments (Fig. 12a and b). However, after 2050 decomposition dominates as temperature further increases leading to loss of a substantial amount of carbon mass. Enhancement of plant photosynthesis due to CO₂ fertilization leads to increasing peat accumulation in both C8.5 and C2.6 experiments. Precipitation increases result in only a slight increase in peat depth in both the experiments (P8.5 and P2.6) because when the system is already saturated, any additional input of water will be removed at faster rates since evaporation and surface runoff are positively correlated to WTP (see Eqs. 8 and 9, respectively). The combined effects of all drivers in FTPC8.5 and FTPC2.6 result in higher peat accumulation initially (see Fig. 12a and b), with reductions after 2050 as carbon mineralization rate increases as a result of higher temperature. The increase in carbon mineralization is also associated with thawing of permafrost. Before 2050 the fraction of ice is higher, restricting the decomposition rate. It is also evident from Fig. A2 that the vegetation and soil carbon fluxes are higher in both the experiments after 2050. In both the experiments (FTPC8.5 and FTPC2.6), there is a loss of carbon after 2050 which stabilizes by the end of the century due to increased NPP (Fig. 12).

4 Discussion

4.1 Model performance

4.1.1 Peat accumulation

Peat formation may be induced by a combination of several factors, among which climate, underlying topography, and local hydrological conditions are the important determinants (Clymo, 1992; Yu et al., 2009). In Stordalen, peat initiation started due to terrestrialisation of an open water area around ca. 4700 cal. BP in the northern part of the mire (Kokfelt et al., 2010) while in Mer Bleue, the peatland formed ca. 8400 cal. BP (Frolking et al., 2010). We used these basal dates to start our model simulations. In the STD experiment, the simulated cumulative peat depth profile for the last 4700 years is consistent with the observed peat accumulation pattern (Kokfelt et al., 2010). In VLD experiment, the average increase in peat depth

was simulated to be 4.2 m, which can be compared to 5 m of observed peat depth (Frolking et al., 2010). The underestimation might be because the simulated annual productivity was slightly low, leading to relatively lower peat depth than observed. This discrepancy may also be traceable to the uncertainty in the climate model-generated palaeoclimate forcing of the peatland model. Studies of the influence of GCM-generated climate uncertainty (i.e. variations in climate output fields among GCMs) on carbon cycle model prediction, underline the high prediction error that can arise, for example in present-day biospheric carbon pools and fluxes (Ahlström et al., 2013; Anav et al., 2013; Ahlström, 2016). Potential bias and errors in the predicted climate may be expected to be even higher in palaeoclimate simulations, not least due to the absence of instrumental observations for validating the models. Furthermore, in this study additional bias could arise due to the interpolation procedure used to transform GCM output fields into monthly anomalies, required to force our model. These were generated by linearly interpolating between the climate model output, which is only available at 1000-year intervals. As such, the applied anomalies do not capture decadal or centennial climate variability that can contribute to climate-forced variable peat accumulation rates and vegetation dynamics on these timescales (Miller et al., 2008). Although the majority of the sites were in good agreement with the observed peat depth values in the regional gradient experiment, several factors may have contributed to poorer agreement for certain sites. In particular, a correct parameterization of local hydrological conditions, bulk density profile, climate forcing data and the right inception period are critical in determining the modelled long-term peat dynamics (Yu et al., 2009), together with inclusion of suitable PFTs. Only the basal age was prescribed on a site-specific basis in our simulations (Table 4).

4.1.2 Coupled vegetation and carbon dynamics

Changes in vegetation cover significantly affect the long-term carbon fluxes due to differences in PFT productivity and decay resistance properties of their litter (Malmer et al., 2005). In Stordalen, mosses and dwarf shrubs are the main peat forming plants present on hummocks and intermediate areas (Malmer and Wallen, 1996). Our results are largely in agreement with the observed changes in major PFTs during the last 4700 years of Stordalen history (Kokfelt et al., 2010). Mosses emerged as the dominant PFT at the beginning of the simulation, while 300–400 years after peat inception shrubs started establishing in the higher elevated patches as a result of a lowering of WTP. Graminoids were not productive during the entire simulation period apart from the period 4–3kyr cal. BP (Kokfelt et al., 2010). The model predicted correctly the dominance of graminoids, characteristic of wet conditions, during 4–3kyr cal. BP. However, a period of graminoid dominance between 700–1700 cal. BP was not accurately captured. One explanation can be the absence of decadal and centennial climate variability in the adopted climate forcing data, resulting in an “averaging out” of moisture status over time that eliminates wet episodes needed for graminoids to be sufficiently competitive. In Mer Bleue, mosses form the dominant vegetation cover together with low shrubs and graminoids. Though in general the model was able to capture these dynamics fairly well, we found some discrepancies in the beginning and at the end of the simulation. In the beginning, there were no

graminoids while at the end the moss-dominated areas were replaced by graminoids due to submergence of lower patches, which is not reflected in the peat core analysis (Frolking et al., 2010).

540 The modelled annual and monthly WTP from 2003-2012 in semi-wet patches and modelled annual ALD 1990-2012 is in good agreement with the observed values for the Stordalen region (Figs. 8, 9 and A5) supporting the ability of model to capture hydrological dynamics that further drive peatland dynamics. For the additional evaluation sites, modelled dominant vegetation cover, LARCA and WTP were in good agreement with the observed values for the three selected sites at which this information was available. Under the present climate, Stordalen was simulated to be a small sink for atmospheric CO₂, in agreement with observed NEE (see Fig 11). NEE interannual range is likewise close to observations for the other Scandinavian sites (Table 5). However it is uncertain whether recent annual observations of NEE necessarily reflect the long-term peatland carbon balance, in view of high variability on multiple timescales. For example, Fajemyr has switched between source (14.3-21.4 g C m⁻² yr⁻¹ in 2005-2006; 23.6 g C m⁻² yr⁻¹ in 2008) and sink (-29.4 g C m⁻² yr⁻¹ in 2007; -28.9 g C m⁻² yr⁻¹ in 2009) conditions in recent years, and this variability has been attributed to disturbances and intermittent drought conditions (Lund et al., 2012).

550 Plant productivity simulated by our model in this study was generally quite low, as is generally observed in subarctic environments (Malmer et al., 2005). However, the NPP of mosses was comparatively higher than the dwarf shrubs because of two factors (Fig. 6a). The presence of permafrost (Fig. 7a) and an ALD near the surface (Fig. 7c) reduced the vascular plants' ability to take up water from the peat soil layers, reducing NPP and in turn affecting the total litter biomass (Fig. 5a). Mosses, however, could access water more easily because their uptake is largely above the ALD. The exposure to wind and snow drift may also contribute to reducing plant productivity (Johansson et al., 2006; Malmer et al., 2005) but these factors are not represented in the model. In the temperate conditions of Mer Bleue, plant productivity is quite high compared to subarctic conditions of Stordalen, as plant water uptake is not limited by permafrost conditions and it is also influenced by a longer growing season. In Mer Bleue, the total simulated NPP was low compared to that used as input to the modelling study by Frolking et al. (2010) but within the observed range reported by Moore et al. (2002). The lower simulated NPP in our model provides one explanation for relatively lower peat accumulation and peat depth, although agreement with the reconstructed peat accumulation trajectory is high for the first 6 kyr (Figs. 4 and 6c).

555 However, estimates of carbon fluxes derived from the flux tower measurements are not directly comparable with the long-term carbon fluxes derived from the peat core analyses (Belyea and Malmer, 2004; Silvola et al., 1996). LARCA for the two sites are 20 and 27.1 g C m⁻² yr⁻¹ respectively, which is near the reported mean for 795 peat cores from Finland (21 g C m⁻² yr⁻¹) (Clymo et al., 1998) and 127 accumulation records from northern peatlands (22.9 g C m⁻² yr⁻¹) (Loisel et al. 2014). The LARCA of all our evaluation sites also fall within reported ranges (see Table 4). Similarly, the mean annual simulated NEE (34.1 g C m⁻² yr⁻¹) for the last three decades (1971-2000) at Stordalen also falls within the recent observed range at the site of

570 8-45 g C m⁻² yr⁻¹ (Malmer et al., 2005; Malmer and Wallen, 1996). Christensen et al. (2012) found that the mean NEE of Stordalen during 2001-2008 was 46 g C m⁻² yr⁻¹ and for 2008-2009 it was 50 ± 17.0 g C m⁻² yr⁻¹ (Olefeldt et al., 2012; Yu, 2012). The mean NEE for 2001-2009 in our simulations was 51.4 g C m⁻² yr⁻¹, which is very near to the observed values. However, as discussed above, an exact comparison cannot yet be made as the carbon fluxes from the wet and semi-wet areas are not properly represented in our model, and the water borne fluxes are also not included in the calculation.

575 Water borne carbon fluxes (DOC) and CH₄ are not yet considered in our model (but are under development; e.g. Tang et al., 2015b) and inclusion of both would alter the NEE values we report above and in Figs. 5c,d and 11. Both release and uptake components of NEE are relatively low in Stordalen compared to other peatlands (Nilsson et al., 2008; Olefeldt et al., 2012). The low ecosystem respiration is associated with low autotrophic respiration (Olefeldt et al., 2012) and the presence of permafrost which keeps the thawed peat soil cool and reduces the decomposition rate in the shallow thawed soil.

580 Temperature increase since the 1970's at Stordalen (Christensen et al., 2012) has caused the permafrost in the peat soil to thaw, leading to a predominance of wet sites dominated by graminoids in parts of the mire, affecting its overall vegetation composition and carbon fluxes (Christensen et al., 2004; Johansson et al., 2006; Swindles et al., 2015). This situation was not captured by our simulation, where there is no such increase in graminoids (Fig. 6b). The increase in wet areas at Stordalen is however associated with peat soil subsidence during permafrost thaw and the resultant change in hydrological networks across the mire landscape (Åkerman & Johansson 2008), a complex physical process not included in our model.
585 Another factor that contributed to the recent dynamics of the site is the influence of the underlying topography on the sub-surface flow and the addition of water through run-on from the surrounding catchment (Tang et al., 2015). Though we incorporated lateral exchange of water between the simulated patches, we ignored the effect of underlying topography that affects the water movement. In Stordalen, the southern and western parts of the mire are normally fed from higher areas centrally and to the east (Johansson et al., 2006), and recent warming has resulted in the runoff rate increasing from the elevated sites to the low lying areas that have slowly become increasingly waterlogged. Tang et al. (2015) showed the importance of including the slope and drainage area in order to distribute water within the catchment area, and demonstrated how these factors influence vegetation distribution and carbon fluxes in LPJ-GUESS.
590

595 4.2 Impact of climate change

4.2.1 Coupled vegetation and carbon dynamics

Some peatlands may sequester more carbon under warming climate conditions (Charman et al., 2013) while some may turn into carbon sources and degrade (Ise et al., 2008; Fan et al., 2013). For Stordalen, our simulations suggested that the temperature (T8.5 and T2.6) is the main factor which accelerates the decomposition in the peat soil after the year 2050.
600 However, the rate of decomposition remains stable in the first half of the 21st century due to the presence of permafrost. The rise in atmospheric CO₂ concentration (C8.5 and C2.6) accelerates the plant productivity. An increase in precipitation (P8.5

and P2.6) has a very limited effect on peat growth as the mire has already been saturated and any additional input of water will be removed at a faster rate because the surface runoff and evaporation are positively correlated with WTP. The warmer and wetter future conditions, in combination with CO₂ fertilization (FTPC8.5 and FTPC2.6), would lead to increased moss productivity and a slight increase in shrub abundance (Figs. 6b and 12). The latter trend is consistent with widespread reports of expansion of tall shrubs in the second half of the 21st century in many parts of the Arctic and beyond (Lorant and Goetz, 2012; Sturm et al., 2005). Higher temperatures will result in earlier snowmelt and a longer growing season (Euskirchen et al., 2006), promoting plant productivity. Our results for both a strong warming (RCP8.5) and low warming (RCP2.6) scenario indicate that the limited increase in decomposition due to soil warming will be more than compensated by the increase in NPP in the first half of the 21st century, resulting in accelerated peat accumulation. Decomposition was, however, simulated to increase after 2040 due to permafrost thawing and high temperature, resulting in the loss of comparatively higher amount of carbon by the end of the 21st century (Fig. 12).

4.2.2 Permafrost and climate warming

Temperature and precipitation are expected to increase at Stordalen in the coming decades (Saelthun and Barkved, 2003) and alongside an increase in snow depth are expected to result in rapid rates of permafrost degradation and a thicker active layer (Christensen et al., 2004; Johansson et al., 2013; Swindles et al., 2015). Due to recent warming the ALD has already increased at Stordalen and surrounding sites over the past three decades (Åkerman and Johansson, 2008). This event has also changed the surface hydrology of the mire and in turn the vegetation distribution within the basin. ALD has increased between 0.7 and 1.3 cm per year in different parts of the mire, accelerating to an average of around 2 cm yr⁻¹ in recent decades. In our results, we found that simulated MAAD was around 0.69 m for 1972-2005, consistent with the observed MAAD of 0.58 m for the same period (Christensen et al., 2004; Johansson et al., 2006). However, it should be noted that our model does not account for the large observed impact of local variation in permafrost thaw on hydrological network and variability in wetness across the mire landscape. According to Fronzek et al. (2006), a slight increase (1 °C) in temperature and precipitation (10% increase) could lead to widespread disappearance of permafrost throughout Scandinavia in the future. In one scenario, they found a complete disappearance of permafrost by the end of the 21st century. Our results for Stordalen are consistent with this scenario: in the FTPC8.5 experiment, permafrost completely disappears by 2050 due to climate warming (Figs. 7b and d). In the more moderate warming of the FTPC2.6 experiment, permafrost thaws but does not disappear after the year 2050, leading to the simulated MAAD of 1.75 m by 2100 (Fig. 7d).

630 5 Conclusion

Our results demonstrate that the incorporation of peatland and permafrost functionality in LPJ-GUESS provides a suitable framework for assessing the combined and interactive responses of peatland vegetation, hydrology and soils to changing drivers under a range of high latitude climates. Modelled peat accumulation, vegetation composition, water table position, and carbon fluxes were found to be broadly consistent with published data for simulated localities in a range of high-latitude

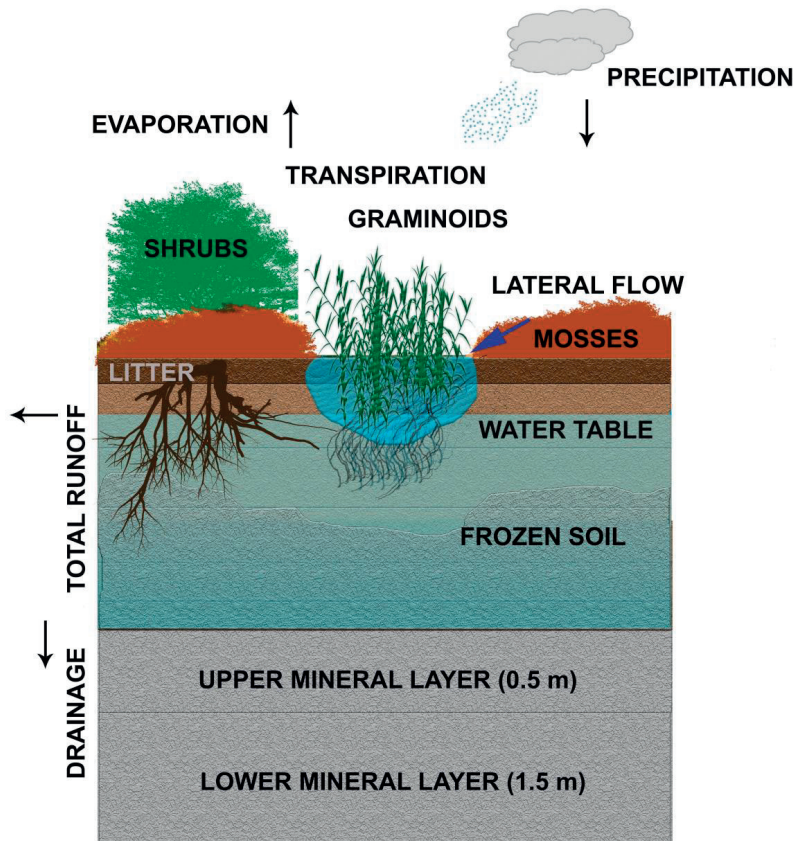
635 climates. Climate change sensitivity simulations for Stordalen suggest that peat will continue to accumulate in the coming
decades, culminating in mid-century (the year 2050), thereafter switching to a CO₂ source as a result of accelerating
decomposition in warming peatland soil. As a complement to empirical studies, our modelling approach can provide an
improved understanding of the long-term dynamics of northern peatland ecosystems at the regional scale, including the fate
of peatland carbon stocks under future climate and atmospheric change. In ongoing work, the model is being extended to
640 incorporate methane biogeochemistry and nutrient dynamics, and will be used to assess impacts of projected future changes
in climate and atmospheric CO₂ on peatland vegetation and greenhouse gas exchange across the Arctic. Coupled to the
atmospheric component of a regional Arctic system model, it is being used to examine the potential for peatland-mediated
biogeochemical and biogeophysical feedbacks processes to amplify or dampen climate change in the Arctic and globally.

645 **Acknowledgements**

This study was funded by the Nordic Top Research Initiative DEFROST and contributes to the strategic research areas Modelling the Regional and Global Earth System (MERGE) and Biodiversity and Ecosystem Services in a Changing Climate (BECC). We also acknowledge support from the Lund University Centre for the study of Climate and Carbon Cycle (LUCCI). We are also thankful to Anders Ahlström for providing the RCP dataset and Ulla Kokfelt for sharing age-depth data of Stordalen mire.

650

Figures:



655

Fig. 1. Schematic representation of peatland structure and function in the implementation described in this paper. Dynamic peat layers deposit above the static mineral soil layers (0.5+1.5 m). In the shallow peat, plant roots are present in both mineral and peat layers. Once the peat becomes sufficiently thick (2 m), all roots are confined to the peat layers.

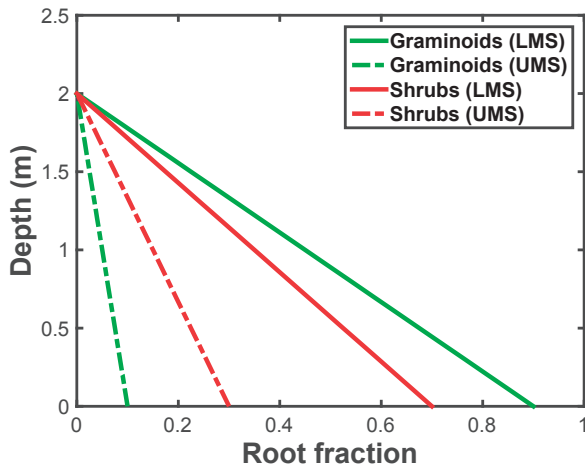
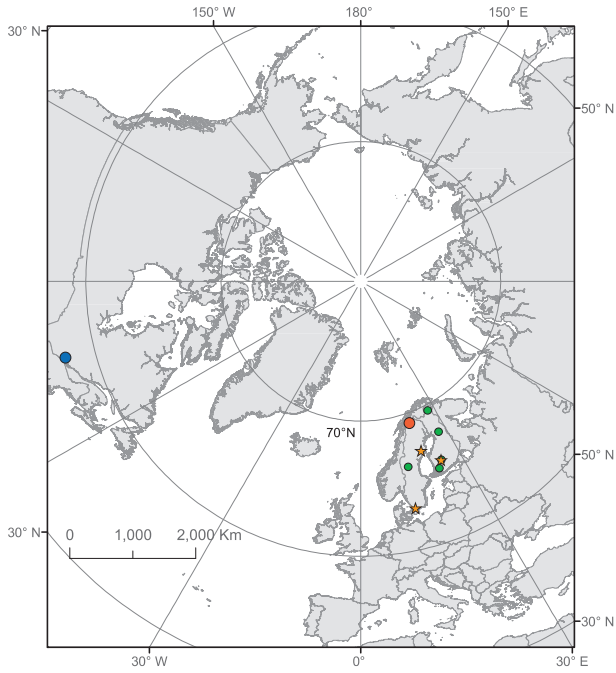
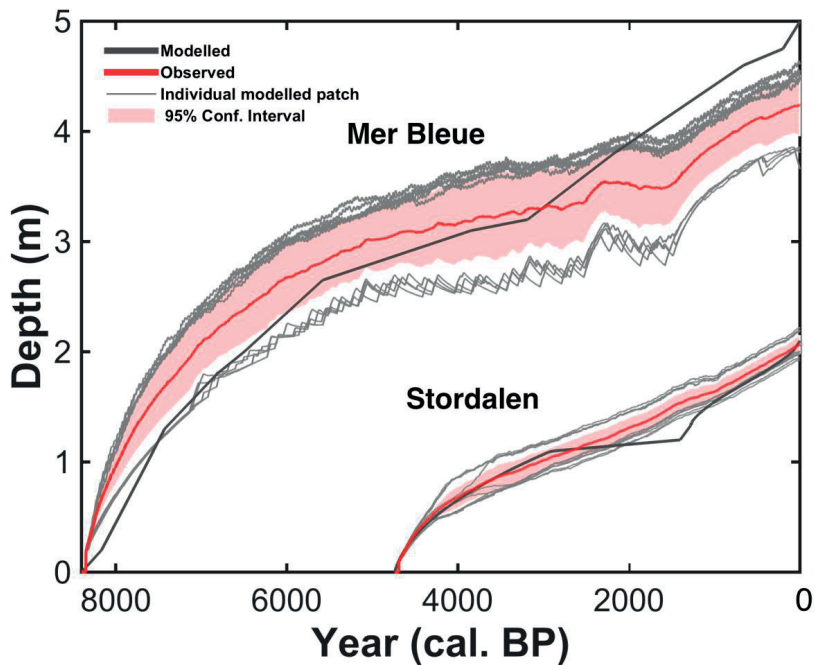


Fig. 2. Root fractions in the upper (UMS) and lower mineral soil (LMS) layers as a function of peat depth (m). The broken lines represent root fractions in UMS and solid lines indicate fractions in the LMS.



665

Fig. 3. Map showing the location of the evaluation site (in red), the validation site (in dark blue) and the distribution of regional gradient points across northern European (in green), used for validating the peat depth. Orange stars show the location of the three points used for the evaluation of peat depth, carbon fluxes, WTP and dominant vegetation cover.



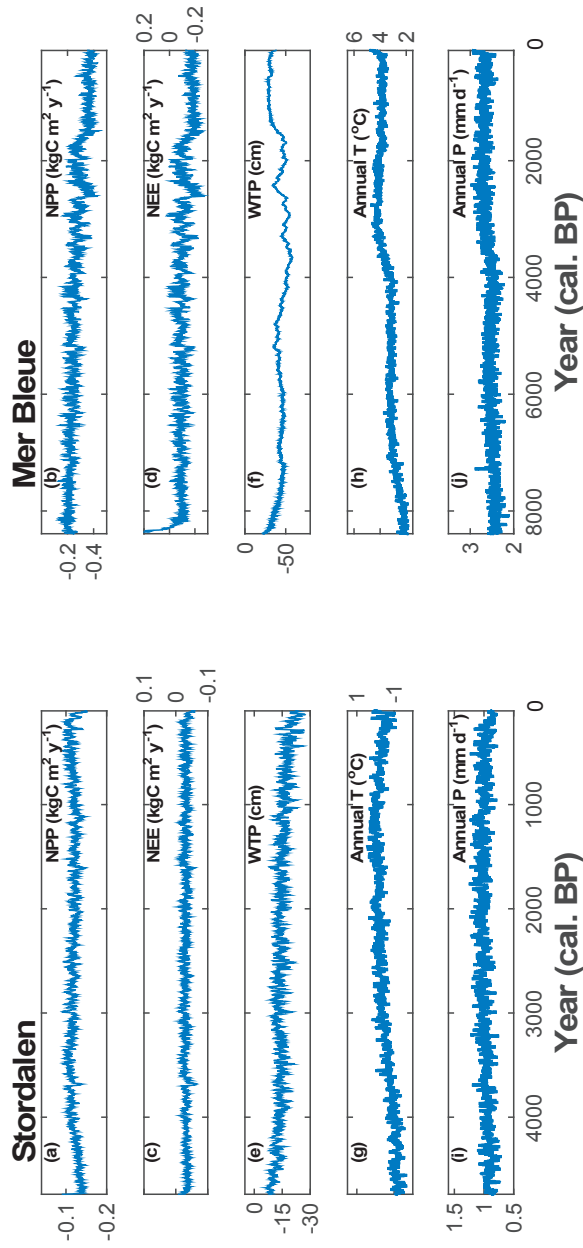
675 **Fig. 4** Comparison of mean landscape simulated peat depth (m) with inferred ages of peat layers of different depths in peat 795 cores from the Stordalen and Mer Bleue sites. The light red shaded area shows the 95% confidence interval (CI)² inferred from the variability among simulated patches at each site (shown in light grey lines).

² $CI = \mu \pm Z_{.95} SE$

where μ is the mean peat depth across all the patches, SE is the standard error of the mean and $Z_{.95}$ is the confidence coefficient from the means of a normal distribution required to contain 0.95 of the area.

676

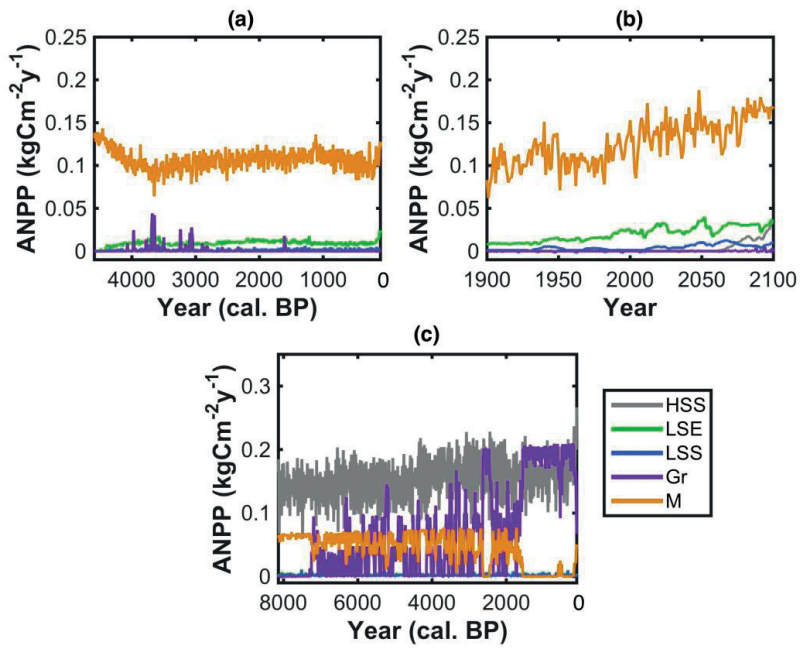
677



678

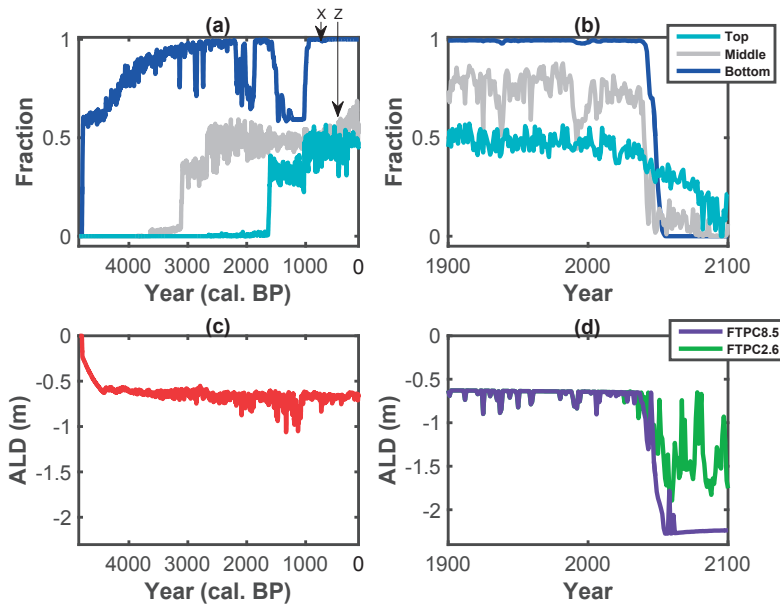
679 **Fig. 5.** Simulated annual average values (10-year moving average) of **(a, b)** net primary productivity (NPP), **(c, d)** net ecosystem exchange (NEE), **(e, f)** water table position
680 (WTP), **(g, h)** temperature and **(i, j)** precipitation for the last 4700 years at Stordalen and for the last 8400 years at Mer Bleue, respectively.

681



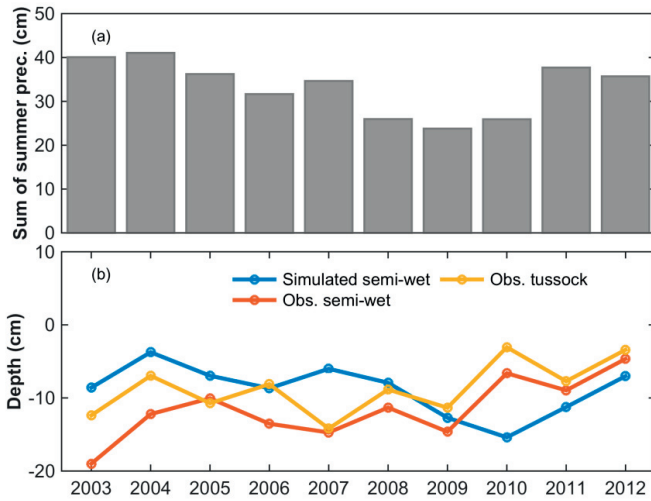
682

683 **Fig. 6.** Simulated annual net primary productivity (ANPP) (10-year moving average) of simulated
684 PFTs (Table 1) (a) for the last 4700 years at Stordalen, (b) for 1900-2100 at Stordalen following
685 RCP8.5 scenario (see Fig. A3 for RCP2.6 scenario) and (c) for the last 8400 years at Mer Bleue.



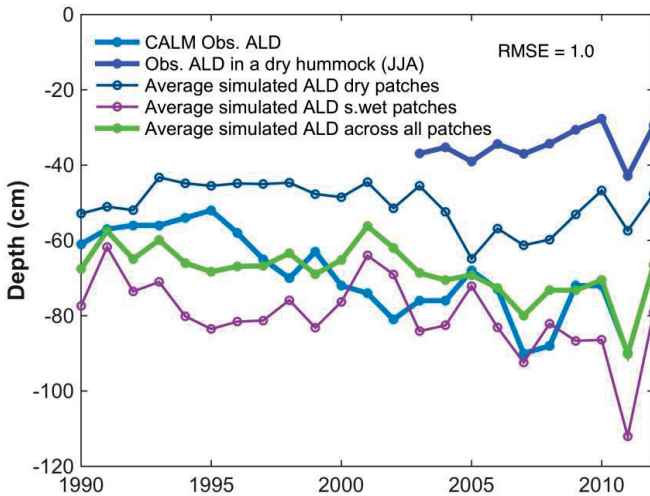
686
 687
 688
 689
 690
 691
 692
 693
 694
 695

Fig. 7. (a) Total simulated peat ice fraction (10-year moving average) over 4700 years at Stordalen. Peat layers corresponding to annual litter cohorts were aggregated to top (top 1 m), middle (middle 1 m) and bottom (lower 1.5 m) for display. (b) Total simulated ice fraction for 1900-2100 following the RCP8.5 scenario (see Fig. A6 for the RCP2.6 scenario results), (c) Total simulated mean September active layer depth for the last 4700 years and (d) for 1900-2100 at Stordalen following the RCP8.5 scenario (FTPC8.5) and RCP2.6 scenario (FTPC2.6).



696

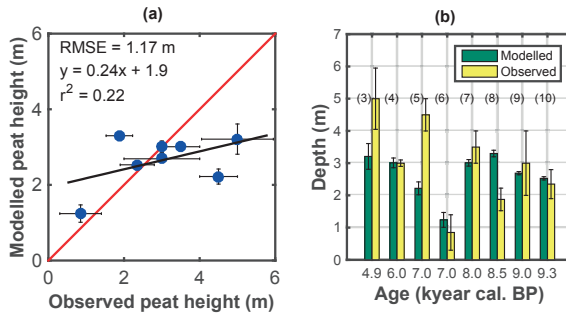
697 **Fig. 8** (a) The total sum of precipitation and (b) comparison between observed and simulated mean
 698 annual WTP for semi-wet patches in Stordalen for 2003-2012.



699

700

701 **Fig. 9.** Comparison between observed and simulated active layer depth for 1990-2012 and average
 702 simulated ALD in semi-wet and dry patches at Stordalen. A separate short mean (June-August) ALD
 703 observation from the Stordalen in a dry elevated hummock site.



705

706

707

708

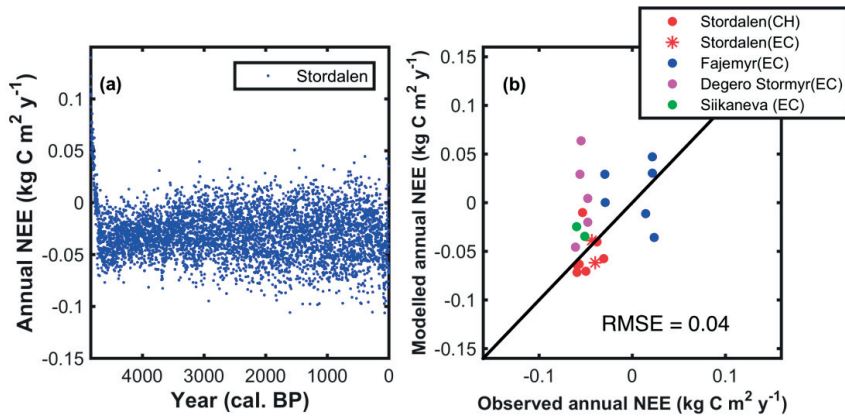
709 **Fig. 10.** (a) Scatter plot with range bars and (b) bar graph showing the comparison between modelled

710 and observed peat depth (m) with reported range bars (in black with yellow bars) at 8 locations

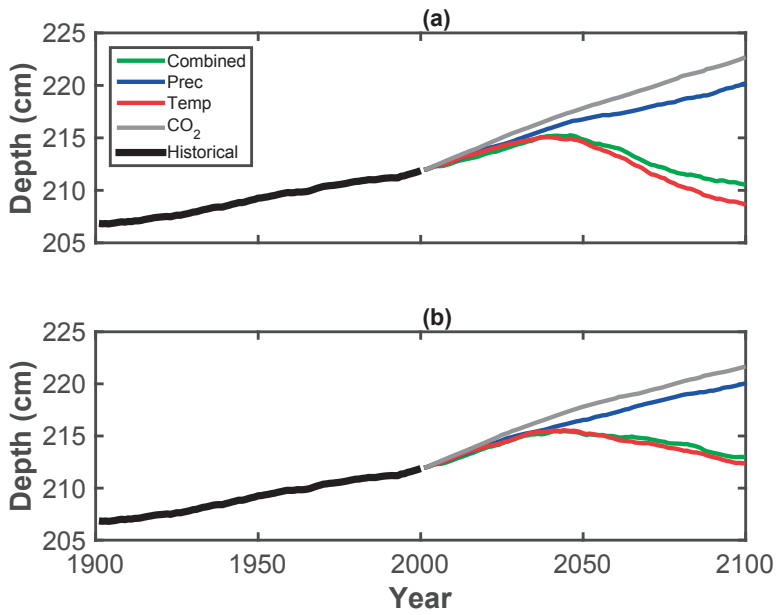
711 (numbered from Table 4) across Scandinavia.

712

713



714
 715 **Fig. 11** (a) Annual simulated NEE (kg C m⁻² yr⁻¹) for Stordalen and (b) relationship between observed
 716 and modeled annual NEE (kg C m⁻² yr⁻¹) for three Scandinavian peatland ecosystems (Table 5;
 717 observed NEE data from Aurela et al., 2007; Lund et al., 2007; Sagerfors et al., 2008; Aslan-Sungur et
 718 al., 2016). EC = eddy covariance (flux tower) data; CH = chamber flux measurements.



719

720

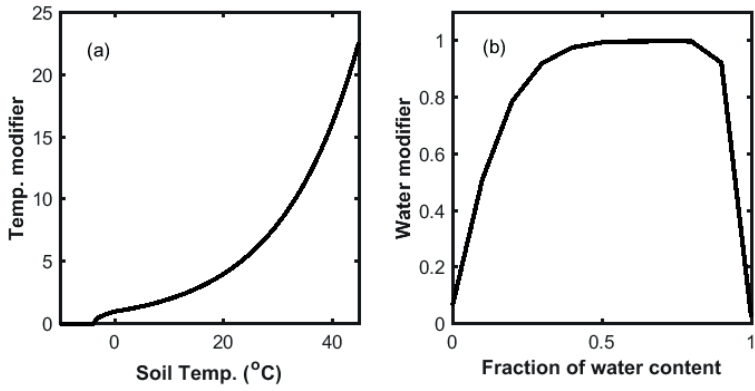
721

722

723 **Fig. 12.** Simulated peat depth (cm) in (a) RCP8.5 and (b) RCP2.6 scenarios simulations at Stordalen.

724

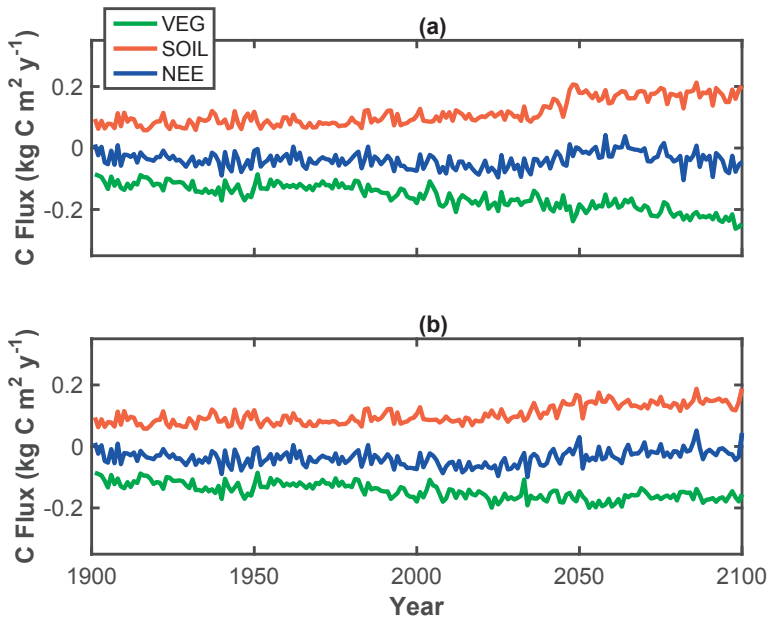
725



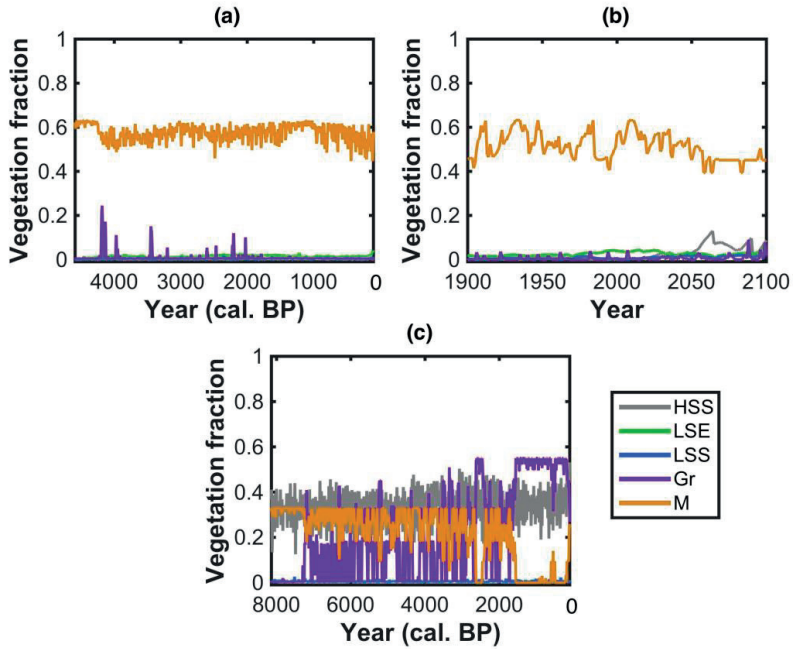
726
727

728 **Fig. A1** Assumed decomposition dependency on (a) soil temperature and (b) soil water content.

729



730
 731 **Fig. A2.** Simulated carbon fluxes and components for 1900-2100 based on historical and (a) RCP8.5
 732 and (b) RCP2.6 future scenarios at Stordalen. VEG = vegetation net primary production (NPP); soil =
 733 heterotrophic respiration; NEE = net ecosystem exchange; negative flux represents uptake from,
 734 positive flux release to the atmosphere.
 735
 736



737

738 **Fig. A3.** Simulated fractional vegetation cover (10-year moving average) of simulated PFTs (Table 1)

739 **(a)** for the last 4700 years at Stordalen, **(b)** for 1900-2100 at Stordalen following the historical

740 simulation and RCP8.5 scenario and **(c)** for the last 8400 years at Mer Bleue.

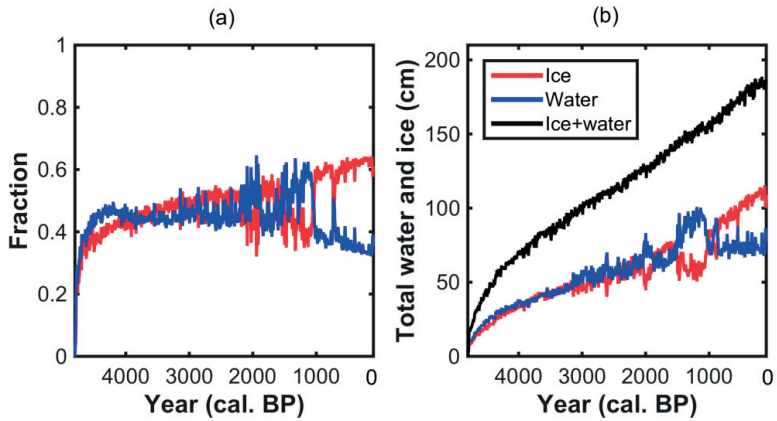
741

742

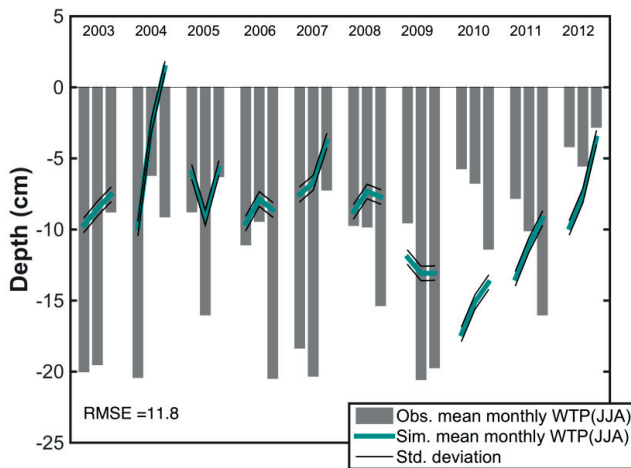
743

744

745

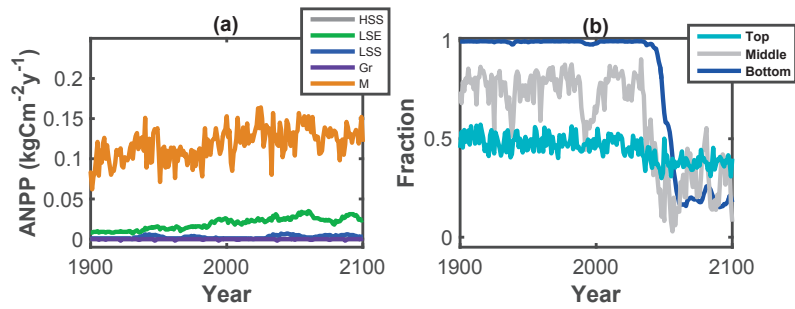


746
 747 **Fig. A4.** (a) Total simulated (10-year moving average) ice and water content in the peat soil and (b)
 748 total simulated water and ice (in cm) for the last 4700 years at Stordalen.



749
 750 **Fig. A5.** Comparison between observed and simulated monthly mean summer (JJA) WTP for semi-
 751 wet patches in Stordalen for 2003-2012.

752



753
754

755 **Fig. A6.** Simulated annual net primary productivity (ANPP) and **(b)** Total simulated ice fraction in the
756 peat sublayers from the year 1900 to 2100 at the Stordalen site using RCP2.6 scenario (FTPC2.6)

757 **Table 1.** Plant functional types (PFTs) simulated in this study, showing representative taxa, phenology, bio-climatic limits, water table position (WTP) threshold for
 758 establishment, prescribed root fractions in mineral soil layers, and initial decomposition rate for different litter fractions.

PFT (abbreviation)	Representative taxa	Phenology	Climate Zone	Growth Form	Min/Max temperature of the coldest month for establishment (°C)	Max GDD for establish- ment (°C.day)	WTP threshold (in cm)	Root fraction		Litter fraction	Initial decompo- sition rate (k_d) ^c (yr ⁻¹)
								Upper mineral soil (UM)	Lower mineral soil (LM)		
High summergreen shrub (HSS)	<i>Salix spp.</i> , <i>Betula nana</i>	Summer green	Boreal- Temperate	Woody	-32.5/-	1000	< -25	0.65	0.35	Wood	0.055
										Leaf	0.1
										Root	0.1
										Seed	0.1
Low evergreen shrub (LSE)	<i>Vaccinium vitis- idaea</i> , <i>Andromeda polifolia</i> L.	Evergreen	Boreal- Temperate	Woody	-32.5/-	100	< -25	0.7	0.3	Wood	0.055
										Leaf	0.1
										Root	0.1
										Seed	0.1
Low summergreen shrub (LSS)	<i>Vaccinium myrtillus</i> , <i>Vaccinium uliginosum</i> , <i>Betula nana</i> L.	Summer green	Boreal- Temperate	Woody	-32.5/-	100	< -25	0.7	0.3	Wood	0.055
										Leaf	0.1
										Root	0.1
										Seed	0.1
Graminoid (Gr)	<i>Carex rotundata</i> <i>Wg.</i> , <i>Eriophorum vaginatum</i> L.	Evergreen	Boreal- Temperate	Herbaceous	-/-	-	> -10	0.9	0.1	Leaf	0.1
										Root	0.1
										Seed	0.1
										Leaf	0.055
Moss (M)	<i>Sphagnum</i> spp.	Evergreen	Boreal- Temperate	Herbaceous	-/15.5	-	< +5 and > -50	-	-	Leaf	0.055
										Seed	0.055

^c Aerts et al. (1999), Frolking et al. (2002) and Moore et al. (2007)

761
762
763

Table 2. Model parameter values used in standard (STD) and validation (VLD) model experiments

Sl. no.	Parameter	Value		Unit	Equation
		STD	VLD		
1.	α	5.0		-	Eq. (4)
2.	β	0.064		-	Eq. (4)
3.	θ_{opt}	0.75		-	Eq. (4)
4.	T_{min}	-4		°C	Eq. (5)
5.	Q_{10}	2		-	Eq. (5)
6.	ρ_{min}	40		kg m ⁻³	Eq. (6)
7.	$\Delta\rho$	80		kg m ⁻³	Eq. (6)
8.	TH	-30	-40	cm	Eq. (9)
9.	u	0.45	0.0	-	Eq. (10)
10.	ρ_o	800		kg m ⁻³	Eq. (12)

764

765

766 **Table 3.** Summary of hindcast and global change experiments
 767
 768

Experiment no.	Experiment name	Description of hindcast and future experiments from 2000 to 2100
1.	STD	Standard model experiment
2.	VLD	Validation model experiment
3.	T8.5	RCP8.5 temperature only
4.	P8.5	RCP8.5 precipitation only
5.	C8.5	RCP8.5 CO ₂ only
6.	FTPC8.5	RCP8.5 including all treatments
7.	T2.6	RCP2.6 temperature only
8.	P2.6	RCP2.6 precipitation only
9.	C2.6	RCP2.6 CO ₂ only
10.	FTPC2.6	RCP2.6 including all treatments

769
 770

771 **Table 4.** Observed peat depth (m) compared with modelled peat depth (m), basal age, climatology, long-term apparent rate of carbon accumulation (LARCA) and total
772 accumulated carbon (kg C m^{-2}) for the calibrated and validation sites together with 8 grid points in the Scandinavian region

Site no.	Site name	Peatland type	Country	Lat. ($^{\circ}\text{N}$)	Lon. ($^{\circ}\text{E}$)	MAAT ($^{\circ}\text{C}$)	MAP (cm yr^{-1})	Basal age (kyear cal. BP)	Modelled		Observed	Reference
									Total carbon (LARCA) $\text{kg C m}^{-2} \text{ yr}^{-1}$	Total peat depth range (average) (in meters)	Total peat depth range (average) (in meters)	
1.	Stordalen	Plasa mire	Sweden	68.5	19.0	-0.7	30	4.7	94.6 (20.0)	1.9 - 2.2 (2.1)	1.9 - 2.3 (2.1)	Kokfelt et al. (2010)
2.	Mer Bleue	Temperate bog	Canada	45.4	-75.5	5.8	91	8.4	227.9 (27.1)	3.6 - 4.4 (4.05)	3.6 - 5.9 (4.9)	Frolking et al. (2010)
3.	Kontolanrahka	Bog	Finland	60.78	22.78	4.6	57.4	4.9	159.7 (32.5)	2.7 - 3.4 (3.2)	4.0 - 6.0 (5.0)	Valiranta et al. (2007)
4.	Lakkasuo	Bog	Finland	61.78	24.30	3.1	70	6.0	162.0 (27.0)	2.9 - 3.2 (3.0)	2.9 - 3.1 (3.0)	Tuittila et al. (2007)
5.	Fajemyr	Temperate tree bog	Sweden	56.27	13.55	6.2	70	7.0	128.2 (18.3)	2.0 - 2.4 (2.2)	4.0 - 5.0 (4.5)	Lund et al. (2007)
6.	Kaamanen	Subarctic poor fen	Finland	69.14	27.30	-1.1	47	7.0	75.3 (10.8)	1.1 - 1.5 (1.2)	0.3 - 1.4 (0.9)	Aurela et al. (2004)

7.	Degerö Stormyr	Boreal poor fen	Sweden	64.18	19.55	1.2	52.3	8.0	166.0 (20.7)	2.9 - 3.1 (3.0)	3.0 - 4.0 (3.5)	Sagerfors et al. (2008)
8.	Lilla Backsjömyren	Mixed mire	Sweden	62.41	14.32	1.6	563	8.5	125.2 (31.3)	3.2 - 3.4 (3.3)	1.5 - 2.2 (1.9)	Andersson and Schoning (2010)
9.	Siikaneva	Boreal poor fen	Finland	61.83	24.18	3.3	713	9.0	156.2 (17.3)	2.6 - 2.7 (2.7)	2.0 - 4.0 (3.0)	Aurela et al. (2007)
10.	Ruosuo	Boreal poor fen	Finland	65.65	27.32	1.0	650	9.3	135.4 (14.5)	2.5 - 2.6 (2.5)	1.9 - 2.8 (2.4)	Makila et al. (2001)

773

774

775

776

777

778

779

780

781

782 **Table 5.** Observed dominant vegetation cover, long-term apparent rate of carbon accumulation
 783 (LARCA), annual net ecosystem exchange (NEE), and mean annual water table position (WTP)
 784 compared with mean modelled values (1990-2000) for the 3 peatland sites in Scandinavia.

785
 786

Site (site no. in Table 4)	Fajemyr (5)	Degerö Stormyr (7)	Siikaneva (9)
Dominant vegetation	M, LSE, T	M, Gr	M, Gr, LSE
Modelled Dominant vegetation	M, LSE	M, Gr	M, Gr, LSE
LARCA (g m⁻² yr⁻¹)	20-35	-	18.5
Modelled LARCA (kg m⁻² yr⁻¹)	18.3	20.7	17.3
NEE (g m⁻² yr⁻¹) (period)	-29.4 to 23.6 (2003-2009)	-48 to -61 (2001-2005)	-50.7 to -59.1 (2004-2005)
Modelled NEE (g m⁻² yr⁻¹)	-35.1 to 47.2	-45 to 63	-24.6 to -34.5
WTP (cm)	0 to -20.0	-4.0 to -20.0	2.0 to -25.0
Modelled WTP (cm)	-15.2 ± 1.83	-2.9 ± 0.99	1.85 ± 0.42
Reference	Lund et al. (2007)	Sagerfors et al. (2008)	Aurela et al. (2007)

787
 788
 789
 790
 791
 792

793 **Table S1.** Comparison of functionality and scope of a representative set of current peatland models.
 794

Schemes Models	Peatland	Permafrost	DGVM	Multiple annual peat layers	Spatial heterogeneity	Methane	Coupled to ESM	Single site	Global/Regi onal application
This study	✓	✓	✓	✓	✓	✗	✗	✓	✓
Wu et al. (2016)	✓	✗	✗	✗	✗	✗	✓	✓	✓
Alexandrov et al. (2016)	✓	✗	✗	✗	✗	✗	✗	✗	✓
Tang et al. (2015b)	✓	✓	✓	✗	✗	✓	✗	✓	✓
Stocker et al. (2014)	✓	✗	✓	✗	✗	✗	✗	✗	✓
Morris et al. (2012)	✓	✗	✗	✗	✓	✗	✗	✓	✗
Schuldt et al. (2013)	✓	✗	✓	✗	✗	✓	✓	✓	✓
Kleinen et al. (2012)	✓	✗	✓	✗	✗	✗	✗	✓	✓
Heinemeyer et al. (2010)	✓	✗	✗	✓	✗	✗	✗	✓	✗
Frolking et al. (2010)	✓	✗	✗	✓	✗	✗	✗	✓	✗
Wania et al. (2009a)	✓	✓	✓	✗	✗	✓	✗	✗	✓
Ise et al. (2008)	✓	✗	✗	✗	✗	✗	✗	✓	✗
Bauer (2004)	✓	✗	✗	✓	✗	✗	✗	✓	✗
Hilbert et al. (2000)	✓	✗	✗	✗	✗	✗	✗	✓	✗
Clymo (1984)	✓	✗	✗	✗	✗	✗	✗	✓	✗
Ingram (1982)	✓	✗	✗	✗	✗	✗	✗	✓	✗

795
 796
 797
 798
 799
 800
 801
 802
 803
 804
 805
 806
 807
 808
 809
 810

References:

- Aerts, R., Verhoeven, J. T. A., and Whigham, D. F.: Plant-mediated controls on nutrient cycling in temperate fens and bogs, *Journal*, 80, 2170-2181, doi: 10.1890/0012-9658(1999)080[2170:pmconc]2.0.co;2, 1999.
- Ahlström, A., Schurgers, G. & Smith, B. : The large influence of climate model bias on terrestrial carbon cycle simulations, *Environmental Research Letters*, in press., 2016.2016.
- Ahlström, A., Smith, B., Lindström, J., Rummukainen, M., and Uvo, C. B.: GCM characteristics explain the majority of uncertainty in projected 21st century terrestrial ecosystem carbon balance, *Biogeosciences*, 10, 1517-1528, doi: 10.5194/bg-10-1517-2013, 2013.
- Åkerman, H. J. and Johansson, M.: Thawing permafrost and thicker active layers in sub-arctic Sweden, *Permafrost Periglacial Process.*, 19, 279-292, doi: 10.1002/ppp.626, 2008.
- Alexandrov, G. A., Brovkin, V. A., and Kleinen, T.: The influence of climate on peatland extent in Western Siberia since the Last Glacial Maximum, *Sci Rep*, 6, doi: ARTN 2478410.1038/srep24784, 2016.
- Anav, A., Friedlingstein, P., Kidston, M., Bopp, L., Ciais, P., Cox, P., Jones, C., Jung, M., Myneni, R., and Zhu, Z.: Evaluating the Land and Ocean Components of the Global Carbon Cycle in the CMIP5 Earth System Models, *J. Clim.*, 26, 6801-6843, doi: 10.1175/Jcli-D-12-00417.1, 2013.
- Andrews, T., Gregory, J. M., Webb, M. J., and Taylor, K. E.: Forcing, feedbacks and climate sensitivity in CMIP5 coupled atmosphere-ocean climate models, *Geophysical Research Letters*, 39, 7, doi: 10.1029/2012gl051607, 2012.
- Aslan-Sungur, G., Lee, X. H., Evrendilek, F., and Karakaya, N.: Large interannual variability in net ecosystem carbon dioxide exchange of a disturbed temperate peatland, *Science of the Total Environment*, 554, 192-202, doi: 10.1016/j.scitotenv.2016.02.153, 2016.
- Baird, A. J., Milner, A. M., Blundell, A., Swindles, G. T., and Morris, P. J.: Microform-scale variations in peatland permeability and their ecohydrological implications, *Journal of Ecology*, 104, 531-544, doi: 10.1111/1365-2745.12530, 2016.
- Bauer, I. E.: Modelling effects of litter quality and environment on peat accumulation over different time-scales, *Journal of Ecology*, 92, 661-674, doi: DOI 10.1111/j.0022-0477.2004.00905.x, 2004.
- Belyea, L. R. and Baird, A. J.: Beyond "The limits to peat bog growth": Cross-scale feedback in peatland development, *Ecol. Monogr.*, 76, 299-322, doi: 10.1890/0012-9615(2006)076[0299:btltpb]2.0.co;2, 2006.
- Belyea, L. R. and Malmer, N.: Carbon sequestration in peatland: patterns and mechanisms of response to climate change, *Global Change Biology*, 10, 1043-1052, doi: 10.1111/j.1529-8817.2003.00783.x, 2004.
- Bubier, J. L., Moore, T. R., and Crosby, G.: Fine-scale vegetation distribution in a cool temperate peatland, *Canadian Journal of Botany-Revue Canadienne De Botanique*, 84, 910-923, doi: 10.1139/b06-044, 2006.
- Callaghan, T. V., Jonasson, C., Thierfelder, T., Yang, Z. L., Hedenas, H., Johansson, M., Molau, U., Van Bogaert, R., Michelsen, A., Olofsson, J., Gwynn-Jones, D., Bokhorst, S., Phoenix, G., Bjerke, J. W., Tommervik, H., Christensen, T. R., Hanna, E., Koller, E. K., and Sloan, V. L.: Ecosystem change and stability over multiple decades in the Swedish subarctic: complex processes and multiple drivers, *Philosophical Transactions of the Royal Society B-Biological Sciences*, 368, doi: 10.1098/rstb.2012.0488, 2013.
- Charman, D. J., Beilman, D. W., Blaauw, M., Booth, R. K., Brewer, S., Chambers, F. M., Christen, J. A., Gallego-Sala, A., Harrison, S. P., Hughes, P. D. M., Jackson, S. T., Korhola, A., Mauquoy, D.,

Mitchell, F. J. G., Prentice, I. C., van der Linden, M., De Vleeschouwer, F., Yu, Z. C., Alm, J., Bauer, I. E., Corish, Y. M. C., Garneau, M., Hohl, V., Huang, Y., Karofeld, E., Le Roux, G., Loisel, J., Moschen, R., Nichols, J. E., Nieminen, T. M., MacDonald, G. M., Phadtare, N. R., Rausch, N., Sillasoo, U., Swindles, G. T., Tuittila, E. S., Ukonmaanaho, L., Valiranta, M., van Bellen, S., van Geel, B., Vitt, D. H., and Zhao, Y.: Climate-related changes in peatland carbon accumulation during the last millennium, *Biogeosciences*, 10, 929-944,doi: 10.5194/bg-10-929-2013, 2013.

Choudhury, B. J., DiGirolamo, N. E., Susskind, J., Darnell, W. L., Gupta, S. K., and Asrar, G.: A biophysical process-based estimate of global land surface evaporation using satellite and ancillary data - II. Regional and global patterns of seasonal and annual variations, *Journal of Hydrology*, 205, 186-204,doi: 10.1016/s0022-1694(97)00149-2, 1998.

Christensen, J. H., B. Hewitson, A. Busiuc, A. Chen, X. Gao, I. Held, R. Jones, R.K. Kolli, W.-T. Kwon, R. Laprise, V. Magaña Rueda, L. Mearns, C.G. Menéndez, J. Räisänen, A. Rinke, Sarr, A., and Whetton, P.: Regional Climate Projections. In: *Climate Change 2007: The Physical Science Basis. Contribution of Working Group I to the Fourth Assessment Report of the Intergovernmental Panel on Climate Change*, [Solomon, S., D. Qin, M. Manning, Z. Chen, M. Marquis, K.B. Averyt, M. Tignor and H.L. Miller (eds.)]. Cambridge University Press, Cambridge, United Kingdom and New York, NY, USA., 2007.2007.

Christensen, T., Jackowicz-Korczynski, M., Aurela, M., Crill, P., Heliasz, M., Mastepanov, M., and Friborg, T.: Monitoring the Multi-Year Carbon Balance of a Subarctic Palsa Mire with Micrometeorological Techniques, *Ambio*, 41, 207-217,doi: 10.1007/s13280-012-0302-5, 2012.

Christensen, T. R., Johansson, T. R., Akerman, H. J., Mastepanov, M., Malmer, N., Friborg, T., Crill, P., and Svensson, B. H.: Thawing sub-arctic permafrost: Effects on vegetation and methane emissions, *Geophysical Research Letters*, 31,doi: L0450110.1029/2003gl018680, 2004.

Clymo, R. S.: The limits to peat bog growth, *Philos. Trans. R. Soc. Lond. Ser. B-Biol. Sci.*, 303, 605-654,doi: 10.1098/rstb.1984.0002, 1984.

Clymo, R. S.: Peat growth, *Quaternary Landscapes*. Eds Shane LCK, Cushing EJ. Minneapolis, University of Minnesota Press., 1991. 76-1121991.

Clymo, R. S.: Models of peat growth, *Suo (Helsinki)*, 43, 127-136,doi: 10.1007/978-3-642-66760-2_9, 1992.

Clymo, R. S., Turunen, J., and Tolonen, K.: Carbon accumulation in peatland, *Oikos*, 81, 368-388,doi: 10.2307/3547057, 1998.

Cramer, W., Bondeau, A., Woodward, F.I., Prentice, I.C., Betts, R.A., Brovkin, V., Cox, P.M., Fisher, V., Foley, J.A., Friend, A.D., Kucharik, C., Lomas, M.R., Ramankutty, N., Sitch, S., Smith, B., White, A. & Young-Molling, C. 2001. Global response of terrestrial ecosystem structure and function to CO₂ and climate change: results from six dynamic global vegetation models. *Global Change Biology* 7: 357-373.

Euskirchen, E. S., McGuire, A. D., Kicklighter, D. W., Zhuang, Q., Clein, J. S., Dargaville, R. J., Dye, D. G., Kimball, J. S., McDonald, K. C., Melillo, J. M., Romanovsky, V. E., and Smith, N. V.: Importance of recent shifts in soil thermal dynamics on growing season length, productivity, and carbon sequestration in terrestrial high-latitude ecosystems, *Global Change Biology*, 12, 731-750,doi: 10.1111/j.1365-2486.2006.01113.x, 2006.

Fan, Z. S., McGuire, A. D., Turetsky, M. R., Harden, J. W., Waddington, J. M., and Kane, E. S.: The response of soil organic carbon of a rich fen peatland in interior Alaska to projected climate change, *Global Change Biology*, 19, 604-620,doi: 10.1111/gcb.12041, 2013.

Friedlingstein, P., Cox, P., Betts, R., Bopp, L., Von Bloh, W., Brovkin, V., Cadule, P., Doney, S., Eby, M., Fung, I., Bala, G., John, J., Jones, C., Joos, F., Kato, T., Kawamiya, M., Knorr, W., Lindsay, K., Matthews, H. D., Raddatz, T., Rayner, P., Reick, C., Roeckner, E., Schnitzler, K. G., Schnur, R., Strassmann, K., Weaver, A. J., Yoshikawa, C., and Zeng, N.: Climate-carbon cycle feedback analysis:

Results from the (CMIP)-M-4 model intercomparison, *J. Clim.*, 19, 3337-3353,doi: 10.1175/jcli3800.1, 2006.

Frolking, S., Roulet, N. T., Moore, T. R., Lafleur, P. M., Bubier, J. L., and Crill, P. M.: Modeling seasonal to annual carbon balance of Mer Bleue Bog, Ontario, Canada, *Glob. Biogeochem. Cycle*, 16,doi: 103010.1029/2001gb001457, 2002.

Frolking, S., Roulet, N. T., Moore, T. R., Richard, P. J. H., Lavoie, M., and Muller, S. D.: Modeling northern peatland decomposition and peat accumulation, *Ecosystems*, 4, 479-498,doi: 10.1007/s10021-001-0105-1, 2001.

Frolking, S., Roulet, N. T., Tuittila, E., Bubier, J. L., Quillet, A., Talbot, J., and Richard, P. J. H.: A new model of Holocene peatland net primary production, decomposition, water balance, and peat accumulation, 1 Article, *Earth System Dynamics*, 1-21 pp., 2010.

Fronzek, S., Luoto, M., and Carter, T. R.: Potential effect of climate change on the distribution of palsa mires in subarctic Fennoscandia, *Climate Research*, 32, 1-12,doi: 10.3354/cr032001, 2006.

Gerten, D., Schaphoff, S., Haberlandt, U., Lucht, W., and Sitch, S.: Terrestrial vegetation and water balance - hydrological evaluation of a dynamic global vegetation model, *Journal of Hydrology*, 286, 249-270,doi: 10.1016/j.jhydrol.2003.09.029, 2004.

Gorham, E.: Northern peatlands - role in the carbon-cycle and probable responses to climatic warming, *Ecological Applications*, 1, 182-195,doi: 10.2307/1941811, 1991.

Hanna, E., Huybrechts, P., Janssens, I., Cappelen, J., Steffen, K., and Stephens, A.: Runoff and mass balance of the Greenland ice sheet: 1958-2003, *J. Geophys. Res.-Atmos.*, 110,doi: 10.1029/2004jd005641, 2005.

Heinemeyer, A., Croft, S., Garnett, M. H., Gloor, E., Holden, J., Lomas, M. R., and Ineson, P.: The MILLENNIA peat cohort model: predicting past, present and future soil carbon budgets and fluxes under changing climates in peatlands, *Climate Research*, 45, 207-226,doi: 10.3354/cr00928, 2010.

Hilbert, D. W., Roulet, N., and Moore, T.: Modelling and analysis of peatlands as dynamical systems, *Journal of Ecology*, 88, 230-242,doi: 10.1046/j.1365-2745.2000.00438.x, 2000.

Hillel, D.: In: *Environmental Soil Physics: Fundamentals, Applications, and Environmental Considerations*, 1998.

Hinzman, L. D., Bettez, N. D., Bolton, W. R., Chapin, F. S., Dyurgerov, M. B., Fastie, C. L., Griffith, B., Hollister, R. D., Hope, A., Huntington, H. P., Jensen, A. M., Jia, G. J., Jorgenson, T., Kane, D. L., Klein, D. R., Kofinas, G., Lynch, A. H., Lloyd, A. H., McGuire, A. D., Nelson, F. E., Oechel, W. C., Osterkamp, T. E., Racine, C. H., Romanovsky, V. E., Stone, R. S., Stow, D. A., Sturm, M., Tweedie, C. E., Vourlitis, G. L., Walker, M. D., Walker, D. A., Webber, P. J., Welker, J. M., Winker, K., and Yoshikawa, K.: Evidence and implications of recent climate change in northern Alaska and other arctic regions, *Clim. Change*, 72, 251-298,doi: 10.1007/s10584-005-5352-2, 2005.

Ingram, H. A. P.: Size and shape in raised mire ecosystems - a geophysical model, *Nature*, 297, 300-303,doi: 10.1038/297300a0, 1982.

IPCC: *Climate Change 2013: The Physical Science Basis, Contribution of Working Group I to the Fifth Assessment Report of the Intergovernmental Panel on Climate Change*, 2013. NY, USA2013.

Ise, T., Dunn, A. L., Wofsy, S. C., and Moorcroft, P. R.: High sensitivity of peat decomposition to climate change through water-table feedback, *Nat. Geosci.*, 1, 763-766,doi: 10.1038/ngeo331, 2008.

Johansson, M., Callaghan, T. V., Bosio, J., Akerman, H. J., Jackowicz-Korczynski, M., and Christensen, T. R.: Rapid responses of permafrost and vegetation to experimentally increased snow cover in sub-arctic Sweden, *Environmental Research Letters*, 8,doi: 10.1088/1748-9326/8/3/035025, 2013.

Johansson, T., Malmer, N., Crill, P. M., Friborg, T., Akerman, J. H., Mastepanov, M., and Christensen, T. R.: Decadal vegetation changes in a northern peatland, greenhouse gas fluxes and net radiative forcing, *Global Change Biology*, 12, 2352-2369, doi: 10.1111/j.1365-2486.2006.01267.x, 2006.

Kleinen, T., Brovkin, V., and Schuldt, R. J.: A dynamic model of wetland extent and peat accumulation: results for the Holocene, *Biogeosciences*, 9, 235-248, doi: 10.5194/bg-9-235-2012, 2012.

Kokfelt, U., Reuss, N., Struyf, E., Sonesson, M., Rundgren, M., Skog, G., Rosen, P., and Hammarlund, D.: Wetland development, permafrost history and nutrient cycling inferred from late Holocene peat and lake sediment records in subarctic Sweden, *J. Paleolimn.*, 44, 327-342, doi: 10.1007/s10933-010-9406-8, 2010.

Lai, D. Y. F.: Methane Dynamics in Northern Peatlands: A Review, *Pedosphere*, 19, 409-421, 2009.

Lindroth, A., Lund, M., Nilsson, M., Aurela, M., Christensen, T. R., Laurila, T., Rinne, J., Riutta, T., Sagerfors, J., Strom, L., Tuovinen, J. P., and Vesala, T.: Environmental controls on the CO₂ exchange in north European mires, *Tellus Ser. B-Chem. Phys. Meteorol.*, 59, 812-825, doi: 10.1111/j.1600-0889.2007.00310.x, 2007.

Lloyd, J. and Taylor, J. A.: On the temperature-dependence of soil respiration, *Funct. Ecol.*, 8, 315-323, doi: 10.2307/2389824, 1994.

Loisel, J., Yu, Z. C., Beilman, D. W., Camill, P., Alm, J., Amesbury, M. J., Anderson, D., Andersson, S., Bochicchio, C., Barber, K., Belyea, L. R., Bunbury, J., Chambers, F. M., Charman, D. J., De Vleeschouwer, F., Fialkiewicz-Koziel, B., Finkelstein, S. A., Galka, M., Garneau, M., Hammarlund, D., Hinchliffe, W., Holmquist, J., Hughes, P., Jones, M. C., Klein, E. S., Kokfelt, U., Korhola, A., Kuhry, P., Lamarre, A., Lamentowicz, M., Large, D., Lavoie, M., MacDonald, G., Magnan, G., Makila, M., Mallon, G., Mathijssen, P., Mauquoy, D., McCarroll, J., Moore, T. R., Nichols, J., O'Reilly, B., Oksanen, P., Packalen, M., Peteet, D., Richard, P. J. H., Robinson, S., Ronkainen, T., Rundgren, M., Sannel, A. B. K., Tarnocai, C., Thom, T., Tuittila, E. S., Turetsky, M., Valiranta, M., van der Linden, M., van Geel, B., van Bellen, S., Vitt, D., Zhao, Y., and Zhou, W. J.: A database and synthesis of northern peatland soil properties and Holocene carbon and nitrogen accumulation, *Holocene*, 24, 1028-1042, doi: 10.1177/0959683614538073, 2014.

Loranty, M. M. and Goetz, S. J.: Shrub expansion and climate feedbacks in Arctic tundra, *Environmental Research Letters*, 7, 3, doi: 10.1088/1748-9326/7/1/011005, 2012.

Lund, M., Christensen, T. R., Lindroth, A., and Schubert, P.: Effects of drought conditions on the carbon dioxide dynamics in a temperate peatland, *Environmental Research Letters*, 7, doi: Artn 04570410.1088/1748-9326/7/4/045704, 2012.

Malmer, N., Johansson, T., Olsrud, M., and Christensen, T. R.: Vegetation, climatic changes and net carbon sequestration in a North-Scandinavian subarctic mire over 30 years, *Global Change Biology*, 11, 1895-1909, doi: 10.1111/j.1365-2486.2005.01042.x, 2005.

Malmer, N. and Wallen, B.: Peat formation and mass balance in subarctic ombrotrophic peatlands around Abisko, northern Scandinavia. In: *Ecological Bulletins; Plant ecology in the subarctic Swedish Lapland*, Karlsson, P. S. and Callaghan, T. V. (Eds.), *Ecological Bulletins*, 1996.

McGuire, A. D., Christensen, T. R., Hayes, D., Heroult, A., Euskirchen, E., Kimball, J. S., Koven, C., Lafleur, P., Miller, P. A., Oechel, W., Peylin, P., Williams, M., and Yi, Y.: An assessment of the carbon balance of Arctic tundra: comparisons among observations, process models, and atmospheric inversions, *Biogeosciences*, 9, 3185-3204, doi: 10.5194/bg-9-3185-2012, 2012.

Miller, P. A., Giesecke, T., Hickler, T., Bradshaw, R. H. W., Smith, B., Seppa, H., Valdes, P. J., and Sykes, M. T.: Exploring climatic and biotic controls on Holocene vegetation change in Fennoscandia, *Journal of Ecology*, 96, 247-259, doi: 10.1111/j.1365-2745.2007.01342.x, 2008.

Miller, P. A. and Smith, B.: Modelling Tundra Vegetation Response to Recent Arctic Warming, *Ambio*, 41, 281-291, doi: 10.1007/s13280-012-0306-1, 2012.

- Mitchell, T. D. and Jones, P. D.: An improved method of constructing a database of monthly climate observations and associated high-resolution grids, *Int. J. Climatol.*, 25, 693-712,doi: 10.1002/joc.1181, 2005.
- Moore, T. R., Bubier, J. L., and Bledzki, L.: Litter decomposition in temperate peatland ecosystems: The effect of substrate and site, *Ecosystems*, 10, 949-963,doi: 10.1007/s10021-007-9064-5, 2007.
- Moore, T. R., Bubier, J. L., Froelking, S. E., Lafleur, P. M., and Roulet, N. T.: Plant biomass and production and CO₂ exchange in an ombrotrophic bog, *Journal of Ecology*, 90, 25-36,doi: 10.1046/j.0022-0477.2001.00633.x, 2002.
- Morris, P. J., Baird, A. J., and Belyea, L. R.: The DigiBog peatland development model 2: ecohydrological simulations in 2D, *Ecohydrology*, 5, 256-268,doi: 10.1002/eco.229, 2012.
- Moss, R. H., Edmonds, J. A., Hibbard, K. A., Manning, M. R., Rose, S. K., van Vuuren, D. P., Carter, T. R., Emori, S., Kainuma, M., Kram, T., Meehl, G. A., Mitchell, J. F. B., Nakicenovic, N., Riahi, K., Smith, S. J., Stouffer, R. J., Thomson, A. M., Weyant, J. P., and Wilbanks, T. J.: The next generation of scenarios for climate change research and assessment, *Nature*, 463, 747-756,doi: 10.1038/nature08823, 2010.
- Nilsson, M., Sagerfors, J., Buffam, I., Laudon, H., Eriksson, T., Grelle, A., Klemetsson, L., Weslien, P., and Lindroth, A.: Contemporary carbon accumulation in a boreal oligotrophic minerogenic mire - a significant sink after accounting for all C-fluxes, *Global Change Biology*, 14, 2317-2332,doi: 10.1111/j.1365-2486.2008.01654.x, 2008.
- Novak, M., Brizova, E., Adamova, M., Erbanova, L., and Bottrell, S. H.: Accumulation of organic carbon over the past 150 years in five freshwater peatlands in western and central Europe, *Science of the Total Environment*, 390, 425-436,doi: 10.1016/j.scitotenv.2007.10.011, 2008.
- Nungesser, M. K.: Modelling microtopography in boreal peatlands: hummocks and hollows, *Ecological Modelling*, 165, 175-207,doi: 10.1016/s0304-3800(03)00067-x, 2003.
- Olefeldt, D., Roulet, N. T., Bergeron, O., Crill, P., Backstrand, K., and Christensen, T. R.: Net carbon accumulation of a high-latitude permafrost tundra mire similar to permafrost-free peatlands, *Geophysical Research Letters*, 39,doi: 10.1029/2011gl050355, 2012.
- Pope, V. D., Gallani, M. L., Rowntree, P. R., and Stratton, R. A.: The impact of new physical parametrizations in the Hadley Centre climate model: HadAM3, *Clim. Dyn.*, 16, 123-146,doi: 10.1007/s003820050009, 2000.
- Pouliot, R., Rochefort, L., Karofeld, E., and Mercier, C.: Initiation of Sphagnum moss hummocks in bogs and the presence of vascular plants: Is there a link?, *Acta Oecol.-Int. J. Ecol.*, 37, 346-354,doi: 10.1016/j.actao.2011.04.001, 2011.
- Robinson, S. D. and Moore, T. R.: The influence of permafrost and fire upon carbon accumulation in high boreal peatlands, Northwest Territories, Canada, *Arct. Antarct. Alp. Res.*, 32, 155-166,doi: 10.2307/1552447, 2000.
- Rosswall, T., Veum, A. K., and Karenlampi, L.: Plant litter decomposition at fennoscandian tundra sites, 1975.
- Roulet, N. T., Lafleur, P. M., Richard, P. J. H., Moore, T. R., Humphreys, E. R., and Bubier, J.: Contemporary carbon balance and late Holocene carbon accumulation in a northern peatland, *Global Change Biology*, 13, 397-411,doi: 10.1111/j.1365-2486.2006.01292.x, 2007.
- Saelthun, N. R. and Barkved, L.: Climate Change Scenarios for the SCANNET Region, Norsk institutt for vannforskning (NIVA), Rep SNO 4663-2003, 742003.

- Schuldt, R. J., Brovkin, V., Kleinen, T., and Winderlich, J.: Modelling Holocene carbon accumulation and methane emissions of boreal wetlands - an Earth system model approach, *Biogeosciences*, 10, 1659-1674,doi: 10.5194/bg-10-1659-2013, 2013.
- Silvola, J., Alm, J., Ahlholm, U., Nykanen, H., and Martikainen, P. J.: CO₂ fluxes from peat in boreal mires under varying temperature and moisture conditions, *Journal of Ecology*, 84, 219-228,doi: 10.2307/2261357, 1996.
- Sitch, S., Huntingford, C., Gedney, N., Levy, P. E., Lomas, M., Piao, S. L., Betts, R., Ciais, P., Cox, P., Friedlingstein, P., Jones, C. D., Prentice, I. C., and Woodward, F. I.: Evaluation of the terrestrial carbon cycle, future plant geography and climate-carbon cycle feedbacks using five Dynamic Global Vegetation Models (DGVMs), *Global Change Biology*, 14, 2015-2039,doi: 10.1111/j.1365-2486.2008.01626.x, 2008.
- Smith, B., Prentice, I. C., and Sykes, M. T.: Representation of vegetation dynamics in the modelling of terrestrial ecosystems: comparing two contrasting approaches within European climate space, *Glob. Ecol. Biogeogr.*, 10, 621-637,doi: 10.1046/j.1466-822X.2001.t01-1-00256.x, 2001.
- Smith, B., Warlind, D., Arneth, A., Hickler, T., Leadley, P., Siltberg, J., and Zaehle, S.: Implications of incorporating N cycling and N limitations on primary production in an individual-based dynamic vegetation model, *Biogeosciences*, 11, 2027-2054,doi: 10.5194/bg-11-2027-2014, 2014.
- Sonesson, M.: Ecology of a subarctic mire, Swedish Natural Science Research Council., Stockholm, Sweden, 1980.
- Stocker, B. D., Spahni, R., and Joos, F.: DYPTOP: a cost-efficient TOPMODEL implementation to simulate sub-grid spatio-temporal dynamics of global wetlands and peatlands, *Geosci. Model Dev.*, 7, 3089-3110,doi: 10.5194/gmd-7-3089-2014, 2014.
- Strandberg, G., Kjellstrom, E., Poska, A., Wagner, S., Gaillard, M. J., Trondman, A. K., Mauri, A., Davis, B. A. S., Kaplan, J. O., Birks, H. J. B., Bjune, A. E., Fyfe, R., Giesecke, T., Kalnina, L., Kangur, M., van der Knaap, W. O., Kokfelt, U., Kunes, P., Latalowa, M., Marquer, L., Mazier, F., Nielsen, A. B., Smith, B., Seppa, H., and Sugita, S.: Regional climate model simulations for Europe at 6 and 0.2 k BP: sensitivity to changes in anthropogenic deforestation, *Climate of the Past*, 10, 661-680,doi: 10.5194/cp-10-661-2014, 2014.
- Sullivan, P. F., Arens, S. J. T., Chimner, R. A., and Welker, J. M.: Temperature and microtopography interact to control carbon cycling in a high arctic fen, *Ecosystems*, 11, 61-76,doi: 10.1007/s10021-007-9107-y, 2008.
- Swindles, G. T., Morris, P. J., Mullan, D., Watson, E. J., Turner, T. E., Roland, T. P., Amesbury, M. J., Kokfelt, U., Schoning, K., Pratte, S., Gallego-Sala, A., Charman, D. J., Sanderson, N., Garneau, M., Carrivick, J. L., Woulds, C., Holden, J., Parry, L., and Galloway, J. M.: The long-term fate of permafrost peatlands under rapid climate warming, *Sci Rep*, 5, 6,doi: 10.1038/srep17951, 2015.
- Tang, J., Miller, P. A., Crill, P. M., Olin, S., and Pilesjo, P.: Investigating the influence of two different flow routing algorithms on soil-water-vegetation interactions using the dynamic ecosystem model LPJ-GUESS, *Ecohydrology*, 8, 570-583,doi: 10.1002/eco.1526, 2015a.
- Tang, J., Miller, P. A., Persson, A., Olefeldt, D., Pilesjo, P., Heliasz, M., Jackowicz-Korczynski, M., Yang, Z., Smith, B., Callaghan, T. V., and Christensen, T. R.: Carbon budget estimation of a subarctic catchment using a dynamic ecosystem model at high spatial resolution, *Biogeosciences*, 12, 2791-2808,doi: 10.5194/bg-12-2791-2015, 2015b.
- Tarnocai, C., Canadell, J. G., Schuur, E. A. G., Kuhry, P., Mazhitova, G., and Zimov, S.: Soil organic carbon pools in the northern circumpolar permafrost region, *Glob. Biogeochem. Cycle*, 23,doi: Artn Gb202310.1029/2008gb003327, 2009.

- Thonicke, K., Venevsky, S., Sitch, S., and Cramer, W.: The role of fire disturbance for global vegetation dynamics: coupling fire into a Dynamic Global Vegetation Model, *Glob. Ecol. Biogeogr.*, 10, 661-677,doi: DOI 10.1046/j.1466-822x.2001.00175.x, 2001.
- Tomlinson, R. W.: Soil carbon stocks and changes in the Republic of Ireland, *Journal of Environmental Management*, 76, 77-93,doi: 10.1016/j.jenvman.2005.02.001, 2005.
- Turunen, J., Tomppo, E., Tolonen, K., and Reinikainen, A.: Estimating carbon accumulation rates of undrained mires in Finland - application to boreal and subarctic regions, *Holocene*, 12, 69-80,doi: 10.1191/0959683602hl522rp, 2002.
- Wania, R., Ross, I., and Prentice, I. C.: Integrating peatlands and permafrost into a dynamic global vegetation model: 1. Evaluation and sensitivity of physical land surface processes, *Glob. Biogeochem. Cycle*, 23,doi: Gb301410.1029/2008gb003412, 2009a.
- Wania, R., Ross, I., and Prentice, I. C.: Integrating peatlands and permafrost into a dynamic global vegetation model: 2. Evaluation and sensitivity of vegetation and carbon cycle processes, *Glob. Biogeochem. Cycle*, 23,doi: Gb301510.1029/2008gb003413, 2009b.
- Weltzin, J. F., Harth, C., Bridgham, S. D., Pastor, J., and Vonderharr, M.: Production and microtopography of bog bryophytes: response to warming and water-table manipulations, *Oecologia*, 128, 557-565,doi: 10.1007/s004420100691, 2001.
- Whiting, G. J. and Chanton, J. P.: Primary production control of methane emission from wetlands, *Nature*, 364, 794-795,doi: 10.1038/364794a0, 1993.
- Wieder, R. K.: Past, present, and future peatland carbon balance: An empirical model based on Pb-210-dated cores, *Ecological Applications*, 11, 327-342,doi: 10.2307/3060892, 2001.
- Wu, Y. Q., Versegny, D. L., and Melton, J. R.: Integrating peatlands into the coupled Canadian Land Surface Scheme (CLASS) v3.6 and the Canadian Terrestrial Ecosystem Model (CTEM) v2.0, *Geosci. Model Dev.*, 9, 2639-2663,doi: 10.5194/gmd-9-2639-2016, 2016.
- Yang, Z., Sykes, M. T., Hanna, E., and Callaghan, T. V.: Linking Fine-Scale Sub-Arctic Vegetation Distribution in Complex Topography with Surface-Air-Temperature Modelled at 50-m Resolution, *Ambio*, 41, 292-302,doi: 10.1007/s13280-012-0307-0, 2012.
- Yu, Z. C.: Northern peatland carbon stocks and dynamics: a review, *Biogeosciences*, 9, 4071-4085,doi: 10.5194/bg-9-4071-2012, 2012.
- Yu, Z. C., Beilman, D. W., and Jones, M. C.: Sensitivity of Northern Peatland Carbon Dynamics to Holocene Climate Change. In: *Carbon Cycling in Northern Peatlands*, Baird, A. J., Belyea, L. R., Comas, X., Reeve, A. S., and Slater, L. D. (Eds.), *Geophysical Monograph Series*, 2009.
- Yu, Z. C., Loisel, J., Brosseau, D. P., Beilman, D. W., and Hunt, S. J.: Global peatland dynamics since the Last Glacial Maximum, *Geophysical Research Letters*, 37, 5,doi: 10.1029/2010gl043584, 2010.
- Yukimoto, S., Adachi, Y., Hosaka, M., Sakami, T., Yoshimura, H., Hirabara, M., Tanaka, T. Y., Shindo, E., Tsujino, H., Deushi, M., Mizuta, R., Yabu, S., Obata, A., Nakano, H., Koshiro, T., Ose, T., and Kitoh, A.: A New Global Climate Model of the Meteorological Research Institute: MRI-CGCM3-Model Description and Basic Performance, *J. Meteorol. Soc. Jpn.*, 90A, 23-64,doi: 10.2151/jmsj.2012-A02, 2012.
- Zhang, W., Jansson, C., Miller, P. A., Smith, B., and Samuelsson, P.: Biogeophysical feedbacks enhance the Arctic terrestrial carbon sink in regional Earth system dynamics, *Biogeosciences*, 11, 5503-5519,doi: 10.5194/bg-11-5503-2014, 2014.
- Zimov, S. A., Schuur, E. A. G., and Chapin, F. S.: Permafrost and the global carbon budget, *Science*, 312, 1612-1613,doi: 10.1126/science.1128908, 2006.

Paper II

Modelling past, present and future peatland carbon accumulation across the pan-Arctic

Nitin Chaudhary, Paul A. Miller and Benjamin Smith

Department of Physical Geography and Ecosystem Science, Lund University,
Sölvegatan 12, SE- 22362 Lund, Sweden

Correspondence to: N. Chaudhary (nitin.chaudhay@nateko.lu.se)

Abstract. Most northern peatlands developed during the Holocene, sequestering large amounts of carbon in terrestrial ecosystems. However, recent syntheses have highlighted the gaps in our understanding of peatland carbon accumulation. Assessments of the long-term carbon accumulation rate and possible warming driven changes in these accumulation rates can therefore benefit from process-based modelling studies. We employed an individual- and patch-based dynamic global ecosystem model with dynamic peatland and permafrost functionality and vegetation dynamics to quantify long-term carbon accumulation rates and to assess the effects of historical and projected climate change on peatland carbon balances across the pan-Arctic. Our results are broadly consistent with published regional and global carbon accumulation estimates. A majority of modelled peatland sites in Scandinavia, Europe, Russia and Central and eastern Canada change from carbon sinks through the Holocene to potential carbon sources in the coming century. In contrast, the carbon sink capacity of modelled sites in Siberia, Far East Russia, Alaska and western and northern Canada was predicted to increase in the coming century. The greatest changes were evident in eastern Siberia, northwest Canada and in Alaska, where peat production, from being hampered by permafrost and low productivity due the cold climate in these regions in the past, was simulated to increase greatly due to warming, wetter climate and greater CO₂ levels by the year 2100. In contrast, our model predicts that sites that are expected to experience reduced precipitation rates and are currently permafrost free will lose more carbon in the future.

1 Introduction

The majority of the northern peatlands developed during the Holocene ca. 8-12 thousand years (kyr) ago, after the deglaciation of the circum-Arctic region (MacDonald et al., 2006). The availability of new land surfaces owing to ice retreat (Dyke et al., 2004; Gorham et al., 2007), climate warming following deglaciation (Kaufman et al., 2004), increased summer insolation (Berger and Loutre, 2003), more pronounced seasonality (Yu et al., 2009), greenhouse gas emissions (MacDonald et al., 2006) and elevated moisture conditions (Wolfe et al., 2000) are some of the factors that promoted the rapid

40 expansion of northern peatlands. Moderate plant productivity together with depressed decomposition
due to saturated conditions led to a surplus of carbon (C) input relative to output, resulting in the
accumulation of peat (Clymo, 1991). Peatlands of the Northern Hemisphere are estimated to have
sequestered approximately 350-500 PgC during the Holocene (Gorham, 1991; Yu, 2012).

45 Peatlands share many characteristics with upland mineral soils and non-peat wetland ecosystems.
However, they constitute a unique ecosystem type with many special characteristics, such as a shallow
water table depth, organic, C-rich soils, a unique vegetation cover dominated by bryophytes (hereinafter
referred to as “mosses”), spatial heterogeneity, anaerobic biogeochemistry and permafrost in many
regions. Due to their high C density, and the sensitivity of their C exchange with the atmosphere to
50 temperature changes, these systems are an important component in the global C cycle and the coupled
Earth system (MacDonald et al., 2006). Lately, considerable effort has been put to incorporating
peatland accumulation processes into models, with the purpose of understanding the role of peatlands in
sequestering C, thereby lowering the radiative forcing of past climate (Frolking and Roulet, 2007;
Wania et al., 2009a; Frolking et al., 2010; Kleinen et al., 2012; Tang et al., 2015), and how they might
55 affect future climate warming and the C cycling (Ise et al., 2008; Swindles et al., 2015).

Clymo (1984) developed a simple one-dimensional peat accumulation model and described the main
processes and mechanisms involved in peat growth and its development. This model became the
starting point for later work in many peat growth modelling studies. Hilbert et al. (2000) developed a
60 theoretical peat growth model with an annual step, modelling the interaction between peat accumulation
and water table depth using two coupled non-linear differential equations. Using a similar approach,
Frolking et al. (2010) developed a complex Holocene peat model by combining the dynamic peat
accumulation model of Hilbert et al. (2000) with a peat decomposition model (Frolking et al., 2001).
They showed that the model performed fairly well in simulating the long-term peat accumulation,
65 vegetation and hydrological dynamics of a temperate ombrotrophic bog in Ontario, Canada. Though the
models mentioned above are detailed enough to capture the peat accumulation and decomposition
processes quite robustly, they lack soil freezing-thawing processes, and this limits their application over
regions where such processes occur. Wania et al. (2009a) were first to account for peat dynamics in a
model for large-area application, incorporating peatland functionality in the LPJ-DGVM model,
70 designed for regional and global simulation of ecosystem responses to climate change (Sitch et al.,
2003). Their approach included a number of novel features - such as a detailed soil freezing-thawing
scheme, peatland-specific plant functional types (PFTs) and a vegetation inundation stress scheme - but
employed a two-layer representation of the peat profile, which is not as detailed as the process-based
dynamic multi-layer approaches taken by Hilbert et al. (2000) and Frolking et al. (2010).

75 Though much information is available about the past and present rates of C accumulation in the literature, recent syntheses have highlighted the existing spatial gaps in data availability across the pan-Arctic (45-75 °N) (Yu et al., 2009; Loisel et al., 2014). The extent and remoteness of many locations present challenges for the reliable estimation of total C, basal ages and C accumulation rates (CAR). In the present study, we use the individual- and patch-based dynamic global ecosystem model LPJ-GUESS (Smith et al., 2001), a climate-driven model of peat accumulation across the pan-Arctic under past, present and future climate. The model is extended to include dynamic peatland functionality and vegetation dynamics as described in Chaudhary et al. (2016) to quantify the spatial and temporal C accumulation rates (CAR) and to assess the potential effects of historical and projected climate and atmospheric CO₂ on peatland C balances at regional scale across the pan-Arctic.

85

2 Methodology

2.1 Model description

90 LPJ-GUESS (Lund-Potsdam-Jena General Ecosystem Simulator) is a process-based model of vegetation dynamics, plant physiology and the biogeochemistry of terrestrial ecosystems. It simulates vegetation structure, composition and dynamics in response to changing climate and soil conditions based on an individual- and patch-based representation of the vegetation and ecosystems of each simulated grid cell and is optimized for regional and global applications (Smith et al., 2001; Sitch et al., 2003; Miller and Smith, 2012). The model has been evaluated in comparison to independent datasets and other models in numerous studies; see e.g. Piao et al. (2013), McGuire et al. (2012), Smith et al. (2014) and Ekici et al. (2015).

We employed a version of LPJ-GUESS customised for studies of Arctic ecosystems (Miller and Smith, 2012) that has been developed to include dynamic, multi-layer peat accumulation functionality and permafrost dynamics. The model represents the major physical and biogeochemical processes in upland and wetland arctic ecosystems, including an expanded set of plant functional types (PFTs) specific to these areas (McGuire et al., 2012; Miller and Smith, 2012). The revised model is described in outline below, while a full description can be found in Chaudhary et al. (2016). In our approach, vegetation and peatland C dynamics are simulated on multiple, connected patches to account for the functional and spatial heterogeneity in peatlands. The simulated PFTs have varied structural and functional characteristics and can establish in each connected patch and compete for soil resources, area and light. The plant population and structure of the plant community is an emergent outcome of this competition. The model is initialised with a random surface constituting 10 patches of uneven height. Heterogeneity in height of adjacent patches is a precondition for hydrological redistribution between them, which mediates vegetation succession and affects the peat accumulation rate, as described below. The soil/peat

110

column is represented by four different vertically-resolved layers. A dynamic single snow layer on overlays the peat column, represented by a dynamic litter/peat layer consisting of a number of sublayers, updated yearly, that depends on its thickness. Underneath the peat column is a fixed 2 m deep mineral soil column consisting of 0.1 m thick sublayers, which is underlain by a 48 m deep “padding” column consisting of relatively thicker sublayers. The soil temperature is updated daily for each sublayer at different depths enabling the simulation of a dynamic soil thermal profile, a basis for the representation of permafrost (Wania et al., 2009a). The fractions of ice and water as well as the mineral and peat fractions in each layer govern the heat capacities and thermal conductivities and affect freezing and thawing processes of soil water in peat and mineral soil layers (Wania et al., 2009a). The fractions of water and ice in the sublayers is updated each day depending upon the variation in the soil temperature and fractional mineral content, following Hillel (1998). A detailed description of permafrost and soil temperature scheme is available in Chaudhary et al. (2016) and Miller and Smith (2012) and references therein.

A water bucket scheme was used to simulate peatland hydrology where the assumption is made that the precipitation is the main input of water. Evapotranspiration, drainage, surface and base runoff are the major water balance processes in the peat layers (Gerten et al., 2004). The model also includes lateral flow of water between patches, an important governing process of vegetation and C dynamics of peatlands that is lacking in most peatland models. From higher elevated patches (hummocks) to lower depressions (hollows), the water flows using a simple lateral flow scheme. In this scheme, water table position (WTP) of individual patches is reset to the mean landscape WTP in each daily time-step. Elevated patches lose water while the depressed patches gain water with respect to the mean landscape WTP, affecting plant productivity and decomposition rates in each patch and resulting in dynamic surface conditions over time.

Five PFTs are used to represent the main functional elements of peatland vegetation: graminoids (Gr), mosses (M), deciduous high shrubs (HSS) and deciduous and evergreen low shrubs (LSS and LSE). PFTs differ in physiological, morphological and life history characteristics that govern their interactions and responses to climate and evolving system state. Key PFT parameters in the present study include C allocation, phenology, rooting depth, tolerance of waterlogging, and decomposability of PFT-derived litter (Miller and Smith, 2012). Prescribed bioclimatic limits (Miller and Smith, 2012) and favoured annual-average WTP (aWTP) ranges determine the PFTs’ establishment and mortality (see Table A1) and reflect their distribution ranges. Shrubs are favoured in dry conditions (Malmer et al., 2005) where aWTP is below -25 cm (we use a sign convention in which a negative value of WTP signifies a water table below the peat surface). Conversely, mosses and graminoids are more vulnerable to dry conditions. Graminoids favour saturated conditions and establish when aWTP is above -10 cm while mosses establish when the aWTP is between +5 and -50 cm. The establishment function is implemented

annually and dependent on aWTP.

150

The balance between the annual addition of new litter layers on top of the mineral soil column and the daily decomposition rate governs the peat accumulation. C originating from different PFTs accrues as litter in the peat layers at variable rates depending on the differences in PFT mortality, productivity and leaf turnover. The accumulated peat decomposes on a daily time step based on the plant litter types in each layer of a patch with decomposition rates that are controlled by soil physical and hydrological properties in each layer. Differences in the peat decomposition rates among PFTs arise from their intrinsic properties and structure, parameterized using an initial decomposition rate k_0 (see Table A1) (Aerts et al., 1999; Frolking et al., 2001; Chaudhary et al., 2016) which is assumed to decline over time (Clymo et al., 1998).

155

160

The way plant access water from the mineral soil and dynamic peat layers in each patch necessitated a readjustment of the soil layer representation relative to the standard version of LPJ-GUESS, taking into account the depth of dynamic peat layers and the mineral soil layers. In the modified water uptake scheme, there are two static underlying mineral soil layers: an upper mineral soil (UMS) layer and a lower mineral soil (LMS) layer, of 0.5 and 1.5 m depth respectively. In the absence of peat, the fraction of roots in these two layers is prescribed for different PFTs (Smith et al., 2001) and determines the daily plant uptake of water from the mineral soil (Table A1) (Chaudhary et al., 2016). We prescribed rooting depth fractions of 0.7 and 0.3 to UMS and LMS, respectively, for shrubs while graminoids are assumed to have relatively shallow rooting depths, with fractions of 0.9 and 0.1 in the UMS and LMS layers respectively (Bernard and Fiala, 1986; Malmer et al., 2005; Wania et al., 2009b). During the initial stages of peat accumulation, plant roots are still present in both in UMS and LMS layers but their root proportion declines linearly as peat builds up while a greater root fraction is added to the peat layers to access water from the peat soil. Mosses are assumed to take up water from the top 50 cm of peat (Shaw et al., 2003; Wania et al., 2009b) once peat height exceeds 50cm. Before this mosses take water only from the mineral soil layers. All other PFTs can take up water from both mineral soil layers and peat layers until peat height reaches 2 m, after which they can only access water from the peat soil layers.

165

170

175

2.2 Simulation Protocol and Data Requirements

180

2.2.1 Hindcast experiments

To initialise the model with vegetation in equilibrium with early Holocene climate, the model was run from bare ground surface conditions for the first 500 years, recycling the first 30 years of the Holocene climate data set (see below), The mineral and peat layers were forced to remain saturated for the entire initialisation period. The peat decomposition, soil temperature and water balance calculations began

185

when the peat column reached a minimum thickness of 0.5 m. We adopted this model initialisation strategy to avoid sudden collapse of the peat column in very dry conditions because shallow peat can become drier or wetter within a very short span and continuous dry periods would increase temperature dependent decomposition rates and reduce the accumulation rate markedly.

190

To adequately represent the peatland history and dynamics across the major bioclimatic domains of the pan-Arctic, the model was applied at 180 grid points (referred to as ‘sites’ below) distributed among 10 geographical zones spanning the circum-Arctic from 45-75 °N (Fig. 1), each zone being represented by 10-20 randomly selected points, (see Fig. 1 and Table 1). Each simulation was run for 10,100 years, and comprised three distinct climate forcing periods. The first, Holocene phase, lasted from 10 kyr before present (BP) until 0 BP, taken to correspond to the year 1900. Details of the source and preparation of the Holocene climate forcing data are explained in Chaudhary et al. (2016). The second, historical phase ran from 1901 until 2000. Finally, the future scenario phase (see Section 2.3.2) ran from 2001 until 2100. We forced the model with daily climate fields (temperature, precipitation and cloudiness) constructed by interpolating between monthly values from 10 kyr BP until 1900, after which the CRU climate data set (Mitchell and Jones, 2005) was used for the historical phase of the simulation until the year 2000. Millennial atmospheric CO₂ concentration values from 10 kyr BP to 1850 AD used as a boundary condition in the Hadley Centre Unified Model (UM) (Miller et al., 2008) were linearly interpolated to yearly values and used to force LPJ-GUESS. Observed annual CO₂ values from atmospheric or ice core measurements were used, to force LPJ-GUESS from 1850 to 2000 (McGuire et al., 2012).

195

200

205

210

215

Accurate prediction of total C accumulation at any particular location depends on selecting the right inception period, the C content and lability of the peat material, its bulk density over time and depth, as well as local hydro-climatic conditions (Clymo, 1992; Clymo et al., 1998). Bulk density and C fraction values vary widely among different peatlands, and reliable estimates are often lacking (Clymo et al., 1998). Basal ages are the proxies of peatland initiation history, are often hard to determine and are not available for many key peatland types. For example, Eastern Siberia and European Russia are regions that have not been well-studied in this regard (Loisel et al., 2014; Yu et al., 2014a). We therefore started simulations at the same time (10 kyr BP) for all 180 sites and fixed initial bulk densities to 40 kg C m⁻³.

220

We calculated rate of C accumulation as long-term (apparent) rate of C accumulation (LARCA) and as actual (net) rate of C accumulation (ARCA) (see Fig. 2). LARCA is the ratio of total cumulative C and the peat column’s basal age. ARCA is the current rate (i.e. the most recent 30 years) at which peatland is sequestering C (Clymo et al., 1998). We also calculated near future rate of C accumulation (NFRCA) from 2001 to 2100 for the 10 studied zones (see below).

2.3.2 Climate change experiments

225 To investigate the sensitivity of CAR to climate change, the future experiments were performed (see
Table 2) by extending the base experiment (BAS) covering the Holocene and recent past climate (to
year 2000) for an additional century to year 2100 (Table 2). Climate output from the Coupled Model
Intercomparison Project Phase 5 (CMIP5) RCP8.5 (Moss et al., 2010) runs performed with the Hadley
Global Environment Model 2 (HadGEM2-ES) (Collins et al., 2011) was used to provide anomalies for
230 future climate forcing. HadGEM2-ES is an updated version of the same model chosen for the Holocene
anomaly fields. It is in the middle-of-the-range of models contributing to the CMIP5 ensemble in terms
of simulated temperature change across the Arctic region (Andrews et al., 2012; Klein et al., 2014).
Model input of atmospheric CO₂ concentrations was taken from the RCP8.5 scenario, extracted from
the International Institute for Applied Systems Analysis website (IIASA;
235 <http://tntcat.iiasa.ac.at/RcpDb/>; page visited 2 Feb 2017). In the first three experiments, the single factor
effect of temperature (T8.5), precipitation (P8.5) and CO₂ (C8.5) was examined, followed by a
combined experiment (FTPC8.5) where change in all three drivers was used to force the model. The
model output variables examined here include total CAR, net primary productivity (NPP), net
ecosystem C exchange (NEE), permafrost distribution, active layer depth (ALD) and regional soil C
240 balance.

2.3.3 Model evaluation

To evaluate the model, we compared the estimates of CAR with regional Holocene C accumulation
245 records synthesised across the pan-Arctic region, hereinafter referred to as “literature range”. Second,
time series were evaluated using observed Holocene LARCA values based on the 127 sites analysed by
Loisel et al. (2014) and the 33 sites analysed by Yu et al. (2009) were averaged in 1000-year periods
which we compared with our model simulations. The Loisel et al. (2014) dataset is more comprehensive
and contains more basal points compared to Yu et al. (2009). In Yu et al. (2009), many key regions such
250 as the Hudson Bay Lowlands, western Europe, and western and eastern Siberia were not present, while
the Loisel et al. (2014) dataset omits some regions such as Eastern Siberia and European Russia.
Furthermore, the points in these two datasets were limited to 69 °N (< 69).

3 Results

255

3.1 Hindcast experiment

While peatland initiation started at ca. 12-13 kyr BP in high latitude areas, the majority of peatlands
formed after 10 kyr BP (See Fig. A1). Mean modelled CAR among all 180 sites was 35.9 g C m⁻² y⁻¹,

260 after which it followed a similar temporal pattern to observed CAR values (Fig. 3a) (Yu et al., 2009;
Loisel et al., 2014). The observed rate calculated by Yu et al. (2009) shows a dip after 5 kyr BP but the
modelled result exhibited no such deviation (Fig. 3a). The observed rate reported by Loisel et al. (2014)
is a little higher than the simulated rate before 4 kyr BP and for the present climate. Modelled CAR was
265 higher at the beginning of the simulation in all the zones apart from Zone J (Fig. 3b). Zones A and B,
covering the Scandinavian and European regions, had high CAR in the beginning of the Holocene,
which then declined through the Holocene phase, while Zone E covering eastern Siberia displays a peak
suggesting an accelerated rate of C accumulation by the year 1900. Almost all regions exhibited similar
CAR for 7-8 kyr BP, following different trajectories thereafter.

270 Scandinavia (Zone A), Europe (B), southwest Siberia (D), central Canada (H) and northern Canada (J)
exhibit lower LARCA values compared to the pan-Arctic average (Fig. 4I) with north Canadian (J) and
European (B) sites accumulating the lowest amounts (14.5 ± 14.8 and 14.2 ± 3.7 g C m⁻² yr⁻¹ respectively)
of C through the Holocene. The other five zones (C, E, F, G and I) showed relatively higher mean
LARCA values and the peatlands in eastern Siberia (E), Alaska (F) and western Canada (G) had the
275 highest mean LARCA values (26.8 ± 13.8 , 26.4 ± 16.3 and 26.6 ± 14.7 g C m⁻² yr⁻¹ respectively). The
global mean LARCA (black dotted line) for the 10 zones was 20.8 ± 12.3 g C m⁻² yr⁻¹ (Fig. 4I and Table
1).

280 Comparing mean ARCA for each zone with the respective LARCA values indicates that the majority of
sites accumulated relatively more C in the last 30 years except Scandinavia (A), and in Europe (B) the
changes were almost negligible (Fig. 4II). The global mean ARCA for the last 30 years was 29.4 ± 27.8
g C m⁻² yr⁻¹ suggesting an upward trend in CARs since the beginning of the Holocene (Fig. 4II and
Table 1).

285 Interpolated values of permafrost (characterised in this study by ice fraction in the peat soil), ALD,
CAR and accumulated litter for the month of September are presented for the recent past and future
climate in Fig. 5, 6, 7 and A2. Figure 5(a) shows that permafrost was widely distributed from Siberia to
Canada and in parts of northern Scandinavia around the end of 20th century according to our model. The
majority of these permafrost areas were associated with shallow active layers (ALD < 0.1 m), while in
290 the southern parts of Siberia and Canada the active layers relatively deeper (Fig. 6a). The presence of
permafrost is associated with diverse levels of peatland CAR (Fig. 7a), ranging from moderate to high
litter accumulation (Fig. A2a). Large parts of western Canada, Alaska and Siberia accumulated
relatively high amounts of C by the year 2000 (Fig. A2a) according to our model.

295

3.2 Climate change experiment

300 In the FTPC8.5 experiment, where all the drivers were combined,, a marginal decrease in global mean
FLARCA ($20.78 \text{ g C m}^{-2} \text{ yr}^{-1}$) compared with the mean LARCA ($20.8 \text{ g C m}^{-2} \text{ yr}^{-1}$) (see Fig. 2) was
noticed. However, the change in CAR was quite evident in certain geographic zones (Fig. 8I and bars).
Some regions showed an increase in their C sequestration capacity while others become C neutral or
sources of C. While Scandinavian (A), European (B), central and eastern Canadian (H, I) sites are
305 projected to become C sources (Fig. 8I and bars), the remaining zones are projected to enhance their C
sink capacity in this scenario. For example, the uptake capacity of northern Canadian (J) sites is
projected to increase fourfold, to $52.3 \pm 37.0 \text{ g C m}^{-2} \text{ y}^{-1}$, from (its LARCA value of) $14.5 \pm 14.8 \text{ g C m}^{-2} \text{ y}^{-1}$
(Table 1 and Fig. 8). All zones showed a decline in CAR in T8.5 experiment, relative to the recent
historical climate (Fig. 8II). This is explained by the positive effects of temperature on soil organic
matter decomposition rates. An exception to this general pattern is seen for northern Canada (Zone J)
310 sites where warming has a positive effect on CAR (Fig. 8II and bars; positive bar value means C
source): higher temperatures create a more suitable environment for plant growth in this region where
cold weather and permafrost limit plant (and therefore litter) production under present climate
conditions (see Fig. A3). The mean modelled global NFRCA in the T8.5 experiment from the year 2000
to 2100 was $1.52 \text{ g C m}^{-2} \text{ yr}^{-1}$. This was a significant drop when compared to modelled LARCA and
315 ARCA. In this experiment, the ESM-derived (Collins et al., 2011) surface air temperature anomalies
used to force our model increase by approximately 5°C by 2100 relative to 2000. Higher temperature is
associated with elevated decomposition rates leading to more C loss and higher heterotrophic
respiration. Projected precipitation increases in the P8.5 experiment resulted in higher CAR in all zones.
Regionally, Siberia and Far East Russia (C, D, E), Alaskan (F) and Canadian (G, H, I, J) sites showed
320 the largest changes, while very little change was seen for the Scandinavia (A) and European (B) sites
(Fig. 8III and bars). Elevated CO_2 in the atmosphere enhanced the rate of plant photosynthesis which
led to higher CAR in the C8.5 experiment in all zones (Fig. 8IV and bars).

Our simulations suggest that the significant temperature increase implied by the RCP8.5 future scenario
325 will lead to disappearance or fragmentation of permafrost from the peat soil, and deeper active layers,
(Fig. 5b). The resultant change in soil water levels and saturation could then either suppress or
accelerate the decomposition rate at many peatland locations (Fig. 8II). In the Siberian (C, D and E) and
Alaskan (F) zones, the projected higher decomposition rates are compensated by higher plant
productivity (Fig. 8III and IV); bars), leading to a net increase in CAR by 2100 in this scenario.

330 From Figure 5(b), it is evident that permafrost area declines, remaining limited to central and eastern
parts of Siberia and the north Canadian region under the future experiment in our model (FTPC8.5).
Permafrost disappears from the large parts of western Siberia and southern parts of Canada with very

335 little remaining presence in Scandinavia (Fig. 5b). This degradation in permafrost leads to deeper active
layers (Fig. 6b,c) and wetter conditions initially in large areas of peatlands currently underlain by
permafrost. Wetter conditions together with CO₂ fertilization lead to high CAR in these areas with high
C build up. In contrast, non-permafrost peatlands showed a decline in CAR and in total litter
accumulation due to higher decomposition rates (Figs. 7b,c and A2b,c) as a result of increases in
evapotranspiration, which draw down the WTP (not shown here).

340

4 Discussion

LARCA expresses the rate of C accumulated in a peatland since its inception (Clymo et al., 1998) and is
a useful metric of the sequestration capacity of peatlands because the current C uptake rate (ARCA) is a
345 snapshot in time that is not expected to reflect the C balance dynamics through the history of the
peatland (Lafleur et al., 2001; Roulet et al., 2007). Recent CAR tends to be higher compared to LARCA
because older peat would have experienced more decay losses, leaching and erosion (Lafleur et al.,
2001). This is clearly reflected in our result (Table 1) where LARCA < ARCA in most cases, even
though in our study only decay losses were considered.

350

The variability in LARCA among sites within a region with relatively similar climate highlights the
influence of local factors (Borren et al., 2004). If climate was the major driving factor behind observed
variations in LARCA then all the peatland types within one climate zone would be expected to have
similar LARCA values. LARCA is highly influenced by local hydrology, topography, climate
355 conditions, permafrost, fire events, substrate, microtopography and vegetation succession (Clymo,
1984; Robinson and Moore, 2000; Beilman, 2001; Turunen et al., 2002; Turetsky et al., 2007).
Furthermore, some studies attribute differences in LARCA values to the overrepresentation of
terrestrialised peatlands and an underrepresentation of paludified or shallow peatlands (Botch et al.,
1995; Tolonen and Turunen, 1996; Clymo et al., 1998) in estimations of this metric. Our model
360 initialisation allowed vegetation to reach an equilibrium with the climate of 10 kyr ago, but the model
ignores the presence of ice over some parts of the study area at this time, thus overestimating the
vegetation cover at the beginning of the simulation, leading to higher CAR than observed (Fig. 3a,b). In
addition, the underlying topography is a major factor for peat initiation and lateral expansion of any
peatland complex but no such data are available for regional simulations. Therefore, we assumed a
365 moist, on average horizontal, soil surface upon which peatland could potentially form at each of our 180
simulation points, ignoring the role of underlying topography and its effects on water movement within
a basin. However, the lateral exchange between higher and lower patches within an overall horizontal
landscape was included in our model (see Section 2).

370 The mean modelled LARCA across the pan-Arctic study area was $20.8 \pm 12.3 \text{ g C m}^{-2} \text{ yr}^{-1}$, a value that
falls within the reported range for northern peatlands, namely $18.6\text{-}22.9 \text{ g C m}^{-2} \text{ yr}^{-1}$ (Yu et al., 2009;
Loisel et al., 2014). However, the Loisel et al. (2014) dataset is not completely representative of the
pan-Arctic region and data from some key regions are missing, such as eastern Siberia and European
Russia (Yu et al., 2014a). The Loisel et al. (2014) dataset includes points that are mainly from
375 deep/central parts and shallow peat basins are underrepresented (MacDonald et al., 2006; Gorham et al.,
2007; Korhola et al., 2010). Furthermore, the dataset is limited to areas north of 69°N . Inclusion of
shallow peatland complexes and more sub-arctic and arctic sites in the synthesis might conceivably
bring down the mean observed LARCA value. Nevertheless, the overall trend of the modelled, global-
averaged CAR ($n = 180$) for the last 10 kyr is quite similar to these published syntheses (Fig. 3a and b
and Table 1).

380 Suitable climate (moist and cool) and optimal local hydrological conditions influenced by favourable
underlying topographical settings accelerated the CAR which led to the formation of large peatland
complexes in the pan-Arctic region (Yu et al., 2009). CAR is the balance between biological inputs
(litter accumulation) and outputs (decomposition and leaching) and these two important processes are
385 quite sensitive to climate variability (Clymo, 1991). High CAR is associated with high plant
productivity and a moist climate leading to shorter residence time in acrotelm layers and generation of
recalcitrant peat, or a combination of any of these factors (Yu, 2006). In many regions, CAR is also
influenced by the presence of permafrost. Under stable or continuous permafrost conditions, the CAR
slows down or ceases (Zoltai, 1995; Blyakharchuk and Sulerzhitsky, 1999) due to low plant
390 productivity. CAR may also become negative due to wind abrasion and thermokast erosion, but these
factors are not considered in our simulations. In contrast, areas underlain by sporadic and discontinuous
permafrost sequester relatively more C (Kuhry and Turunen, 2006).

395 Significant increases in temperature are expected at high latitudes in the coming century, even under the
most optimistic emissions reduction scenarios. Under these conditions, some peatlands could sequester
more C (Charman et al., 2013) while others could turn into C sources and degrade (Ise et al., 2008; Fan
et al., 2013). Permafrost peatlands are sensitive ecosystems and respond quite rapidly to temperature
change as well as other aspects of climate (Christensen et al., 2004). The formation of thermokast lakes,
400 degradation of palsas, flooding and subsidence of the land surface are key features that might be
indicators of and the result of rapid warming and permafrost decay. Soil subsidence-driven pond
formation has been observed to lead to a total shift from a recalcitrant moss-dominated vegetation
community to dominance by non-peat forming plant types such as *Carex* sp. (Malmer et al., 2005).
However, the complex physical process inducing such changes is not included in this model.

405 In our scenario simulations (Table 2), we find that higher temperature leads to thawing of permafrost
that in turn increases the moisture availability, at least initially. The rise in temperature also results in
early spring snowmelt and a longer growing season (Euskirchen et al., 2006) while, in the same time
frame, atmospheric CO₂ concentration will also increase. These factors lead to increases in plant
productivity, leading to higher CAR (Klein et al., 2013), even in cases where moisture- and
410 temperature-driven peat decomposition also speeds up.

High temperature and limited moisture conditions with limited or no permafrost are associated with an
increase in the Bowen ratio, implying a shift towards drier conditions which accelerates the peat
decomposition and in turn reduces CAR (Franzén, 2006; Ise et al., 2008; Bragazza et al., 2016). This
415 will also result in draw down of water position and dominance of woody shrubs. The latter trend,
namely an expansion of shrubs across the Arctic and beyond in the next half of the 21st century, is in
keeping with other studies (Sturm et al., 2005; Loranty and Goetz, 2012). Conversely, warmer and
wetter future climate conditions, in combination with CO₂ fertilization, could lead to increased CAR in
areas projected to have a higher precipitation rate, compensating temperature enhancement of
420 decomposition.

Simulated responses of peatland to the differential climate conditions of the studied regions reflect a
range of model responses, and are discussed in relation to available literature knowledge below.

425 **4.1 Scandinavia and Europe (Zones A and B)**

In the Scandinavian region (Zone A), observed mean LARCA values vary between 11.8 and 26.1 g C
m⁻² y⁻¹ (Tolonen and Turunen, 1996; Makila, 1997; Clymo et al., 1998; Makila et al., 2001; Makila and
Moisanen, 2007). Modelled averaged LARCA for this zone (17.2 ± 7.4 g C m⁻² y⁻¹) is within the
430 reported literature range (Fig. 4 Zone A and Table 3). A more representative LARCA estimate derived
from 1302 dated peat cores from all Finnish undrained peatlands is 18.5 g C m⁻² y⁻¹ (Turunen et al.,
2002), which is also quite close to our estimate. LARCA estimates from 10 sites in northern Sweden
range from 8-32 g C m⁻² y⁻¹, with an average of 16 g C m⁻² y⁻¹ (Klarqvist et al., 2001a). Estimates of
LARCA from Russian Karelia, adjacent to Scandinavia, are reported as 20 g C m⁻² yr⁻¹ (Elina et al.,
435 1984). The recent observed rate (ARCA) ranges between 8.1-23.0 g C m⁻² yr⁻¹ (mean 12.1 g C m⁻² y⁻¹)
for Scandinavia (Korhola et al., 1995) which can be compared to the modelled ARCA value ($13.6 \pm$
18.2 g C m⁻² y⁻¹) in this zone.

The modelled LARCA (14.2 ± 3.7 g C m⁻² y⁻¹) for central and eastern Europe (Zone B) is relatively low.
However, while some sites in this region are reported as being quite productive (21.3 ± 3.7 g C m⁻² y⁻¹;
440 Anderson (2002)), long-term CAR estimates are available for relatively few sites (Charman, 1995;

Anderson, 1998), making a comparison difficult. The points that fall in the British Isles showed lower modelled LARCA ($12\text{--}14 \text{ g C m}^{-2} \text{ y}^{-1}$) values than observed literature range indicating shortcomings in the simulation of local hydrological conditions, or a possible bias in the climate forcing of our model. A decline in CAR in Scandinavia and Europe over recent decades is apparent in our simulations. Some observational studies also point to a reduced rate of C accumulation in recent years for this region (Clymo et al., 1998; Klarqvist et al., 2001b; Gorham et al., 2003). This slowing has been attributed to an increase in decay rates due to climate and hydrological changes, the development of a stable structure (Malmer and Wallen, 1999), divergence in the rate of nutrient supply, or a combination of these factors (Franzén, 2006). Our model predicts that the C sequestration capacity of the Scandinavian region will decrease after 2050 and become C neutral, with peatland in the European region becoming a C source in the same time frame (Fig. 8(I) Zones A and B). The simulated future C losses are associated with increase in the decomposition rate due to higher temperatures and a lower soil water table, the latter resulting from the combination of marginal or no increase in precipitation and soil water loss due to higher evapotranspiration.

4.2 Siberia (Zones C and D) and Far East Russia (Zone E)

Large peatland complexes were formed in western Siberia during the Holocene and around 40% of the world's peat deposits are found in this region, covering more than 300 million ha (Turunen et al., 2001; Bleuten et al., 2006). LARCA for west Siberia has been estimated at 5.4 to 38.1 $\text{g C m}^{-2} \text{ y}^{-1}$ (Beilman et al., 2009). The modelled LARCA for the northwest and southwest region is 24.6 ± 14.6 and 16.7 ± 8.6 respectively (Fig. 5 Zones C and D and Table 3). The combined average modelled LARCA for the north and southwest Siberian (C+D) zones is $20.6 \text{ g C m}^{-2} \text{ y}^{-1}$. Turunen et al. (2001) report average LARCA from 11 sites in northwestern Siberia at $17.2 \text{ g C m}^{-2} \text{ yr}^{-1}$ (range from 12.1 to 23.7 $\text{g C m}^{-2} \text{ yr}^{-1}$). Botch (1995) estimated relatively higher LARCA (31.4–38.1 $\text{g C m}^{-2} \text{ y}^{-1}$) for the raised string bogs in western Siberia. These observations are in line with our modelled range of $24.6 \pm 14.6 \text{ g C m}^{-2} \text{ yr}^{-1}$ for the northwestern sites.

Borren et al. (2004) found LARCA values between 19–69 $\text{g C m}^{-2} \text{ y}^{-1}$ for the southern taiga zones of southwestern Siberia. The modelled LARCA value for the southwestern zone (D) is $16.7 \pm 8.6 \text{ g C m}^{-2} \text{ y}^{-1}$. The apparent underestimation by our model could be explained by the relatively larger area encompassed by our simulations, extending into warmer southerly areas with limited peat accumulation, compared to the aforementioned studies (Fig. 5 Zones C and D and Table 3). Borren and Bleuten (2006) modelled a LARCA range of 10–85 $\text{g C m}^{-2} \text{ y}^{-1}$ (mean 16 $\text{g C m}^{-2} \text{ y}^{-1}$) for a large mire complex in southwestern Siberia and our value falls within this range.

The mean observed LARCA was $10.6 \pm 5.5 \text{ g C m}^{-2} \text{ y}^{-1}$ for a permafrost polygon peatland of Far East Russia (Gao and Couwenberg, 2015). Botch et al. (1995) cite CAR values of $44.8 \text{ g C m}^{-2} \text{ y}^{-1}$ for both Kamchatka and Sakhalin regions and $33.6 \text{ g C m}^{-2} \text{ y}^{-1}$ for Far East regions. Our modelled estimate $26.8 \pm 13.8 \text{ g C m}^{-2} \text{ y}^{-1}$ is broadly comparable to the range of these observations.

480

Our model predicted that the sink capacity ($22.7 \text{ g C m}^{-2} \text{ y}^{-1}$) of the entire Russian region (C, D and E) was higher than the pan-Arctic average (Fig. 4 and Table 3). In future, higher temperature and precipitation, together with increases in snow depth, result in permafrost degradation that will lead to a deeper active layer in the western part of Siberia (Fig. 5b, 6b). Plants experience improved hydrological conditions due to a deeper ALD. Thawing of the permafrost in the peat and mineral soils coupled with a longer growing season and CO_2 fertilization leads to higher plant productivity, offsetting the higher decomposition rate leading to an increase in CAR (Fig. 7b, c). Hence, this region is projected to act as a C sink in the future (Fig. 8 a). It is notable in our simulations that temperature increases in the T8.5 experiment have a very limited overall effect on decomposition rate in Russia (Zones C, D and E) while precipitation and CO_2 fertilization have a positive effect on C build up (Fig. 8 b, c and d).

485

490

4.3 Canada (zones G to J) and Alaska (zone F)

Canada's Mackenzie River Basin and Hudson Bay Lowlands are two of the largest peatland basins in the world (Beilman et al., 2008). The individual observed C accumulation rates vary considerably across Canada and the LARCA for the entire Canadian region ranges from 0.2 to $45 \text{ g C m}^{-2} \text{ y}^{-1}$ (see Table 3). The modelled mean LARCA value averaged among zones G-J (the entire Canadian region) is $21.2 \text{ g C m}^{-2} \text{ y}^{-1}$. Most observational studies have been carried out in the western and central regions of Canada (Halsey et al., 1998; Vitt et al., 2000; Beilman, 2001; Yu et al., 2003; Sannel and Kuhry, 2009).

500

However, in recent years, studies have been conducted in the Hudson Bay and James Bay Lowlands of eastern Canada (Loisel and Garneau, 2010; van Bellen et al., 2011; Bunbury et al., 2012; Lamarre et al., 2012; Garneau et al., 2014; Holmquist and MacDonald, 2014; Packalen and Finkelstein, 2014).

505

Observed LARCA in zone I is relatively low, as peatlands initiated later in this region due to a late Holocene thermal maximum (5.0–3.0 kyr; Yu et al., 2009) and the presence of the remnants of the Laurentide ice sheet (Gorham et al., 2007). In our model simulations, all peatlands were initiated at the same time and we have not considered the influence of ice sheet cover, explaining the higher modelled CARs ($25.3 \pm 11.8 \text{ g C m}^{-2} \text{ y}^{-1}$) in the eastern region. The observed LARCA of the three main eastern regions in Canada is: Quebec ($26.1 \text{ g C m}^{-2} \text{ y}^{-1}$; Garneau et al., 2014), Hudson Bay Lowlands ($18.5 \text{ g C m}^{-2} \text{ y}^{-1}$; Packalen and Finkelstein, 2014) and James Bay Lowlands ($23.9 \text{ g C m}^{-2} \text{ y}^{-1}$; Holmquist and MacDonald, 2014), and other studies in the area have similar values (see Table 3). Our simulations suggest that permafrost will disappear from large areas of southern Canada under the RCP8.5 climate change scenario, leading to deeper ALD (Fig. 5b, 6b). While western and northern Canadian regions

510

sequester C at higher rates from 2001 to 2100 in our simulations, central and eastern parts turn into a C source over the same time period. Decomposition rate will increase due to higher temperatures, overriding the positive gains due to precipitation and C fertilization in central and eastern regions (Fig. 8 zones H and I).

The majority of simulated points in northern Canada (Zone J) are in the continuous or discontinuous permafrost region (Sannel and Kuhry, 2009). Observed LARCA values in this zone vary from 0.2 to 16.5 g C m⁻² y⁻¹ (see Table 3). Similarly, the modelled CAR of the northern Canadian sites was lowest (14.5 ±14.8 g C m⁻² y⁻¹) as a result of cold climate conditions (Table 4). The mean temperature in this zone is around -15 °C, with short growing seasons and low precipitation rates, the majority of which falls as snow. In some sites, negligible CARs were noticed due to extremely cold climate conditions that limited plant productivity. In other sub-arctic regions, similar effects of cold climate and permafrost conditions have been observed. For instance, LARCA ranges from 12.5 to 16.5 g C m⁻² y⁻¹ for the center polygon peatlands in western Canada (Vardy et al., 2000) and 11 g C m⁻² y⁻¹ in the northern Yukon (Ovenden, 1990). Similarly, polygon peat plateaus in eastern Siberia have sequestered C at low rates (10.2 g C m⁻² y⁻¹) (Gao and Couwenberg, 2015). Lately, owing to recent climate warming and permafrost thaw, bioclimatic conditions have changed in these peatlands and many of them have seen two to threefold increases in CAR (Ali et al., 2008; Loisel and Garneau, 2010), indicating a recent shift toward an increased C sink capacity. A fourfold increase in CAR, associated with permafrost thaw and increased primary productivity, was simulated under future warming by our model (Table 1 and Fig. 8 Zone J).

Alaska hosts around 40 million ha of peatland area (Kivinen and Pakarinen, 1981). Studies show that LARCA in this region ranges from 5 to 20 g C m⁻² yr⁻¹ (see Table 3). Our modelling results (26.4 ±16.3 gC m⁻² yr⁻¹) may be overestimations (Table 1 and Fig. 4 Zone F). The higher CAR values in our simulations are caused by high plant productivity, moist climate conditions, the generation of recalcitrant peat or a combination of these factors. This overestimation of CAR in Alaska casts doubt on the simulated large future sink capacity of the study area (55.5 ±16.3 gC m⁻² yr⁻¹) under the RCP8.5 scenario.

4.4 Future climate impacts on peatlands

Our simulations under the strong RCP8.5 forcing scenario indicate a sharp reduction in the area underlain by permafrost in e.g. western Siberia and western Canada, leading to an initial increase in moisture conditions or wet surfaces there. The increase in moisture conditions can dampen the amplifying effects of temperature on decomposition rates, leading to net increase in CAR (Figs. 6, 7 and

550 8). By 2100, our model indicates that permafrost areas will be limited to eastern Siberia, northern and western Canada and parts of Alaska (Fig. 7).

In future, areas currently devoid of permafrost, mainly Europe and Scandinavia, eastern parts of Canada and European Russia, could lose a substantial amount of C due to drying of peat in conjunction with a deeper WTP (Fig. 8). In a modelling study, (Ise et al., 2008) used a coupled physical–biogeochemical soil model at a site in northern Manitoba, Canada, and found that peatlands could respond quickly to warming, losing labile soil organic carbon during dry periods. Similarly, Borren and Bleuten (2006), using a three-dimensional dynamic model with imposed artificial drainage to simulate the Bakchar bog in western Siberia, indicated that LARCA will drop from 16.2 to 5.2 g C m⁻² y⁻¹ during the 21st century due to higher decomposition linked to reduced peat moisture content. Our simulations are based on climate forcing derived from the RCP8.5 scenario output from one earth system model (HadGEM2-ES). We expect that simulated changes in permafrost and C accumulation would be more moderate and slower if the model were forced with more moderate levels of climate change.

565 Overall, we found that Scandinavia, Europe, Russia and Central and eastern Canadian sites could turn into C sources while the C sink capacity could be enhanced at other sites (Fig. 8). The greatest changes were evident in eastern Siberia, northwest Canada and in Alaska. Peat production was initially hampered by permafrost and low productivity due to the cold climate in these regions but initial warming coupled with a moisture rich environment and greater CO₂ levels could lead to rapid increases in CAR by 2100 in this scenario. In contrast, sites that experience reduced precipitation rates and that are currently without permafrost could lose more C in the future.

570 **5 Conclusion**

Our model, which uniquely among large-scale models of high-latitude ecosystems accounts for feedbacks between hydrology, peat properties, permafrost dynamics and dynamic, climate-sensitive vegetation composition, is able to reproduce broad, observed patterns of peatland C and permafrost dynamics across the pan-Arctic region. Under a business-as-usual future climate scenario, we showed that non-permafrost peatlands may be expected to become a C source due to soil moisture limitations, while permafrost peatlands gain C in our simulations due to initial increase in soil moisture as a result of permafrost thawing, which suppresses decomposition while enhancing plant production. We also demonstrate that the extant permafrost area will be reduced and limited to central and eastern parts of Siberia and the north Canadian region by the late 21st century, disappearing from large parts of western Siberia and southern parts of Canada with very little presence in Scandinavia. Our modelling approach contributes to our understanding of the long-term peatland dynamics at regional and global scale. The implications of future climate change for peatland C stocks is also discussed. As such it complements

empirical research in this field but also requires its output for model development and evaluation. We
585 plan to incorporate methane biogeochemistry and nutrient dynamics in the next model update. In future,
the model will be coupled to the atmospheric component of a regional Earth system model to examine
the role of peatland-mediated biogeochemical and biophysical feedbacks to climate change in the Arctic
and globally.

590

Acknowledgements

595 This study was funded by the Nordic Top Research Initiative DEFROST and contributes to the strategic research areas Modelling the Regional and Global Earth System (MERGE) and Biodiversity and Ecosystem Services in a Changing Climate (BECC). We also acknowledge support from the Lund University Centre for the study of Climate and Carbon Cycle (LUCCI). Simulations were performed on the Aurora resource of the Swedish National Infrastructure for Computing (SNIC) at the Lund University Centre for Scientific and Technical Computing (Lunarc), project no. 2016/1-441.

600 **Table 1.** Mean modeled C accumulation rates at different timescales in 10 zones

Zone	Region	Latitude range (λ)	Longitude range (ϕ)	No. of points (n)	LARCA ($\text{gCm}^{-2} \text{y}^{-1}$)	ARCA ($\text{gCm}^{-2} \text{y}^{-1}$)	NFRCA (FTPC8.5) ($\text{gCm}^{-2} \text{y}^{-1}$)
A	Scandinavia	50 to 75	0 to 30	20	17.2 ± 7.4	13.6 ± 18.2	-5.2 ± 18.4
B	Europe	45 to 75	-10 to 60	20	14.2 ± 3.7	14.2 ± 14.6	-28.1 ± 28.5
C	Northwest Siberia	60 to 75	50 to 120	20	24.6 ± 14.6	35.9 ± 18.9	40.3 ± 12.1
D	Southwest Siberia and parts of central Asia	45 to 60	50 to 120	20	16.7 ± 8.6	39.1 ± 25.1	20.1 ± 21.2
E	Far east Russia and parts of central Asia	45 to 75	120 to 180	20	26.8 ± 13.8	50.7 ± 43.6	42.1 ± 23.5
F	Alaska	55 to 75	190 to 220	12	26.4 ± 16.3	32.2 ± 31.3	55.5 ± 16.3
G	Western Canada	50 to 75	220 to 240	13	26.6 ± 14.7	32.2 ± 36.5	38.5 ± 16.2
H	Central Canada and parts of US	45 to 60	240 to 270	20	18.3 ± 7.9	24.8 ± 12.2	3.1 ± 21.0
I	Eastern Canada and parts of US	45 to 60	270 to 300	20	25.3 ± 11.8	28.2 ± 22.1	-5.21 ± 26.1
J	Northern Canada	60 to 75	240 to 300	15	14.5 ± 14.8	23.7 ± 28.9	52.3 ± 19.2
-	pan-Arctic	45 to 75	0 to 360	180	20.8 ± 12.3	29.4 ± 27.8	18.3 ± 47.2

Table 2. Summary of hindcast and global change experiments

Experiment no.	Experiment name	Description of hindcast and future experiments
1.	BAS	Base experiment
2.	T8.5	RCP8.5 temperature only
3.	P8.5	RCP8.5 precipitation only
4.	C8.5	RCP8.5 CO ₂ only
5.	FTPC8.5	RCP8.5 including all treatments

Table 3. Observed regional long-term rate of peatland C accumulation across northern latitude areas

Individual zone	Country	Extent	Type	No. of cores (sites)	Climate zone	LARCA mean (range) (gCm ⁻² y ⁻¹)	Reference
Zone A and B	Scandinavia and Europe						
1.	Finland	Entire	Bogs and fens	1028	Sub-arctic and boreal	26.1 (2.8-88.6)	Tolonen and Turunen (1996)
2.	Finland	Haukkasuo	Bogs	79	Boreal	19.1 (16.7-22.3)	Makila (1997)
3.	Finland	Entire	Bogs and fens	-	Sub-arctic and boreal	21.0	Clymo et al. (1998)
4.	Sweden	North	Bogs and fens	10	Boreal	16.0 (8-32)	Klarqvist et al. (2001a)
5.	Finland	Entire	Bogs and fens	1302	Sub-arctic and boreal	18.5 (16.9-20.8)	Turunen et al. (2002)
6.	Finland	Luovuoma	Fen	58	Sub-arctic	11.8 (5-30)	Makila and Moisanen (2007)
7.	Finland	South and central	Bogs and Fens	10	Sub-arctic and boreal	21.7 (19.4-24.0)	Makila (2011)
8.	Scotland	North	Bogs	3	Boreal	21.3 (11.5-35.2)	Anderson (2002)
Zone C, D and E	Siberia and Far East Russia						
1.	FSU ¹	Entire	Bogs and fens	-	Sub-arctic and boreal	30	Botch et al. (1995)
	Siberia	West	Bogs	-	Sub-arctic and boreal	31.4 - 38.1	Botch et al. (1995)
2.	Siberia	Northwest	Bogs and fens	11	Boreal	17.29 (12.1-23.7)	Turunen et al. (2001)
3.	Siberia	Northwest	Bogs and fens	23	Sub-arctic	17.1 (5.4-35.9)	Beilman et al. (2009)
4.	Siberia	Southwest	Bogs and fens	8	Boreal	19-69	Borren et al. (2004)
5.	Siberia	Kamchatka	Bogs	-	-	44.8	Botch et al. (1995)
6.	Siberia	Sakhalin	Bogs	-	-	44.8	Botch et al. (1995)
7.	Siberia	Far East region	Bogs	-	-	33.6	Botch et al. (1995)

¹ FSU- Former Soviet Union

8.	Siberia	Yakutia	Polygon peatland	4	Sub-arctic	10.6 (8.9-13.8)	Gao and Couwenberg (2015)
Zone F and G	Western Canada and Alaska						
1.	W. Canada	-	Bogs and fens	-	Arctic, sub-arctic and boreal	19.4	Vitt et al. (2000)
2.	Alaska	South-central	Bogs and fens	4	Boreal	15 (5-20)	Jones and Yu (2010)
3.	Alaska	South-central	Bogs and fens	4	Boreal	11.5 ²	Loisel and Yu (2013)
4.	Alaska	-	Bogs and fens	-	Sub-arctic and boreal	12.6 (8.6-16.6)	Gorham (1991)
Zone H and I	Central and Eastern Canada						
1.	E. Canada	Hudson Bay Lowlands, Ontario	Bogs and fens	17	Sub-arctic	18.5 (14-38)	Packalen and Finkelstein (2014)
2.	E. Canada	Hudson Bay Lowlands, Ontario	Bogs and fens	1	Sub-arctic	18.9 (8.1- 36.7)	Bunbury et al. (2012)
3.	E. Canada	Hudson Bay Lowlands, Quebec	Bogs and fens	2	Sub-arctic	24 (23.19-24.19)	Lamarre et al. (2012)
4.	E. Canada	James Bay Lowlands, Quebec	Bog	3	Boreal	16.2 (14.4-18.9)	van Bellen et al. (2011)
5.	E. Canada	James Bay Lowlands, Quebec	Bogs and fens	13	Sub-arctic and boreal	23.6 (17.6-38.5)	Gorham et al. (2003)
6.	N. America and E. Canada	Maine, Newfoundland and Nova Scotia	Bogs	3	Boreal	34.8 (28.5-45)	Charman et al. (2015)
7.	E. Canada	New Brunswick, Quebec, Ontario, Prince Edward Island, Nova Scotia	Bogs	15	Sub-arctic and boreal	19 (5.1-34.6)	Turunen et al. (2004)
8.	C. Canada	Upper Pinto fen, Alberta	Fen	1	Boreal	31.1	Yu et al. (2003)
9.	C. Canada	Goldeye Lake	Fen	1	Boreal	25.5 (7.8-113)	Yu (2006)

² CAR over past 4000 years

10.	C. Canada	Central	Bogs and fens	14	Sub-arctic and boreal	24.8 (8-37.5)	Yu (2006)
11.	C. Canada	Alberta	Fens	4	Boreal	32.5 (21.4-44.2)	Yu et al. (2014b)
12.	C. Canada	Mariana	Fen		Boreal	33.6 (7.0-70.6)	Nicholson and Vitt (1990)
13.	E. Canada	Hudson Bay and James Bay Lowlands	Bogs	8	Sub-arctic and boreal	23.95 (16.5-33.9)	Holmquist and MacDonald (2014)
14.	E. Canada	James Bay Lowlands, Quebec	Bogs	4	Boreal	22.5 (9.1-41.7)	Loisel and Garneau (2010)
15.	E. Canada	Quebec	Bogs	21	Sub-arctic and boreal	26.1 (10-70)	Garneau et al. (2014)
Zone J	Northern Canada						
1.	N. Canada	-	-	22	Sub-arctic	0.2 -13.1	Robinson and Moore (1999)
2.	N. Canada	Nunavut, Northwest Territories	Polygon peatlands	4	Sub-arctic and low arctic	14.1 (12.5-16.5)	Vardy et al. (2000)
3.	N. Canada	Yukon	-	-	Sub-arctic	11.0	Ovenden (1990)
4.	N. Canada	-	-	-	Sub-arctic	9.0	Tarnocai (1988)
5.	N and C. Canada	Selwyn Lake and Ennadai Lake	Peat plateau	2	Sub-arctic	12.5-12.7	Sannel and Kuhry (2009)
6.	N. Canada	Baffin Island	-	-	Arctic and sub-arctic	0.2-2.4	Schlesinger (1990)

Figures:

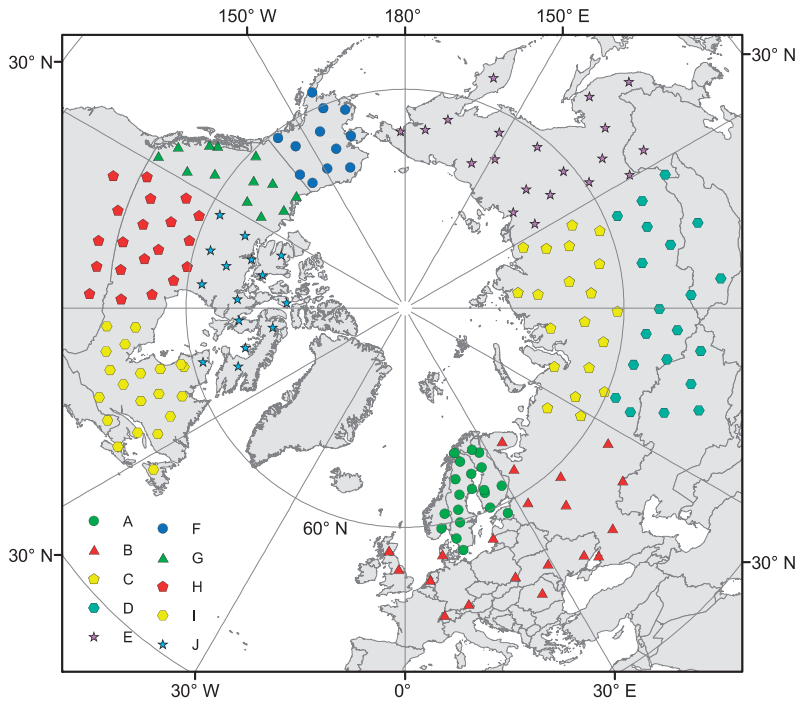


Fig. 1 Location of 180 randomly selected simulation sites spread across 10 geographical zones between 45 and 75°N.

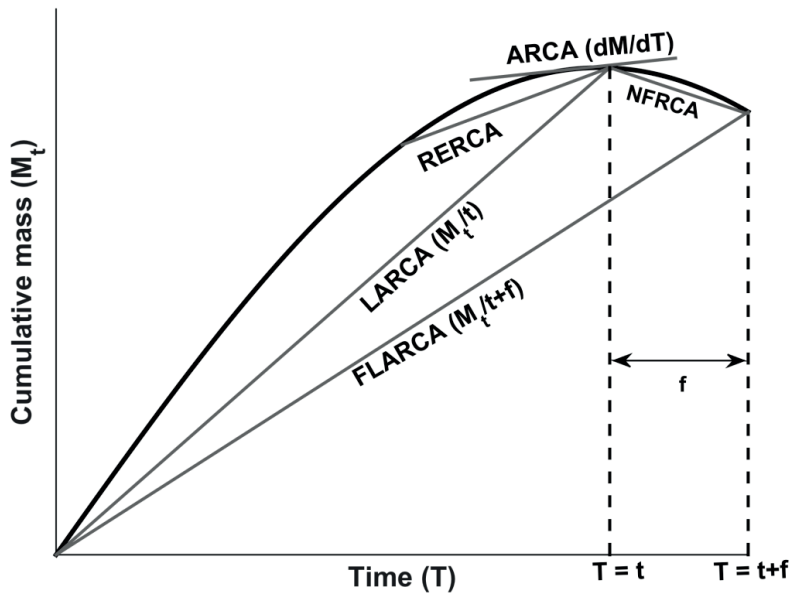


Fig. 2 Commonly used measures of peat accumulation rate: long-term (apparent) rate of C accumulation (LARCA), recent rate of C accumulation (RERCA), actual rate of C accumulation (ARCA), simulated future long-term (apparent) rate of C accumulation (FLARCA), and near future rate of C accumulation rate (NFRCA) (Adapted from Rydin and Jeglum (2013))

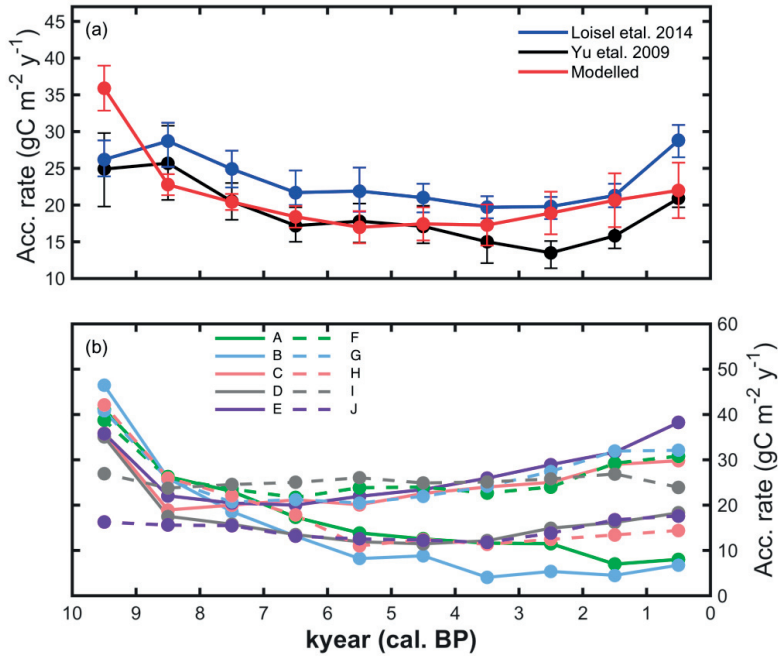


Fig. 3 (a) Simulated and observed mean C accumulation rate ($\text{g C m}^{-2} \text{y}^{-1}$) for each 1000-year period for the last 10,000 years. Red: simulated mean (and standard error of the means) CAR based on 180 random sites. Blue and black points observed C accumulation rates ($\text{g C m}^{-2} \text{y}^{-1}$) based on 127 (Loisel et al., 2014) (blue points) and 33 sites (Yu et al., 2009) (black points) across northern peatlands with error bars showing standard errors of the means, (b) mean C accumulation rate ($\text{g C m}^{-2} \text{y}^{-1}$) for each zone (Fig 1) for each 1000-year period for the last 10,000 years

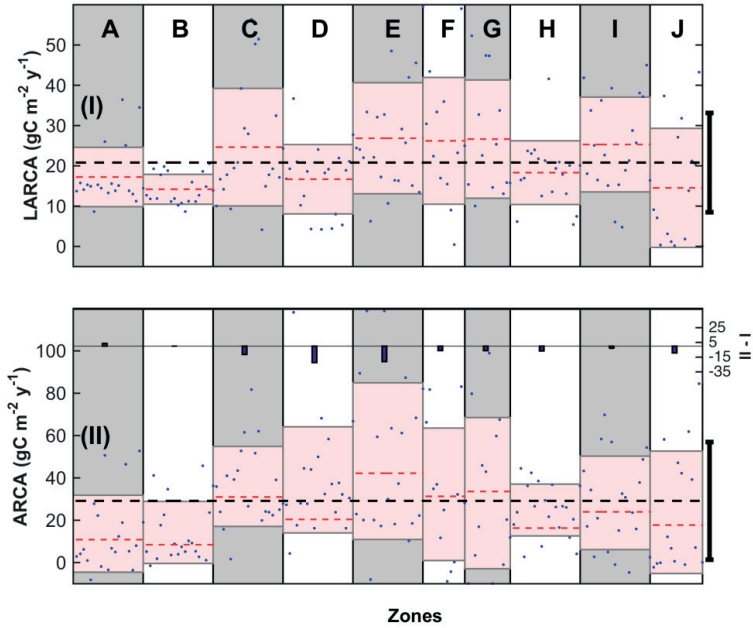


Fig. 4 Simulated Holocene peat accumulation rates across the 10 zones considered in this study (blue dots) and for the pan-Arctic region as a whole (black lines). The x-axis shows the number of sites partitioned into 10 zones. The black dotted line is the global average with standard deviation (black line outside the y-axis) and the red dotted line is the average among zones with standard deviation in light red patch. (I) simulated long-term (apparent) rate of C accumulation (LARCA); (II) simulated actual rate of C accumulation (ARCA) for the last 30 years. Blue bars show the difference between ARCA and LARCA mean values for the respective zone (II-I)

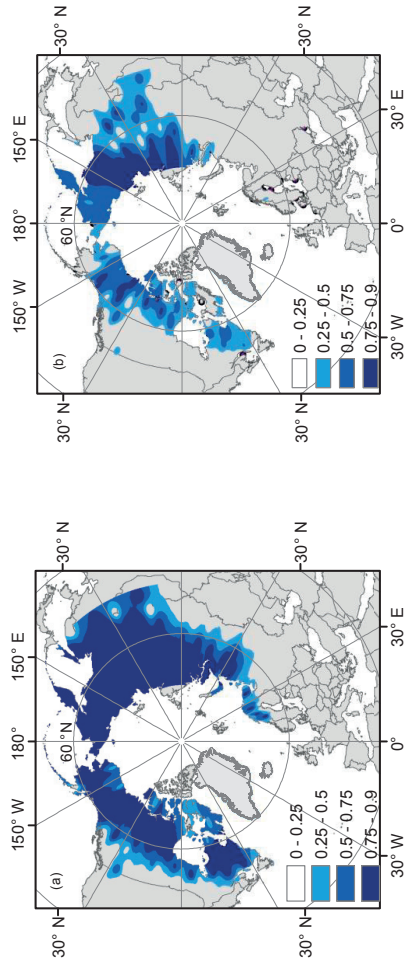


Fig. 5 Modelled September ice fraction (0-1) in the peat soil (as a proxy for permafrost distribution) interpolated among simulation points, averaged over (a) 1990-2000 and (b) 2090-2100.

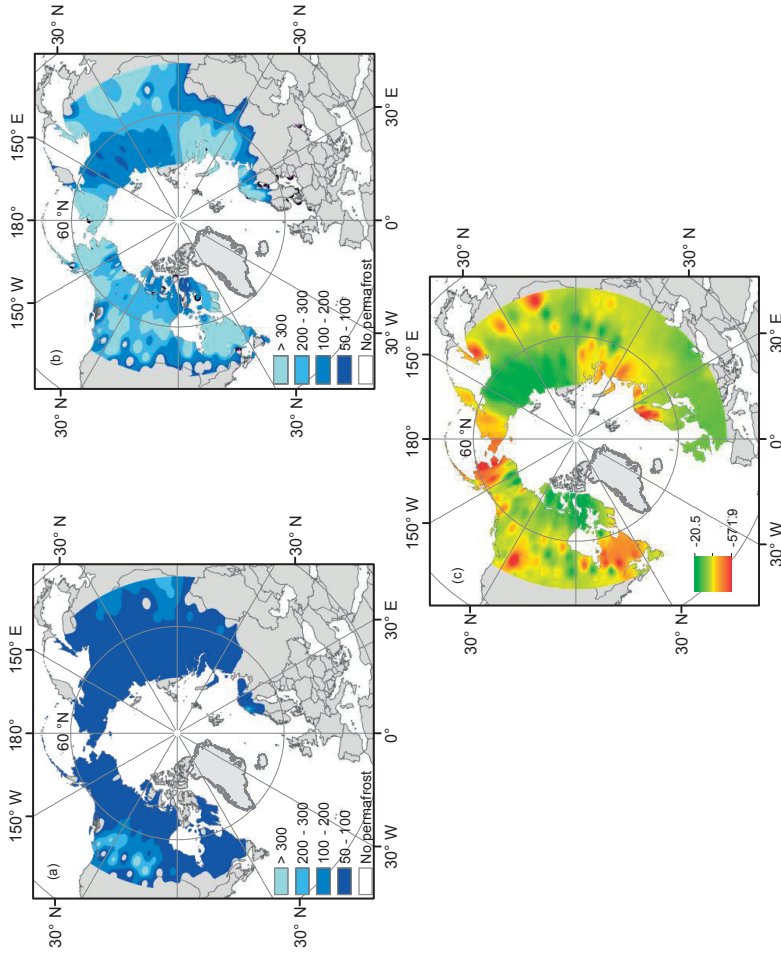


Fig. 6 Modelled mean September active layer depth (ALD in cm) interpolated among simulation points for (a) 1990-2000, (b) 2090-2100; (c) Net change in total ALD (b-a).

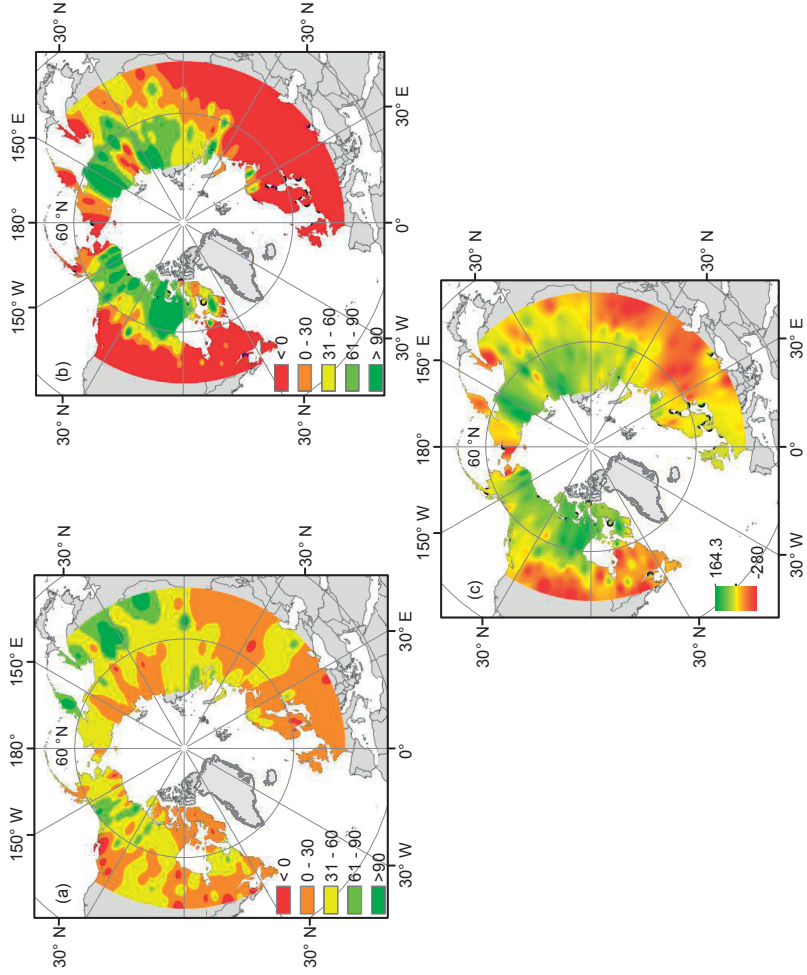


Fig. 7 Modelled mean C accumulation rate ($\text{g C m}^{-2} \text{y}^{-1}$) interpolated among simulation points for (a) 1990-2000, (b) 2090-2100; (c) Net change in total accumulation rate (b-a).

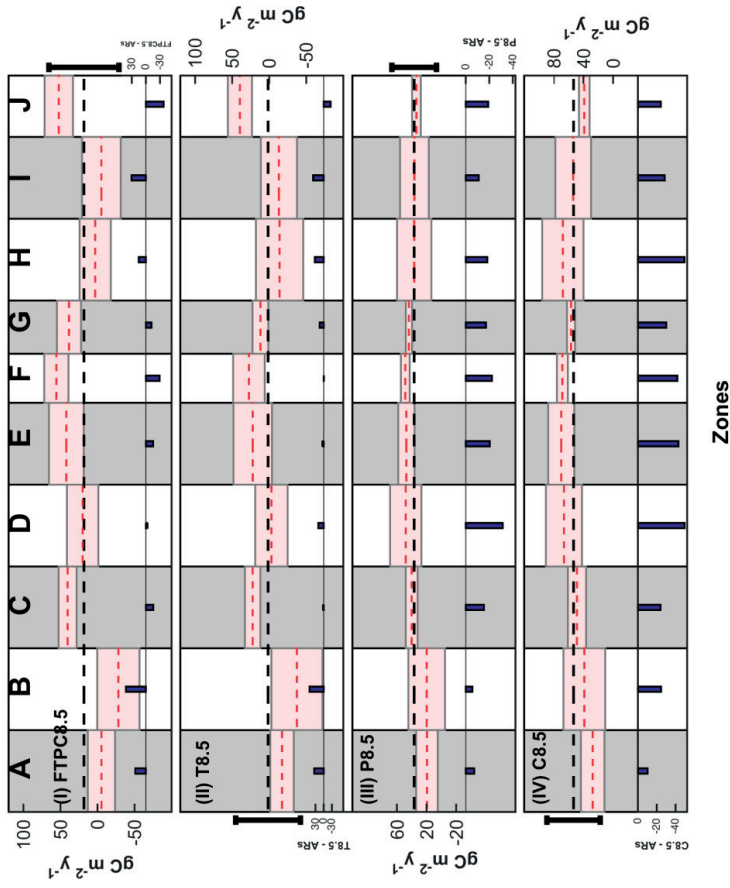


Fig. 8 Simulated C accumulation rate (blue lines) for each zone (refer Fig. 1 and 4) and across the pan-Arctic. The black dotted line is the pan-Arctic average with standard deviation (black line outside); red dotted line is the average for the respective zone with standard deviation in light red patch (I) average simulated near future rate of C accumulation (NFRCA) from the year 2001-2100 in FTPC8.5 experiment; (II) simulated NFRCA in T8.5 experiment, (III) simulated NFRCA in P8.5 experiment and (IV) simulated NFRCA in C8.5 experiment. Blue bars show the difference between NFRCA and LARCA values for each zone.

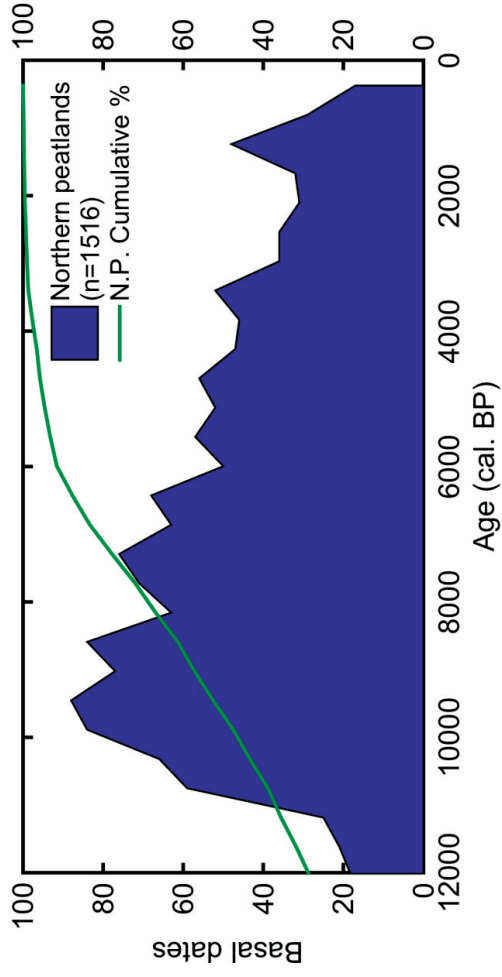


Fig. A1 Observed peat basal ages plotted as a frequency curve and cumulative percentage (in green) for northern peatlands (n = 1516; MacDonald et al. (2006))

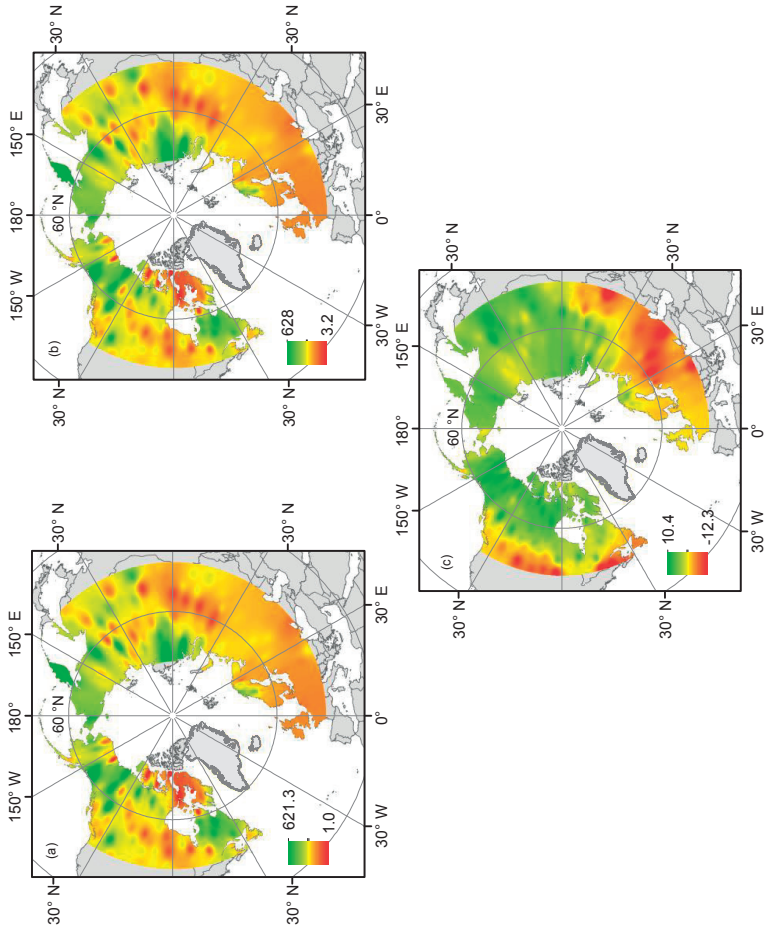


Fig. A2 Modelled total accumulated C interpolated (kg C m^{-2}) among simulation points for (a) 1990-2000, (b) 2090-2100; (c) Net change in total C accumulation (b-a).

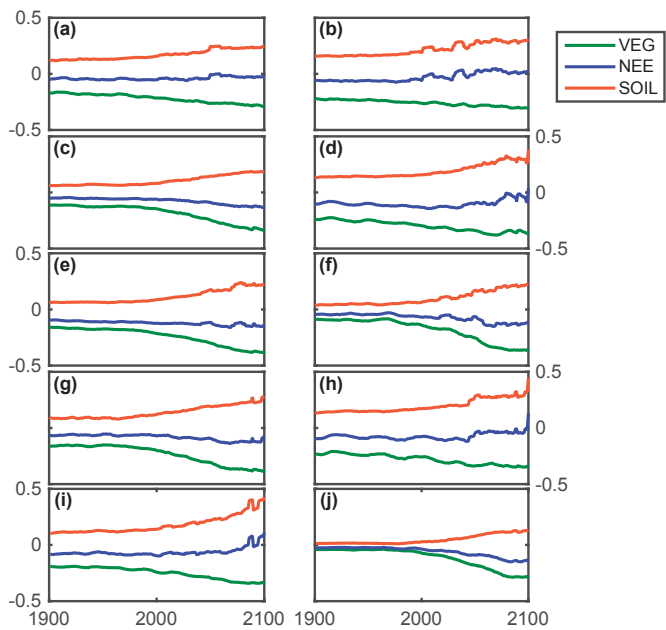


Fig. A3 Total simulated carbon fluxes (10-year moving average) (in $\text{kg C m}^{-2} \text{y}^{-1}$) for each zone for 1900-2100, including the RCP8.5 (FTPC8.5) forcing scenario for 2001-2100: vegetation NPP (VEG), litter and soil respiration (SOIL) and net ecosystem exchange (NEE).

Table A1. Plant functional types (PFTs) simulated in this study, showing representative taxa, phenology, bio-climatic limits, water table position (WTP) threshold for establishment, prescribed root fractions in mineral soil layers, and initial decomposition rate for different litter fractions.

PFT (abbreviation)	Representative taxa	Phenology	Climate Zone	Growth Form	Min/Max temperature of the coldest month for establishment (°C)	Max GDD for establishment (°C day)	WTP threshold (in mm)	Root fraction		Litter fraction	Initial decomposition rate (k_d) ³ (yr ⁻¹)
								Upper mineral soil (UM)	Lower mineral soil (LM)		
High summergreen shrub (HSS)	<i>Salix spp.</i> , <i>Betula nana</i>	Summer green	Boreal-Temperate	Woody	-32.5/-	1000	< -250	0.7	0.3	Wood	0.055
										Leaf	0.1
										Root	0.1
										Seed	0.1
Low evergreen shrub (LSE)	<i>Vaccinium vitis-idaea</i> , <i>Andromeda polifolia</i> L.	Evergreen	Boreal-Temperate	Woody	-32.5/-	100	< -250	0.7	0.3	Wood	0.055
										Leaf	0.1
										Root	0.1
										Seed	0.1
Low summergreen shrub (LSS)	<i>Vaccinium myrtillus</i> , <i>Vaccinium uliginosum</i> , <i>Betula nana</i> L.	Summer green	Boreal-Temperate	Woody	-32.5/-	100	< -250	0.7	0.3	Wood	0.055
										Leaf	0.1
										Root	0.1
										Seed	0.1
Graminoid (Gr)	<i>Carex rotundata</i> Wg., <i>Eriophorum vaginatum</i> L.	Evergreen	Boreal-Temperate	Herbaceous	-/-	-	> -100	0.9	0.1	Leaf	0.1
										Root	0.1
										Seed	0.1
										Leaf	0.055
Moss (M)	<i>Sphagnum</i> spp.	Evergreen	Boreal-Temperate	Herbaceous	-/15.5	-	< +50 and > -500	-	-	Leaf	0.055
								Seed	0.055		

³ Aerts et al. (1999), Frolking et al. (2002) and Moore et al. (2007)

References

- Aerts, R., Verhoeven, J. T. A., and Whigham, D. F.: Plant-mediated controls on nutrient cycling in temperate fens and bogs, *Journal*, 80, 2170-2181,doi: 10.1890/0012-9658(1999)080[2170:pmconc]2.0.co;2, 1999.
- Ali, A. A., Ghaleb, B., Garneau, M., Asnong, H., and Loisel, J.: Recent peat accumulation rates in minerotrophic peatlands of the Bay James region, Eastern Canada, inferred by ²¹⁰Pb and ¹³⁷Cs radiometric techniques, *Appl Radiat Isot*, 66, 1350-1358,doi: 10.1016/j.apradiso.2008.02.091, 2008.
- Anderson, D. E.: A reconstruction of Holocene climatic changes from peat bogs in north-west Scotland, *Boreas*, 27, 208-224,1998.
- Anderson, D. E.: Carbon accumulation and C/N ratios of peat bogs in North-West Scotland, *Scot Geogr J*, 118, 323-341,doi: Doi 10.1080/00369220218737155, 2002.
- Andrews, T., Gregory, J. M., Webb, M. J., and Taylor, K. E.: Forcing, feedbacks and climate sensitivity in CMIP5 coupled atmosphere-ocean climate models, *Geophysical Research Letters*, 39, 7,doi: 10.1029/2012gl051607, 2012.
- Beilman, D. W.: Plant community and diversity change due to localized permafrost dynamics in bogs of western Canada, *Canadian Journal of Botany-Revue Canadienne De Botanique*, 79, 983-993,2001.
- Beilman, D. W., MacDonald, G. M., Smith, L. C., and Reimer, P. J.: Carbon accumulation in peatlands of West Siberia over the last 2000 years, *Glob. Biogeochem. Cycle*, 23, 12,doi: 10.1029/2007gb003112, 2009.
- Beilman, D. W., Vitt, D. H., Bhatti, J. S., and Forest, S.: Peat carbon stocks in the southern Mackenzie River Basin: uncertainties revealed in a high-resolution case study, *Global Change Biology*, 14, 1221-1232,doi: 10.1111/j.1365-2486.2008.01565.x, 2008.
- Berger, A. and Loutr, M. F.: Insolation values for the climate of the last 10 million years, *Quaternary Science Reviews*, 10, 297-317,2003.
- Bernard, J. M. and Fiala, K.: Distribution and Standing Crop of Living and Dead Roots in Three Wetland *Carex* Species, *Bulletin of the Torrey Botanical Club*, 113, 1-5,doi: 10.2307/2996226, 1986.
- Bleuten, W., Borren, W., Glaser, P. H., Tsuchihara, T., Lapshina, E. D., Makila, M., Siegel, D., Joosten, H., and Wassen, M. J.: Hydrological processes, nutrient flows and patterns of fens and bogs. In: *Wetlands and Natural Resource Management*, Verheven, J. T. A., Beltman, B., Bobbink, R., and Whigham, D. F. (Eds.), *Ecological Studies : Analysis and Synthesis*, Springer-Verlag Berlin, Berlin, 2006.
- Blyakharchuk, T. A. and Sulerzhitsky, L. D.: Holocene vegetational and climatic changes in the forest zone of Western Siberia according to pollen records from the extrazonal palsa bog Bugristoye, *Holocene*, 9, 621-628,doi: Doi 10.1191/095968399676614561, 1999.

Borren, W. and Bleuten, W.: Simulating Holocene carbon accumulation in a western Siberian watershed mire using a three-dimensional dynamic modeling approach, *Water Resources Research*, 42, 13, doi: 10.1029/2006wr004885, 2006.

Borren, W., Bleuten, W., and Lapshina, E. D.: Holocene peat and carbon accumulation rates in the southern taiga of western Siberia, *Quaternary Research*, 61, 42-51, doi: 10.1016/j.yqres.2003.09.002, 2004.

Botch, M. S., Kobak, K. I., Vinson, T. S., and Kolchugina, T. P.: CARBON POOLS AND ACCUMULATION IN PEATLANDS OF THE FORMER SOVIET-UNION, *Glob. Biogeochem. Cycle*, 9, 37-46, doi: 10.1029/94gb03156, 1995.

Bragazza, L., Buttler, A., Robroek, B. J. M., Albrecht, R., Zaccone, C., Jassey, V. E. J., and Signarbieux, C.: Persistent high temperature and low precipitation reduce peat carbon accumulation, *Global Change Biology*, 22, 4114-4123, doi: 10.1111/gcb.13319, 2016.

Bunbury, J., Finkelstein, S. A., and Bollmann, J.: Holocene hydro-climatic change and effects on carbon accumulation inferred from a peat bog in the Attawapiskat River watershed, Hudson Bay Lowlands, Canada, *Quaternary Research*, 78, 275-284, doi: 10.1016/j.yqres.2012.05.013, 2012.

Charman, D. J.: Patterned fen development in northern Scotland: Hypothesis testing and comparison with ombrotrophic blanket peats, *Journal of Quaternary Science*, 10, 327-342, doi: 10.1002/jqs.3390100403, 1995.

Charman, D. J., Amesbury, M. J., Hinchliffe, W., Hughes, P. D. M., Mallon, G., Blake, W. H., Daley, T. J., Gallego-Sala, A. V., and Mauquoy, D.: Drivers of Holocene peatland carbon accumulation across a climate gradient in northeastern North America, *Quaternary Science Reviews*, 121, 110-119, doi: 10.1016/j.quascirev.2015.05.012, 2015.

Charman, D. J., Beilman, D. W., Blaauw, M., Booth, R. K., Brewer, S., Chambers, F. M., Christen, J. A., Gallego-Sala, A., Harrison, S. P., Hughes, P. D. M., Jackson, S. T., Korhola, A., Mauquoy, D., Mitchell, F. J. G., Prentice, I. C., van der Linden, M., De Vleeschouwer, F., Yu, Z. C., Alm, J., Bauer, I. E., Corish, Y. M. C., Garneau, M., Hohl, V., Huang, Y., Karofeld, E., Le Roux, G., Loisel, J., Moschen, R., Nichols, J. E., Nieminen, T. M., MacDonald, G. M., Phadtare, N. R., Rausch, N., Sillasoo, U., Swindles, G. T., Tuittila, E. S., Ukonmaanaho, L., Valiranta, M., van Bellen, S., van Geel, B., Vitt, D. H., and Zhao, Y.: Climate-related changes in peatland carbon accumulation during the last millennium, *Biogeosciences*, 10, 929-944, doi: 10.5194/bg-10-929-2013, 2013.

Chaudhary, N., Miller, P. A., and Smith, B.: Modelling Holocene peatland dynamics with an individual-based dynamic vegetation model, *Biogeosciences* (in review), 2016.2016.

Christensen, T. R., Johansson, T. R., Akerman, H. J., Mastepanov, M., Malmer, N., Friborg, T., Crill, P., and Svensson, B. H.: Thawing sub-arctic permafrost: Effects on vegetation and methane emissions, *Geophysical Research Letters*, 31, doi: L04501 10.1029/2003gl018680, 2004.

Clymo, R. S.: The limits to peat bog growth, *Philos. Trans. R. Soc. Lond. Ser. B-Biol. Sci.*, 303, 605-654,doi: 10.1098/rstb.1984.0002, 1984.

Clymo, R. S.: Peat growth, *Quaternary Landscapes*. Eds Shane LCK, Cushing EJ. Minneapolis, University of Minnesota Press., 1991. 76-1121991.

Clymo, R. S.: Models of peat growth, *Suo (Helsinki)*, 43, 127-136,doi: 10.1007/978-3-642-66760-2_9, 1992.

Clymo, R. S., Turunen, J., and Tolonen, K.: Carbon accumulation in peatland, *Oikos*, 81, 368-388,doi: 10.2307/3547057, 1998.

Collins, W. J., Bellouin, N., Doutriaux-Boucher, M., Gedney, N., Halloran, P., Hinton, T., Hughes, J., Jones, C. D., Joshi, M., Liddicoat, S., Martin, G., O'Connor, F., Rae, J., Senior, C., Sitch, S., Totterdell, I., Wiltshire, A., and Woodward, S.: Development and evaluation of an Earth-System model-HadGEM2, *Geosci. Model Dev.*, 4, 1051-1075,doi: 10.5194/gmd-4-1051-2011, 2011.

Dyke, A. S., Giroux, D., and Robertson, L.: *Paleovegetation Maps, Northern North America, 18000 to 1000 BP*, *Geol. Surv. Can. Open File 4682*, Ottawa, Canada., 2004.2004.

Ekici, A., Chadburn, S., Chaudhary, N., Hajdu, L. H., Marmy, A., Peng, S., Boike, J., Burke, E., Friend, A. D., Hauck, C., Krinner, G., Langer, M., Miller, P. A., and Beer, C.: Site-level model intercomparison of high latitude and high altitude soil thermal dynamics in tundra and barren landscapes, *The Cryosphere*, 9, 1343-1361,doi: 10.5194/tc-9-1343-2015, 2015.

Elina, G., Kuznecov, O. L., and Maksimov, A. I.: *StrukturnoFunktional'naja Organizatsija i Dinamika Bolotnyh Ekosistem Karelii*, *Nauka, Leningrad, Russia*, pp. 128, 1984.1984.

Euskirchen, E. S., McGuire, A. D., Kicklighter, D. W., Zhuang, Q., Clein, J. S., Dargaville, R. J., Dye, D. G., Kimball, J. S., McDonald, K. C., Melillo, J. M., Romanovsky, V. E., and Smith, N. V.: Importance of recent shifts in soil thermal dynamics on growing season length, productivity, and carbon sequestration in terrestrial high-latitude ecosystems, *Global Change Biology*, 12, 731-750,doi: 10.1111/j.1365-2486.2006.01113.x, 2006.

Fan, Z. S., McGuire, A. D., Turetsky, M. R., Harden, J. W., Waddington, J. M., and Kane, E. S.: The response of soil organic carbon of a rich fen peatland in interior Alaska to projected climate change, *Global Change Biology*, 19, 604-620,doi: 10.1111/gcb.12041, 2013.

Franzén, L. G.: Increased decomposition of subsurface peat in Swedish raised bogs: are temperate peatlands still net sinks of carbon? , *Mires and Peat 1: Art. 3.* , 2006.2006.

Frolking, S. and Roulet, N. T.: Holocene radiative forcing impact of northern peatland carbon accumulation and methane emissions, *Global Change Biology*, 13, 1079-1088,doi: 10.1111/j.1365-2486.2007.01339.x, 2007.

Frolking, S., Roulet, N. T., Moore, T. R., Richard, P. J. H., Lavoie, M., and Muller, S. D.: Modeling northern peatland decomposition and peat accumulation, *Ecosystems*, 4, 479-498,doi: 10.1007/s10021-001-0105-1, 2001.

Frolking, S., Roulet, N. T., Tuittila, E., Bubier, J. L., Quillet, A., Talbot, J., and Richard, P. J. H.: A new model of Holocene peatland net primary production, decomposition, water balance, and peat accumulation, 1 Article, *Earth System Dynamics*, 1-21 pp., 2010.

Gao, Y. and Couwenberg, J.: Carbon accumulation in a permafrost polygon peatland: steady long-term rates in spite of shifts between dry and wet conditions, *Glob Chang Biol*, 21, 803-815,doi: 10.1111/gcb.12742, 2015.

Garneau, M., van Bellen, S., Magnan, G., Beaulieu-Audy, V., Lamarre, A., and Asnong, H.: Holocene carbon dynamics of boreal and subarctic peatlands from Quebec, Canada, *Holocene*, 24, 1043-1053,doi: 10.1177/0959683614538076, 2014.

Gerten, D., Schaphoff, S., Haberlandt, U., Lucht, W., and Sitch, S.: Terrestrial vegetation and water balance - hydrological evaluation of a dynamic global vegetation model, *Journal of Hydrology*, 286, 249-270,doi: 10.1016/j.jhydrol.2003.09.029, 2004.

Gorham, E.: Northern peatlands - role in the carbon-cycle and probable responses to climatic warming, *Ecological Applications*, 1, 182-195,doi: 10.2307/1941811, 1991.

Gorham, E., Janssens, J. A., and Glaser, P. H.: Rates of peat accumulation during the postglacial period in 32 sites from Alaska to Newfoundland, with special emphasis on northern Minnesota, *Canadian Journal of Botany-Revue Canadienne De Botanique*, 81, 429-438,doi: 10.1139/b03-036, 2003.

Gorham, E., Lehman, C., Dyke, A., Janssens, J., and Dyke, L.: Temporal and spatial aspects of peatland initiation following deglaciation in North America, *Quaternary Science Reviews*, 26, 300-311,doi: 10.1016/j.quascirev.2006.08.008, 2007.

Halsey, L. A., Vitt, D. H., and Bauer, I. E.: Peatland initiation during the Holocene in continental western Canada, *Clim. Change*, 40, 315-342,doi: 10.1023/a:1005425124749, 1998.

Hilbert, D. W., Roulet, N., and Moore, T.: Modelling and analysis of peatlands as dynamical systems, *Journal of Ecology*, 88, 230-242,doi: 10.1046/j.1365-2745.2000.00438.x, 2000.

Hillel, D.: In: *Environmental Soil Physics: Fundamentals, Applications, and Environmental Considerations*, 1998.

Holmquist, J. R. and MacDonald, G. M.: Peatland succession and long-term apparent carbon accumulation in central and northern Ontario, Canada, *Holocene*, 24, 1075-1089,doi: 10.1177/0959683614538074, 2014.

Ise, T., Dunn, A. L., Wofsy, S. C., and Moorcroft, P. R.: High sensitivity of peat decomposition to climate change through water-table feedback, *Nat. Geosci.*, 1, 763-766,doi: 10.1038/ngeo331, 2008.

Jones, M. C. and Yu, Z. C.: Rapid deglacial and early Holocene expansion of peatlands in Alaska, *Proceedings of the National Academy of Sciences of the United States of America*, 107, 7347-7352,doi: 10.1073/pnas.0911387107, 2010.

Kaufman, D. S., Ager, T. A., Anderson, N. J., Anderson, P. M., Andrews, J. T., Bartlein, P. J., Brubaker, L. B., Coats, L. L., Cwynar, L. C., Duvall, M. L., Dyke, A. S., Edwards, M. E., Eisner, W. R., Gajewski, K., Geirsdottir, A., Hu, F. S., Jennings, A. E., Kaplan, M. R., Kerwin, M. N., Lozhkin, A. V., MacDonald, G. M., Miller, G. H., Mock, C. J., Oswald, W. W., Otto-Bliesner, B. L., Porinchu, D. F., Ruhland, K., Smol, J. P., Steig, E. J., and Wolfe, B. B.: Holocene thermal maximum in the western Arctic (0-180 degrees W), *Quaternary Science Reviews*, 23, 529-560, doi: 10.1016/j.quascirev.2003.09.007, 2004.

Kivinen, E. and Pakarinen, P.: Geographical distribution of peat resources and major peatland 582 complex types in the world., *Annales Academiae Scientiarum Fennicae, Series A, Number 132:1-28*, 1981.1981.

Klarqvist, M., Bolin, E., and M., N.: Factors controlling peat growth and carbon accumulation rates in boreal mires during the Holocene, In Klarqvist, M (ed.): *Peat Growth and Carbon Accumulation Rates during the Holocene in Boreal Mires. Acta Universitatis Agriculturae Sueciae, Silvestria 203, Paper IV, 1 31, 2001a.2001a.*

Klarqvist, M., Bolin, E., and M., N.: Long-term decline in apparent peat carbon accumulation in boreal mires in northern Sweden, In Klarqvist, M. (ed.): *Peat Growth and Carbon Accumulation Rates during the Holocene in Boreal Mires. Acta Universitatis Agriculturae Sueciae, Silvestria 203, Paper III, 1 22., 2001b.2001b.*

Klein, E. S., Yu, Z., and Booth, R. K.: Recent increase in peatland carbon accumulation in a thermokarst lake basin in southwestern Alaska, *Journal*, 392, 186-195, doi: 10.1016/j.palaeo.2013.09.009, 2013.

Klein, F., Goosse, H., Mairesse, A., and de Vernal, A.: Model-data comparison and data assimilation of mid-Holocene Arctic sea ice concentration, *Climate of the Past*, 10, 1145-1163, doi: 10.5194/cp-10-1145-2014, 2014.

Kleinen, T., Brovkin, V., and Schuldt, R. J.: A dynamic model of wetland extent and peat accumulation: results for the Holocene, *Biogeosciences*, 9, 235-248, doi: 10.5194/bg-9-235-2012, 2012.

Korhola, A., Ruppel, M., Seppa, H., Valiranta, M., Virtanen, T., and Weckstrom, J.: The importance of northern peatland expansion to the late-Holocene rise of atmospheric methane, *Quaternary Science Reviews*, 29, 611-617, doi: 10.1016/j.quascirev.2009.12.010, 2010.

Korhola, A., Tolonen, K., Turunen, J., and Jungner, H.: Estimating long-term carbon accumulation rates in boreal peatlands by radiocarbon dating, *Radiocarbon*, 37, 575-584, 1995.

Kuhry, P. and Turunen, J.: The Postglacial Development of Boreal and Subarctic Peatlands. In: *Boreal Peatland Ecosystems*, Wieder, R. K. and Vitt, D. H. (Eds.), Springer Berlin Heidelberg, Berlin, Heidelberg, 2006.

Lafleur, P. M., Roulet, N. T., and Admiral, S. W.: Annual cycle of CO₂ exchange at a bog peatland, *J. Geophys. Res.-Atmos.*, 106, 3071-3081, doi: Doi 10.1029/2000jd900588, 2001.

Lamarre, A., Garneau, M., and Asnong, H.: Holocene paleohydrological reconstruction and carbon accumulation of a permafrost peatland using testate amoeba and macrofossil analyses, Kuujjuarapik, subarctic Quebec, Canada, *Review of Palaeobotany and Palynology*, 186, 131-141, doi: 10.1016/j.revpalbo.2012.04.009, 2012.

Loisel, J. and Garneau, M.: Late Holocene paleoecohydrology and carbon accumulation estimates from two boreal peat bogs in eastern Canada: Potential and limits of multi-proxy archives, *Palaeogeography Palaeoclimatology Palaeoecology*, 291, 493-533, doi: 10.1016/j.palaeo.2010.03.020, 2010.

Loisel, J. and Yu, Z. C.: Recent acceleration of carbon accumulation in a boreal peatland, south central Alaska, *Journal of Geophysical Research-Biogeosciences*, 118, 41-53, doi: 10.1029/2012jg001978, 2013.

Loisel, J., Yu, Z. C., Beilman, D. W., Camill, P., Alm, J., Amesbury, M. J., Anderson, D., Andersson, S., Bochicchio, C., Barber, K., Belyea, L. R., Bunbury, J., Chambers, F. M., Charman, D. J., De Vleeschouwer, F., Fialkiewicz-Koziel, B., Finkelstein, S. A., Galka, M., Garneau, M., Hammarlund, D., Hinchcliffe, W., Holmquist, J., Hughes, P., Jones, M. C., Klein, E. S., Kokfelt, U., Korhola, A., Kuhry, P., Lamarre, A., Lamentowicz, M., Large, D., Lavoie, M., MacDonald, G., Magnan, G., Makila, M., Mallon, G., Mathijssen, P., Mauquoy, D., McCarroll, J., Moore, T. R., Nichols, J., O'Reilly, B., Oksanen, P., Packalen, M., Petet, D., Richard, P. J. H., Robinson, S., Ronkainen, T., Rundgren, M., Sannel, A. B. K., Tarnocai, C., Thom, T., Tuittila, E. S., Turetsky, M., Valiranta, M., van der Linden, M., van Geel, B., van Bellen, S., Vitt, D., Zhao, Y., and Zhou, W. J.: A database and synthesis of northern peatland soil properties and Holocene carbon and nitrogen accumulation, *Holocene*, 24, 1028-1042, doi: 10.1177/0959683614538073, 2014.

Loranty, M. M. and Goetz, S. J.: Shrub expansion and climate feedbacks in Arctic tundra, *Environmental Research Letters*, 7, 3, doi: 10.1088/1748-9326/7/1/011005, 2012.

MacDonald, G. M., Beilman, D. W., Kremenetski, K. V., Sheng, Y., Smith, L. C., and Velichko, A. A.: Rapid early development of circumarctic peatlands and atmospheric CH₄ and CO₂ variations, *Science*, 314, 285-288, doi: 10.1126/science.1131722, 2006.

Makila, M.: Holocene lateral expansion, peat growth and carbon accumulation on Haukkasuo, a raised bog in southeastern Finland, *Boreas*, 26, 1-14, 1997.

Makila, M.: CARBON ACCUMULATION IN PRISTINE AND DRAINED MIRES
Geological Survey of Finland, Special Paper, 49, 171-177, 2011.

Makila, M. and Moisanen, M.: Holocene lateral expansion and carbon accumulation of Luovuoma, a northern fen in Finnish Lapland, *Boreas*, 36, 198-210, doi: 10.1080/03009480600994460, 2007.

Makila, M., Saarnisto, M., and Kankainen, T.: Aapa mires as a carbon sink and source during the Holocene, *Journal of Ecology*, 89, 589-599, doi: 10.1046/j.0022-0477.2001.00586.x, 2001.

Malmer, N., Johansson, T., Olsrud, M., and Christensen, T. R.: Vegetation, climatic changes and net carbon sequestration in a North-Scandinavian subarctic mire over 30 years, *Global Change Biology*, 11, 1895-1909, doi: 10.1111/j.1365-2486.2005.01042.x, 2005.

Malmer, N. and Wallen, B.: The dynamics of peat accumulation on bogs: mass balance of hummocks and hollows and its variation throughout a millennium, *Ecography*, 22, 736-750, doi: 10.1111/j.1600-0587.1999.tb00523.x, 1999.

McGuire, A. D., Christensen, T. R., Hayes, D., Heroult, A., Euskirchen, E., Kimball, J. S., Koven, C., Laflour, P., Miller, P. A., Oechel, W., Peylin, P., Williams, M., and Yi, Y.: An assessment of the carbon balance of Arctic tundra: comparisons among observations, process models, and atmospheric inversions, *Biogeosciences*, 9, 3185-3204, doi: 10.5194/bg-9-3185-2012, 2012.

Miller, P. A., Giesecke, T., Hickler, T., Bradshaw, R. H. W., Smith, B., Seppa, H., Valdes, P. J., and Sykes, M. T.: Exploring climatic and biotic controls on Holocene vegetation change in Fennoscandia, *Journal of Ecology*, 96, 247-259, doi: 10.1111/j.1365-2745.2007.01342.x, 2008.

Miller, P. A. and Smith, B.: Modelling Tundra Vegetation Response to Recent Arctic Warming, *Ambio*, 41, 281-291, doi: 10.1007/s13280-012-0306-1, 2012.

Mitchell, T. D. and Jones, P. D.: An improved method of constructing a database of monthly climate observations and associated high-resolution grids, *International Journal of Climatology*, 25, 693-712, doi: 10.1002/joc.1181, 2005.

Moss, R. H., Edmonds, J. A., Hibbard, K. A., Manning, M. R., Rose, S. K., van Vuuren, D. P., Carter, T. R., Emori, S., Kainuma, M., Kram, T., Meehl, G. A., Mitchell, J. F. B., Nakicenovic, N., Riahi, K., Smith, S. J., Stouffer, R. J., Thomson, A. M., Weyant, J. P., and Wilbanks, T. J.: The next generation of scenarios for climate change research and assessment, *Nature*, 463, 747-756, doi: 10.1038/nature08823, 2010.

Ovenden, L.: Peat Accumulation in Northern Wetlands, *Quaternary Research*, 33, 377-386, doi: doi 10.1016/0033-5894(90)90063-Q, 1990.

Packalen, M. S. and Finkelstein, S. A.: Quantifying Holocene variability in carbon uptake and release since peat initiation in the Hudson Bay Lowlands, Canada, *Holocene*, 24, 1063-1074, doi: 10.1177/0959683614540728, 2014.

Piao, S., Sitch, S., Ciais, P., Friedlingstein, P., Peylin, P., Wang, X., Ahlstrom, A., Anav, A., Canadell, J. G., Cong, N., Huntingford, C., Jung, M., Levis, S., Levy, P. E., Li, J., Lin, X., Lomas, M. R., Lu, M., Luo, Y., Ma, Y., Myneni, R. B., Poulter, B., Sun, Z., Wang, T., Viovy, N., Zaehle, S., and Zeng, N.: Evaluation of terrestrial carbon cycle models for their response to climate variability and to CO₂ trends, *Global Change Biology*, 19, 2117-2132, doi: 10.1111/gcb.12187, 2013.

Robinson, S. D. and Moore, T. R.: Carbon and peat accumulation over the past 1200 years in a landscape with discontinuous permafrost, northwestern Canada, *Glob. Biogeochem. Cycle*, 13, 591-601, doi: 10.1029/1999gb900008, 1999.

- Robinson, S. D. and Moore, T. R.: The influence of permafrost and fire upon carbon accumulation in high boreal peatlands, Northwest Territories, Canada, *Arct. Antarct. Alp. Res.*, 32, 155-166,doi: 10.2307/1552447, 2000.
- Roulet, N. T., Lafleur, P. M., Richard, P. J. H., Moore, T. R., Humphreys, E. R., and Bubier, J.: Contemporary carbon balance and late Holocene carbon accumulation in a northern peatland, *Global Change Biology*, 13, 397-411,doi: 10.1111/j.1365-2486.2006.01292.x, 2007.
- Rydin, H. and Jeglum, J. K.: *The Biology of Peatlands*, 2e, Oxford University Press, 2013.
- Sannel, A. B. K. and Kuhry, P.: Holocene peat growth and decay dynamics in sub-arctic peat plateaus, west-central Canada, *Boreas*, 38, 13-24,doi: 10.1111/j.1502-3885.2008.00048.x, 2009.
- Schlesinger, W. H.: Evidence from Chronosequence Studies for a Low Carbon-Storage Potential of Soils, *Nature*, 348, 232-234,doi: DOI 10.1038/348232a0, 1990.
- Shaw, A. J., Cox, C. J., and Boles, S. B.: Polarity of peatmoss (*Sphagnum*) evolution: who says bryophytes have no roots?, *American Journal of Botany*, 90, 1777-1787,doi: 10.3732/ajb.90.12.1777, 2003.
- Sitch, S., Smith, B., Prentice, I. C., Arneth, A., Bondeau, A., Cramer, W., Kaplan, J. O., Levis, S., Lucht, W., Sykes, M. T., Thonicke, K., and Venevsky, S.: Evaluation of ecosystem dynamics, plant geography and terrestrial carbon cycling in the LPJ dynamic global vegetation model, *Global Change Biology*, 9, 161-185,doi: 10.1046/j.1365-2486.2003.00569.x, 2003.
- Smith, B., Prentice, I. C., and Sykes, M. T.: Representation of vegetation dynamics in the modelling of terrestrial ecosystems: comparing two contrasting approaches within European climate space, *Glob. Ecol. Biogeogr.*, 10, 621-637,doi: 10.1046/j.1466-822X.2001.t01-1-00256.x, 2001.
- Smith, B., Warlind, D., Arneth, A., Hickler, T., Leadley, P., Silberg, J., and Zaehle, S.: Implications of incorporating N cycling and N limitations on primary production in an individual-based dynamic vegetation model, *Biogeosciences*, 11, 2027-2054,doi: 10.5194/bg-11-2027-2014, 2014.
- Sturm, M., Schimel, J., Michaelson, G., Welker, J. M., Oberbauer, S. F., Liston, G. E., Fahnestock, J., and Romanovsky, V. E.: Winter biological processes could help convert arctic tundra to shrubland, *Bioscience*, 55, 17-26,doi: 10.1641/0006-3568(2005)055[0017:wbpchc]2.0.co;2, 2005.
- Swindles, G. T., Morris, P. J., Mullan, D., Watson, E. J., Turner, T. E., Roland, T. P., Amesbury, M. J., Kokfelt, U., Schoning, K., Pratte, S., Gallego-Sala, A., Charman, D. J., Sanderson, N., Garneau, M., Carrivick, J. L., Woulds, C., Holden, J., Parry, L., and Galloway, J. M.: The long-term fate of permafrost peatlands under rapid climate warming, *Sci Rep*, 5, 6,doi: 10.1038/srep17951, 2015.

Tang, J., Miller, P. A., Persson, A., Olefeldt, D., Pilesjo, P., Heliasz, M., Jackowicz-Korczynski, M., Yang, Z., Smith, B., Callaghan, T. V., and Christensen, T. R.: Carbon budget estimation of a subarctic catchment using a dynamic ecosystem model at high spatial resolution, *Biogeosciences*, 12, 2791-2808,doi: 10.5194/bg-12-2791-2015, 2015.

Tolonen, K. and Turunen, J.: Accumulation rates of carbon in mires in Finland and implications for climate change, *Holocene*, 6, 171-178,doi: 10.1177/095968369600600204, 1996.

Turetsky, M. R., Wieder, R. K., Vitt, D. H., Evans, R. J., and Scott, K. D.: The disappearance of relict permafrost in boreal north America: Effects on peatland carbon storage and fluxes, *Global Change Biology*, 13, 1922-1934,doi: 10.1111/j.1365-2486.2007.01381.x, 2007.

Turunen, J., Roulet, N. T., Moore, T. R., and Richard, P. J. H.: Nitrogen deposition and increased carbon accumulation in ombrotrophic peatlands in eastern Canada, *Glob. Biogeochem. Cycle*, 18, 12,doi: 10.1029/2003gb002154, 2004.

Turunen, J., Tahvanainen, T., Tolonen, K., and Pitkanen, A.: Carbon accumulation in West Siberian mires, Russia, *Glob. Biogeochem. Cycle*, 15, 285-296,doi: 10.1029/2000gb001312, 2001.

Turunen, J., Tomppo, E., Tolonen, K., and Reinikainen, A.: Estimating carbon accumulation rates of undrained mires in Finland - application to boreal and subarctic regions, *Holocene*, 12, 69-80,doi: 10.1191/0959683602hl522rp, 2002.

van Bellen, S., Dallaire, P.-L., Garneau, M., and Bergeron, Y.: Quantifying spatial and temporal Holocene carbon accumulation in ombrotrophic peatlands of the Eastmain region, Quebec, Canada, *Glob. Biogeochem. Cycle*, 25,doi: 10.1029/2010gb003877, 2011.

Vardy, S. R., Warner, B. G., Turunen, J., and Aravena, R.: Carbon accumulation in permafrost peatlands in the Northwest Territories and Nunavut, Canada, *Holocene*, 10, 273-280,doi: 10.1191/095968300671749538, 2000.

Vitt, D. H., Halsey, L. A., Bauer, I. E., and Campbell, C.: Spatial and temporal trends in carbon storage of peatlands of continental western Canada through the Holocene, *Can. J. Earth Sci.*, 37, 683-693,doi: 10.1139/e99-097, 2000.

Wania, R., Ross, I., and Prentice, I. C.: Integrating peatlands and permafrost into a dynamic global vegetation model: 1. Evaluation and sensitivity of physical land surface processes, *Glob. Biogeochem. Cycle*, 23,doi: Gb3014
10.1029/2008gb003412, 2009a.

Wania, R., Ross, I., and Prentice, I. C.: Integrating peatlands and permafrost into a dynamic global vegetation model: 2. Evaluation and sensitivity of vegetation and carbon cycle processes, *Glob. Biogeochem. Cycle*, 23,doi: Gb3015
10.1029/2008gb003413, 2009b.

Wolfe, B. B., Edwards, T. W. D., Aravena, R., Forman, S. L., Warner, B. G., Velichko, A. A., and MacDonald, G. M.: Holocene paleohydrology and paleoclimate at treeline, north-

central Russia, inferred from oxygen isotope records in lake sediment cellulose, *Quaternary Research*, 53, 319-329, doi: 10.1006/qres.2000.2124, 2000.

Yu, Z. C.: Holocene carbon accumulation of fen peatlands in boreal western Canada: A complex ecosystem response to climate variation and disturbance, *Ecosystems*, 9, 1278-1288, doi: 10.1007/s10021-006-0174-2, 2006.

Yu, Z. C.: Northern peatland carbon stocks and dynamics: a review, *Biogeosciences*, 9, 4071-4085, doi: 10.5194/bg-9-4071-2012, 2012.

Yu, Z. C., Beilman, D. W., and Jones, M. C.: Sensitivity of Northern Peatland Carbon Dynamics to Holocene Climate Change. In: *Carbon Cycling in Northern Peatlands*, Baird, A. J., Belyea, L. R., Comas, X., Reeve, A. S., and Slater, L. D. (Eds.), *Geophysical Monograph Series*, 2009.

Yu, Z. C., Loisel, J., Charman, D. J., Beilman, D. W., and Camill, P.: Holocene peatland carbon dynamics in the circum-Arctic region: An introduction, *Holocene*, 24, 1021-1027, doi: 10.1177/0959683614540730, 2014a.

Yu, Z. C., Vitt, D. H., Campbell, I. D., and Apps, M. J.: Understanding Holocene peat accumulation pattern of continental fens in western Canada, *Canadian Journal of Botany- Revue Canadienne De Botanique*, 81, 267-282, doi: 10.1139/b03-016, 2003.

Yu, Z. C., Vitt, D. H., and Wieder, R. K.: Continental fens in western Canada as effective carbon sinks during the Holocene, *Holocene*, 24, 1090-1104, doi: 10.1177/0959683614538075, 2014b.

Zoltai, S. C.: Permafrost Distribution in Peatlands of West-Central Canada during the Holocene Warm Period 6000 Years Bp, *Geogr Phys Quatern*, 49, 45-54, 1995.

Paper III

Biotic and abiotic drivers of peatland growth and microtopography: a model demonstration

5 **Nitin Chaudhary, Paul A. Miller and Benjamin Smith**

Department of Physical Geography and Ecosystem Science, Lund University,
Sölvegatan 12, SE- 22362 Lund, Sweden

10 *Correspondence to:* **N. Chaudhary (nitin.chj@gmail.com)**

Abstract

15 Peatlands are important carbon reserves in terrestrial ecosystems. The
microtopography of a peatland area has a strong influence on its carbon balance,
determining carbon fluxes at a range of spatial scales. These patterned surfaces are
very sensitive to changing climatic conditions. There are open research questions
concerning the stability, behaviour and transformation of these microstructures, and
the implications of these changes for the long-term accumulation of organic matter
20 in peatlands. A simple two-dimensional peat microtopographical model was
developed which accounts for the effects of microtopographic variations and a
dynamic water table on competitive interactions between peat forming plants. In a
case study of a subarctic mire in northern Sweden, we examined the consequences
of such interactions on peat accumulation patterns and the transformation of
25 microtopographic structure. The simulations demonstrate plausible interactions
between peatland growth, water table position (WTP) and microtopography,
consistent with many observational studies, including an observed peat age profile
from the study area. Our model also suggests that peatlands could exhibit
alternative compositional and structural dynamics depending on the initial
30 topographical and climatic conditions, and plant characteristics. Our model
approach represents a step towards improved representation of peatland vegetation
dynamics and net carbon balance in Earth system models, allowing their potentially
important implications for regional and global carbon balances and biogeochemical
and biophysical feedbacks to the atmosphere to be explored and quantified.

35

40

45

50

Keywords: Peatlands, Microtopography, Carbon accumulation, Decomposition,
55 Vegetation dynamics, Ecosystem modelling

1. Introduction

Northern peatlands are one of the biggest carbon reserves among terrestrial ecosystems (Yu et al., 2010). They have low net primary productivity (NPP) relative to other ecosystems globally but due to an even lower decomposition rate they have sequestered considerable amounts of carbon over the course of centuries (Clymo, 1991; Thormann and Bayley, 1997; Froelking et al., 2001). Northern peatlands have accumulated carbon at a rate of 15-30 g C m⁻² yr⁻¹ in the last 5000 to 10,000 years (Yu et al., 2009; Loisel et al., 2014). Overall, this imbalanced process has created a repository of approximately 200-550 PgC covering about 3.5 million km² of peatland areas (Gorham, 1991; Turunen et al., 2002; Yu, 2012).

Global climate models have projected a warming of more than 5°C by the end of the century in northern peatland areas (Christensen et al., 2007; IPCC, 2013). The magnitude of this warming will be exacerbated by the associated arctic climate-carbon feedbacks (Bridgman et al., 1995; Davidson and Janssens, 2006; Zhang et al., 2014). Constraints on biological activity imposed by low temperature would be reduced, accelerating plant productivity as well as decomposition rates (Klein et al., 2013). Potentially, the resulting shift in the balance between production and decomposition might be sufficient to influence the existing sink capacity of these peatlands (Wieder, 2001; Ise et al., 2008; Fan et al., 2013). Studies have also highlighted the implications of alterations in precipitation patterns and rapid rates of permafrost degradation on the peatland carbon cycle and climate (Christensen et al., 2004; Åkerman and Johansson, 2008; Bragazza et al., 2013). These altered patterns have the potential to modify local and regional hydrology and moisture balances, which could in turn affect the vegetation composition and carbon balance of many northern peatlands. For instance, abrupt changes in environmental conditions may create unfavorable settings for existing plant species and provide opportunities for new (non-resident) species to flourish in those areas (Malmer et al., 2005; Johansson et al., 2006; Zhang et al., 2013).

Hummock and hollow microtopography is a distinctive feature of many northern peatland ecosystems, with microtopographical position playing a critical role in carbon balance (Gorham, 1991; Weltzin et al., 2001; Pouliot et al., 2011). Local climate conditions, surface hydrology and vegetation cover are the main factors controlling the dynamics of patterned surfaces. These micro-formations develop distinctive conditions with plant species, hydrology, nutrient status, plant productivity, and decomposition rates varying systematically at a range of spatial scales (Bridgman et al., 1995; Waddington and Roulet, 1996; Nungesser, 2003). Changes in regional climatic conditions could have a profound impact on these micro-formations, modifying the peatland carbon balance from micro (1-10 m) to macro (>10⁴ m) scales. For example, in a well-studied peatland in subarctic northern Sweden, Stordalen mire, permafrost underlying elevated areas is being degraded as a result of recent climate warming, with an increase in wet depressions

100 modifying the vegetation composition and overall carbon sink capacity of the mire
(Christensen et al., 2004; Malmer et al., 2005; Johansson et al., 2006).

The microtopography of peatlands comprises hummocks, hollows and intermediate
areas. Hollows are dominated by tall productive graminoids while dwarf shrubs are
105 favoured in hummock areas where the water table position (WTP) remains
relatively low. Between these two extremes, different species of moss can thrive in
distinctive hydrological gradients - dry, wet and intermediate (where the WTP
remains close to the surface) (Seppa, 2002; Malmer et al., 2005; Johansson et al.,
2006; Trudeau et al., 2014). These plant species accumulate carbon at different
110 rates according to their morphological and structural makeup (Aerts et al., 1999).
Early studies such as those of VonPost and Sernander (1910) and Osvald (1923)
postulated that deposition of organic plant material at dissimilar rates leads to a
cyclic transformation of hummocks into hollows and vice versa. Later studies have
challenged this “cyclical succession” hypothesis, emphasising instead the
115 importance of variable decomposition rates on the microtopography of peatlands
(Tolonen, 1971; Barber, 1981; Seppa, 2002). Litter derived from plant species
growing in hollow areas decomposes more quickly than that derived from the
vegetation of hummocks and intermediate areas, with the result that peatland
microtopography can remain stable with little alterations for long periods of time.
120 By contrast, studies in some peatland areas have found that spatial heterogeneity or
surface roughness decreases over time due to differential rates of peat accumulation
in hummocks and hollows, leading to a flatter surface (Clymo and Hayward, 1982;
Hayward and Clymo, 1983). These varied and contradictory observations on
growth patterns and surface microstructure dynamics complicate the construction
125 of suitable models of the responses of peatland microtopography, vegetation cover
and carbon dynamics at the regional scale, for instance in climate change impact
(McGuire et al., 2012) and Earth system modelling (Zhang et al., 2013) studies.

In this study, we propose and demonstrate a novel two-dimensional (2-D) model
130 representation of peat microsite dynamics. Earlier, similar models have generally
focused on peat accumulation and decomposition patterns, overlooking the tight
coupling between vegetation dynamics and microtopographical transformation and
their role in peatland carbon balance. The proposed model fills this gap by testing
the adequacy of simple but empirically defensible assumptions about the dynamic
135 responses of the major peatland plant functional groups to microtopography and
water table variations, taking into account the feedbacks of plant compositional
shift on hydrology, decomposition and peat accumulation. The model is designed to
allow it be embedded within the biogeochemistry component of a regional Earth
system (climate) model, accounting for the effects of vegetation dynamics on
140 peatland carbon balance and vegetation cover at much larger (regional) scales
(Smith et al., 2011). With this goal in mind, we choose to adopt a parsimonious
approach by restricting the number of inputs required by the model (common
climate variables and primary productivity estimates) and adopting process

representations that do not rely on the availability of detailed local-scale
145 measurements (e.g. soil temperature calculations). We employ the model to address
the relative merits of alternative theories as to the origin and stability of peatland
microtopography, in turn shedding light on the potential influence of the explored
mechanisms on peatlands and their role in the global carbon balance under a
changing climate. We also perform sensitivity analyses to determine the impact of
150 model parameters and initialisation on simulated microtopography, vegetation and
long-term peatland carbon balance.

2. Materials and Methods

155 2.1. Model Overview

The structure of the model is presented schematically in Fig. 1. Relative
abundances of shrubs, graminoids and mosses in adjacent patches in a shared
landscape are represented, changing over time in response to small-scale
hydrology, productivity and decomposition rates that govern the rate of peat
160 accumulation (or depletion) in each patch. These processes are assumed to
determine the growth pattern, behavior and transformation of microtopographical
structures. The key formulations are adopted from previously developed peat
growth models (see below). The novel feature is the inclusion of dynamic
vegetation composition and the resulting impacts on peat accumulation or loss and
165 small-scale hydrology. The input variables are annual NPP at the mean landscape
level (distributed based on plant productivity), daily temperature and precipitation.
The focus of the study is on the recent peat deposition and surface microstructures
and its transformations during the last 1000 years and due to this brief period of
peat accumulation history. As little variation in peat bulk density with respect to
170 depth is expected in such a time frame, a constant dry bulk density is assumed in
this study (Table 1).

2.1.1. Peat Accumulation and Decomposition

Annual peat accumulation and decomposition follow Clymo (1984), and Frolking
175 et al. (2001) and Bauer (2004). The acrotelm and catotelm are two functionally-
distinct layers typical of most peatland soils. The acrotelm is the comparatively
aerated upper layer which plays the main role in determining vegetation
composition. Vegetation growth results in deposits of organic material (litter) being
transferred into the acrotelm. The water table fluctuates in the acrotelm, depending
180 on microtopography, rainfall, snowmelt, evapotranspiration and runoff, with some
areas remaining drier while other parts remain completely saturated. Due to this
uneven wetness, litter decomposes aerobically as well as anaerobically in the
acrotelm (Clymo, 1991; Frolking et al., 2002). The catotelm exists below the
permanent annual WTP and remains waterlogged throughout the year, creating
185 anoxic conditions which in turn attenuate the decomposition rate and promote peat
accumulation.

This model implicitly divides the total peat column into two parts—acrotelm and catotelm—demarcated by WTP (WTP takes negative (positive) values when the WTP is below (above) the peat surface). Annually, plant biomass is deposited as a new layer over previously accumulated peat layers in each patch (see below) based on the fractional projective cover (FPC) of the vegetation across the assumed landscape. Decomposition transforms the litter biomass in each layer into peat as time passes (Clymo, 1991). The rate of change in peat mass is the total peat production minus total peat loss due to decomposition, modelled as:

$$\frac{dM}{dt} = A - K M \quad (1)$$

where M is the total peat mass (kg C m^{-2}), A is the total peat input ($\text{kg C m}^{-2} \text{ yr}^{-1}$), and K (yr^{-1}) is the decomposition rate (see Eq. 3). Peat height may be derived from M using the assumed constant value for bulk density shown in Table 1. Peat decomposition is simulated on a daily time step based on decomposability which varies depending on the source plant type (Table 1). Litter generated from mosses (all types) has relatively low decomposition rates, shrub litter decomposes at a relatively higher rate, and graminoid litter has the highest decomposition rate; initial decomposition rates (k_o – see Eq. 2) of 0.1, 0.05 and 0.075 yr^{-1} for wet, intermediate and dry mosses species respectively and 0.15, and 0.25 yr^{-1} for shrubs and graminoids, respectively, were assumed (Aerts et al., 1999; Frolking et al., 2001). The turnover rates for different source plant types decline and converge over time, with the rate of dampening being calculated using a simplified reduction equation proposed by Clymo et al. (1998):

$$k_i = k_o \left(\frac{m_t}{m_o} \right)^n \quad (2)$$

where k_o is the initial decomposition rate, the decay parameter n determines the rate of peat decay, m_o is the initial mass and m_t is the mass remaining at some point in time (t).

Peat water content (θ) and soil temperature (T_s) have multiplicative effects on the daily decomposition rate (K_i) in each layer following Ise et al. (2008) and Lloyd and Taylor (1994):

$$K_i = k_i T_m W_m \quad (3)$$

where k_i is the decomposition rate of layer i given in Eq. 2, and T_m and W_m are the temperature and moisture multipliers, respectively. We assumed that at field capacity (θ_{opt}), peat decomposes very quickly but when the area is waterlogged its decomposition rate decreases. We allowed the peat to decompose in very dry conditions when the WTP drops below -40 cm and water content goes below 0.01 in the peat layers.

$$W_m = \begin{cases} 1.0 - 0.975 \left(\frac{\theta - \theta_{opt}}{1.0 - \theta_{opt}} \right)^\alpha, & \theta > \theta_{opt} \\ 1.0 - \left(\frac{\theta_{opt} - \theta}{\theta_{opt}} \right)^\alpha, & \theta \geq 0.01 \text{ and } \theta \leq \theta_{opt} \\ \beta, & \theta < 0.01 \text{ and } WTP < -40 \end{cases} \quad (4)$$

235 where θ is the volumetric peat water content and θ_{opt} is the field capacity and optimum volumetric water content where W_m becomes 1.0. The decomposition rate is exponentially affected by soil temperature:

$$T_m = \exp(308.56 (1.0/Z - 1.0/(T_i + Z))) \quad (5)$$

240 where T_i (°C) is the peat temperature in peat layer (i) and Z is a parameter affecting the slope of the exponential function (Table 1).

2.1.2. Hydrology

245 The hydrology module simulates the daily WTP which in turn determines the local vegetation cover and affects decomposition rates. A traditional water bucket scheme is adopted:

$$W = P - ET - ROF \quad (6)$$

250 where W is the total water input, P is the precipitation, ET is the evapotranspiration rate and ROF is the surface runoff. Using this scheme, peat water content (θ) is updated daily in each layer of each patch (see below). Precipitation is the major source of water in ombrotrophic bogs and provides the water input to the system. Precipitation comes in the form of rain or snow depending upon the daily surface
255 air temperature (T). When the temperature falls below the freezing point (0 °C assumed), water is stored in the snow pack above the peat layers. Snow melts when the temperature rises above the freezing point and melt rate is also influenced by daily precipitation (Choudhury et al., 1998):

$$260 \quad M = \min(1.5 + 0.007 \cdot P \cdot (T - T_s), SP) \quad (7)$$

where M is the daily total snow melt (mm), P is the daily precipitation (mm), T is the daily surface temperature (°C), $T_s = 0.0$, is the maximum temperature (°C) at which precipitation remains snow and SP is the current snowpack (mm).

265 Evapotranspiration and runoff remove water from the peat column. In Stordalen, summer evaporation can reach 2-3 mm day⁻¹ while remaining around 0.5-1 mm day⁻¹ in winter (Rosswall et al., 1975). Evapotranspiration is a decreasing function of WTP (Frolking et al., 2010) and is calculated using:

$$270 \quad ET(WTP) = \begin{cases} E_o, & WTP > -100 \\ 5.7 \cdot \exp(0.0105 \cdot WTP), & WTP \leq -100 \end{cases} \quad (8)$$

where E_0 is the maximum evapotranspiration rate (Table 1) and WTP is expressed in mm. Runoff is computed following a relationship modified from Wania et al. (2009a): maximum runoff can reach up to 2-3 mm day⁻¹ when the WTP reaches +15 cm above the surface, and there is negligible water loss from runoff below a WTP of -500 mm.

$$R = e^{-0.005 \text{ WTP}} \quad (9)$$

Patches can hold water up to +15 cm above the surface giving suitable conditions for graminoids to flourish (see below). Warmer and drier conditions deepen the WTP which in turn increases acrotelm depth. This prolongs peat residence time in the acrotelm, reducing the amount of carbon that passes down to the catotelm. Peat layers above the WTP in each patch are assumed to remain unsaturated.

2.1.3. Patch structure and lateral water flow

The model is run for a landscape consisting of 50 random patches of uneven height representing small-scale spatial heterogeneity typically present in peatlands. Each patch has its unique vegetation cover, hydrology, productivity and decomposition rates. Soil water across the landscape (i.e. all patches) is aggregated and redistributed among patches each day through lateral flow effecting in a simple way horizontal water flow between patches. The elevated areas lose water based on the mean landscape level WTP while depressed areas receive water from the adjacent patches. In normal conditions, elevated areas have lower WTP while hollows remain waterlogged, in turn affecting the vegetation, productivity and decomposition dynamics in each patch.

We calculate the landscape WTP and add and remove the amount of water from each patch required to match the landscape WTP:

$$MWTP = \sum PWTP_i / n \quad (10)$$

where MWTP is the mean WTP across all the patches, $PWTP_i$ is the water table position in individual patches (i) and n is the total number of patches. The water to be added to or removed from each patch with respect to mean water table position (MWTP) in each patch, i.e. lateral flow (LF), is given by:

$$DWTP_i = PWTP_i - MWTP \quad (11)$$

$$LF_i = DWTP_i \cdot \Phi_a \quad (12)$$

where $DWTP_i$ is the difference in the patch (i) and MWTP and LF_i is the total water to be added or removed with respect to MWTP in each patch (i). If the WTP is below the surface then the total water transfer is calculated by the difference in WTP (water heights) multiplied by average porosity (Φ_a) while when the WTP is

above the surface then Φ_a is not included in the calculation. The daily water balance is implemented before the exchange of water between patches.

2.1.4. Vegetation dynamics

320 Vegetation dynamics are affected both by autogenic (WTP and carbon mineralization) and allogenic (temperature and precipitation) factors influencing plant litter quality and quantity, microtopography and the total amount of peat. In this study, a fractional area approach is used to determine and update annually the percentage of patch area each plant type occupies based on annual WTP. Five plant
325 types – shrubs (Sh), graminoids (Gr), hummocks, hollows and lawn mosses (Mhu, Mho and Mim respectively) — are considered in this study. These five plant types are the main elements of the northern subarctic peatland vegetation. Shrubs such as *Betula nana*, *Andromeda polifolia* and *Vaccinium uliginosum* prefer to grow in dry hummock areas where the WTP remains relatively deeper while water filled
330 hollows are mainly dominated by tall productive graminoids, e.g. *Carex rotundata* and *Eriophorum vaginatum*. Mosses such as *Sphagnum lindbergi* are mainly present in intermediate areas where the WTP remains close to the surface. Hummock mosses such as *S. fuscum* and *S. russowii* dominate relatively drier and elevated areas while hollow mosses such as *S. balticum* and *S. riparium* thrive in
335 waterlogged conditions (Malmer et al., 2005). We assume a sigmoid relationship between annual WTP and plant productivity reduction (Yin et al., 2003), expressed here through the use of a multiplicative FPC reduction term, applied annually to the FPC values of the plant types (Fig. 2). Annual WTP influences productivity differentially for each of the plant types. Mho experience optimal productivity (no
340 FPC reduction) when annual WTP is between +10 cm above and -5 cm below the surface, declining at higher and lower WTPs while Mim and Mhu optimal productivity is between -5 to -20 cm and -20 to -35 cm respectively. They approach extinction (FPC reduction= 0.99) when annual WTP exceeds 10 cm above or below the optimal condition. Graminoids are characteristic for saturated conditions,
345 experiencing optimal productivity at annual WTP > +10 cm and approaching extinction at a WTP of -5 cm or more. At -35 cm WTP shrubs begin to occur, coming to dominate the entire patch when WTP remains below -50 cm (Fig. 2):

$$FPC_x(AWTP) = FPC_x - FPC_x (1 - 1/(1 + \exp(a \cdot b \cdot AWTP - c))) \quad (13)$$

350 where FPC_x is the FPC for plant type x: graminoid, shrub or mosses, AWTP is the annual WTP and a, b and c are parameters defined in Table 2 for each plant type. There is, however, a lag in the system, whereby WTP changes cause marginal shifts in the relative FPCs of the plant types in each patch, each year, through multiplication of the FPC reduction term in Fig 2. The FPC of any plant type is constrained never to drop below 10^{-5} allowing for recovery under suitable
355 conditions. Emulating lags due to population dynamics and community interactions in real peatland ecosystems, the model does not determine a new equilibrium vegetation composition instantaneously. This mechanism allows vegetation to withstand short-term climatic fluctuations and also to maintain a smooth transition

360 between the composition of plant species, expected as an outcome of the lagged effects of competition on the relative growth and mortality of the five plant types.

Biomass for each plant type is initialised randomly in the first year of a simulation. FPC summed across the five plant types is constrained always sum to 1, representing full vegetation coverage with no bare ground. Plant types compete with one another within but not among patches. Graminoids are known to have a significantly higher productivity than the other plant types (Malmer et al., 2005; 365 Johansson et al., 2006) whereas shrubs are typically least productive (Malmer et al., 2005). The landscape-average NPP, provided as annual input to the model (see below), was thus partitioned among plant types reflecting their relative productivities, but maintaining the prescribed average NPP value (see Eqs. (14 and 370 B.1), respectively):

$$\text{ANPP}_x = D \cdot \text{ANPP} \quad (14)$$

where ANPP is the annual NPP at mean landscape level, ANPP_x is the annual NPP for x plant types: shrubs, graminoids and three mosses, distributed according to D = 375 2.0, 1.5, 1.2, 1.0 and 1.0 for shrubs, graminoids, lawn, hummock and hollow mosses respectively.

2.1.3 Permafrost/Freezing-thawing cycle

Freezing and thawing of peat soil is typical of arctic and subarctic conditions and 380 leads to cryogenic landscape structures affecting plant productivity, decomposition and hydrological dynamics (Christensen et al., 2004; Johansson et al., 2006; Wania et al., 2009b). In order to correctly calculate the fraction of ice and water in the peat soil, soil temperature at different depths must be estimated. We calculated the peat temperature at the center of the each layer by adopting the simple analytical 385 approach used in the LPJ-GUESS ecosystem model (Smith et al., 2001; Sitch et al., 2003):

$$T_L = m + n (30 - AL \cdot L) \quad (15)$$

$$EL = \exp(-AL) \quad (16)$$

$$390 \quad T_s = T_m + EL (T_L - T_m) \quad (17)$$

where T_m is the mean of monthly mean temperatures for the last year (°C), EL is the exponential of oscillation lag, T_s is the soil temperature at the center of the peat layers, m and n are the regression parameters, AL is the oscillation lag in angular units at depth (from the surface to the center of the peat layer) (see Table 1) and L 395 is the conversion factor for oscillation lag from angular units to days (=365/2π). Soil temperature is driven by surface air temperature which acts as the upper boundary condition.

400 The fraction of air, water and ice in each layer is updated daily based on the soil

temperature in that layer, following the treatment of phase change described by (Wania et al., 2009a). If the soil temperature calculated by Eqs 15-17 passes 0 °C, ice content is set to zero and a corresponding amount of liquid water is added to the layer. Water and ice content are calculated by dividing the amount of frozen and melted water with total water holding capacity. If a layer is totally frozen (100% ice), then it cannot hold additional water. In partially frozen soil, the sum of the fractions of water and ice is limited to water holding capacity of that layer. The water and ice present in a particular peat layer influence soil thermal conductivity and heat capacity for that layer.

405

410

2.2. Study area and data requirements

The model was applied based on the conditions at Stordalen, a subarctic mire in northern Sweden (68.36°N, 19.05°E, elevation 360 m a.s.l.) located 9.5 km east of the Abisko Research Station (Oquist and Svensson, 2002). Stordalen is one of the most studied mixed mire sites in the world and was therefore suitable for developing and evaluating our model. The annual average temperature of Stordalen was -0.7 °C for the period 1913-2003 (Christensen et al., 2004) and 0.49 °C for the period 2002-2011 (Callaghan et al., 2013). The warmest month is July and the coldest month is February. The mean annual precipitation is low but has recently increased from 304 mm (1961-1990) to 362 mm (1997-2007) (Johansson et al., 2013). Overviews of the ecology and biogeochemistry of Stordalen are provided by Sonesson (1980), Malmer et al. (2005) and Johansson et al. (2006). Ecosystem respiration of Stordalen is lower relative to other northern peatlands due to low mean temperatures, a short frost-free season and the presence of discontinuous permafrost that keeps the thawed soil cooler and restricts decomposition rates (Lindroth et al., 2007).

415

420

425

The model was forced with daily average air temperature and precipitation derived by combining millennium climate anomalies with the CRU climate dataset (Mitchell and Jones, 2005). The method was explained in Chaudhary et al. (2016). From 1901-1912, the CRU TS 3.0 dataset of Mitchell and Jones (2005) and from the period 1913-2000 the observed dataset of Yang et al. (2012) was used to force the model. The high spatial resolution (50 m), modern observed climate dataset was developed by Yang et al. (2012) for the Stordalen site. In this dataset, the observations from the nearest weather stations and local observations were included to take into account the effects of the Torneträsk lake close to the Stordalen catchment on seasonal temperatures. The monthly precipitation data (1913-2000) for Stordalen at 50 m resolution were downscaled from 10 min resolution using CRU TS 1.2 data (Mitchell and Jones, 2005), a technique common for cold regions (Hanna et al., 2005). The precipitation data were also corrected by including the influences of topography and by using historical measurements of precipitation from the Abisko Research Station record.

430

435

440

NPP values to force the model were simulated by the “northern peatlands”

component of the LPJ-GUESS dynamic vegetation model (DGVM) (Smith et al., 2001; McGuire et al., 2012; Miller and Smith, 2012); configured and set up to the simulate ecosystem of the Stordalen study site as described in Chaudhary et al. (2016).

To evaluate our model, simulation results were compared to an observed peat accumulation profile for last 1000 years inferred from radio-isotope dating of peat core sequences. The peat initiation started ca. 4700 years before present (BP) in the northern part and ca. 6000 BP in the southern part of the mire as a result of terrestrialisation (Kokfelt et al., 2010).

2.3. Simulation Protocol

In order to test hypotheses relating to peatland microtopography and peat accumulation, typical Stordalen initial conditions were maintained where all the five plant types competed with each other based on the annual WTP with varying productivities and decomposition rates. The base model simulation (referred to as BAS in Table 3) was run for 1000 years with 50 patches. The model was initialised with a stochastically-generated, uneven surface having sufficient water and ice, leading to a reasonably fixed WTP so that some areas remained drier while some became completely saturated. Emulating the observed distribution of different microsites in the 1970's (Malmer et al. 2005), the simulation was started from 1000 BP with almost 50% elevated patches, 30% patches representing intermediate areas and 20% representing depressions. This assumes no major shift in topographical, ecological and climate patterns prior to 1970.

A series of sensitivity tests was performed in order to determine the effects of key drivers and assumptions on the simulated peat accumulation and microtopographical dynamics (Table 3). In these experiments, the effects of $\pm 50\%$ precipitation rates (P+50 and P-50) and ± 5 °C temperature (T+5 and T-5) changes were simulated in order to ascertain the consequences of climate modifications on peat accumulation and microtopographical changes. Implications of adjusting the homogenous species cover (HOM) and low surface roughness (LSR) on model outputs were also analyzed. In order to isolate the effects of small-scale microtopography on peat accumulation, we removed the effects of source plant type on litter decomposition by running the model with only a single plant type (intermediate moss) in the HOM experiment. The LSR experiment enabled the influence of surface roughness on peat accumulation to be determined. Finally, to determine the effects of initial topographical structure on model output, in the RAN1 experiment the model was initialised repeatedly 50 times with randomly varying topographical structure.

480

3. Results

3.1. Model Simulations

In the BAS experiment, the average total peat accumulation across 50 patches was 51.9 kg C m⁻² yr⁻¹ in the last 1000 years BP making a total cumulative peat depth increment of 49.5 cm (Fig. 3 and Table 4). The simulated cumulative peat height is near to the observation-based estimate of 56 cm for the last 1000 years (Kokfelt et al., 2010) and follows a similar trajectory. Areas dominated by hollow mosses (71.6 cm; 75.1 kg C m⁻² yr⁻¹) and lawn mosses (64.9 cm; 65.5 kg C m⁻² yr⁻¹) accumulated more peat relative to areas dominated by graminoids (58.2 cm; 61.1 kg C m⁻² yr⁻¹), and dry mosses (31.1 cm; 32.6 kg C m⁻² yr⁻¹) (Fig 4. a and b and Fig. 5). The patches co-dominated by shrubs and hummocks mosses accumulated the least peat (25.67 cm; 26.9 kg C m⁻² yr⁻¹). Although the initial decomposition rate of hollow mosses (0.1 yr⁻¹) and graminoids (0.25 yr⁻¹) was relatively higher, the saturated conditions in those patches limit daily decomposition rate leading to faster peat accumulation (Table 4). On the other hand, a fluctuating WTP increased the rate of decay in lawn mosses-covered ground despite a lower initial decomposition rate (0.05 yr⁻¹) and they accumulated less peat than patches dominated by hollow mosses. Shrubs and hummock mosses were assumed to have a moderate initial tissue decomposition rate (0.15 and 0.075 yr⁻¹ – see Table 1) yet showed the lowest peat accumulation in our simulations. This low rate of peat accumulation is the result of greater temperature- and dryness-driven rates of decomposition in elevated patches. Thus, the average rate of peat formation across the modelled landscape is ranked in the following order: Mho > Mim > Gr > Mhu > Sh (Fig. 5).

The mean annual simulated WTP fluctuated between -5 and -20 cm from the surface (Fig. 4c). The mean annual simulated ALD was shallow (20-30 cm) initially but reached 40-60 cm below the surface by the end of the simulation. The peatland's spatial heterogeneity, quantified by the standard deviation of patch height, declined over time (Fig. 4d). It is notable that graminoid-covered hollows deposited peat at faster rates compared to the elevated areas. Peat growth in intermediate areas was limited by high decomposition rates in elevated areas (a negative feedback). Therefore, we found that the spatial heterogeneity of the peatland decreased over the course of the simulation (Fig. 4d).

We found that many patches could be dominated by one or two plant types for a long period of time before reaching a threshold whereby an abrupt transition in dominance from one plant type to another occurred within a decade (not shown). On the other hand, in some patches, it was found that a new plant type could increase in abundance, after many years replacing the initial dominant plant types (Fig. 6 a, b). The vegetation transition periods and FPC fluctuations differ between patches

wherever this occurs and during such transitions both types of vegetation coexist in different proportions.

525

Cyclicity between shrubs and hummock mosses was simulated in some elevated patches. The vegetation transition period lasts for 50-150 years during which time both types of vegetation can coexist (Fig. 6 a). We found that a high rate of deposition of organic matter by hummock mosses could lead to a decline in moss fractional cover as the annual WTP drew down from the surface, resulting in a shift towards dominance by shrubs. However, the comparatively high decomposition rate of shrubs then slowed the growth of the peat column and the WTP again approached the surface in time, leading to suitable conditions for hummock mosses. A similar phenomenon results in a short cyclical transition between lawn and hummock mosses (Fig. 6 b).

530

535

3.2. Sensitivity analysis

Results from analysis of the model sensitivity to its forcing and initialisation are shown in Table 5.

540

An increase in air temperature by 5 °C (T+5) resulted in thawing of permafrost and a lowering of the WTP owing to a higher evapotranspiration rate. Higher temperature also accelerated the microbial decomposition rate (see Eq. 5). This resulted in a lower peat accumulation relative to the BAS experiment (Fig. 8). As decomposition increases due to lowering of WTP, a vegetation shift occurs and hummock mosses and shrubs completely occupy most of the patches. A lowering of the surface air temperature by 5 °C (T-5) substantially increased peat accumulation as result of slower decomposition in cooler soils. The ALD became deeper and patches hold less water (not shown). Evapotranspiration driven water loss was decreased, further lowering the decomposition rate but runoff rate increased as WTP neared the surface.

545

550

On decreasing the precipitation rate (P-50), we noticed a marginal decrease in peat accumulation because the peat column was almost frozen and only the upper 40-60 cm were active which can easily replenish even with such low levels of precipitation. Conversely, when the system is already saturated, any additional input of water (P+50) will be removed because evaporation and surface runoff are increasing functions of WTP (see Eqs. 8 and 9, respectively). However, a slightly higher average WTP in this simulation led to slightly higher peat deposition (Fig. 7).

555

560

When heterogeneity between the patches was decreased (LSR) compared to the BAS experiment, the WTP approached the surface rather quickly leading to dominance by graminoids, hollow and lawn mosses and higher rates of peat accumulation (Fig. 7). Over the course of the simulation, the patches dominated by

565

hollow and lawn mosses increased more in height than graminoid-dominated areas, leading to a rougher surface by the end of the simulation.

In the HOM experiment, a homogenous cover of lawn moss accumulated 62.7 kg C m⁻² (59.8 cm) of peat in 1000 years, which is high compared to the BAS experiment. When plant type-specific effects are removed, hydrological differences between microsites control the rate of peat accumulation and decomposition. Hollows added relatively more carbon than hummocks and intermediate areas due to their saturated conditions decreasing the overall decomposition rate. These differential rates of peat accumulation tended to cause convergence among patches, leading to a smoother peatland surface, in contrast to the LSR experiments described above. It can be seen from Figure 7 that the peat accumulation trajectory was quite sensitive to its initial microtopographical conditions (RAN1 experiments). This is because topography has a strong control on landscape WTP with cascading effects on plant distribution and peat accumulation and their distribution among patches within the landscape.

4 Discussion

Classic peatland research focused mainly on the permanently saturated zone, the catotelm (Ingram, 1982; Clymo, 1984, 1992). The role of surface structures was highly generalised or ignored in earlier modelling studies. Our results demonstrate that surface structures may potentially play a critical role in determining the composition of the vegetation in different microsites depending upon the WTP, which in turn affects the plant litter quantity and quality, influencing the net rate of peat formation and overall peatland development. Other recent studies have likewise emphasised the importance of surface micro-formations in peatland dynamics (Belyea and Malmer, 2004; Belyea and Baird, 2006; Pouliot et al., 2011; Belyea, 2013). The patterned surface creates a distinctive environment with unique plant cover, nutrient status, productivity and decomposition rates, constraining carbon fluxes at a range of scales, and affecting not just the peatland carbon balance but also its development.

Vegetation cover is important due to the consequences of plant litter quality on the accumulation rate of peat (Johnson and Damman, 1991; Belyea, 1996; Thormann and Bayley, 1997; Belyea, 2013). Different plant species differ in productivity, and produce litter that decomposes at different rates depending on its structural properties and chemical composition. This leads to highly variable spatial and temporal rates of carbon accumulation depending on vegetation type. Peat largely originating from graminoids and shrubs tends to decay faster than peat derived from *Sphagnum* mosses (Johnson and Damman, 1991; Aerts et al., 1999; Moore et al., 2007; Strakova et al., 2010). As a result, areas dominated by mosses accumulated comparatively more peat than the areas dominated by graminoids and shrubs in respective microforms (hummocks and hollows).

610

The BAS experiment highlighted the implications of plant litter quality on the net peat accumulation. Though graminoids are more productive than hollow mosses, their initial decomposition was also greater which led to relatively less peat accumulation in depressed sites. Likewise, areas co-dominated by shrubs and hummock mosses accumulated less peat than hummock moss areas despite shrubs being more productive (see Table 4). These results suggest that the inherent plant litter quality significantly affects the peatland growth and could be more important than the amount of litter deposited by the plant species.

615

620

Among mosses, *Sphagnum* species associated with hummock sites accumulated relatively less peat than hollow and lawn mosses due to a thicker aerated zone (Figs. 3a and 3b). Our simulation results suggest a hump-backed relationship between the average rate of peat formation and water-table position, and this is dictated by the differential WTP preferences assumed for the simulated plant types (Fig 5). A hump-backed curve was similarly found to describe the relationship between the rate of peat formation and acrotelm depth at Ellergower Moss site by Belyea and Clymo (2001).

625

630

This hump-backed relationship was used to explain ecohydrological feedbacks and the nonlinearity that exists in the peatland system by (Belyea and Clymo, 2001; Belyea, 2013). There are two forces at work during the peatland microtopographical dynamics. One is stabilization force (negative feedback) and other is a destabilization force (a positive feedback) (Belyea, 2013) as shown in Fig. 5. As a result of an external perturbation, a stable state is either pushed toward saturated (arrow I) or drier conditions (arrow II). The rising limb of the curve is considered unstable as any small climate perturbation may push the system toward drier and elevated path but if the water saturation limit increases then the depressed patches may turn into deep-water pool, an irreversible stage (not represented in our model). On the other hand, to dampen the effects of external forcing and to control the elevated microstructures to grow disproportionately, a negative feedback (arrow IV) pushes back the system to the stable state. If this were not the case, the differences between the microforms would become exceptionally large. We introduced a condition mimicking a stabilization force where drier patches restricted to become too large and decompose at minimal rate (0.01) when AWTP falls below -40 cm below the surface (see Eq. 4).

635

640

645

650

The total accumulated peat from the mixture of five plant types in the BAS experiment was lower than the HOM experiment, where only a single plant (lawn moss) cover was considered (Fig. 7). The latter experiment was conducted to ascertain whether the decay rate is regulated by microhabitats or by plant species. We found that hollows accumulate more carbon when there are no differences in litter quality. Weltzin et al. (2001) conducted an experiment in a homogeneously covered peatland and likewise observed higher peat accumulation in wet

depressions. Our results suggest that the interaction of both initial decomposition
655 rate and peat hydrology determine the amount of carbon deposited in patches.

Although empirical studies show that peatland microstructures may often remain
stable for long periods of time, our findings demonstrate that while some areas
660 (patches) may exhibit stability, overall a peatland can lose its heterogeneity in time
(Figs. 4a and 4d). Furthermore, in some cases they may potentially also exhibit
cyclic succession, as has often been discussed and hypothesized in early peatland
vegetation studies (VonPost and Sernander, 1910; Osvald, 1923). In the BAS
experiment, the cyclicality was simulated between the hummock mosses and shrubs,
and between lawn and hummock mosses. They regenerated and replaced each other
665 under a stable environment (Fig. 6 a). In the former case (hummock mosses-
shrubs), the main reason for the cyclic transformation was the initial loss of surface
roughness creating conditions suitable both for hummock mosses and shrubs over
higher areas. The elevated areas composed mainly of the peat derived from shrubs
quickly lost peat mass as their decomposition rate was relatively high, forcing the
670 peat column downward (or to grow less quickly). This in turn created suitable
conditions for hummock mosses as water neared the surface. When hummock
mosses occupied these areas they deposit enough carbon to cause the WTP to
decline relative to the surface which again favored dominance by shrubs. A similar
cyclical phenomenon was noticed between lawn and hummock mosses (Fig 6b) but
675 soon disappeared as initial differences in patch height were reduced (Fig 4d),
resulting in higher WTP in all patches and a more favourable setting for lawn
mosses. Tolonen (1985) showed continuous alternate streaks of dark and light
layers from the peat sample of a raised bog in Maine and New Brunswick. These
streaks were believed to correspond to lichen and *Sphagnum* peat, respectively,
680 indicating that they are associated with hummocks and intermediate areas but not
with hollows. Reflecting contrasting patterns of variability or stability among real
peatlands, depending on hydromorphic factors, our results were generally
consistent with the stable structure hypothesis (Tolonen, 1971; Barber, 1981;
Seppa, 2002) but also suggest that cyclic transformation may occur in intermediate
685 and elevated areas under certain circumstances, or for transient periods. Such
dynamics may be important for the evolution of large-scale peatland carbon
balance under changing conditions such as climate warming, but may be
challenging to predict with accuracy due to the strong influence of internal
feedbacks suggested by our simulation results.

690 In general, heterogeneity was found to decrease over time in our simulations (Fig.
4d) and the peat landscape becomes progressively more dominated by *Sphagnum*
species (Belyea and Malmer, 2004). Hollow mosses dominate the deeper sites
while hummock mosses flourish in elevated areas. A stable state is attained where
695 the *Sphagnum* species become increasingly dominant and occupy their own niche,
as often seen in many peatlands (Belyea and Lancaster, 2002) while the proportion
of graminoid and shrub dominated patches decreases slowly over time (Fig. 4a).

The decrease in aerated zone and dominance of *Sphagnum* species in turn promoted greater carbon accumulation and peat formation. We have also noticed that an abrupt transition from one dominant vegetation state to another state can lead to sudden shifts in the carbon accumulation trajectory (see grey lines in Fig. 3).

In the BAS experiment, the vegetation composition in many peatland patches remained stable for a long period of time until the gradual climate forcing lead to a step-like shift in their vegetation states (not shown). Belyea and Malmer (2004) also noted that in many peatlands long periods of little or no change can end with a sudden, abrupt shift in vegetation composition and carbon balance. Subject to very strong forcing, these patches may follow a number of alternative pathways instead of following the dominant path, as can be seen (Fig. 3 and 5) in our BAS and sensitivity experiments (T+5 and T-5). Our results are line with other studies and support the idea that successional dynamics can be nonlinear. The main identification of a nonlinear system is its sensitivity to initial conditions that in turn can cause it to follow number of alternative pathways, as reflected in our RAN1 experiment (Fig. 7). Consistent with these findings, a regional compilation of paleoecological records showed a diversity of histories of peatland development at different sites (Bunting and Warner (1998)).

When the surface roughness was reduced (LSR), a total dominance of graminoids, hollow and lawn mosses was noticed as the annual WTP came closer to the surface on average. Over time, hollow and intermediate patches grew relative to graminoid-dominated patches leading to a rougher peat surface and by the end of the simulation some patches were occupied by hummock mosses indicating that system itself transforms, from smooth to heterogeneous surface and then stabilizes.

Peatland may lose or gain carbon due to future climate warming. In our T+5 experiment, higher temperatures lead to thawing of permafrost, higher soil temperatures and an increase of aerated (less waterlogged) soils due to higher evapotranspiration. These factors accelerate microbial decomposition (Eq. 5) leading to lower peat accumulation (Ise et al., 2008; Dorrepaal et al., 2009). As annual WTP drops, some patches come to be dominated by shrubs, which affects litter quality and peat accumulation. Studies have shown that NPP may also increase in some regions due to higher temperatures, a longer growing season and CO₂ fertilisation. This could compensate for the type of loss of carbon from the system seen in our simulations, negating a potential positive feedback to climate warming (Beilman et al., 2009; Jones and Yu, 2010; Loisel et al., 2012). Charman et al. (2013) showed that variability in NPP has more influence than peat decomposition in determining peat accumulation patterns. Therefore, it is important to take into account both the modifications of NPP in a warming climate and higher peat decay rates in order to determine future peat accumulation rates.

In Stordalen, water table dynamics are largely controlled by underlying permafrost

(Christensen et al., 2004). This is taken into account in the LPJ-GUESS model generated data on NPP and explain why no major change in annual WTP was noticed in the P±50. As the majority of peat was frozen, only the upper 30-50 cm were biologically active to any great degree, which was quickly replenished under the restricted precipitation experiment (P-50) in turn negligibly affected the peat accumulation relative to the BAS experiment. In the climate of Stordalen, soil freezing causes water holding capacity of the patch to decrease with the result that the peatland requires less water to achieve a near-surface WTP compared to a non-permafrost peatland. Conversely, in the P+50 experiment, we found that adding extra water to peatlands which are already waterlogged with a high WTP (Fig. 4) would not make much difference to their WTP, vegetation cover and peat accumulation.

In a warmer climate (T+5), the model predicted that Stordalen would lose carbon as higher evapotranspiration lowers WTP, increasing peat residence time in the acrotelm, causing rapid aerobic decomposition. Similarly, recent studies have shown that a drier mire surface reduces the carbon accumulation rate by increasing the peat residence time in the acrotelm (Scanlon and Moore, 2000; Frohling et al., 2002; Malmer and Wallen, 2004; Morris and Waddington, 2011). These studies also showed that colder and wetter conditions decreased the peat decay rate due to an increase in anaerobic conditions and a lower substrate temperature, leading to higher peat deposition. This is also in line with our findings (T-5 simulation – see Fig 6).

Some recent studies have pointed out that permafrost thawing may lead to an additional water input in low-lying and collapsed areas in high-latitude peatlands (Johansson et al., 2006; Johansson et al., 2013) under warming conditions. This may be expected to result in a shift in vegetation composition favouring graminoids and mosses, thereby affecting the carbon balance. In the Stordalen mire, permafrost underlying elevated areas is being degraded as a result of recent climate warming, with an increase in wet depressions modifying the overall carbon sink capacity of the mire (Christensen et al., 2004; Malmer et al., 2005; Johansson et al., 2006). However, there is no soil subsidence functionality in our model, which explains in part why an increase in the wet patches was not simulated in the final years of the simulation.

Our results show that peatlands could exhibit different compositional and structural dynamics based on their initial topographical and climatic conditions, and plant characteristics. These dynamics in turn will affect the net carbon balance from annual to millennial time scales. Peatlands microtopographical structure may remain stable in some places but overall its heterogeneity decreases if the surface is initially highly heterogeneous. Peatlands can also exhibit cyclicity in terms of vegetation and microtopographical structure under certain conditions (Figs. 3 and 4). This implies that it may not be very easy to generalise the future behavior of

these microstructures in climate change impact studies and Earth system modelling. However, by highlighting the processes and parameters contributing the most variability in terms of carbon balance and vegetation cover, our parsimonious model approach represents a step towards the representation of such dynamics in regional vegetation and Earth system models, allowing their potentially important implications for regional and global carbon balance and biogeochemical feedbacks on the atmosphere to be explored and quantified.

5 Conclusion

The present study demonstrates that the simple 2-D microtopographical model was able to produce reasonable peatland dynamics. Though the results would be more realistic if we included the effects of permafrost contraction and expansion on the peatland hydrology, thermal conductivity and vegetation dynamics, the simulations in our study demonstrate in a transparent and plausible way interactions between peatland growth, WTP and microtopography that are consistent with many observational studies. Preliminary work with this model suggests that peatlands could exhibit alternative compositional and structural dynamics depending on initial topographical and climatic conditions, and plant characteristics. By highlighting those processes and interactions that it will be vital to consider, our model approach represents a step towards the representation of such dynamics and their climate feedbacks in regional earth system models.

810

Acknowledgements

815 This study was funded by the Nordic Top Research Initiative DEFROST and contributes to the strategic research areas Modelling the Regional and Global Earth System (MERGE) and Biodiversity and Ecosystem Services in a Changing Climate (BECC). We also acknowledge support from the Lund University Centre for the study of Climate and Carbon Cycle (LUCCI).

820

Table 1. Parameters used in the model

Parameter	Value	Units	Reference
Bulk density	105	kg C m ⁻³	(Rosswall et al., 1975; Wallen, 1986)
Initial decomposition rate of shrub	0.15	yr ⁻¹	(Aerts et al., 1999; Frohking et al., 2002; Moore et al., 2007)
Initial decomposition rate of graminoid	0.25	yr ⁻¹	
Initial decomposition rate of lawn moss	0.05	yr ⁻¹	
Initial decomposition rate of hummock moss	0.075	yr ⁻¹	
Initial decomposition rate of hollow moss	0.1	yr ⁻¹	
Decay parameter (n)	0.55	-	(Clymo, 1992)
Water modifier parameter 1 (α)	5.0	-	(Ise et al., 2008)
Water modifier parameter 2 (β)	0.6	-	
The field capacity (θ_{opt})	0.6	-	
Temperature modifier parameter (Z)	45.02	°C	-
Maximum evapotranspiration (E_o)	2.0	mm day ⁻¹	(Rosswall et al., 1975)
Soil temperature parameter (AL)	0.25	m	-

825 **Table 2.** Parameters used in fraction reduction function (Eq. 10)

Plant type	WTP (cm)	a	b	c
Graminoid	all	0.05	-20	-5
Hollow moss	> 0	0.05	-20	-12
	≤ 0	0.05	-20	10
Lawn moss	> -15	0.05	-15	0
	≤ -15	0.02	35	25
Hummock moss	> -30	0.05	-15	15
	≤ -30	0.02	51	40
Shrub	all	0.02	36	46

Table 3. Summary of sensitivity experiments

830

Experiment no.	Experiment name	Changes w.r.t BAS experiment
1.	BAS	Base model run (1000 yr)
2.	P+50	Precipitation rate uniformly increased by 50%
3.	P-50	Precipitation rate uniformly decreased by 50%
4.	T+5	Temperature uniformly increased by 5°C
5.	T-5	Temperature uniformly decreased by 5°C
6.	LSR	Spatial heterogeneity decreased
7.	HOM	Single plant type- lawn moss cover
8.	RAN1	Surface initialised with random topography

835

840

845

850

855

Table 4. Simulated peat accumulated in microstructures, expressed in terms of carbon density and height.

Dominant microstructure/ plant types (> 0.5 fraction for the last 1000 years)	Peat accumulation (kg C m ⁻²)	Peat height (cm) ⁸⁶⁰
Hollow (Gr)	65.5	64.9 ⁸⁶⁵
Hollow (Mho)	75.1	71.6
Lawn (Mim)	65.5	64.9
Hummock (Mhu)	61.1	58.2 ⁸⁷⁰
Hummock (Mhu) and (Sh)	32.6	31.1
Mean	51.9	49.5

875

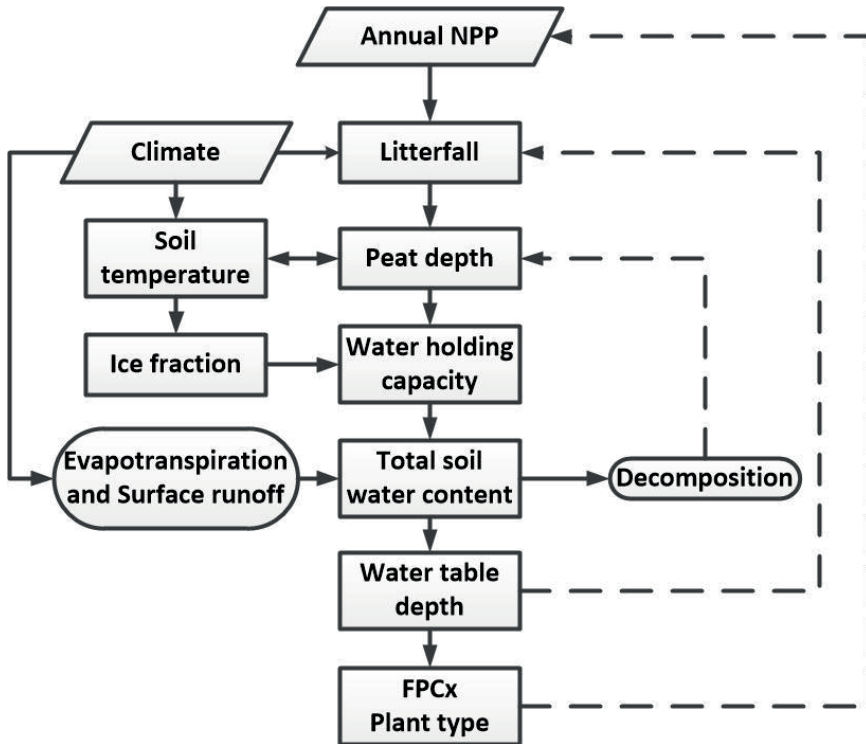
880 **Table 5.** Results of sensitivity experiments

Experiment no.	Experiment	Peat accumulated (kg C m ⁻²)	Change in peat height (cm)	Change w.r.t BAS (in kg C m ⁻² / cm)	Evidence of cyclicity?
1.	BAS	51.9	49.5	-	Yes
2.	T+5	43.4	41.4	-8.5/-8.1	No
3.	T-5	68.7	65.4	16.8/15.9	Yes
4.	P+50	52.0	49.5	0.08/0.01	Yes
5.	P-50	51.5	49.1	-0.4/-0.4	Yes
6.	LSR	75.5	71.9	23.6/22.4	No
7.	HOM	62.7	59.8	10.8/10.3	No

885

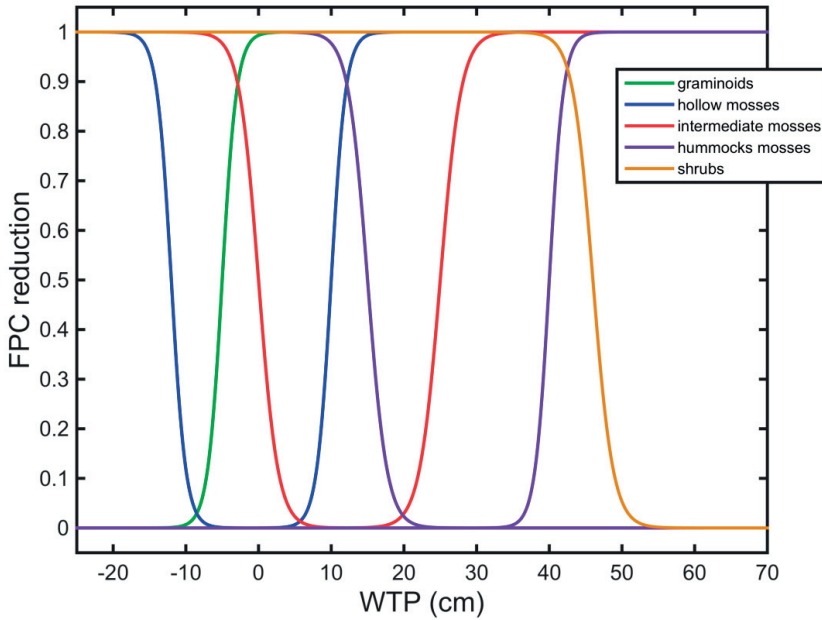
Figures:

890

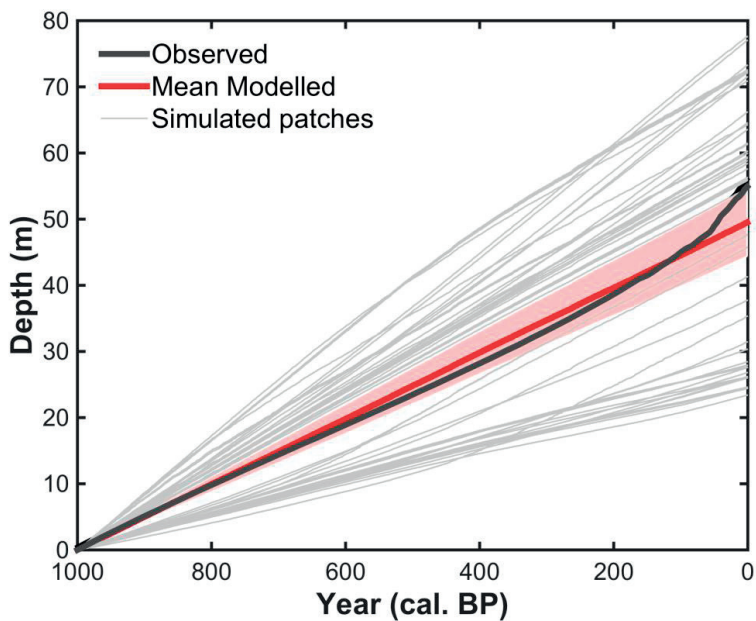


895 **Fig. 1.** Schematic representation of the two-dimensional peat microtopographical model. Model inputs are depicted by parallelograms, state variables are in rectangle boxes and processes are present in round boxes.

900



905 **Fig. 2.** Annual reduction factors for the fractional projective cover (FPC) for
 graminoids, shrubs (S), hummock mosses (Mhu), hollow mosses (Mho) and lawn
 (intermediate) mosses (Mim), respectively, as a function of annual water table
 position (WTP). FPC is adjusted sigmoidally every year using these values to
 approach the target FPC = 1 given the current WTP. Negative WTP values occur
 910 when the water table is below the surface.



915 **Fig. 3.** Comparison between observed and mean simulated peat accumulation profiles (cm) across 50 patches over 1000 years at Stordalen mire. The light red shaded area shows the 95% confidence interval inferred from the simulation data, and the light grey lines depict the simulated patches

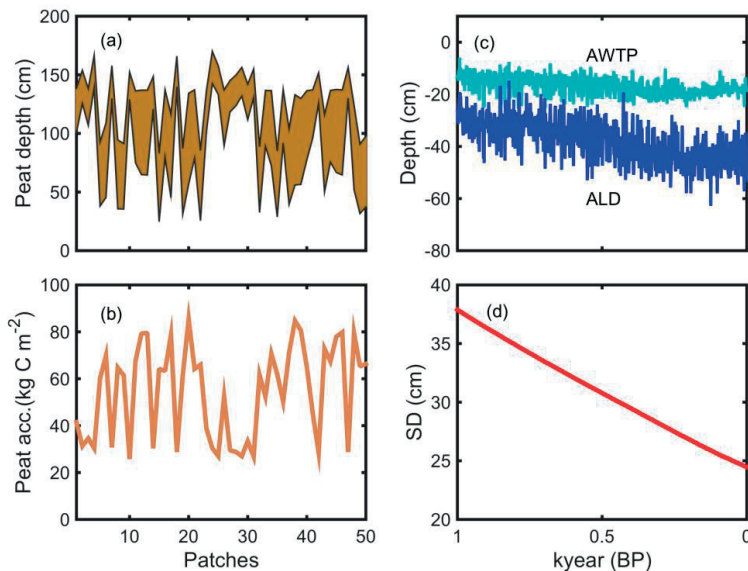
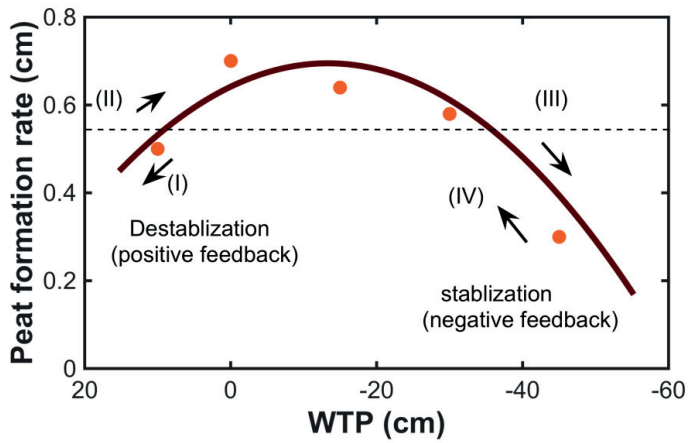


Fig. 4. Output from the two-dimensional (2-D) model representing microtopography and total peat growth (cm) of a subarctic peatland (with hummock and hollow formations), with horizontal axes showing adjacent patches representing 1 m² of a peatland area. (a) Initial and final height (black lines) with brown colour depicting total peat accumulated in 1000 simulation years; (b) total carbon accumulated (kg C m⁻²) after 1000 years; (c) annual water table position (in light blue) and annual active layer depth (in dark blue) and (d) temporal evolution of the height difference between the highest and lowest patches (cm).



935 **Fig. 5.** Average peat formation rate (cm y^{-1}) across the peat surface in relation to
 940 water table position (dotted line). The red points are the average peat formation
 rates in each microforms plotted against the mean favourable WTP limit for five
 plant types, and the black line is the second order polynomial fit to these points.
 Black arrows show the ecohydrological feedbacks involved during the peat
 formation processes (Adapted from Belyea (2013))

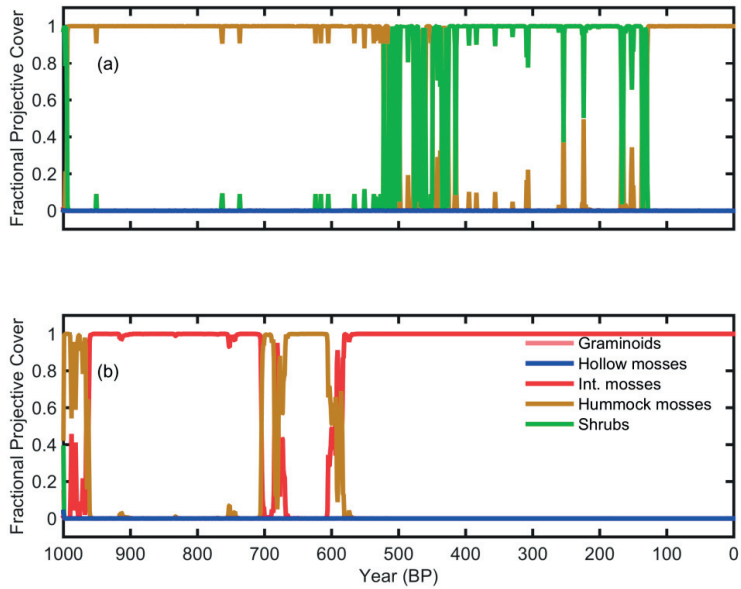
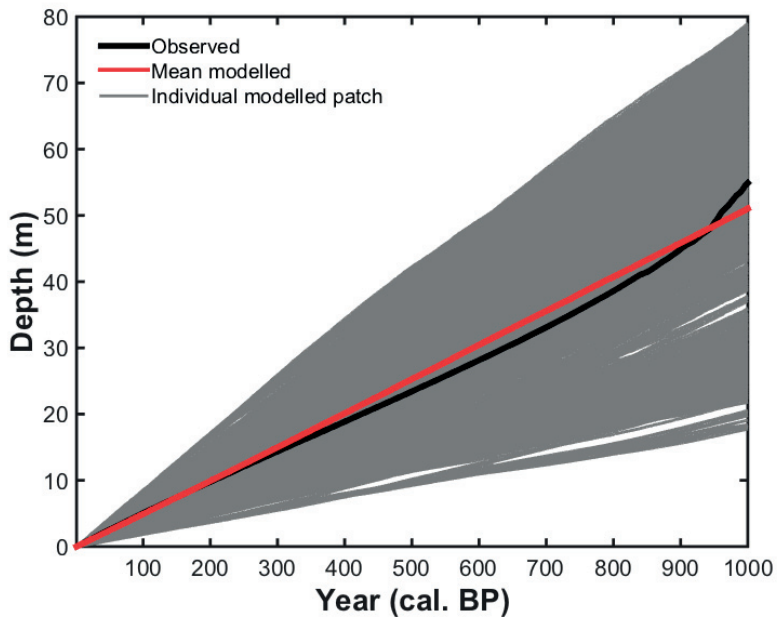


Fig. 6. The fractional projective cover (FPC) of each co-occurring plant type over the course of the base experiment (BAS) in (a) a patch representing an elevated site, and (b) a patch representing intermediate site. The cyclicity between shrubs and hummock mosses is apparent from c. 600 years in (a) and intermediate and hummock mosses in (b).

945

950



955 **Fig. 7.** Comparison between observed and simulated peat accumulation over 1000 years. The model was initialised 50 times with randomly varying topographical structure and vegetation cover. Here we show the mean of the ensemble (Mean modelled) and the individual members of the ensemble (50×50 - grey lines).

960

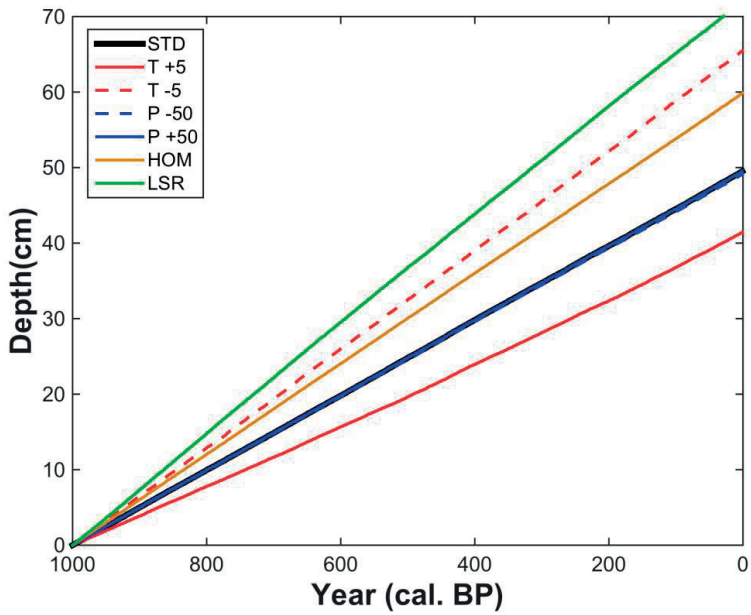


Fig. 8. Peat accumulation over 1000 years in the sensitivity experiments (see Table 3 for details).

965

970

975

980

985

Appendix B. Supplementary equations

990 Eq. B.1. The equation for normalization of NPP

$$aNPPx = k_o \cdot ANPP$$

$$TNPP = aNPPg + aNPPs + aNPPmho + aNPPmim + aNPPmhu$$

$$k = aNPPx/TNPP$$

995 $aNPPx = k ANPP$

where ANPP is the annual NPP at mean landscape level, aNPPx is the annual NPP for x plant types: graminoids, shrubs and three mosses distributed according to $k_o = 2, 1, 0.5$ for graminoids, mosses and shrubs respectively and TNPP is the total NPP

1000

1005

References:

- 1010 Aerts R, Verhoeven JTA, Whigham DF. 1999. Plant-mediated controls on nutrient cycling in temperate fens and bogs. *Ecology*, p2170-2181.
- Åkerman HJ, Johansson M. 2008. Thawing permafrost and thicker active layers in sub-arctic Sweden. *Permafrost and Periglacial Processes* 19: 279-292.
- Barber KE. 1981. Peat stratigraphy and climatic change a paleo ecological test of the theory of cyclic peat bog regeneration. XII+219Pp.
- 1015 Bauer IE. 2004. Modelling effects of litter quality and environment on peat accumulation over different time-scales. *Journal of Ecology* 92: 661-674.
- Beilman DW, MacDonald GM, Smith LC, Reimer PJ. 2009. Carbon accumulation in peatlands of West Siberia over the last 2000 years. *Global Biogeochemical Cycles* 23.
- 1020 Belyea LR. 1996. Separating the effects of litter quality and microenvironment on decomposition rates in a patterned peatland. *Oikos* 77: 529-539.
- Belyea LR. 2013. Nonlinear Dynamics of Peatlands and Potential Feedbacks on the Climate System. *Carbon Cycling in Northern Peatlands: American Geophysical Union*, p5-18.
- 1025 Belyea LR, Baird AJ. 2006. Beyond "The limits to peat bog growth": Cross-scale feedback in peatland development. *Ecological Monographs* 76: 299-322.
- Belyea LR, Clymo RS. 2001. Feedback control of the rate of peat formation. *Proceedings of the Royal Society B-Biological Sciences* 268: 1315-1321.
- 1030 Belyea LR, Lancaster J. 2002. Inferring landscape dynamics of bog pools from scaling relationships and spatial patterns. *Journal of Ecology* 90: 223-234.
- Belyea LR, Malmer N. 2004. Carbon sequestration in peatland: patterns and mechanisms of response to climate change. *Global Change Biology* 10: 1043-1052.
- Bragazza L, Parisod J, Buttler A, Bardgett RD. 2013. Biogeochemical plant-soil microbe feedback in response to climate warming in peatlands. *Nature Climate Change* 3: 273-277.
- 1035 Bridgman SD, Johnston CA, Pastor J, Updegraff K. 1995. Potential feedbacks of northern wetlands on climate-change - an outline of an approach to predict climate-change impact. *Bioscience* 45: 262-274.
- Bunting MJ, Warner BG. 1998. Hydrosere development in southern Ontario: patterns and controls. *Journal of Biogeography* 25: 3-18.
- 1040 Callaghan TV, Jonasson C, Thierfelder T, Yang ZL, Hedenas H, Johansson M, Molau U, Van Bogaert R, Michelsen A, Olofsson J, Gwynn-Jones D, Bokhorst S, Phoenix G, Bjerke JW, Tommervik H, Christensen TR, Hanna E, Koller EK, Sloan VL. 2013. Ecosystem change and stability over multiple decades in the Swedish

- 1045 subarctic: complex processes and multiple drivers. *Philosophical Transactions of the Royal Society B-Biological Sciences* 368: 18.
- Charman DJ, Beilman DW, Blaauw M, Booth RK, Brewer S, Chambers FM, Christen JA, Gallego-Sala A, Harrison SP, Hughes PDM, Jackson ST, Korhola A, Mauquoy D, Mitchell FJG, Prentice IC, van der Linden M, De Vleeschouwer F, Yu
 1050 ZC, Alm J, Bauer IE, Corish YMC, Garneau M, Hohl V, Huang Y, Karofeld E, Le Roux G, Loisel J, Moschen R, Nichols JE, Nieminen TM, MacDonald GM, Phadtare NR, Rausch N, Sillasoo U, Swindles GT, Tuittila ES, Ukonmaanaho L, Valiranta M, van Bellen S, van Geel B, Vitt DH, Zhao Y. 2013. Climate-related changes in peatland carbon accumulation during the last millennium.
 1055 *Biogeosciences* 10: 929-944.
- Chaudhary N, Miller PA, Smith B. 2016. Modelling Holocene peatland dynamics with an individual-based dynamic vegetation model. *Biogeosciences* (in review).
- Choudhury BJ, DiGirolamo NE, Susskind J, Darnell WL, Gupta SK, Asrar G. 1998. A biophysical process-based estimate of global land surface evaporation using satellite and ancillary data - II. Regional and global patterns of seasonal and
 1060 annual variations. *Journal of Hydrology* 205: 186-204.
- Christensen JH, B. Hewitson, A. Busuioc, A. Chen, X. Gao, I. Held, R. Jones, R.K. Kolli, W.-T. Kwon, R. Laprise, V. Magaña Rueda, L. Mearns, C.G. Menéndez, J. Räisänen, A. Rinke, Sarr A, Whetton P. 2007. Regional Climate Projections. In: *Climate Change 2007: The Physical Science Basis. Contribution of Working Group I to the Fourth Assessment Report of the Intergovernmental Panel on Climate Change*. [Solomon, S., D. Qin, M. Manning, Z. Chen, M. Marquis, K.B. Averyt, M. Tignor and H.L. Miller (eds.)]. Cambridge University Press, Cambridge, United Kingdom and New York, NY, USA.
 1065
- 1070 Christensen TR, Johansson TR, Akerman HJ, Mastepanov M, Malmer N, Friborg T, Crill P, Svensson BH. 2004. Thawing sub-arctic permafrost: Effects on vegetation and methane emissions. *Geophysical Research Letters* 31.
- Clymo RS. 1984. The limits to peat bog growth. *Philosophical Transactions of the Royal Society of London Series B-Biological Sciences* 303: 605-654.
- 1075 Clymo RS. 1991. Peat growth. *Quaternary Landscapes*. Eds Shane LCK, Cushing EJ. Minneapolis, University of Minnesota Press.: 76-112.
- Clymo RS. 1992. Models of peat growth. *Suo (Helsinki)* 43: 127-136.
- Clymo RS, Hayward PM. 1982. The ecology of Sphagnum. *The Ecology of Bryophytes*. Ed Smith AJE. London, Chapman and Hall: 229-289.
- 1080 Clymo RS, Turunen J, Tolonen K. 1998. Carbon accumulation in peatland. *Oikos* 81: 368-388.
- Davidson EA, Janssens IA. 2006. Temperature sensitivity of soil carbon decomposition and feedbacks to climate change. *Nature* 440: 165-173.

- 1085 Dorrepaal E, Toet S, van Logtestijn RSP, Swart E, van de Weg MJ, Callaghan TV, Aerts R. 2009. Carbon respiration from subsurface peat accelerated by climate warming in the subarctic. *Nature* 460: 616-U679.
- Fan ZS, McGuire AD, Turetsky MR, Harden JW, Waddington JM, Kane ES. 2013. The response of soil organic carbon of a rich fen peatland in interior Alaska to projected climate change. *Global Change Biology* 19: 604-620.
- 1090 Frohling S, Roulet NT, Moore TR, Lafleur PM, Bubier JL, Crill PM. 2002. Modeling seasonal to annual carbon balance of Mer Bleue Bog, Ontario, Canada. *GLOBAL BIOGEOCHEMICAL CYCLES* 16.
- Frohling S, Roulet NT, Moore TR, Richard PJH, Lavoie M, Muller SD. 2001. Modeling northern peatland decomposition and peat accumulation. *Ecosystems* 4: 479-498.
- 1095 Frohling S, Roulet NT, Tuittila E, Bubier JL, Quillet A, Talbot J, Richard PJH. 2010. A new model of Holocene peatland net primary production, decomposition, water balance, and peat accumulation. *Earth System Dynamics*, p1-21.
- Gorham E. 1991. Northern peatlands - role in the carbon-cycle and probable responses to climatic warming. *Ecological Applications* 1: 182-195.
- 1100 Hanna E, Huybrechts P, Janssens I, Cappelen J, Steffen K, Stephens A. 2005. Runoff and mass balance of the Greenland ice sheet: 1958-2003. *Journal of Geophysical Research-Atmospheres* 110: 16.
- Hayward PM, Clymo RS. 1983. The growth of sphagnum - experiments on, and simulation of, some effects of light-flux and water-table depth. *Journal of Ecology* 71: 845-863.
- 1105 Ingram HAP. 1982. Size and shape in raised mire ecosystems - a geophysical model. *Nature* 297: 300-303.
- IPCC. 2013. *Climate Change 2013: The Physical Science Basis. Contribution of Working Group I to the Fifth Assessment Report of the Intergovernmental Panel on Climate Change*: NY, USA.
- 1110 Ise T, Dunn AL, Wofsy SC, Moorcroft PR. 2008. High sensitivity of peat decomposition to climate change through water-table feedback. *Nature Geoscience* 1: 763-766.
- 1115 Johansson M, Callaghan TV, Bosio J, Akerman HJ, Jackowicz-Korczynski M, Christensen TR. 2013. Rapid responses of permafrost and vegetation to experimentally increased snow cover in sub-arctic Sweden. *Environmental Research Letters* 8.
- Johansson T, Malmer N, Crill PM, Friborg T, Akerman JH, Mastepanov M, Christensen TR. 2006. Decadal vegetation changes in a northern peatland, greenhouse gas fluxes and net radiative forcing. *Global Change Biology* 12: 2352-2369.
- 1120

- Johnson LC, Damman AWH. 1991. Species-controlled sphagnum decay on a south Swedish raised bog. *Oikos* 61: 234-242.
- 1125 Jones MC, Yu Z. 2010. Rapid deglacial and early Holocene expansion of peatlands in Alaska. *Proceedings of the National Academy of Sciences of the United States of America* 107: 7347-7352.
- Klein ES, Yu Z, Booth RK. 2013. Recent increase in peatland carbon accumulation in a thermokarst lake basin in southwestern Alaska. *Palaeogeography Palaeoclimatology Palaeoecology*, p186-195.
- 1130 Kokfelt U, Reuss N, Struyf E, Sonesson M, Rundgren M, Skog G, Rosen P, Hammarlund D. 2010. Wetland development, permafrost history and nutrient cycling inferred from late Holocene peat and lake sediment records in subarctic Sweden. *Journal of Paleolimnology* 44: 327-342.
- 1135 Lindroth A, Lund M, Nilsson M, Aurela M, Christensen TR, Laurila T, Rinne J, Riutta T, Sagerfors J, Strom L, Tuovinen JP, Vesala T. 2007. Environmental controls on the CO₂ exchange in north European mires. *Tellus Series B-Chemical and Physical Meteorology* 59: 812-825.
- Lloyd J, Taylor JA. 1994. On the temperature-dependence of soil respiration. *Functional Ecology* 8: 315-323.
- 1140 Loisel J, Gallego-Sala AV, Yu Z. 2012. Global-scale pattern of peatland Sphagnum growth driven by photosynthetically active radiation and growing season length. *Biogeosciences* 9: 2737-2746.
- Loisel J, Yu ZC, Beilman DW, Camill P, Alm J, Amesbury MJ, Anderson D, Andersson S, Bochicchio C, Barber K, Belyea LR, Bunbury J, Chambers FM, Charman DJ, De Vleeschouwer F, Fialkiewicz-Koziel B, Finkelstein SA, Galka M, Garneau M, Hammarlund D, Hinchcliffé W, Holmquist J, Hughes P, Jones MC, Klein ES, Kokfelt U, Korhola A, Kuhry P, Lamarre A, Lamentowicz M, Large D, Lavoie M, MacDonald G, Magnan G, Makila M, Mallon G, Mathijssen P, Mauquoy D, McCarroll J, Moore TR, Nichols J, O'Reilly B, Oksanen P, Packalen M, Peteet D, Richard PJH, Robinson S, Ronkainen T, Rundgren M, Sannel ABK, Tarnocai C, Thom T, Tuittila ES, Turetsky M, Valiranta M, van der Linden M, van Geel B, van Bellen S, Vitt D, Zhao Y, Zhou WJ. 2014. A database and synthesis of northern peatland soil properties and Holocene carbon and nitrogen accumulation. *Holocene* 24: 1028-1042.
- 1145
- 1150
- 1155 Malmer N, Johansson T, Olsrud M, Christensen TR. 2005. Vegetation, climatic changes and net carbon sequestration in a North-Scandinavian subarctic mire over 30 years. *Global Change Biology* 11: 1895-1909.
- Malmer N, Wallen B. 2004. Input rates, decay losses and accumulation rates of carbon in bogs during the last millennium: internal processes and environmental changes. *Holocene* 14: 111-117.
- 1160
- McGuire AD, Christensen TR, Hayes D, Heroult A, Euskirchen E, Kimball JS, Koven C, Lafleur P, Miller PA, Oechel W, Peylin P, Williams M, Yi Y. 2012. An assessment of the carbon balance of Arctic tundra: comparisons among

- 1165 observations, process models, and atmospheric inversions. *Biogeosciences* 9: 3185-3204.
- Miller PA, Smith B. 2012. Modelling Tundra Vegetation Response to Recent Arctic Warming. *Ambio* 41: 281-291.
- 1170 Mitchell TD, Jones PD. 2005. An improved method of constructing a database of monthly climate observations and associated high-resolution grids. *International Journal of Climatology* 25: 693-712.
- Moore TR, Bubier JL, Bledzki L. 2007. Litter decomposition in temperate peatland ecosystems: The effect of substrate and site. *Ecosystems* 10: 949-963.
- 1175 Morris PJ, Waddington JM. 2011. Groundwater residence time distributions in peatlands: Implications for peat decomposition and accumulation. *Water Resources Research* 47: 12.
- Nungesser MK. 2003. Modelling microtopography in boreal peatlands: hummocks and hollows. *Ecological Modelling* 165: 175-207.
- 1180 Oquist MG, Svensson BH. 2002. Vascular plants as regulators of methane emissions from a subarctic mire ecosystem. *Journal of Geophysical Research-Atmospheres* 107: 10.
- Osvald H. 1923. Die Vegetation des Hochmoores Komosse. Svenska Växtsociologiska Sällskapets Handlingar 1. Uppsala.
- 1185 Pouliot R, Rochefort L, Karofeld E, Mercier C. 2011. Initiation of Sphagnum moss hummocks in bogs and the presence of vascular plants: Is there a link? *Acta Oecologica-International Journal of Ecology* 37: 346-354.
- Rosswall T, Veum AK, Karenlampi L. 1975. Plant litter decomposition at fennoscandian tundra sites. 268-278p.
- 1190 Scanlon D, Moore T. 2000. Carbon dioxide production from peatland soil profiles: The influence of temperature, oxic/anoxic conditions and substrate. *Soil Science* 165: 153-160.
- Seppa H. 2002. Mires of Finland: regional and local controls of vegetation, landforms, and long-term dynamics. *Fennia* 180: 43-60.
- 1195 Sitch S, Smith B, Prentice IC, Arneth A, Bondeau A, Cramer W, Kaplan JO, Levis S, Lucht W, Sykes MT, Thonicke K, Venevsky S. 2003. Evaluation of ecosystem dynamics, plant geography and terrestrial carbon cycling in the LPJ dynamic global vegetation model. *Global Change Biology* 9: 161-185.
- 1200 Smith B, Prentice IC, Sykes MT. 2001. Representation of vegetation dynamics in the modelling of terrestrial ecosystems: comparing two contrasting approaches within European climate space. *Global Ecology and Biogeography* 10: 621-637.
- Smith B, Samuelsson P, Wramneby A, Rummukainen M. 2011. A model of the coupled dynamics of climate, vegetation and terrestrial ecosystem biogeochemistry

- for regional applications. *Tellus Series a-Dynamic Meteorology and Oceanography* 63: 87-106.
- 1205 Sonesson M. 1980. Ecology of a subarctic mire. Stockholm, Sweden: Swedish Natural Science Research Council. 313pp.p.
- Strakova P, Anttila J, Spetz P, Kitunen V, Tapanila T, Laiho R. 2010. Litter quality and its response to water level drawdown in boreal peatlands at plant species and community level. *Plant and Soil* 335: 501-520.
- 1210 Thormann MN, Bayley SE. 1997. Decomposition along a moderate-rich fen-marsh peatland gradient in boreal Alberta, Canada. *Wetlands* 17: 123-137.
- Tolonen K. 1971. On the regeneration of north european bogs part 1 Klaukkalan Isosuo in southern Finland. *Suomen Maataloustieteellisen Seuran Julkaisuja* 123: 143-166.
- 1215 Tolonen M. 1985. Paleoeological record of local fire history from a peat deposit in SW Finland. *Annales Botanici Fennici* 22: 15-29.
- Trudeau NC, Garneau M, Pelletier L. 2014. Interannual variability in the CO2 balance of a boreal patterned fen, James Bay, Canada. *Biogeochemistry* 118: 371-387.
- 1220 Turunen J, Tomppo E, Tolonen K, Reinikainen A. 2002. Estimating carbon accumulation rates of undrained mires in Finland - application to boreal and subarctic regions. *Holocene* 12: 69-80.
- VonPost L, Sernander R. 1910. Pflanzen-physiognomische Studien auf Torfmooren in Närke. *Livretguide des excursions en Suede du Xle Congr. Geol. Int.* 14
- 1225 Stockholm: 48.
- Waddington JM, Roulet NT. 1996. Atmosphere-wetland carbon exchanges: Scale dependency of CO2 and CH4 exchange on the developmental topography of a peatland. *GLOBAL BIOGEOCHEMICAL CYCLES* 10: 233-245.
- Wallen B. 1986. ABOVE AND BELOW GROUND DRY MASS OF THE 3 MAIN VASCULAR PLANTS ON HUMMOCKS ON A SUB-ARCTIC PEAT BOG. *Oikos* 46: 51-56.
- 1230 Wania R, Ross I, Prentice IC. 2009a. Integrating peatlands and permafrost into a dynamic global vegetation model: 1. Evaluation and sensitivity of physical land surface processes. *GLOBAL BIOGEOCHEMICAL CYCLES* 23.
- 1235 Wania R, Ross I, Prentice IC. 2009b. Integrating peatlands and permafrost into a dynamic global vegetation model: 2. Evaluation and sensitivity of vegetation and carbon cycle processes. *GLOBAL BIOGEOCHEMICAL CYCLES* 23.
- Weltzin JF, Harth C, Bridgham SD, Pastor J, Vonderharr M. 2001. Production and microtopography of bog bryophytes: response to warming and water-table manipulations. *Oecologia* 128: 557-565.
- 1240

- Wieder RK. 2001. Past, present, and future peatland carbon balance: An empirical model based on Pb-210-dated cores. *Ecological Applications* 11: 327-342.
- 1245 Yang Z, Sykes MT, Hanna E, Callaghan TV. 2012. Linking Fine-Scale Sub-Arctic Vegetation Distribution in Complex Topography with Surface-Air-Temperature Modelled at 50-m Resolution. *Ambio* 41: 292-302.
- Yin XY, Goudriaan J, Lantinga EA, Vos J, Spiertz HJ. 2003. A flexible sigmoid function of determinate growth. *Annals of Botany* 91: 361-371.
- Yu ZC. 2012. Northern peatland carbon stocks and dynamics: a review. *Biogeosciences* 9: 4071-4085.
- 1250 Yu ZC, Beilman DW, Jones MC. 2009. Sensitivity of Northern Peatland Carbon Dynamics to Holocene Climate Change. Baird AJ, Belyea LR, Comas X, Reeve AS, Slater LD editors. *Carbon Cycling in Northern Peatlands*, p55-69.
- Yu ZC, Loisel J, Brosseau DP, Beilman DW, Hunt SJ. 2010. Global peatland dynamics since the Last Glacial Maximum. *Geophysical Research Letters* 37: 5.
- 1255 Zhang W, Jansson C, Miller PA, Smith B, Samuelsson P. 2014. Biogeophysical feedbacks enhance the Arctic terrestrial carbon sink in regional Earth system dynamics. *Biogeosciences* 11: 5503-5519.
- 1260 Zhang W, Miller PA, Smith B, Wania R, Koenigk T, Doscher R. 2013. Tundra shrubification and tree-line advance amplify arctic climate warming: results from an individual-based dynamic vegetation model. *Environmental Research Letters* 8.

Paper IV



Site-level model intercomparison of high latitude and high altitude soil thermal dynamics in tundra and barren landscapes

A. Ekici^{1,10}, S. Chadburn², N. Chaudhary³, L. H. Hajdu⁴, A. Marmy⁵, S. Peng^{6,7}, J. Boike⁸, E. Burke⁹, A. D. Friend⁴, C. Hauck⁵, G. Krinner⁶, M. Langer^{6,8}, P. A. Miller³, and C. Beer¹⁰

¹Department of Biogeochemical Integration, Max Planck Institute for Biogeochemistry, Jena, Germany

²Earth System Sciences, Laver Building, University of Exeter, Exeter, UK

³Department of Physical Geography and Ecosystem Science, Lund University, Lund, Sweden

⁴Department of Geography, University of Cambridge, Cambridge, England

⁵Department of Geosciences, University of Fribourg, Fribourg, Switzerland

⁶CNRS and Université Grenoble Alpes, LGGE, 38041, Grenoble, France

⁷Laboratoire des Sciences du Climat et de l'Environnement, Gif-sur-Yvette, France

⁸Alfred-Wegener-Institut, Helmholtz-Zentrum für Polar- und Meeresforschung, Potsdam, Germany

⁹Met Office Hadley Centre, Exeter, UK

¹⁰Department of Applied Environmental Science (ITM) and Bolin Centre for Climate Research, Stockholm University, Stockholm, Sweden

Correspondence to: A. Ekici (a.ekici@exeter.ac.uk)

Received: 8 July 2014 – Published in The Cryosphere Discuss.: 18 September 2014

Revised: 19 June 2015 – Accepted: 2 July 2015 – Published: 22 July 2015

Abstract. Modeling soil thermal dynamics at high latitudes and altitudes requires representations of physical processes such as snow insulation, soil freezing and thawing and sub-surface conditions like soil water/ice content and soil texture. We have compared six different land models: JSBACH, ORCHIDEE, JULES, COUP, HYBRID8 and LPJ-GUESS, at four different sites with distinct cold region landscape types, to identify the importance of physical processes in capturing observed temperature dynamics in soils. The sites include alpine, high Arctic, wet polygonal tundra and non-permafrost Arctic, thus showing how a range of models can represent distinct soil temperature regimes. For all sites, snow insulation is of major importance for estimating topsoil conditions. However, soil physics is essential for the subsoil temperature dynamics and thus the active layer thicknesses. This analysis shows that land models need more realistic surface processes, such as detailed snow dynamics and moss cover with changing thickness and wetness, along with better representations of subsoil thermal dynamics.

1 Introduction

Recent atmospheric warming trends are affecting terrestrial systems by increasing soil temperatures and causing changes in the hydrological cycle. Especially in high latitudes and altitudes, clear signs of change have been observed (Serreze et al., 2000; ACIA, 2005; IPCC AR5, 2013). These relatively colder regions are characterized by the frozen state of terrestrial water, which brings additional risks associated with shifting soils into an unfrozen state. Such changes will have broad implications for the physical (Romanovsky et al., 2010), biogeochemical (Schuur et al., 2008) and structural (Larsen et al., 2008) conditions of the local, regional and global climate system. Therefore, predicting the future state of the soil thermal regime at high latitudes and altitudes holds major importance for Earth system modeling.

There are increasing concerns as to how land models perform at capturing high latitude soil thermal dynamics, in particular in permafrost regions. Recent studies (Koven et al., 2013; Slater and Lawrence, 2013) have provided detailed assessments of commonly used earth system models (ESMs) in simulating soil temperatures of present and future state

of the Arctic. By using the Coupled Model Intercomparison Project phase 5 – CMIP5 (Taylor et al., 2009) results, Koven et al. (2013) have shown a broad range of model outputs in simulated soil temperature. They attributed most of the inter-model discrepancies to air–land surface coupling and snow representations in the models. Similar to those findings, Slater and Lawrence (2013) confirmed the high uncertainty of CMIP5 models in predicting the permafrost state and its future trajectories. They concluded that these model versions are not appropriate for such experiments, since they lack critical processes for cold region soils. Snow insulation, land model physics and vertical model resolutions were identified as the major sources of uncertainty.

For the cold regions, one of the most important factors modifying soil temperature range is the surface snow cover. As discussed in many previous studies (Zhang, 2005; Koven et al., 2013; Scherler et al., 2013; Marmy et al., 2013; Langer et al., 2013; Boike et al., 2003; Gubler et al., 2013; Fiddes et al., 2015), snow dynamics are quite complex and the insulation effects of snow can be extremely important for the soil thermal regime. Model representations of snow cover are lacking many fine-scale processes such as snow ablation, depth hoar formation, snow metamorphism, wind effects on snow distribution and explicit heat and water transfer within snow layers. These issues bring additional uncertainties to global projections.

Current land surface schemes, and most vegetation and soil models, represent energy and mass exchange between the land surface and atmosphere in one dimension. Using a grid cell approach, such exchanges are estimated for the entire land surface or specific regions. However, comparing simulated and observed time series of states or fluxes at point scale rather than grid averaging is an important component of model evaluation, for understanding remaining limitations of models (Ekici et al., 2014; Mahecha et al., 2010). In such “site-level runs”, we assume that lateral processes can be ignored and that the ground thermal dynamics are mainly controlled by vertical processes. Then, models are driven by observed climate and variables of interest can be compared to observations at different temporal scales. Even though such idealized field conditions never exist, a careful interpretation of site-level runs can identify major gaps in process representations in models.

In recent years, land models have improved their representations of the soil physical environment in cold regions. Model enhancements include the addition of soil freezing and thawing, detailed snow representations, prescribed moss cover, extended soil columns and coupling of soil heat transfer with hydrology (Ekici et al., 2014; Gouttevin et al., 2012a; Dankers et al., 2011; Lawrence et al., 2008; Wania et al., 2009a). Also active layer thickness (ALT) estimates have improved in the current model versions. Simple relationships between surface temperature and ALT were used in the early modeling studies (Lunardini, 1981; Kudryavtsev et al., 1974; Romanovsky and Osterkamp, 1997; Shiklo-

manov and Nelson, 1999; Stendel et al., 2007; Anisimov et al., 1997). These approaches assume an equilibrium condition, whereas a transient numerical method is better suited within a climate change context. A good review of widely used analytical approximations and differences to numerical approaches is given by Riseborough et al. (2008). With the advanced soil physics in many models, these transient approaches are more widely used, especially in long-term simulations. Such improvements highlight the need for an updated assessment of model performances in representing high latitude/altitude soil thermal dynamics.

We have compared the performances of six different land models in simulating soil thermal dynamics at four contrasting sites. In contrast to previous work (Koven et al., 2013; Slater and Lawrence, 2013), we used advanced model versions specifically improved for cold regions and our model simulations are driven by (and evaluated with) site observations. To represent a wider range of assessment and model structures, we used both land components of ESMs (JSBACH, ORCHIDEE, JULES) and stand-alone models (COUP, HYBRID8, LPJ-GUESS), and compared them at Arctic permafrost, Alpine permafrost and Arctic non-permafrost sites. By doing so, we aimed to quantify the importance of different processes, to determine the general shortcomings of current model versions and finally to highlight the key processes for future model developments.

2 Methods

2.1 Model descriptions

2.1.1 JSBACH

Jena Scheme for Biosphere–Atmosphere Coupling in Hamburg (JSBACH) is the land surface component of the Max Planck Institute earth system model (MPI-ESM), which comprises ECHAM6 for the atmosphere (Stevens et al., 2012) and MPIOM for the ocean (Jungclaus et al., 2013). JSBACH provides the land surface boundary for the atmosphere in coupled simulations; however, it can also be used offline driven by atmospheric forcing. The current version of JSBACH (Ekici et al., 2014) employs soil heat transfer coupled to hydrology with freezing and thawing processes included. The soil model is discretized as five layers with increasing thicknesses of up to 10 m depth. There are up to five snow layers with constant density and heat transfer parameters. JSBACH also simulates a simple moss/organic matter insulation layer again with constant parameters.

2.1.2 ORCHIDEE

ORCHIDEE is a global land surface model, which can be used coupled to the Institut Pierre Simon Laplace (IPSL) climate model or driven offline by prescribed atmospheric forcing (Krinner et al., 2005). ORCHIDEE computes all the

soil–atmosphere–vegetation-relevant energy and water exchange processes in 30 min time steps. It combines a soil–vegetation–atmosphere transfer model with a carbon cycle module, computing vertically detailed soil carbon dynamics. The high latitude version of ORCHIDEE includes a dynamic three-layer snow module (Wang et al., 2013), soil freeze–thaw processes (Gouttevin et al., 2012a), and a vertical permafrost soil thermal and carbon module (Koven et al., 2011). The soil hydrology is vertically discretized as 11 numerical nodes with 2 m depth (Gouttevin et al., 2012a), and soil thermal and carbon modules are vertically discretized as 32 layers with ~47 m depth (Koven et al., 2011). A one-dimensional Fourier equation was applied to calculate soil thermal dynamics, and both soil thermal conductivity and heat capacity are functions of the frozen and unfrozen soil water content and of dry and saturated soil thermal properties (Gouttevin et al., 2012b).

2.1.3 JULES

JULES (Joint UK Land Environment Simulator) is the land-surface scheme used in the Hadley Centre climate model (Best et al., 2011; Clark et al., 2011), which can also be run offline, driven by atmospheric forcing data. It is based on the Met Office Surface Exchange Scheme, MOSES (Cox et al., 1999). JULES simulates surface exchange, vegetation dynamics and soil physical processes. It can be run at a single point, or as a set of points representing a 2-D grid. In each grid cell, the surface is tiled into different surface types, and the soil is treated as a single column, discretized vertically into layers (four in the standard setup). JULES simulates fluxes of moisture and energy between the atmosphere, surface and soil, and the soil freezing and thawing. It includes a carbon cycle that can simulate carbon exchange between the atmosphere, vegetation and soil. It also includes a multi-layer snow model (Best et al., 2011), with layers that have variable thickness, density and thermal properties. The snow scheme significantly improves the soil thermal regime in comparison with the old, single-layer scheme (Burke et al., 2013). The model can be run with a time step of between 30 min and 3 h, depending on user preference.

2.1.4 COUP

COUP is a stand-alone, one-dimensional heat and mass transfer model for the soil–snow–atmosphere system (Jansson and Karlberg, 2011) and is capable of simulating transient hydrothermal processes in the subsurface including seasonal or perennial frozen ground (see e.g., Hollesen et al., 2011; Scherler et al., 2010, 2013). Two coupled partial differential equations for water and heat flow are the core of the COUP Model. They are calculated over up to 50 vertical layers of arbitrary depth. Processes that are important for permafrost simulations, such as the freezing and thawing of soil as well as the accumulation, metamorphosis and

melt of snow cover are included in the model (Lundin, 1990; Gustafsson et al., 2001). Freezing processes in the soil are based on a function of freezing point depression and on an analogy of freezing–thawing and wetting–drying (Harlan, 1973; Jansson and Karlberg, 2011). Snow cover is simulated as one layer of variable height, density, and water content.

The upper boundary condition is given by a surface energy balance at the soil–snow–atmosphere boundary layer, driven by climatic variables. The lower boundary condition at the bottom of the soil column is usually given by the geothermal heat flux (or zero heat flux) and a seepage flow of percolating water. Water transfer in the soil depends on texture, porosity, water, and ice content. Bypass flow through macropores, lateral runoff and rapid lateral drainage due to steep terrain can also be considered (e.g., Scherler et al., 2013). A detailed description of the model including all its equations and parameters is given in Jansson and Karlberg (2011) and Jansson (2012).

2.1.5 HYBRID8

HYBRID8 is a stand-alone land surface model, which computes the carbon and water cycling within the biosphere and between the biosphere and atmosphere. It is driven by the daily/sub-daily climate variables above the canopy, and the atmospheric CO₂ concentration. Computations are performed on a 30 min time step for the energy fluxes and exchanges of carbon and water with the atmosphere and the soil. Litter production and soil decomposition are calculated at a daily time step. HYBRID8 uses the surface physics and the latest parameterization of turbulent surface fluxes from the GISS ModelE (Schmidt et al., 2006; Friend and Kiang, 2005), but has no representation of vegetation dynamics. The snow dynamics from ModelE are also not yet fully incorporated. Heat dynamics are described in Rosenzweig et al. (1997) and moisture dynamics in Abramopoulos et al. (1988).

In HYBRID8 the prognostic variable for the heat transfer is the heat in the different soil layers, and from that, the model evaluates the soil temperature. The processes governing this are diffusion from the surface to the sub-surface layers, and conduction and advection between the soil layers. The bottom boundary layer in HYBRID8 is impermeable, resulting in zero heat flux from the soil layers below. The version used in this project has no representation of the snow dynamics and has no insulating vegetation cover. However, the canopy provides a simple heat buffer due its separate heat capacity calculations.

2.1.6 LPJ-GUESS

Lund-Potsdam-Jena General Ecosystem Simulator (LPJ-GUESS) is a process-based model of vegetation dynamics and biogeochemistry optimized for regional and global applications (Smith et al., 2001). Mechanistic representations

of biophysical and biogeochemical processes are shared with those in the Lund-Potsdam-Jena dynamic global vegetation model LPJ-DGVM (Sitch et al., 2003; Gerten et al., 2004). However, LPJ-GUESS replaces the large area parameterization scheme in LPJ-DGVM, whereby vegetation is averaged out over a larger area, allowing several state variables to be calculated in a simpler and faster manner, with more robust and mechanistic schemes of individual- and patch-based resource competition and woody plant population dynamics. Detailed descriptions are given by Smith et al. (2001), Sitch et al. (2003), Wolf et al. (2008), Miller and Smith (2012) and Zhang et al. (2013).

LPJ-GUESS has recently been updated to simulate Arctic upland and peatland ecosystems (McGuire et al., 2012; Zhang et al., 2013). It shares the numerical soil thawing–freezing processes, peatland hydrology and the model of wetland methane emission with LPJ-DGVM WHyMe, as described by Wania et al. (2009a, b, 2010). To simulate soil temperatures and active layer depths, the soil column in LPJ-GUESS is divided into a single snow layer of fixed density and variable thickness, a litter layer of fixed thickness (10 cm for these simulations, except for Schilthorn where it is set to 2.5 cm), a soil column of 2 m depth (with sublayers of thickness 0.1 m, each with a prescribed fraction of mineral and organic material, but with fractions of soil water and air that are updated daily), and finally a “padding” column of depth 48 m (with thicker sublayers), to simulate soil thermal dynamics. Insulation effects of snow, phase changes in soil water, daily precipitation input and air temperature forcing are important determinants of daily soil temperature dynamics at different sublayers.

2.2 Study sites

2.2.1 Nuuk

The Nuuk observational site is located in southwestern Greenland. The site is situated in a valley in Kobbefjord at 500 m altitude above sea level, and ambient conditions show Arctic climate properties, with a mean annual temperature of -1.5°C in 2008 and -1.3°C in 2009 (Jensen and Rasch, 2009, 2010). Vegetation types consist of *Empetrum nigrum* with *Betula nana* and *Ledum groenlandicum*, with a vegetation height of 3–5 cm. The study site soil lacks mineral soil horizons due to cryoturbation and lack of podsol development, as it is situated in a dry location. The soil is composed of 43 % sand, 34 % loam, 13 % clay and 10 % organic materials. No soil ice or permafrost formations have been observed within the drainage basin. Snow cover is measured at the Climate Basic station, 1.65 km from the soil station but at the same altitude. At the time of the annual Nuuk Basic snow survey in mid-April, the snow depth at the soil station was very similar to the snow depth at the Climate Basic station: ± 0.1 m when the snow depth is high (near 1 m). Strong winds ($> 20\text{ m s}^{-1}$) have a strong influence on the redistribu-

tion of newly fallen snow, especially in the beginning of the snow season, so the formation of a permanent snow cover at the soil station can be delayed as much as 1 week, while the end of the snow cover season is similar to that at the Climate Basic station (B. U. Hansen, personal communication, 2013; ZackenbergGIS, 2012).

2.2.2 Schilthorn

The Schilthorn massif (Bernese Alps, Switzerland) is situated at 2970 m altitude in the northcentral part of the European Alps. Its non-vegetated lithology is dominated by deeply weathered limestone schists, forming a surface layer of mainly sandy and gravelly debris up to 5 m thick, which lies over presumably strongly jointed bedrock. Following the first indications of permafrost (ice lenses) during the construction of the summit station between 1965 and 1967, the site was chosen for long-term permafrost observation within the framework of the European PACE project and consequently integrated into the Swiss permafrost monitoring network PERMOS as one of its reference sites (PERMOS, 2013).

The measurements at the monitoring station at 2900 m altitude are located on a flat plateau on the north-facing slope and comprise a meteorological station and three boreholes (14 m vertical, 100 m vertical and 100 m inclined), with continuous ground temperature measurements since 1999 (Vonder Mühll et al., 2000; Hoelzle and Gruber, 2008; Harris et al., 2009). Borehole data indicate permafrost of at least 100 m thickness, which is characterized by ice-poor conditions close to the melting point. Maximum active-layer depths recorded since the start of measurements in 1999 are generally around 4–6 m, but during the exceptionally warm summer of the year 2003 the active-layer depth increased to 8.6 m, reflecting the potential for degradation of permafrost at this site (Hilbich et al., 2008).

The monitoring station has been complemented by soil moisture measurements since 2007 and geophysical (mainly geoelectrical) monitoring since 1999 (Hauck, 2002; Hilbich et al., 2011). The snow cover at Schilthorn can reach maximum depths of about 2–3 m and usually lasts from October through to June/July. One-dimensional soil model sensitivity studies showed that impacts of long-term atmospheric changes would be strongest in summer and autumn, due to this late snowmelt and the long decoupling of the atmosphere from the surface. So, increasing air temperatures could lead to a severe increase in active-layer thickness (Engelhardt et al., 2010; Marmy et al., 2013; Scherler et al., 2013).

2.2.3 Samoylov

Samoylov Island belongs to an alluvial river terrace of the Lena River delta. The island is elevated about 20 m above the normal river water level and covers an area of about 3.4 km^2 (Boike et al., 2013). The western part of the island constitutes

Table 1. Model details related to soil heat transfer.

	JSBACH	ORCHIDEE	JULES	COUP	HYBRID8	LPJ-GUESS
Soil freezing	Yes	Yes	Yes	Yes	Yes	Yes
Soil heat transfer method	Conduction	Conduction	Conduction advection	Conduction advection	Conduction advection	Conduction
Dynamic soil heat transfer parameters	Yes	Yes	Yes	Yes	Yes	Yes
Soil depth	10 m	43 m	3 m	Variable (> 5 m)	Variable (> 5 m)	2 m
Bottom boundary condition	Zero heat flux	Geothermal heat flux (0.057 W m ⁻²)	Zero heat flux	Geothermal heat flux (0.011 W m ⁻²)	Zero heat flux	Zero heat flux
Snow layering	Five layers	Three layers	Three layers	One layer	No snow representation	One layer
Dynamic snow heat transfer parameters	No	Yes	Yes	Yes	–	Yes (only heat capacity)
Insulating vegetation cover	10 cm moss layer	–	–	–	–	Site-specific litter layer
Model time step	30 min	30 min	30 min	30 min	30 min	1 day

Table 2. Site details.

	Nuuk	Schilthorn	Samoylov	Bayelva
Latitude	64.13° N	46.56° N	72.4° N	78.91° N
Longitude	51.37° W	7.08° E	126.5° E	11.95° E
Mean annual air temperature	−1.3 °C	−2.7 °C	−13 °C	−4.4 °C
Mean annual ground temperature	3.2 °C	−0.45 °C	−10 °C	−2/−3 °C
Annual precipitation	900 mm	1963 mm	200 mm	400 mm
Avg. length of snow cover	7 months	9.5 months	9 months	9 months
Vegetation cover	Tundra	Barren	Tundra	Tundra

a modern floodplain, which is lower compared with the rest of the island and is often flooded during ice break-up of the Lena River in spring. The eastern part of the island belongs to the elevated river terrace, which is mainly characterized by moss- and sedge-vegetated tundra (Kutzbach et al., 2007). In addition, several lakes and ponds occur, which make up about 25 % of the surface area of Samoylov (Muster et al., 2012).

The land surface of the island is characterized by the typical micro-relief of polygonal patterned ground, caused by frost cracking and subsequent ice-wedge formation. The polygonal structures usually consist of depressed centers surrounded by elevated rims, which can be found in a partly or completely collapsed state (Kutzbach et al., 2007). The soil in the polygonal centers usually consists of water-saturated sandy peat, with the water table standing a few centimeters above or below the surface. The elevated rims are usually covered with a dry moss layer, underlain by wet sandy soils, with massive ice wedges underneath. The cryogenic soil complex of the river terrace reaches depths of 10 to 15 m and is underlain by sandy to silty river deposits. These river deposits reach depths of at least 1 km in the delta region (Langer et al., 2013).

There are strong spatial differences in surface energy balance due to heterogeneous surface and subsurface properties. Due to thermo-erosion, there is an ongoing expansion of thermokarst lakes and small ponds (Abnizova et al., 2012). Soil water drainage is strongly related to active layer dynamics, with lateral water flow occurring from late sum-

mer to autumn (Helbig et al., 2013). Site conditions include strong snow–microtopography and snow–vegetation interactions due to wind drift (Boike et al., 2013).

2.2.4 Bayelva

The Bayelva climate and soil-monitoring site is located in the Kongsfjord region on the west coast of Svalbard Island. The North Atlantic Current warms this area to an average air temperature of about −13 °C in January and +5 °C in July, and provides about 400 mm precipitation annually, falling mostly as snow between September and May. The annual mean temperature of 1994 to 2010 in the village of Ny-Ålesund has been increasing by +1.3 K per decade (Maturilli et al., 2013). The observation site is located in the Bayelva River catchment on the Brøgger peninsula, about 3 km from Ny-Ålesund. The Bayelva catchment is bordered by two mountains, the Zeppelinfjellet and the Scheteligfjellet, between which the glacial Bayelva River originates from the two branches of the Brøggerbreen glacier moraine rubble. To the north of the study site, the terrain flattens, and after about 1 km, the Bayelva River reaches the shoreline of the Kongsfjorden (Arctic Ocean). In the catchment area, sparse vegetation alternates with exposed soil and sand and rock fields. Typical permafrost features, such as mud boils and non-sorted circles, are found in many parts of the study area. The Bayelva permafrost site itself is located at 25 m a.s.l., on top of the small Leirhaugen hill. The domi-

Table 3. Details of driving data preparation for site simulations.

	Nuuk	Schilthorn	Samoylov	Bayelva	
Atmospheric forcing variables	Air temperature	in situ	in situ	in situ	
	Precipitation	in situ	in situ	in situ	
	Air pressure	in situ	WATCH	WATCH	in situ
	Atm. humidity	in situ	in situ	in situ	in situ
	Incoming longwave radiation	in situ	in situ	in situ	WATCH
	Incoming shortwave radiation	in situ	in situ	WATCH	in situ
	Net radiation	in situ	–	in situ	–
	Wind speed	in situ	in situ	in situ	in situ
	Wind direction	in situ	–	in situ	–
	Time period	26/06/2008–31/12/2011	01/10/1999–30/09/2008	14/07/2003–11/10/2005	01/01/1998–31/12/2009
Static soil parameters	Soil porosity	46 %	50 %	60 %	41 %
	Soil field capacity	36 %	44 %	31 %	22 %
	Mineral soil depth	36 cm	710 cm	800 cm	30 cm
	Dry soil heat capacity	$2.213 \times 10^6 \text{ (Jm}^{-3} \text{ K}^{-1}\text{)}$	$2.203 \times 10^6 \text{ (Jm}^{-3} \text{ K}^{-1}\text{)}$	$2.1 \times 10^6 \text{ (Jm}^{-3} \text{ K}^{-1}\text{)}$	$2.165 \times 10^6 \text{ (Jm}^{-3} \text{ K}^{-1}\text{)}$
	Dry soil heat conductivity	$6.84 \text{ (Wm}^{-1} \text{ K}^{-1}\text{)}$	$7.06 \text{ (Wm}^{-1} \text{ K}^{-1}\text{)}$	$5.77 \text{ (Wm}^{-1} \text{ K}^{-1}\text{)}$	$7.93 \text{ (Wm}^{-1} \text{ K}^{-1}\text{)}$
	Sat. hydraulic conductivity	$2.42 \times 10^{-6} \text{ (ms}^{-1}\text{)}$	$4.19 \times 10^{-6} \text{ (ms}^{-1}\text{)}$	$2.84 \times 10^{-6} \text{ (ms}^{-1}\text{)}$	$7.11 \times 10^{-6} \text{ (ms}^{-1}\text{)}$
	Saturated moisture potential	0.00519 (m)	0.2703 (m)	0.28 (m)	0.1318 (m)

Table 4. Details of model spin up procedures.

	JSBACH	ORCHIDEE	JULES	COUP	HYBRID8	LPJ-GUESS
Spin-up data	Observed climate	Observed climate	Observed climate	Observed climate	Observed climate	WATCH* data
Spin-up duration	50 years	10 000 years	50 years	10 years	50 years	500 years

* 500 years forced with monthly WATCH reanalysis data from the 1901–1930 period, followed by daily WATCH forcing from 1901–until YYYY-MM-DD, then daily site data.

nant ground pattern at the study site consists of non-sorted soil circles. The bare soil circle centers are about 1 m in diameter and are surrounded by a vegetated rim, consisting of a mixture of low vascular plants of different species of grass and sedges (*Carex spec.*, *Deschampsia spec.*, *Eriophorum spec.*, *Festuca spec.*, *Luzula spec.*), catchfly, saxifrage, willow and some other local common species (*Dryas octopetala*, *Oxyria digyna*, *Polygonum viviparum*) and unclassified species of mosses and lichens. The vegetation cover at the measurement site was estimated to be approximately 60 %, with the remainder being bare soil with a small proportion of stones. The silty clay soil has a high mineral content, while the organic content is low, with organic fractions below 10 % (Boike et al., 2007). In the study period, the permafrost at Leirhaugen hill had a mean annual temperature of about -2°C at the top of the permafrost at 1.5 m depth.

Over the past decade, the Bayelva catchment has been the focus of intensive investigations into soil and permafrost conditions (Roth and Boike, 2001; Boike et al., 2007; Westermann et al., 2010, 2011), the winter surface energy balance (Boike et al., 2003), and the annual balance of energy, H_2O and CO_2 , and micrometeorological processes controlling these fluxes (Westermann et al., 2009; Lüers et al., 2014).

2.3 Intercomparison setup and simulation protocol

In order solely to compare model representations of physical processes and to eliminate any other source of uncertainty (e.g., climate forcing, spatial resolution, soil parameters), model simulations were driven by the same atmospheric forcing and soil properties at site-scale. Driving data for all site simulations were prepared and distributed uniformly. Site observations were converted into continuous time series with minor gap-filling. Where the observed variable set lacked the variable needed by the models, extended WATCH reanalysis data (Weedon et al., 2010; Beer et al., 2014) were used to complement the data sets. Soil thermal properties are based on the sand, silt, and clay fractions of the Harmonized World Soil database v1.1 (FAO et al., 2009). All model simulations were forced with these data sets. Table 3 summarizes the details of site-driving data preparation together with soil static parameters.

To bring the state variables into equilibrium with climate, models are spun up with climate forcing. Spin-up procedure is part of the model structure, in some cases a full biogeochemical and physical spin up is implemented, whereas in some models a simpler physical spin up is possible. This brings different requirements for the spin-up time length, so each model was independently spun up depending on its model formulations and discretization scheme, and the details are given in Table 4. However, the common practice in

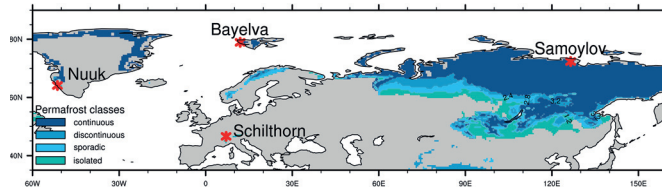


Figure 1. Location map of the sites used in this study. The background map is color-coded with the IPA permafrost classes from Brown et al. (2002).

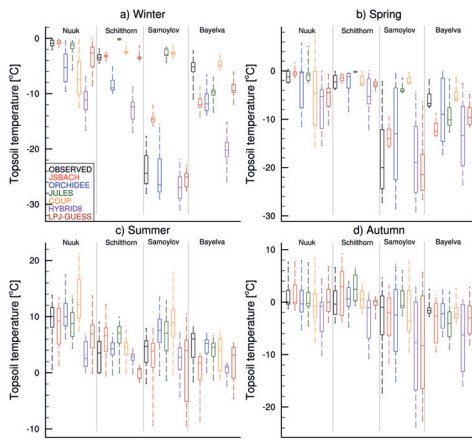


Figure 2. Box plots showing the topsoil temperature for observation and models for different seasons. Boxes are drawn with the 25th percentile and mean and 75th percentiles, while the whiskers show the min and max values. Seasonal averages of soil temperatures are used for calculating seasonal values. Each plot includes four study sites divided by the gray lines. Black boxes show observed values, and colored boxes distinguish models. See Table A1 in Appendix A for exact soil depths used in this plot.

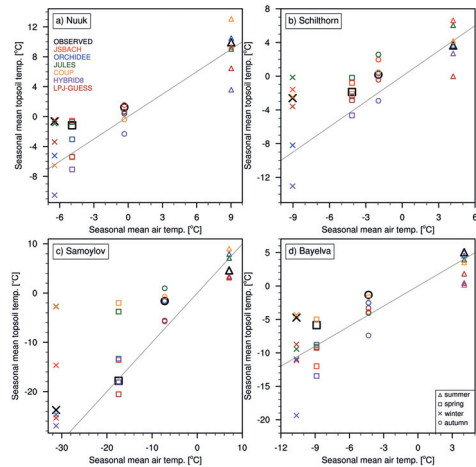


Figure 3. Scatter plots showing air–topsoil temperature relation from observations and models at each site for different seasons. Seasonal mean observed air temperature is plotted against the seasonal mean modeled topsoil temperature separately for each site. Black markers are observed values, colors distinguish models and markers distinguish seasons. Gray lines represent the 1 : 1 line. See Table A1 in Appendix A for exact soil depths used in this plot.

all model spin-up procedures was to keep the mean annual soil temperature change less than 0.01 °C in all soil layers.

Most of the analysis focuses on the upper part of the soil. The term “topsoil” is used from now on to indicate the chosen upper soil layer in each model, and the first depth of soil temperature observations. The details of layer selection are given in Table A1 of Appendix A.

3 Results

3.1 Topsoil temperature and surface insulation effects

As all our study sites are located in cold climate zones (Fig. 1), there is significant seasonality, which necessitates a separate analysis for each season. Figure 2 shows average seasonal topsoil temperature distributions (see Table A1 in the Appendix for layer depths) extracted from the six models, along with the observed values at the four different sites. In this figure, observed and simulated temperatures show a wide range of values depending on site-specific conditions and model formulations. Observations show that dur-

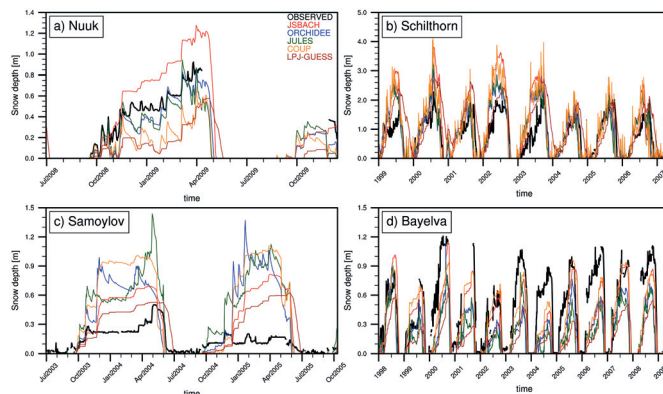


Figure 4. Time-series plots of observed and simulated snow depths for each site. Thick black lines are observed values and colored lines distinguish simulated snow depths from models.

ing winter and spring, Samoylov is much colder than the other sites (Fig. 2a, b). Observed summer and autumn temperatures are similar at all sites (Fig. 2c, d), with Nuuk being the warmest site in general. For the modeled values, the greatest inconsistency with observations is in matching the observed winter temperatures, especially at Samoylov and Schilthorn (Fig. 2a). The modeled temperature range increases in spring (Fig. 2b), and even though the mean modeled temperatures in summer are closer to observed means, the maximum and minimum values show a wide range during this season (Fig. 2c). Autumn shows a more uniform distribution of modeled temperatures compared with the other seasons (Fig. 2d).

A proper assessment of critical processes entails examining seasonal changes in surface cover and the consequent insulation effects for the topsoil temperature. To investigate these effects, Fig. 3 shows the seasonal relations between air and topsoil temperature at each study site. Air temperature values are the same for all models, as they are driven with the same atmospheric forcing. Observations show that topsoil temperatures are warmer than the air during autumn, winter, and spring at all sites, but the summer conditions are dependent on the site (Fig. 3). In the models, winter topsoil temperatures are warmer than the air in most cases, as observed. However, the models show a wide range of values, especially at Samoylov (Fig. 3c), where the topsoil temperatures differ by up to 25 °C between models. In summer, the models do not show consistent relationships between soil and air temperatures, and the model range is highest at the Nuuk and Schilthorn sites.

To analyze the difference in modeled and observed snow isolation effect in more detail, Fig. 4 shows the changes in snow depth from observed and modeled values. Schilthorn

has the highest snow depth values (> 1.5 m), while all other sites have a maximum snow height between 0.5 and 1 m (Fig. 4). Compared with observations, the models usually overestimate the snow depth at Schilthorn and Samoylov (Fig. 4b, c) and underestimate it at Nuuk and Bayelva (Fig. 4a, d).

For our study sites, the amount of modeled snow depth bias is correlated with the amount of modeled topsoil temperature bias (Fig. 5). With overestimated (underestimated) snow depth, models generally simulate warmer (colder) topsoil temperatures. As seen in Fig. 5a, almost all models underestimate the snow depth at Nuuk and Bayelva, and this creates colder topsoil temperatures. The opposite is seen for Samoylov and Schilthorn, where higher snow depth bias is accompanied by higher topsoil temperature bias (except for ORCHIDEE and LPJ-GUESS models).

As snow can be persistent over spring and summer seasons in cold regions (Fig. 4), it is worthwhile to separate snow and snow-free seasons for these comparisons. Figure 6 shows the same atmosphere–topsoil temperature comparison as in Fig. 3 but using individual (for each model and site) snow and snow-free seasons instead of conventional seasons. In this figure, all site observations show a warmer topsoil temperature than air, except for the snow-free season at Samoylov. Models, however, show different patterns at each site. For the snow season, models underestimate the observed values at Nuuk and Bayelva, whereas they overestimate it at Schilthorn and Samoylov, except for the previously mentioned ORCHIDEE and LPJ-GUESS models. Modeled snow-free season values, however, do not show consistent patterns.

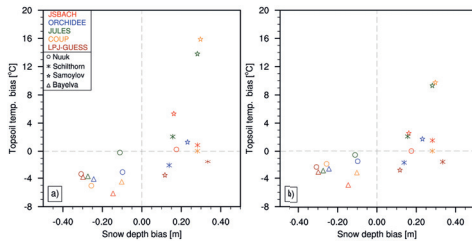


Figure 5. Scatter plots showing the relation between snow depth bias and topsoil temperature bias during snow season (a) and the whole year (b). Snow season is defined separately for each model, by taking snow depth values over 5 cm to represent the snow-covered period. The average temperature bias of all snow-covered days is used in (a), and the temperature bias in all days (snow covered and snow-free seasons) is used in (b). Markers distinguish sites and colors distinguish models. See Table A1 in Appendix A for exact soil depths used in this plot.

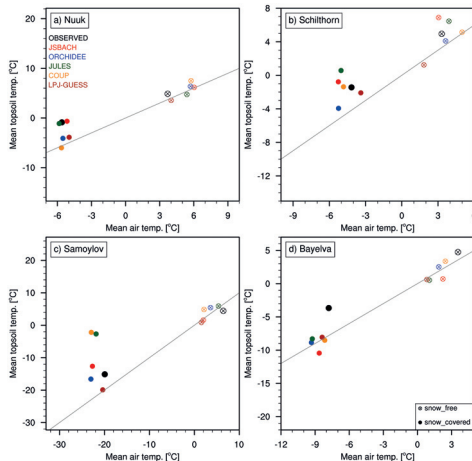


Figure 6. Scatter plots showing air–topsoil temperature relation from observations and models at each site for snow and snow-free seasons. Snow season is defined separately for observations and each model, by taking snow depth values over 5 cm to represent the snow-covered period. The average temperature of all snow covered (or snow-free) days of the simulation period is used in the plots. Markers distinguish snow and snow-free seasons and colors distinguish models. Gray lines represent the 1 : 1 line. See Table A1 in Appendix A for exact soil depths used in this plot.

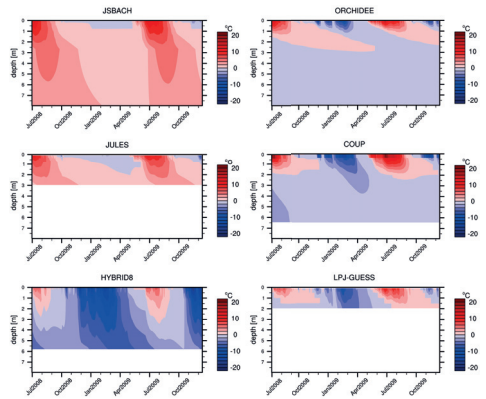


Figure 7. Time–depth plot of soil temperature evolution at the Nuuk site for each model. Simulated soil temperatures are interpolated into 200 evenly spaced nodes to represent a continuous vertical temperature profile. The deepest soil temperature calculation is taken as the bottom limit for each model (no extrapolation applied).

3.2 Subsurface thermal regime

Assessing soil thermal dynamics necessitates scrutinizing subsurface temperature dynamics as well as surface conditions. Soil temperature evolutions of simulated soil layers are plotted for each model at each site in Figs. 7–10. Strong seasonal temperature changes are observed close to the surface, whereas temperature amplitudes are reduced in deeper layers and eventually a constant temperature is simulated at depths with zero annual amplitude (DZAA).

Although Nuuk is a non-permafrost site, most of the models simulate subzero temperatures below 2–3 m at this site (Fig. 7). Here, only ORCHIDEE and COUP simulate a true DZAA at around 2.5–3 m, while all other models show a minor temperature change even at their deepest layers. At the high altitude Schilthorn site (Fig. 8), JSBACH and JULES simulate above 0 °C temperatures (non-permafrost conditions) in deeper layers. Compared with other models with snow representation, ORCHIDEE and LPJ-GUESS show colder subsurface temperatures at this site (Fig. 8). The simulated soil thermal regime at Samoylov reflects the colder climate at this site. All models show subzero temperatures below 1 m (Fig. 9). However, compared with other models, JULES and COUP show values much closer to 0 °C. At the high-Arctic Bayelva site, all models simulate permafrost conditions (Fig. 10). The JULES and COUP models again show warmer temperature profiles than the other models.

The soil thermal regime can also be investigated by studying the vertical temperature profiles regarding the annual means (Fig. 11), and minimum and maximum values

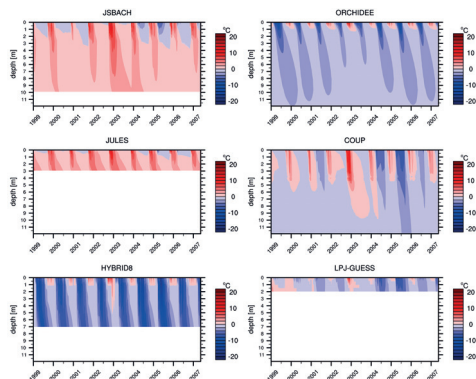


Figure 8. Time–depth plot of soil temperature evolution at Schilthorn site for each model. Simulated soil temperatures are interpolated into 200 evenly spaced nodes to represent a continuous vertical temperature profile. The deepest soil temperature calculation is taken as the bottom limit for each model (no extrapolation applied).

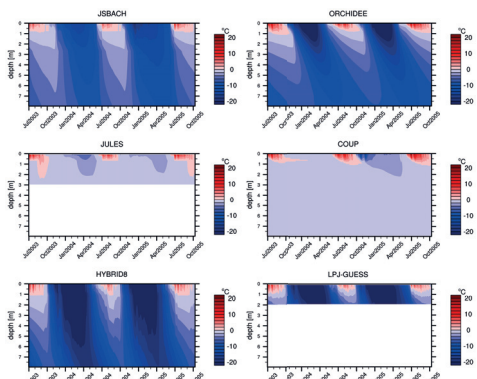


Figure 9. Time–depth plot of soil temperature evolution at Samoylov site for each model. Simulated soil temperatures are interpolated into 200 evenly spaced nodes to represent a continuous vertical temperature profile. The deepest soil temperature calculation is taken as the bottom limit for each model (no extrapolation applied).

(Fig. 12). In Figure 11, the distribution of mean values is similar to the analysis of topsoil conditions. The mean subsoil temperature is coldest at Samoylov followed by Bayelva, while Schilthorn is almost at the 0 °C boundary (no deep soil temperature data were available from Nuuk for this comparison). JSBACH, JULES, and COUP overestimate the temperatures at Schilthorn and Samoylov, but almost all models underestimate it at Bayelva. Figure 12 shows the temperature envelopes of observed and simulated values at each site. The minimum (maximum) temperature curve represents the coldest (warmest) possible conditions for the soil thermal regime at a certain depth. The models agree more on the maximum curve than the minimum curve (Fig. 12), indicating the differences in soil temperature simulation for colder periods. The HYBRID8 model almost always shows the coldest conditions, whereas the pattern of the other models changes depending on the site.

Figure 13 shows the yearly change of ALT for the three permafrost sites. Observations indicate a shallow ALT at Samoylov (Fig. 13b) and very deep ALT for Schilthorn (Fig. 13a). All models overestimate the ALT at Samoylov (Fig. 13b), but there is disagreement among models in over- or underestimating the ALT at Schilthorn (Fig. 13a) and Bayelva (Fig. 13c).

4 Discussion

4.1 Topsoil temperature and surface insulation effects

Figure 2 has shown a large range among modeled temperature values, especially during winter and spring. As mentioned in the introduction, modeled mean soil temperatures are strongly related to the atmosphere–surface thermal connection, which is strongly influenced by snow cover and its properties.

Observations show warmer topsoil temperatures than air during autumn, winter, and spring (Fig. 3). This situation indicates that soil is insulated when compared to colder air temperatures. This can be attributed to the snow cover during these seasons (Fig. 4). The insulating property of snow keeps the soil warmer than air, while not having snow can result in colder topsoil temperatures than air (as for the HYBRID8 model, cf. Fig. 3). Even though the high albedo of snow provides a cooling effect for soil, the warming due to insulation dominates during most of the year. Depending on their snow depth bias, models show different relations between air and topsoil temperature. The amount of winter warm bias from snow depth overestimation in models depends on whether the site has a “sub- or supra-critical” snow height. With supra-critical conditions (e.g., at Schilthorn), the snow depth is so high that a small over- or underestimation in the model makes very little difference to the insulation. Only the timing of the snow arrival and melt-out is important. In sub-critical conditions (e.g., at Samoylov), the snow depth is so low that any overestimation leads to a strong warm bias in the simula-

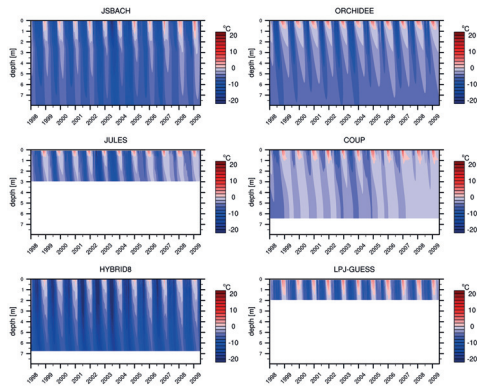


Figure 10. Time–depth plot of soil temperature evolution at Bayvelva site for each model. Simulated soil temperatures are interpolated into 200 evenly spaced nodes to represent a continuous vertical temperature profile. The deepest soil temperature calculation is taken as the bottom limit for each model (no extrapolation applied).

tion e.g., for JULES/COUP. This effect is also mentioned in Zhang (2005), where it is stated that snow depths of less than 50 cm have the greatest impact on soil temperatures. However, overestimated snow depth at Samoylov and Schilthorn does not always result in warmer soil temperatures in models as expected (Fig. 3b, c). At these sites, even though JSBACH, JULES and COUP show warmer soil temperatures in parallel to their snow depth overestimations, ORCHIDEE and LPJ-GUESS show the opposite. This behavior indicates different processes working in opposite ways. Nevertheless, most of the winter, autumn and spring topsoil temperature biases can be explained by snow conditions (Fig. 5a). Figure 5b shows that snow depth bias can explain the topsoil temperature bias even when the snow-free season is considered, which is due to the long snow period at these sites (Table 2). This confirms the importance of snow representation in models for capturing topsoil temperatures at high latitudes and high altitudes.

On the other hand, considering dynamic heat transfer parameters (volumetric heat capacity and heat conductivity) in snow representation seems to be of lesser importance (JSBACH vs. other models, see Table 1). This is likely because a greater uncertainty comes from processes that are still missing in the models, such as wind drift, depth hoar formation and snow metamorphism. As an example, the landscape heterogeneity at Samoylov forms different soil thermal profiles for polygon center and rim. While the soil temperature comparisons were performed for the polygon rim, snow depth observations were taken from polygon center. Due to strong wind drift, almost all snow is removed from the rim and also limited to ca. 50 cm (average polygon height) at

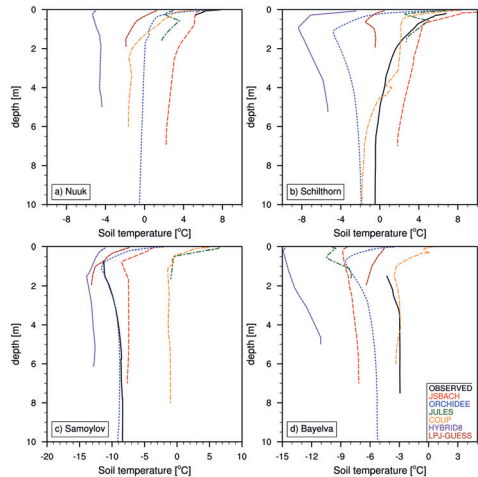


Figure 11. Vertical profiles of annual soil temperature means of observed and modeled values at each site. Black thick lines are the observed values, while colored dashed lines distinguish models. (Samoylov and Bayvelva observations are from borehole data).

the center (Boike et al., 2008). This way, models inevitably overestimate snow depth and insulation, in particular on the rim where soil temperature measurements have been taken. Hence, a resulting winter warm bias is expected (Fig. 2a, models JSBACH, JULES, COUP).

During the snow-free season, Samoylov has colder soil temperatures than air (Fig. 6c). Thicker moss cover and higher soil moisture content at Samoylov (Boike et al., 2008) are the reasons for cooler summer topsoil temperatures at this site. Increasing moss thickness changes the heat storage of the moss cover and it acts as a stronger insulator (Gornall et al., 2007), especially when dry (Soudzilovskaia et al., 2013). Additionally, high water content in the soil requires additional input of latent heat for thawing and there is less heat available to warm the soil.

Insulation strength during the snow-free season is related to model vegetation/litter layer representations. 10 cm fixed moss cover in JSBACH and a 10 cm litter layer in LPJ-GUESS bring similar amounts of insulation. At Samoylov, where strong vegetation cover is observed in the field, these models perform better for the snow-free season (Fig. 6c). However, at Bayvelva, where vegetation effects are not that strong, 10 cm insulating layer proves to be too much and creates colder topsoil temperatures than observations (Fig. 6d). And for the bare Schilthorn site, even a thin layer of surface cover (2.5 cm litter layer) creates colder topsoil temperatures in LPJ-GUESS (Fig. 6b).

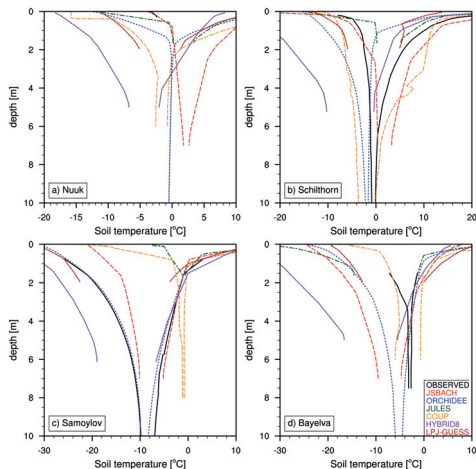


Figure 12. Soil temperature envelopes showing the vertical profiles of soil temperature amplitudes of each model at each site. Soil temperature values of observations (except Nuuak) and each model are interpolated to finer vertical resolution and max and min values are calculated for each depth to construct max and min curves. For each color, the right line is the maximum and the left line is the minimum temperature curve. Black thick lines are the observed values, while colored dashed lines distinguish models.

At Bayelva, all models underestimate the observed topsoil temperatures all year long (Fig. 6d). With underestimated snow depth (Fig. 4d) and winter cold bias in topsoil temperature (Fig. 3d), models create a colder soil thermal profile that results in cooling of the surface from below even during the snow-free season. Furthermore, using global reanalysis products instead of site observations (Table 3) might cause biases in incoming longwave radiation, which can also affect the soil temperature calculations. In order to assess model performance in capturing observed soil temperature dynamics, it is important to drive the models with a complete set of site observations.

These analyses support the need for better vegetation insulation in models during the snow-free season. The spatial heterogeneity of surface vegetation thickness remains an important source of uncertainty. More detailed moss representations were used in Porada et al. (2013) and Rinke et al. (2008), and such approaches can improve the snow-free season insulation in models.

4.2 Soil thermal regime

Model differences in representing subsurface temperature dynamics are related to the surface conditions (especially snow) and soil heat transfer formulations. The ideal way

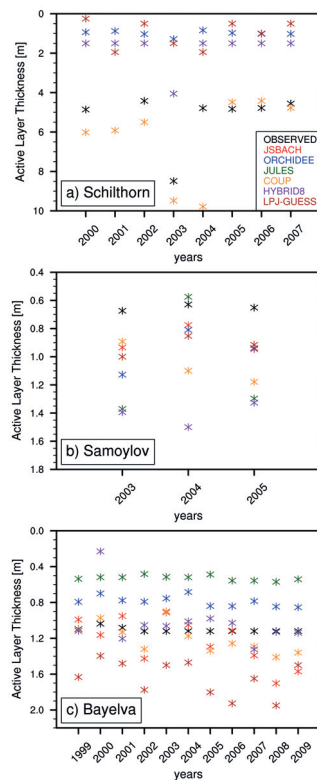


Figure 13. Active layer thickness (ALT) values for each model and observation at the three permafrost sites. ALT calculation is performed separately for models and observations by interpolating the soil temperature profile into finer resolution and estimating the maximum depth of 0 °C for each year. (a), (b) and (c) show the temporal change of ALT at Schillthorn (2001 is omitted because observations have major gaps, also JSBACH and JULES are excluded as they simulate no permafrost at this site), Samoylov and Bayelva, respectively. Colors distinguish models and observations.

to assess the soil internal processes would be to use the same snow forcing or under snow temperature for all models. However most of the land models used in this study are not that modular. Hence, intertwined effects of surface and soil internal processes must be discussed together here.

Figures 7–10 show the mismatch in modeled DZAA representations. Together with the soil water and ice contents, simulating DZAA is partly related to the model soil depth and some models are limited by their shallow depth representations (Fig. A1 in the Appendix, Table 1). Apart from

the different temperature values, models also simulate permafrost conditions very differently. As seen in Fig. 8, JSBACH and JULES do not simulate permafrost conditions at Schilthorn. In reality, there are almost isothermal conditions of about -0.7°C between 7 m and at least 100 m depth at this site (PERMOS, 2013), which are partly caused by the three-dimensional thermal effects due to steep topography (Noetzi et al., 2008). Temperatures near the surface will not be strongly affected by three-dimensional effects, as the monitoring station is situated on a small but flat plateau (Scherler et al., 2013), but larger depths get additional heat input from the opposite southern slope, causing slightly warmer temperatures at depth than for completely flat topography (Noetzi et al., 2008). The warm and isothermal conditions close to the freezing point at Schilthorn mean that a small temperature mismatch (on the order of 1°C) can result in non-permafrost conditions. This kind of temperature bias would not affect the permafrost condition at colder sites (e.g., Samoylov). In addition, having low water and ice content, and a comparatively low albedo, make the Schilthorn site very sensitive to interannual variations and make it more difficult for models to capture the soil thermal dynamics (Scherler et al., 2013). Compared to the other models with snow representation, ORCHIDEE and LPJ-GUESS show colder subsurface temperatures at this site (Fig. 8). A thin surface litter layer (2.5 cm) in LPJ-GUESS contributes to the cooler Schilthorn soil temperatures in summer.

Differences at Samoylov are more related to the snow depth biases. As previously mentioned, subcritical snow conditions at this site amplify the soil temperature overestimation coming from snow depth bias (Fig. 5). Considering their better match during snow-free season (Fig. 6c), the warmer temperatures in deeper layers of JULES and COUP can be attributed to overestimated snow depths for this site by these two models (Fig. 9). Additionally, JULES and COUP models simulate generally warmer soils conditions than the other models, because these models include heat transfer via advection in addition to heat conduction. Heat transfer by advection of water is an additional heat source for the subsurface in JULES and COUP, which can also be seen in the results for Bayelva (Fig. 10). In combination with that, COUP has a greater snow depth at Samoylov (Fig. 5), resulting in even warmer subsurface conditions than JULES. Such conditions demonstrate the importance of the combined effects of surface processes together with internal soil physics.

Due to different heat transfer rates among models, internal soil processes can impede the heat transfer and result in delayed warming or cooling of the deeper layers. JSBACH, ORCHIDEE, JULES and COUP show a more pronounced time lag of the heat/cold penetration into the soil, while HYBRID8 and LPJ-GUESS show either a very small lag or no lag at all (Figs. 7–10). This time lag is affected by the method of heat transfer (e.g., advection and conduction, see above), soil heat transfer parameters (soil heat capacity/conductivity), the amount of simulated phase change,

vertical soil model resolution and internal model time step. Given that all models use some sort of heat transfer method including phase change (Table 1) and similar soil parameters (Table 3), the reason for the rapid warming/cooling at deeper layers of some models can be missing latent heat of phase change, vertical resolution or model time step. Even though the mineral (dry) heat transfer parameters are shared among models, they are modified afterwards due to the coupling of hydrology and thermal schemes. This leads to changes in the model heat conductivities depending on how much water and ice they simulate in that particular layer. Unfortunately, not all models output soil water and ice contents in a layered structure similar to soil temperature. This makes it difficult to assess the differences in modeled phase change, and the consequent changes to soil heat transfer parameters. A better quantification of heat transfer rates would require a comparison of simulated water contents and soil heat conductivities among models, which is beyond the scope of this paper.

The model biases in matching the vertical temperature curves (minimum, maximum, mean) are related to the topsoil temperature bias in each model for each site, but also the above-mentioned soil heat transfer mechanisms and bottom boundary conditions. Obviously, models without snow representation (e.g., HYBRID8) cannot match the minimum curve in Fig. 12. However, snow depth bias (Fig. 5) cannot explain the minimum curve mismatch for ORCHIDEE, COUP, and LPJ-GUESS at Schilthorn (Fig. 12b). This highlights the effects of soil heat transfer schemes once again.

In general, permafrost specific model experiments require deeper soil representation than 5–10 m. As discussed in Alexeev et al. (2007), more than 30 m soil depth is needed for capturing decadal temperature variations in permafrost soils. The improvements from having such extended soil depth are shown in Lawrence et al. (2012), when compared to their older model version with shallow soil depth (Lawrence and Slater, 2005). Additionally, soil layer discretization plays an important role for the accuracy of heat and water transfer within the soil, and hence can effect the ALT estimations. Most of the model setups in our intercomparison have less than 10 m depths, so they lack some effects of processes within deeper soil layers. However, most of the models used in global climate simulations have similar soil depth representations and the scope here is to compare models that are not only aimed to simulate site-specific permafrost conditions at high resolution but to show general guidelines for future model developments.

Adding to all these outcomes, some models match the site observations better than others at specific sites. For example, the mean annual soil thermal profiles are better captured by JSBACH at Nuuk, by JULES and COUP at Schilthorn, by ORCHIDEE at Samoylov, and by COUP at Bayelva (Fig. 11). Comparing just the topsoil conditions at the non-permafrost Nuuk site, JSBACH better matches the observations due to its moss layer. On the other hand, by having better snow depth dynamics (Fig. 4), JULES and COUP mod-

els are better suited for sites with deeper snow depths like Schilthorn and Bayelva. Contrarily, the wet Samoylov site is better represented by ORCHIDEE in snow season (Fig. 2a) due to lower snow depths in this model (Fig. 4) and thus colder soil temperatures. However, the snow-free season is better captured by the JSBACH model (Fig. 2c) due to its effective moss insulation and LPJ-GUESS model due to its insulating litter layer.

4.3 Active layer thickness

As seen above, surface conditions (e.g., insulation) alone are not enough to explain the soil thermal regime, as subsoil temperatures and soil water and ice contents affect the ALT as well. For Schilthorn, LPJ-GUESS generally shows shallower ALT values than other models (Fig. 13a); it also shows the largest snow depth bias (Fig. 5), excluding snow as a possible cause for this shallow ALT result. However, if snow depth bias alone could explain the ALT difference, ORCHIDEE would show different values than HYBRID8, which completely lacks any snow representation. At Schilthorn, COUP has a high snow depth bias (Fig. 5) but still shows a very good match with the observed ALT (Fig. 13a), mainly because snow cover values at Schilthorn are very high so ALT estimations are insensitive to snow depth biases as long as modeled snow cover is still sufficiently thick to have the full insulation effect (Scherler et al., 2013).

All models overestimate the snow depth at Samoylov (Fig. 5) and most of them lack a proper moss insulation (Fig. 6c), which seems to bring deeper ALT estimates in Samoylov (Fig. 13b). However, HYBRID8 does not have snow representation, yet it shows the deepest ALT values, which means lack of snow insulation is not the reason for deeper ALT values in this model. As well as lacking any vegetation insulation, soil heat transfer is also much faster in HYBRID8 (see Sect. 3.2), which allows deeper penetration of summer warming into the soil column.

Surface conditions alone cannot describe the ALT bias in Bayelva either. LPJ-GUESS shows the lowest snow depth (Fig. 5) together with deepest ALT (Fig. 13c), while JULES shows similar snow depth bias as LPJ-GUESS but the shallowest ALT values. As seen from Fig. 10, LPJ-GUESS allows deeper heat penetration at this site. So, not only the snow conditions, but also the model's heat transfer rate is critical for correctly simulating the ALT.

5 Conclusions

We have evaluated different land models' soil thermal dynamics against observations using a site-level approach. The analysis of the simulated soil thermal regime clearly reveals the importance of reliable surface insulation for topsoil temperature dynamics and of reliable soil heat transfer formula-

tions for subsoil temperature and permafrost conditions. Our findings include the following conclusions.

1. At high latitudes and altitudes, model snow depth bias explains most of the topsoil temperature biases.
2. The sensitivity of soil temperature to snow insulation depends on site snow conditions (sub-/supra-critical).
3. Surface vegetation cover and litter/organic layer insulation is important for topsoil temperatures in the snow-free season, therefore models need more detailed representation of moss and top organic layers.
4. Model heat transfer rates differ due to coupled heat transfer and hydrological processes. This leads to discrepancies in subsoil thermal dynamics.
5. Surface processes alone cannot explain the whole soil thermal regime; subsoil conditions and model formulations affect the soil thermal dynamics.

For permafrost and cold-region-related soil experiments, it is important for models to simulate the soil temperatures accurately, because permafrost extent, active layer thickness and permafrost soil carbon processes are strongly related to soil temperatures. There is major concern about how the soil thermal state of these areas affects the ecosystem functions, and about the mechanisms (physical/biogeochemical) relating atmosphere, oceans and soils in cold regions. With the currently changing climate, the strength of these couplings will be altered, bringing additional uncertainty into future projections.

In this paper, we have shown the current state of a selection of land models with regard to capturing surface and subsurface temperatures in different cold-region landscapes. It is evident that there is much uncertainty, both in model formulations of soil internal physics and especially in surface processes. To achieve better confidence in future simulations, model developments should include better insulation processes (for snow: compaction, metamorphism, depth hoar, wind drift; for moss: dynamic thickness and wetness). Models should also perform more detailed evaluation of their soil heat transfer rates with observed data, for example comparing simulated soil moisture and soil heat conductivities.

Appendix A: Model layering schemes and depths of soil temperature observations

Exact depths of each soil layer used in model formulations:

JSBACH: 0.065, 0.254, 0.913, 2.902, 5.7 m

ORCHIDEE: 0.04, 0.05, 0.06, 0.07, 0.08, 0.1, 0.11, 0.14, 0.16, 0.19, 0.22, 0.27, 0.31, 0.37, 0.43, 0.52, 0.61, 0.72, 0.84, 1.00, 1.17, 1.39, 1.64, 1.93, 2.28, 2.69, 3.17, 3.75, 4.42, 5.22, 6.16, 7.27 m

JULES: 0.1, 0.25, 0.65, 2.0 m

COUP: different for each site

Nuuk: 0.01 m intervals until 0.36 m, then 0.1 m intervals until 2 m and then 0.5 m intervals until 6 m

Schilthorn: 0.05 m then 0.1 m intervals until 7 m, and then 0.5 m intervals until 13 m

Samoylov: 0.05 m then 0.1 m intervals until 5 m, and then 0.5 m intervals until 8 m

Bayelva: 0.01 m intervals until 0.3 m, then 0.1 m intervals until 1 m and then 0.5 m intervals until 6 m

HYBRID8: different for each site

Nuuk: 0.07, 0.29, 1.50, 5.00 m

Schilthorn: 0.07, 0.30, 1.50, 5.23 m

Samoylov: 0.07, 0.30, 1.50, 6.13 m

Bayelva: 0.07, 0.23, 1.50, 5.00 m

LPJ-GUESS: 0.1 m intervals until 2 m (additional padding layer of 48 m depth).

Table A1. Selected depths of observed and modeled soil temperatures referred as “topsoil temperature” in Figs. 1, 2, 4, 5 and 6.

	Nuuk	Schilthorn	Samoylov	Bayelva
OBSERVATION	5 cm	20 cm	6 cm	6 cm
JSBACH	3.25 cm	18.5 cm	3.25 cm	3.25 cm
ORCHIDEE	6.5 cm	18.5 cm	6.5 cm	6.5 cm
JULES	5 cm	22.5 cm	5 cm	5 cm
COUP	5.5 cm	20 cm	2.5 cm	5.5 cm
HYBRID8	3.5 cm	22 cm	3.5 cm	3.5 cm
LPJ-GUESS	5 cm	25 cm	5 cm	5 cm

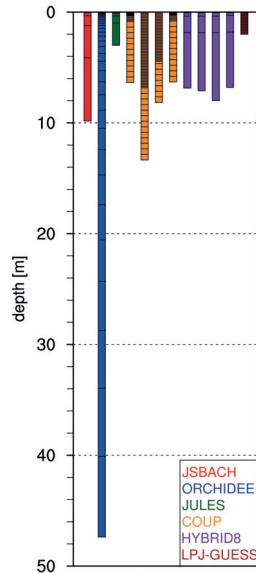


Figure A1. Soil layering schemes of each model. COUP and HYBRID8 models use different layering schemes for each study site, which are represented with different bars (from left to right: Nuuk, Schilthorn, Samoylov and Bayelva).

Depths of soil temperature observations for each site:

Nuuk: 0.01, 0.05, 0.10, 0.30 m

Schilthorn: 0.20, 0.40, 0.80, 1.20, 1.60, 2.00, 2.50, 3.00, 3.50, 4.00, 5.00, 7.00, 9.00, 10.00 m

Samoylov: 0.02, 0.06, 0.11, 0.16, 0.21, 0.27, 0.33, 0.38, 0.51, 0.61, 0.71 m

Bayelva: 0.06, 0.24, 0.40, 0.62, 0.76, 0.99, 1.12 m

The Supplement related to this article is available online at doi:10.5194/tc-9-1343-2015-supplement.

Acknowledgements. The research leading to these results has received funding from the European Community's Seventh Framework Programme (FP7 2007–2013) under grant agreement no. 238366. Authors also acknowledge the BMBF project CarboPerm for the funding. Nuuk site monitoring data for this paper were provided by the GeoBasis program run by Department of Geography, University of Copenhagen and Department of Bioscience, Aarhus University, Denmark. The program is part of the Greenland Environmental Monitoring (GEM) Program (www.g-e-m.dk) and financed by the Danish Environmental Protection Agency, Danish Ministry of the Environment. We would like to acknowledge a grant of the Swiss National Science Foundation (Sinergia TEMPS project, no. CRSII2 136279) for the COUP model intercomparison, as well as the Swiss PERMOS network for the Schilthorn data provided. Authors also acknowledge financial support from DEFROST, a Nordic Centre of Excellence (NCoE) under the Nordic Top-level Research Initiative (TRI), and the Lund University Centre for Studies of Carbon Cycle and Climate Interactions (LUCCI). Eleanor Burke was supported by the Joint UK DECC/Defra Met Office Hadley Centre Climate Programme (GA01101) and the European Union Seventh Framework Programme (FP7/2007-2013) under grant agreement no. 282700, which also provided the Samoylov site data.

The article processing charges for this open-access publication were covered by the Max Planck Society.

Edited by: T. Zhang

References

- Abnizova, A., Siemens, J., Langer, M., and Boike, J.: Small ponds with major impact: The relevance of ponds and lakes in permafrost landscapes to carbon dioxide emissions, *Global Biogeochem. Cy.*, 26, GB2041, doi:10.1029/2011GB004237, 2012.
- Abramopoulos, F., Rosenzweig, C., and Choudhury, B.: Improved ground hydrology calculations for global climate models (GCMs): Soil water movement and evapotranspiration, *J. Climate*, 1, 921–941, doi:10.1175/1520-0442(1988)001<0921:IGHCFG>2.0.CO;2, 1988.
- ACIA: Arctic Climate Impact Assessment, Cambridge University Press, New York, USA, 1042 pp., 2005.
- Alexeev, V. A., Nicolovsky, D. J., Romanovsky, V. E., and Lawrence, D. M.: An evaluation of deep soil configurations in the CLM3 for improved representation of permafrost, *Geophys. Res. Lett.*, 34, L09502, doi:10.1029/2007GL029536, 2007.
- Anisimov, O. A. and Nelson, F. E.: Permafrost zonation and climate change in the northern hemisphere: results from transient general circulation models, *Climatic Change*, 35, 241–258, doi:10.1023/A:1005315409698, 1997.
- Beer, C., Weber, U., Tomelleri, E., Carvalhais, N., Mahecha, M., and Reichstein, M.: Harmonized European long-term climate data for assessing the effect of changing temporal variability on land-atmosphere CO₂ fluxes, *J. Climate*, 27, 4815–4834, doi:10.1175/JCLI-D-13-00543.1, 2014.
- Best, M. J., Pryor, M., Clark, D. B., Rooney, G. G., Essery, R. L. H., Ménard, C. B., Edwards, J. M., Hendry, M. A., Porson, A., Gedney, N., Mercado, L. M., Sitch, S., Blyth, E., Boucher, O., Cox, P. M., Grimmond, C. S. B., and Harding, R. J.: The Joint UK Land Environment Simulator (JULES), model description – Part 1: Energy and water fluxes, *Geosci. Model Dev.*, 4, 677–699, doi:10.5194/gmd-4-677-2011, 2011.
- Boike, J., Roth, K., and Ippisch, O.: Seasonal snow cover on frozen ground: Energy balance calculations of a permafrost site near Ny-Ålesund, Spitsbergen, *J. Geophys. Res.-Atmos.*, 108, 8163, doi:10.1029/2001JD000939, 2003.
- Boike, J., Ippisch, O., Overduin, P. P., Hagedorn, B., and Roth, K.: Water, heat and solute dynamics of a mud boil, Spitsbergen, *Geomorphology*, 95, 61–73, doi:10.1016/j.geomorph.2006.07.033, 2007.
- Boike, J., Wille, C., and Abnizova, A.: Climatology and summer energy and water balance of polygonal tundra in the Lena River Delta, Siberia, *J. Geophys. Res.*, 113, G03025, doi:10.1029/2007JG000540, 2008.
- Boike, J., Kattenstroth, B., Abramova, K., Bornemann, N., Chetverova, A., Fedorova, I., Fröb, K., Grigoriev, M., Grüber, M., Kutzbach, L., Langer, M., Minke, M., Muster, S., Piel, K., Pfeiffer, E.-M., Stoeff, G., Westermann, S., Wischnewski, K., Wille, C., and Hubberten, H.-W.: Baseline characteristics of climate, permafrost and land cover from a new permafrost observatory in the Lena River Delta, Siberia (1998–2011), *Biogeosciences*, 10, 2105–2128, doi:10.5194/bg-10-2105-2013, 2013.
- Brown, J., Ferrians Jr., O. J., Heginbottom, J. A., and Melnikov, E. S.: Circum-Arctic map of permafrost and ground-ice conditions (Version 2), National Snow and Ice Data Center, Boulder, CO, USA, available at: <http://nsidc.org/data/ggd318.html> (last access: 10 September 2012), 2002.
- Burke, E. J., Dankers, R., Jones, C. D., and Wiltshire, A. J.: A retrospective analysis of pan Arctic permafrost using the JULES land surface model, *Clim. Dynam.*, Volume 41, 1025–1038, 2013.
- Clark, D. B., Mercado, L. M., Sitch, S., Jones, C. D., Gedney, N., Best, M. J., Pryor, M., Rooney, G. G., Essery, R. L. H., Blyth, E., Boucher, O., Harding, R. J., Huntingford, C., and Cox, P. M.: The Joint UK Land Environment Simulator (JULES), model description – Part 2: Carbon fluxes and vegetation dynamics, *Geosci. Model Dev.*, 4, 701–722, doi:10.5194/gmd-4-701-2011, 2011.
- Cox, P. M., Betts, R. A., Bunton, C. B., Essery, R. L. H., Rowntree, P. R., and Smith, J.: The impact of new land surface physics on the GCM simulation of climate and climate sensitivity, *Clim. Dynam.*, 15, 183–203, 1999.
- Dankers, R., Burke, E. J., and Price, J.: Simulation of permafrost and seasonal thaw depth in the JULES land surface scheme, *The Cryosphere*, 5, 773–790, doi:10.5194/tc-5-773-2011, 2011.
- Ekici, A., Beer, C., Hagemann, S., Boike, J., Langer, M., and Hauck, C.: Simulating high-latitude permafrost regions by the JSBACH terrestrial ecosystem model, *Geosci. Model Dev.*, 7, 631–647, doi:10.5194/gmd-7-631-2014, 2014.
- Engelhardt, M., Hauck, C., and Salzmann, N.: Influence of atmospheric forcing parameters on modelled mountain permafrost evolution, *Meteorol. Zeitschr.*, 19, 491–500, 2010.

- FAO, IIASA, ISRIC, ISS-CAS, and JRC: Harmonized World Soil Database (version 1.1) FAO, Rome, Italy and IIASA, Laxenburg, Austria, 2009.
- Fiddes, J., Endrizzi, S., and Gruber, S.: Large-area land surface simulations in heterogeneous terrain driven by global data sets: application to mountain permafrost, *The Cryosphere*, 9, 411–426, doi:10.5194/tc-9-411-2015, 2015.
- Friend, A. D. and Kiang, N. Y.: Land-surface model development for the GISS GCM: Effects of improved canopy physiology on simulated climate, *J. Climate*, 18, 2883–2902, doi:10.1175/JCLI13425.1, 2005.
- Gerten, D., Schaphoff, S., Haberlandt, U., Lucht, W., and Sitch, S.: Terrestrial vegetation and water balance – hydrological evaluation of a dynamic global vegetation model, *J. Hydrol.*, 286, 249–270, 2004.
- Gornall, J. L., Jonsdottir, I. S., Woodin, S. J., and Van der Wal, R.: Arctic mosses govern below-ground environment and ecosystem processes, *Oecologia*, 153, 931–941, doi:10.1007/s00442-007-0785-0, 2007.
- Gouttevin, I., Krinner, G., Ciais, P., Polcher, J., and Legout, C.: Multi-scale validation of a new soil freezing scheme for a land-surface model with physically-based hydrology, *The Cryosphere*, 6, 407–430, doi:10.5194/tc-6-407-2012, 2012a.
- Gouttevin, I., Menegoz, M., Domine, F., Krinner, G., Koven, C. D., Ciais, P., Tarnocai, C., and Boike, J.: How the insulating properties of snow affect soil carbon distribution in the continental pan-Arctic area, *J. Geophys. Res.*, 117, G02020, doi:10.1029/2011JG001916, 2012b.
- Gubler, S., Endrizzi, S., Gruber, S., and Purves, R. S.: Sensitivities and uncertainties of modeled ground temperatures in mountain environments, *Geosci. Model Dev.*, 6, 1319–1336, doi:10.5194/gmd-6-1319-2013, 2013.
- Gustafsson, D., Stähli, M., and Jansson, P.-E.: The surface energy balance of a snow cover: comparing measurements to two different simulation models, *Theor. Appl. Climatol.*, 70, 81–96, 2001.
- Harlan, R. L.: Analysis of coupled heat-fluid transport in partially frozen soil, *Water Resour. Res.*, 9, 1314–1323, 1973.
- Harris, C., Arenson, L., Christiansen, H., Etzelmüller, B., Frauenfelder, R., Gruber, S., Haeberli, W., Hauck, C., Hoelzle, M., Humlum, O., Isaksen, K., Kääb, A., Kern-Lütschg, M., Lehning, M., Matsuoka, N., Murton, J., Nötzli, J., Phillips, M., Ross, N., Seppälä, M., Springman, S., and Vonder Mühll, D.: Permafrost and climate in Europe: monitoring and modelling thermal, geomorphological and geotechnical responses, *Earth Sci. Rev.*, 92, 117–171, 2009.
- Hauck, C.: Frozen ground monitoring using DC resistivity tomography, *Geophys. Res. Lett.*, 29, 2016, doi:10.1029/2002GL014995, 2002.
- Helbig, M., Boike, J., Langer, M., Schreiber, P., Runkle, B. R., and Kutzbach, L.: Spatial and seasonal variability of polygonal tundra water balance: Lena River Delta, northern Siberia (Russia), *Hydrogeol. J.* 21, 133–147, 2013.
- Hilbich, C., Hauck, C., Hoelzle, M., Scherler, M., Schudel, L., Völkisch, I., Vonder Mühll, D., and Mäusbacher, R.: Monitoring mountain permafrost evolution using electrical resistivity tomography: A 7-year study of seasonal, annual, and long-term variations at Schilthorn, Swiss Alps, *J. Geophys. Res.*, 113, F01S90, doi:10.1029/2007JF000799, 2008.
- Hilbich, C., Fuss, C., and Hauck, C.: Automated time-lapse ERT for improved process analysis and monitoring of frozen ground, *Permafrost. Periglac. Proc.* 22, 306–319, doi:10.1002/ppp.732, 2011.
- Hoelzle, M., Gruber, S.: Borehole and ground surface temperatures and their relationship to meteorological conditions in the Swiss Alps, edited by: Kane, D. L. and Hinkel, K. M., in: Proceedings Ninth International Conference on Permafrost, 29 June–3 July, Fairbanks Alaska, vol. 1. Institute of Northern Engineering, University of Alaska Fairbanks, 723–728, 2008.
- Hollesen, J., Elberling, B., and Jansson, P. E.: Future active layer dynamics and carbon dioxide production from thawing permafrost layers in Northeast Greenland, *Global Change Biol.*, 17, 911–926, doi:10.1111/j.1365-2486.2010.02256.x, 2011.
- IPCC AR5: Summary for Policymakers, Climate Change 2013, The Physical Science Basis, Contribution of Working Group I to the Fifth Assessment Report of the Intergovernmental Panel on Climate Change, edited by: Stocker, T. F., Qin, D., Plattner, G.-K., Tignor, M., Allen, S. K., Boschung, J., Nauels, A., Xia, Y., Bex, V., and Midgley, P. M., Cambridge University Press, Cambridge, UK and New York, NY, USA, 2013.
- Jansson, P. E.: CoupModel: model use, calibration, and validation, *Transactions of the ASABE* 55.4, 1335–1344, 2012.
- Jansson, P.-E. and Karlberg, L.: Coupled heat and mass transfer model for soil-plant-atmosphere systems, Royal Institute of Technology, Dept of Civil and Environmental Engineering, Stockholm, available at: <http://www.lwr.kth.se/VaraDatorprogram/CoupModel/index.htm> (last access: 17 September 2014), 2011.
- Jensen, L. M. and Rasch, M.: Nuuk Ecological Research Operations, 2nd Annual Report, 2008, Roskilde, National Environmental Research Institute, Aarhus University, Denmark, 80 pp., 2009.
- Jensen, L. M. and Rasch, M.: Nuuk Ecological Research Operations, 3rd Annual Report, 2009, Roskilde, National Environmental Research Institute, Aarhus University, Denmark, 80 pp., 2010.
- Jungclaus, J. H., Fischer, N., Haak, H., Lohmann, K., Marotzke, J., Matei, D., Mikolajewicz, U., Notz, D., and von Storch, J. S.: Characteristics of the ocean simulations in MPIOM, the ocean component of the MPI-Earth System Model, *J. Adv. Model. Earth Syst.*, 5, 422–446, doi:10.1002/jame.20023, 2013.
- Koven, C. D., Ringeval, B., Friedlingstein, P., Ciais, P., Cadule, P., Khvorostyanov, D., Krinner, G., and Tarnocai, C.: Permafrost carbon-climate feedbacks accelerate global warming, *P. Natl. Acad. Sci.*, 108, 14769–14774, 2011.
- Koven, C. D., William, J. R., and Alex, S.: Analysis of Permafrost Thermal Dynamics and Response to Climate Change in the CMIP5 Earth System Models, *J. Climate*, 26, 1877–1900, doi:10.1175/JCLI-D-12-00228.1, 2013.
- Krinner, G., Viovy, N., de Noblet-Ducoudré, N., Ogée, J., Polcher, J., Friedlingstein, P., Ciais, P., Sitch, S., and Prentice, I. C.: A dynamic global vegetation model for studies of the coupled atmosphere-biosphere system, *Global Biogeochem. Cy.*, 19, GB1015, doi:10.1029/2003GB002199, 2005.
- Kudryavtsev, V. A., Garagulya, L. S., Kondrat'yeva, K. A., and Melamed, V. G.: Fundamentals of Frost Forecasting in Geological Engineering Investigations, Cold Regions Research and Engineering Laboratory: Hanover, NH, 1974.
- Kutzbach, L., Wille, C., and Pfeiffer, E.-M.: The exchange of carbon dioxide between wet arctic tundra and the atmosphere at the

- Lena River Delta, Northern Siberia, *Biogeosciences*, 4, 869–890, doi:10.5194/bg-4-869-2007, 2007.
- Langer, M., Westermann, S., Heikenfeld, M., Dorn, W., and Boike, J.: Satellite-based modeling of permafrost temperatures in a tundra lowland landscape, *Remote Sens. Environ.*, 135, 12–24, doi:10.1016/j.rse.2013.03.011, 2013.
- Larsen, P. H., Goldsmith, S., Smith, O., Wilson, M. L., Strzepek, K., Chinowsky, P., and Saylor, B.: Estimating future costs for Alaska public infrastructure at risk from climate change, *Global Environ. Change*, 18, 442–457, doi:10.1016/j.gloenvcha.2008.03.005, 2008.
- Lawrence, D. M. and Slater, A. G.: A projection of severe near-surface permafrost degradation during the 21st century, *Geophys. Res. Lett.*, 32, L24401, doi:10.1029/2005GL025080, 2005.
- Lawrence, D. M., Slater, A. G., Romanovsky, V. E., and Nicolsky, D. J.: Sensitivity of a model projection of near-surface permafrost degradation to soil column depth and representation of soil organic matter, *J. Geophys. Res.*, 113, 1–14, 2008.
- Lawrence, D. M., Slater, A. G., and Swenson, S. C.: Simulation of Present-Day and Future Permafrost and Seasonally Frozen Ground Conditions in CCSM4, *J. Climate*, 25, 2207–2225, 2012.
- Lunardini, V. J.: Heat transfer in cold climates, Van Nostrand Reinhold, New York, 731 pp., 1981.
- Lundin, L. C.: Hydraulic properties in an operational model of frozen soil, *J. Hydrol.*, 118, 289–310, 1990.
- Lüers, J., Westermann, S., Piel, K., and Boike, J.: Annual CO₂ budget and seasonal CO₂ exchange signals at a High Arctic permafrost site on Spitsbergen, Svalbard archipelago, *Biogeosciences*, 11, 6307–6322, doi:10.5194/bg-11-6307-2014, 2014.
- Mahecha, M. D., Reichstein, M., Jung, M., Seneviratne, S. I., Zaehle, S., Beer, C., Braakhekke, M. C., Carvalhais, N., Lange, H., Le Maire, G., and Moors, E.: Comparing observations and process-based simulations of biosphere-atmosphere exchanges on multiple timescales, *J. Geophys. Res.*, 115, G02003, doi:10.1029/2009JG001016, 2010.
- Marmy, A., Salzmann, N., Scherler, M., and Hauck, C.: Permafrost model sensitivity to seasonal climatic changes and extreme events in mountainous regions, *Environ. Res. Lett.*, 8, 035048, doi:10.1088/1748-9326/8/3/035048, 2013.
- Maturilli, M., Herber, A., and König-Langlo, G.: Climatology and time series of surface meteorology in Ny-Ålesund, Svalbard, *Earth Syst. Sci. Data*, 5, 155–163, doi:10.5194/essd-5-155-2013, 2013.
- McGuire, A. D., Christensen, T. R., Hayes, D., Herault, A., Euskirchen, E., Kimball, J. S., Koven, C., Lafleur, P., Miller, P. A., Oechel, W., Peylin, P., Williams, M., and Yi, Y.: An assessment of the carbon balance of Arctic tundra: comparisons among observations, process models, and atmospheric inversions, *Biogeosciences*, 9, 3185–3204, doi:10.5194/bg-9-3185-2012, 2012.
- Miller, P. A. and Smith, B.: Modeling tundra vegetation response to recent Arctic warming, *AMBIO, J. Human. Environ.*, 21, 281–291, 2012.
- Muster, S., Langer, M., Heim, B., Westermann, S., and Boike, J.: Subpixel heterogeneity of ice-wedge polygonal tundra: a multi-scale analysis of land cover and evapotranspiration in the Lena River Delta, Siberia, *Tellus B*, 64, 2012.
- Noetzi, J., Hilbich, C., Hauck, C., Hoelzle, M., and Gruber, S.: Comparison of simulated 2D temperature profiles with time-lapse electrical resistivity data at the Schilthorn crest, Switzerland, 9th International Conference on Permafrost, Fairbanks, US, 1293–1298, 2008.
- PERMOS: Permafrost in Switzerland 2008/2009 and 2009/2010, edited by: Noetzi, J., Glaciological Report (Permafrost) No. 10/11 of the Cryospheric Commission of the Swiss Academy of Sciences (SCNAT), Zurich, Switzerland, 2013.
- Porada, P., Weber, B., Elbert, W., Pöschl, U., and Kleidon, A.: Estimating global carbon uptake by Lichens and Bryophytes with a process-based model, *Biogeosciences*, 10, 6989–7033, doi:10.5194/bg-10-6989-2013, 2013.
- Rinke, A., Kuhry, P., and Dethloff, K.: Importance of a soil organic layer for Arctic climate: A sensitivity study with an Arctic RCM, *Geophys. Res. Lett.*, 35, L13709, doi:10.1029/2008GL034052, 2008.
- Riseborough, D., Shiklomanov, N., Eitzmuller, B., Gruber, S., and Marchenko, S.: Recent Advances in Permafrost Modelling, *Permafrost: Periglac. Process.*, 19, 137–156, 2008.
- Romanovsky, V. E. and Osterkamp, T. E.: Thawing of the active layer on the coastal plain of the Alaskan Arctic, *Permafrost: Periglac. Proc.*, 8, 1–22, doi:10.1002/(SICI)1099-1530(199701)8:1<1::AID-PPP243>3.0.CO;2-U, 1997.
- Romanovsky, V. E., Smith, S. L., and Christiansen, H. H.: Permafrost thermal state in the polar Northern Hemisphere during the international polar year 2007–2009: a synthesis, *Permafrost: Periglac. Process.*, 21, 106–116, 2010.
- Rosenzweig, C. and Abramopoulos, F.: Land-surface model development for the GISS GCM, *J. Climate*, 10, 2040–2054, doi:10.1175/1520-0442(1997)010<2040:LSDMTF>2.0.CO;2, 1997.
- Roth, K. and Boike, J.: Quantifying the thermal dynamics of a permafrost site near Ny-Ålesund, Svalbard, *Water Resour. Res.*, 37, 2901–2914, doi:10.1029/2000WR000163, 2001.
- Scherler, M., Hauck, C., Hoelzle, M., Stähli, M., and Völsch, I.: Meltwater infiltration into the frozen active layer at an alpine permafrost site, *Permafrost Periglac. Process.*, 21, 325–334, doi:10.1002/ppp.694, 2010.
- Scherler, M., Hauck, C., Hoelzle, M., and Salzmann, N.: Modeled sensitivity of two alpine permafrost sites to RCM-based climate scenarios, *J. Geophys. Res. Earth Surf.*, 118, 780–794, doi:10.1002/jgrf.20069, 2013.
- Schmidt, G. A., Ruedy, R., Hansen, J. E., Aleinov, I., Bell, N., Bauer, M., Bauer, S., Cairns, B., Canuto, V., Cheng, Y., Del Genio, A., Faluvegi, G., Friend, A. D., Hall, T. M., Hu, Y., Kelley, M., Kiang, N. Y., Koch, D., Laci, A. A., Lerner, J., Lo, K. K., Miller, R. L., Nazarenko, L., Oinas, V., Perlwitz, J., Perlwitz, J., Rind, D., Romanou, A., Russell, G. L., Sato, M. K., Shindell, D. T., Stone, P. H., Sun, S., Tausnev, N., Thresher, D., and Yao, M. S.: Present day atmospheric simulations using GISS ModelE: Comparison to in-situ, satellite and reanalysis data, *J. Climate* 19, 153–192, 2006.
- Schuur, E. A. G., Bockheim, J., Canadell, J. G., Euskirchen, E., Field, C. B., Goryachkin, S. V., Hagemann, S., Kuhry, P., Lafleur, P. M., Lee, H., Mazhitova, G., Nelson, F. E., Rinke, A., Romanovsky, V. E., Shiklomanov, N., Tarnocai, C., Venevsky, S., Vogel, J. G., and Zimov, S. A.: Vulnerability of Permafrost Carbon to Climate Change: Implications for the Global Carbon Cycle, *BioScience*, 58, 701–714, 2008.
- Serreze, M., Walsh, J., Chapin, F., Osterkamp, T., Dyurgerov, M., Romanovsky, V., Oechel, W., Morison, J., Zhang, T., and Barry,

- R.: Observational evidence of recent change in the northern high-latitude environment, *Clim. Change*, 46, 159–207, 2000.
- Shiklomanov, N. I. and Nelson, F. E.: Analytic representation of the active layer thickness field, Kuparuk River Basin, Alaska, *Ecological Modeling*, 123, 105–125, doi:10.1016/S0304-3800(99)00127-1, 1999.
- Sitch, S., Smith, B., Prentice, I. C., Arneth, A., Bondeau, A., Cramer, W., Kaplan, J. O., Levis, S., Lucht, W., Sykes, M. T., Thonicke, K., and Venevsky, S.: Evaluation of ecosystem dynamics, plant geography and terrestrial carbon cycling in the LPJ dynamic global vegetation model, *Global Change Biology*, 9, 161–185, 2003.
- Slater, A. G. and Lawrence, D. M.: Diagnosing Present and Future Permafrost from Climate Models, *J. Clim.*, 26, 5608–5623, doi:10.1175/JCLI-D-12-00341.1, 2013.
- Smith, B., Prentice, I. C., and Sykes, M. T.: Representation of vegetation dynamics in the modelling of terrestrial ecosystems: comparing two contrasting approaches within European climate space, *Global Ecol. Biogeogr.*, 10, 621–637, doi:10.1046/j.1466-822X.2001.t01-1-00256, 2001.
- Soudzilovskaia, N. A., van Bodegom, P. M., and Cornelissen, J. H. C.: Dominant bryophyte control over high-latitude soil temperature fluctuations predicted by heat transfer traits, field moisture regime and laws of thermal insulation, *Funct. Ecol.*, 27, 1442–1454, doi:10.1111/1365-2435.12127S, 2013.
- Stendel M., Romanovsky, V. E., Christensen, J. H., and Sazonova T.: Using dynamical downscaling to close the gap between global change scenarios and local permafrost dynamics, *Global Planet. Change*, 56, 203–214, doi:10.1016/j.gloplacha.2006.07.014, 2007.
- Stevens, B., Giorgetta, M., Esch, M., Mauritsen, T., Crueger, T., Rast, S., Salzmann, M., Schmidt, H., Bader, J., Block, K., Brokopf, R., Fast, I., Kinne, S., Kornblueh, L., Lohmann, U., Pincus, R., Reichler, T., and Roeckner, E.: The atmospheric component of the MPI-M Earth System Model: ECHAM6, *J. Adv. Model. Earth Syst.*, 5, 146–172, doi:10.1002/jame.20015, 2012.
- Taylor, K. E., Stouffer, R. J., and Meehl, G. A.: A summary of the CMIP5 experiment design. PCMDI Tech. Rep., 33 pp., available at: http://cmip-pcmdi.llnl.gov/cmip5/docs/Taylor_CMIP5_design.pdf, 2009.
- Vonder Mühl, D., Hauck, C., and Lehmann, F.: Verification of geophysical models in Alpine permafrost using borehole information, *Ann. Glaciol.*, 31, 300–306, 2000.
- Wang, T., Otle, C., Boone, A., Ciais, P., Brun, E., Morin, S., Krinner, G., Piao, S., and Peng, S.: Evaluation of an improved intermediate complexity snow scheme in the ORCHIDEE land surface model, *J. Geophys. Res.-Atmos.*, 118, 6064–6079, doi:10.1002/jgrd.50395, 2013.
- Wania, R., Ross, I., and Prentice, I. C.: Integrating peatlands and permafrost into a dynamic global vegetation model: 1. Evaluation and sensitivity of physical land surface processes, *Global Biogeochem. Cy.*, 23, doi:10.1029/2008GB003412, 2009a.
- Wania, R., Ross, I., and Prentice, I. C.: Integrating peatlands and permafrost into a dynamic global vegetation model: 2. Evaluation and sensitivity of vegetation and carbon cycle processes, *Global Biogeochem. Cy.*, 23, doi:10.1029/2008GB003413, 2009b.
- Wania, R., Ross, I., and Prentice, I. C.: Implementation and evaluation of a new methane model within a dynamic global vegetation model: LPJ-WHyMe v1.3.1, *Geoscientific Model Development* 3, 565–584, 2010.
- Weedon, G., Gomes, S., Viterbo, P., Österle, H., Adam, J., Bellouin, N., Boucher, O., and Best, M.: The WATCH forcing data 1958–2001: A meteorological forcing dataset for land surface and hydrological models WATCH Tech. Rep. 22, 41 pp., available at: <http://www.eu-watch.org/publications/technical-reports>, 2010.
- Westermann, S., Lüers, J., Langer, M., Piel, K., and Boike, J.: The annual surface energy budget of a high-arctic permafrost site on Svalbard, Norway, *The Cryosphere*, 3, 245–263, doi:10.5194/tc-3-245-2009, 2009.
- Westermann, S., Wollschläger, U., and Boike, J.: Monitoring of active layer dynamics at a permafrost site on Svalbard using multi-channel ground-penetrating radar, *The Cryosphere*, 4, 475–487, doi:10.5194/tc-4-475-2010, 2010.
- Westermann, S., Langer, M., and Boike, J.: Spatial and temporal variations of summer surface temperatures of high-arctic tundra on Svalbard – Implications for MODIS LST based permafrost monitoring, *Remote Sens. Environ.*, 115, 908–922, doi:10.1016/j.rse.2010.11.018, 2011.
- Wolf, A., Callaghan, T., and Larson, K.: Future changes in vegetation and ecosystem function of the Barents Region, *Clim. Change*, 87, 51–73, 2008.
- ZackenbergGIS, available at: <http://dmugisweb.dmu.dk/zackenberggis/datapage.aspx>, last access: 10 September 2012.
- Zhang, T.: Influence of the seasonal snow cover on the ground thermal regime: An overview, *Rev. Geophys.*, 43, RG4002, doi:10.1029/2004RG000157, 2005.
- Zhang, W., Miller, P. A., Smith, B., Wania, R., Koenigk, T., and Döscher, R.: Tundra shrubification and tree-line advance amplify arctic climate warming: results from an individual-based dynamic vegetation model, *Environ. Res. Lett.*, 8, 034023, doi:10.1088/1748-9326/8/3/034023, 2013.

**Avhandlingar från Institutionen för naturgeografi och ekosystemanalys (INES),
Lunds universitet**

**Dissertations from Department of Physical Geography and Ecosystem Science,
University of Lund**

Martin Sjöström, 2012: Satellite remote sensing of primary production in semi-arid Africa.

Zhenlin Yang, 2012: Small-scale climate variability and its ecosystem impacts in the sub-Arctic.

Ara Toomanian, 2012: Methods to improve and evaluate spatial data infrastructures.

Michal Heliasz, 2012: Spatial and temporal dynamics of subarctic birch forest carbon exchange.

Abdulghani Hasan, 2012: Spatially distributed hydrological modelling : wetness derived from digital elevation models to estimate peatland carbon.

Julia Bosiö, 2013: A green future with thawing permafrost mires? : a study of climate-vegetation interactions in European subarctic peatlands. (Lic.)

Anders Ahlström, 2013: Terrestrial ecosystem interactions with global climate and socio-economics.

Kerstin Baumanns, 2013: Drivers of global land use change : are increasing demands for food and bioenergy offset by technological change and yield increase? (Lic.)

Yengoh Genesis Tambang, 2013: Explaining agricultural yield gaps in Cameroon.

Jörgen Olofsson, 2013: The Earth : climate and anthropogenic interactions in a long time perspective.

David Wårlind, 2013: The role of carbon-nitrogen interactions for terrestrial ecosystem dynamics under global change : a modelling perspective.

Elin Sundqvist, 2014: Methane exchange in a boreal forest : the role of soils, vegetation and forest management.

Julie Mari Falk, 2014: Plant-soil-herbivore interactions in a high Arctic wetland : feedbacks to the carbon cycle.

Finn Hedefalk, 2014: Life histories across space and time : methods for including geographic factors on the micro-level in longitudinal demographic research. (Lic.)

Sadegh Jamali, 2014: Analyzing vegetation trends with sensor data from earth observation satellites.

Cecilia Olsson, 2014: Tree phenology modelling in the boreal and temperate climate zones : timing of spring and autumn events.

Jing Tang, 2014: Linking distributed hydrological processes with ecosystem vegetation dynamics and carbon cycling : modelling studies in a subarctic catchment of northern Sweden.

Zhang Wenxin, 2015: The role of biogeophysical feedbacks and their impacts in the arctic and boreal climate system.

Lina Eklund, 2015: “No Friends but the Mountains” : understanding population mobility and land dynamics in Iraqi Kurdistan.

Stefan Olin, 2015: Ecosystems in the Anthropocene : the role of cropland management for carbon and nitrogen cycle processes.

Thomas Möckel, 2015: Hyperspectral and multispectral remote sensing for mapping grassland vegetation.

Hongxiao Jin, 2015: Remote sensing phenology at European northern latitudes : from ground spectral towers to satellites.

Bakhtiyor Pulatov, 2015: Potential impact of climate change on European agriculture : a case study of potato and Colorado potato beetle.

Christian Stiegler, 2016: Surface energy exchange and land-atmosphere interactions of Arctic and subarctic tundra ecosystems under climate change.

Per-Ola Olsson, 2016: Monitoring insect defoliation in forests with time-series of satellite based remote sensing data : near real-time methods and impact on the carbon balance.

Jonas Dalmayne, 2016: Monitoring biodiversity in cultural landscapes : development of remote sensing- and GIS-based methods.

Balathandayuthabani Panneer Selvam, 2016: Reactive dissolved organic carbon dynamics in a changing environment : experimental evidence from soil and water.

Kerstin Engström, 2016: Pathways to future cropland : assessing uncertainties in socio-economic processes by applying a global land-use model.

Finn Hedefalk, 2016: Life paths through space and time : adding the micro-level geographic context to longitudinal historical demographic research.

Ehsan Abdolmajidi, 2016: Modeling and improving Spatial Data Infrastructure (SDI).

Giuliana Zanchi, 2016: Modelling nutrient transport from forest ecosystems to surface waters.

Florian Sallaba, 2016: Biophysical and human controls of land productivity under global change : development and demonstration of parsimonious modelling techniques.

Norbert Pirk, 2017: Tundra meets atmosphere : seasonal dynamics of trace gas exchange in the High Arctic.

Minchao Wu, 2017: Land-atmosphere interactions and regional Earth system dynamics due to natural and anthropogenic vegetation changes.

Niklas Bocke-Olén, 2017: Global savannah phenology : integrating earth observation, ecosystem modelling, and PhenoCams.

Abdulhakim M. Abdi, 2017: Primary production in African drylands: quantifying supply and demand using earth observation and socio-ecological data.

Nitin Chaudhary, 2017: Peatland dynamics in response to past and potential future climate change.

